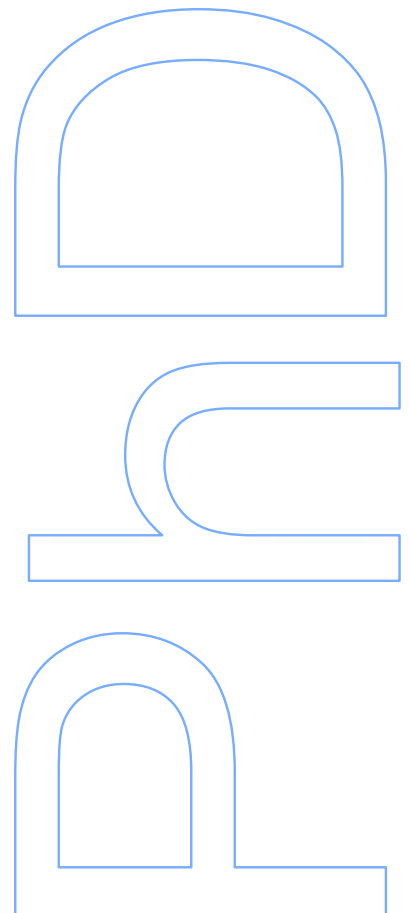# Unraveling the metabolism and transmembrane transport of the highly valuable medicinal alkaloids from *Catharanthus roseus*

Inês Carqueijeiro
Doutoramento em Biologia
Departamento de Biologia
2012

Orientador
Mariana Sottomayor, Professora Auxiliar, Faculdade de Ciências
Universidade do Porto

À minha irmã

ACKNOWLEDGMENTS

First and foremost I want to thank my supervisor Professor Mariana Sottomayor. It has been an honour to be her Ph.D. student. She has taught me, both consciously and unconsciously, how to become a better scientist, and most of all how to become a better person. I appreciate all her contributions of time, brainstorming, experience, wisdom and encouragement. The joy and enthusiasm she has for her research, and for my work was contagious and motivational for me, even during tough times in the Ph.D. quest. I am also thankful for the excellent example she has provided me as a successful woman.

To the members of the Bioactive Natural Products (BNP) group that have contributed immensely to my personal and professional time at IBMC. The group has been a source of friendship as well as good advice and collaboration. I am especially grateful for the fun group of the original BNP group members who stuck with me. A special thanks to Raquel, Luisa, Gisela and Ju, past members of our group, who were always alongside with me. Raquel, one of my first teachers at the bench. Jorge Gutierrez, nuestro niño, mi compañero, gracias por los buenos ratos. Lorena llegaste tarde a nuestro grupo, pero ya eres parte de nosotras y fuiste una gran ayuda para mi, nunca te voy a perdonar que hubieras llegado tan tarde, mi estancia en Oporto hubiera sido mucho mas agradable contigo – gracias cariño.

To Patrícia, my second pair of hands and many times my spare brain, my psychologist and my mum!!! At least I gave you the opportunity to experience how to be a mum, before your real Inês arrived. All the words won't be enough to thank you. This PhD is also your second PhD.

Sara, a little Big woman, who was always there when I needed it, without asking for what/why or when… just "what do you need me to do…" the true example of how two different people can build a good work (friend) relationship.

To Professor Alain Goossens thank you so much for welcoming me in your lab and having the opportunity to learn with such a bright scientist. You are to blame for raising my standards, and making me much more demanding not only with myself and with my work, but also with the ones that surround me. The most valuable lesson that I learned from you in these four years was – "don't complain or find excuses, just present the best work" (I tried!).

To Prof Hernâni Gerós, you were much more than a co-supervisor! Your patience, kindness and everlasting good-will was always a comfort during the hard journey of membrane transport. Thank you so much for accepting me in your lab and making me feel like I was part of the team.

My time at Porto was made enjoyable in large part due to the many friends and groups that became a part of my life. To Rita, Daniela, Margarida, Patrícia Carneiro, my friends of all hours, that made my time in Porto more cosy and homey, and for making the weekends look and feel like real weekends.

To the members of Molecular Biology of Nitrogen Assimilation group at IBMC, for hosting us in the last years and for all the support, assistance and exchange of knowledge. A special thanks to Liliana and Ana Rita Seabra.

To Marta Vaz Mendes my voice of conscience – thank you for all. Filipe, who else had the patience for such a demanding lab neighbour?

To the members of the Alain Goossens Laboratory, for integrating me in the work group. A special thanks to Tessa and Jacob, part of my journey was much easier with your precious help. Having the fortune of knowing you and learn with you was a real life experience.

To the members of the Hernâni Gerós group, Artur, Henrique, Jorge, Richard, Viviana for welcoming me for almost two years (back and forth). Henrique, when grow up I want to be just like you.

A special thanks to my IGC family, Rui Gardner (thank you for embracing with me in this idioblasts journey), Telma, Pedro (how come next to you the sun always shine and hard work sound like party I will never know…), what a pleasure to work in such a place. Work almost feels like "a fun camping week". With you guys I learned that it doesn't matter the number of working hours, but instead the quality… and what a good quality is your work.

I would like to thank Professor Alberto Dias for spending time to teaching and helping me with the HPLC. Thank you.

To Frederico Silva, Paula Sampaio, Rui Fernandes, heads of IBMC core facilities, for the precious advice and help, crucial for the achievement of large part of the results presented in this thesis. Frederico, thank you for becoming my friend and sharing your knowledge with me. You are my personal proteomic google.

I would also like to acknowledge the IBMC Information Systems Department members, Pedro Martins and Nuno Leite de Faria. Thank you for all your help.

Last but not least, I would like to thank my family for all their love and encouragement. To my parents, who raised me with a love for science and supported me in all my pursuits and adventures. Thank you for your love, support, and never ending encouragement. To my mum for allowing me to embrace my dreams, and to my father for teaching me how to dream. A special thanks to my sister, my better version, my best friend, many times my only friend - who never allows me to feel alone. With you by my side I can do anything and everything!!!

To my uncles, Tia e Tio, my second parents. To Edmundo and Mena, my extended family – thank you. To my cousins Tita and João (special thanks to you João, for always opening the doors of your house to me and never asking until when!!). Paco, my precious…My friends Beijocas, Ganhão, Marta, Domingos, Fadinha … at least now I can come back…thank you for waiting.

And last, the person I most miss today… my Grandfather. Not everyone has the fortune to meet their one true hero - I was very lucky. Much of what I am I owe to you, and the will to achieve your standards will always guide me.

FCUP 5

Unravelling the metabolism and transmembrane transport of the highly valuable medicinal alkaloids from *Catharanthus roseus*

Ao abrigo do disposto no número 2 do Artigo 8o da Decreto Lei no 388/70

This dissertation is based on the following publications, as well as in some unpublished results:

I. Carqueijeiro I, Noronha H, Duarte P, Gerôs HV, Sottomayor M (2013) Vacuolar transport of the medicinal alkaloids from *Catharanthus roseus* is mediated by a proton driven antiport. Plant Physiology. DOI: 10.1104/pp.113.220558.

Under revision to be submitted:

I. Carqueijeiro I., Lima F., Bettencourt S., Claverol S., Bonneu M., Duarte P., Sottomayor M. The proteome of a toxic vacuole: analysis of the leaf vacuoles from the alkaloid producing plant *Catharanthus roseus.*

II. Carqueijeiro I, Gardner R., Lopes T, Lima F, Duarte P, Sottomayor M. A fluorescence activated cell sorting method for isolation of *Catharanthus roseus* leaf cells accumulating medicinal alkaloids.

III. Carqueijeiro I., Poiller J., Gardner R., Lopes T., Lima F., Duarte P., Goossens A., Sottomayor M. A targeted transcriptomic approach to unravel the metabolism of the highly valuable medicinal alkaloids from *Catharanthus roseus.*

Supplementary data (Chapter III and V) can be consulted in the CD that accompanies this thesis.

Given that some of the results that integrate this dissertation were published in international scientific journals (Chapters II) with distinct graphical presentations, a standardization of the text and figures format was carried out, without any change in their content. The articles mentioned above are reproduced in this thesis with the permission of the copyright holder.

ABSTRACT

Catharanthus roseus (L.) G. Don. accumulates in the leaves low levels of the important anticancer terpenoid indole alkaloids (TIAs) vinblastine (VLB) and vincristine (VCR), making of this plant one of the best characterized medicinal plants. However, although much is known about the biosynthesis and regulation of TIAs in *C. roseus*, gene / enzyme characterization is still lacking for many biosynthetic steps, the membrane transport mechanisms of TIAs are basically uncharacterized despite their importance for TIA accumulation, and no effective regulatory master switch of the TIA pathway has been identified to date.

In this thesis, the metabolism and transmembrane transport of the highly valuable medicinal alkaloids from *C. roseus* was investigated, using biochemical and omic approaches. Investigation of the vacuolar accumulation of TIAs showed that they are transported into the vacuoles of mesophyll cells by a specific proton antiport system, dependent on the transtonoplast pH gradient generated by the vacuolar H^+-ATPase and the vacuolar H^+-PPase, in agreement with previous observations for the alkaloids berberine in *Coptis japonica* and nicotine in tobacco. These results further support the H^+ antiport mechanism as a general system for vacuolar accumulation of alkaloids in plants.

The proteome of the toxic vacuoles of *C. roseus* leaf cells was investigated and it revealed several candidate multidrug and toxic compound extrusion (MATE) transporter candidate genes to the vacuolar proton / TIA antiport. As a whole, the proteome of the toxic vacuoles from *C. roseus* leaves indicated, apart from the well-known involvement in lytic reactions and in ion and sugar homeostasis, a high commitment of this organelle with secondary metabolism and defence indicated by the high levels of strictosidine synthase, a newly discovered and very significant role in redox homeostasis, the presence of a significant metabolic activity, and the possible association of innumerable transporters and signalling proteins in membrane microdomains.

Finally, a differential transcription profiling of leaf idioblast cells specialized in the late, bottleneck steps of VLB biosynthesis was performed. For this, a fluorescence activated cell sorting method enabling the isolation of idioblast protoplasts from the remaining leaf protoplasts was established, and the isolated idioblast cells were then submitted to differential transcription profiling by cDNA- amplified fragment length polymorphism. This transcriptional screening showed that the idioblast cells from *C. roseus* leaves present a very distinctive expression profile relative to all other cells in the leaves, and it was possible to identify a number of very strong candidate genes to

important functions within the TIA pathway, namely to the bottleneck hydroxylation of α-3',4'-anhydrovinblastine into VLB, to the transmembrane transport of TIA intermediates (several ATP binding cassette transporters) and to transcriptional regulation of the early and late steps of the TIA pathway.

Overall, the results obtained in the course of this thesis have provided novel and important information regarding the transmembrane transport of TIAs, as well as a set of highly relevant candidate genes for TIA metabolism that may lead to the successful manipulation of *C. roseus* to produce higher levels of the anticancer VLB and VCR in the near future.

RESUMO

Catharanthus roseus (L.) G. Don. acumula nas suas folhas níveis muito baixos dos alcalóides indólicos terpenóides (TIAs), vimblastina (VLB) e vincristina (VCR), que são importantes medicamentos anticancerígenos. Como consequência desta importância, *C. roseus* tornou-se uma das plantas medicinais mais bem caracterizadas. No entanto, embora se saiba muito sobre a biossíntese e regulação dos TIAs em *C. roseus*, ainda não foi realizada a caracterização dos genes / enzimas para muitas das etapas biossintéticas, os mecanismos de transporte transmembranar dos TIAs são basicamente desconhecidos, apesar de sua importância para a acumulação dos TIAs, e não foi identificado nenhum regulador geral da via dos TIAs até ao momento.

Nesta tese, o metabolismo e o transporte transmembranar dos alcalóides medicinais altamente valiosos de *C. roseus* foram investigadas utilizando abordagens bioquímicas e ómicas. Investigação da acumulação vacuolar dos TIAs mostrou que estes são transportados para os vacúolos das células do mesófilo por um sistema de antiporte protónico específico, dependente do gradiente de pH através do tonoplasto gerado pela H^+-ATPase vacuolar e pela H^+-PPase vacuolar, como observado anteriormente para a berberina em *Coptis japonica* alcalóides para a nicotina no tabaco. Estes resultados apoiam o mecanismo de antiporte proteónico como um sistema geral de acumulação vacuolar dos alcalóides nas plantas.

O proteoma dos vacúolos tóxicos das células de folha de *C. roseus* foi investigado e revelou vários genes de transportadores MATE (multidrug and toxic compound extrusion) candidatos para o sistema de antiporte protónico do vacúolo. Como um todo, o proteoma dos vacúolos tóxicos das folhas de *C. roseus* mostrou, para além do envolvimento já conhecido em reacções líticas e na homeostase iónica e de açúcares, um elevado envolvimento deste organelo com o metabolismo secundário e defesa, indicado pelos níveis elevados da enz«ima estrictosidina sintase, um papel novo e muito significativo na homeostase redox da célula, a presença de uma actividade metabólica significativa, e a possível associação de inúmeros transportadores e proteínas de sinalização em microdomínios de membrana.

Finalmente, foi efetuado um rastreio transcricional diferencial de idioblastos de folha, que são células especializadas nas etapas finais e limitantes da biossíntese de VLB. Para isso, foi estabelecido um método de separação de células por FACS (fluorescence activated cell sorting) permitindo o isolamento de protoplastos de idioblastos a partir dos protoplastos totais de folha, e os idioblastos isolados foram então submetidos a rastreio transcricional diferencial por cDNA-AFPL (amplified fragment

length polymorphism). Este rastreio mostrou que os idioblastos das folhas de *C. roseus* apresentam um perfil de expressão marcadamente distinto das outras células presentes nas folhas, e foi possível identificar um conjunto de genes candidatos muito fortes para funções importantes na via dos TIAs, nomeadamente para a hidroxilação limitante de α-3',4'-anidrovimblastine em VLB, para o transporte transmembranar de TIAs (vários transportadores ABC - ATP binding cassette) e para a regulação transcricional das etapas precoces e tardias da via dos TIAs.

Globalmente, os resultados obtidos no decurso deste trabalho proporcionaram informação nova e importante sobre o transporte transmembranar dos TIAs, bem como a identificação de um conjunto de genes candidatos altamente relevantes para o metabolismo dos TIAs, que poderão conduzir num futuro próximo à manipulação bem sucedida de *C. roseus* para produzir níveis mais elevados dos TIAs anticancerígenos VLB e VCR.

FCUP 11

Unravelling the metabolism and transmembrane transport of the highly valuable medicinal alkaloids from *Catharanthus roseus*

TABLE OF CONTENTS

FCUP 13

Unravelling the metabolism and transmembrane transport of the highly valuable medicinal alkaloids from *Catharanthus roseus*

ABREVIATIONS

10HGO – 10-hydroxygeraniol oxidoreductase

35S – Cauliflower Mosaic virus promoter

ABC – ATP-binding cassette protein

ADP – Adenosine diphosphate

ADP2 – ADP-ribosylation factor 2

AGP – Arabinogalactan protein

AGP58 - Arabinogalactan protein 58

APX – Ascorbate peroxidase

ATP – Adenosine-5'-triphosphate

ACMA – 9-amino-2-methoxy-6-chloroacridinic monocation

AVLB – α-3',4'-anhydrovinblastine

AS – anthranilate synthase

B5 – Gamborg's B5 medium

cDNA - Complementary DNA

cDNA-AFLP - cDNA-Amplified Fragment Length Polymorphism

CFP - Cyan fluorescent protein

Cys Aminoacid cystein

CroPrx1 *Catharanthus roseus* Prx1

CroPrx5 *Catharanthus roseus* Prx5

CroPrx7 *Catharanthus roseus* Prx7

CroPrx50 *Catharanthus roseus* Prx50

CTE– C-terminal extensión

DHA - dehydrascorbate

D4H - Deacetoxyvindoline-4-hydroxylase

DAT - Deacetylvindoline-4-O-acetyltransferase

DMSO - Dimethylsulfoxide

DNA - Deoxyribonucleic acid

dNTPs - Deoxyribonucleotide triphosphates of purine bases (adenine, guanine), and pyrimidine
    bases (uracil, thymine, cytosine)

Fluo-4 AM – Fluorescent calcium indicator Fluo-4

F-H$^+$-ATPase – Mitochondria-type H+-ATPase

FM1- 43 – Fluorescent membrane probe

FDA – Fluorescein diacetate

EDTA – Ethylenediaminetetraacetic acid

ER – Endoplasmic reticulum

G10H – Geraniol 10-hydroxylase

GFP – Green Fluorescent Protein (originally isolated from *Aequorea victoria*)

GPI – Glycosylphosphatidylinositol

GSP – Gene Specific Primers

GSSG – oxidized glutathione

GSH – glutathione

HPLC – High-performance liquid chromatography

LAMT – loganic acid methyltransferase,

K_M – Michaelis-Menten constant

MATE – Multidrug and toxic compound extrusion

MDHA – monodehydroascorbate reductase

MPGR - Medicinal Plant Genomics Resource

mRNA - messenger ribonucleic acid

MRP - Multidrug resistance-associated protein

m/z – mass to charge ratio

NADP – nicotinamide adenine dinucleotide

NADPH – Nicotinamide adenine dinucleotide phosphate

NBD – Nucleotide-binding domain

NMT – *N*-methyltransferase,

nos ter - NOS terminator from the *nopaline synthase* gene from *A.tumefaciens*

ORCAE – Online Resource for Community Annotation of Eukaryotes

OMT – 16-hydoxytabersonine 16-*O*-methyltransferase

ON - Overnight

PCR - Polymerase chain reaction

pDNA – plasmid DNA

PEG - Polyethylene glycol

Prx1 - *Catharanthus roseus* Peroxidase 1 50 7 5

PCA - Principal Components Analysisintri

PPi - Pyrophosphate

Pi – phosphate

PIP – intrinsic plasma membrane protein

P-H$^+$-ATPase – Plasma membrane-type H+-ATPase

RNA - Ribonucleic acid

RPs28 - 40S ribosomal protein S28

RPL24 - 60S ribosomal protein L24

RPS9 - 40S ribosomal protein S9

RT-PCR - Reverse transcription PCR

SDS-PAGE – SDS-Polyacrylamide gel electrophoresis

SNARE – Soluble N-ethylmaleimide sensitive factor adaptor protein receptor

Semi-qPCR - Semi-quantitative PCR

SGD – strictosidine β-D-glucosidase

SLS – secologanin synthase

STR – Strictosidine synthase

FCUP 15

Unravelling the metabolism and transmembrane transport of the highly valuable medicinal alkaloids from *Catharanthus roseus*

SD – Standard deviation

T16H – tabersonine 16-hydroxylase

T_a – Annealing temperature

TDC – Tryptophan decarboxylase

TIPs – intrinsic tonoplast protein

TIA – Terpenoid indole alkaloid

TMD – Transmembrane domain

T_m – Melting temperature

UV – Ultra-violet

VCR – vincristine

VLB – vinblastine

V-H$^+$-ATPase – Vacuolar-type H+-ATPase

V-H$^+$-PPase – Vacuolar -type pyrosphosphatese

v/v – volume/volume

w/v – weight/volume

LIST OF FIGURES

FCUP 19

Unravelling the metabolism and transmembrane transport of the highly valuable medicinal alkaloids from *Catharanthus roseus*

LIST OF TABLES

µM) and the F-H$^+$-ATPase inhibitor azide (5 mM), to detect only the V-H$^+$-ATPase activity.

Chapter

I

General Introduction

1. GENERAL INTRODUCTION

Natural products, also referred as secondary metabolites, are not essential for the growth or reproduction of plants, and are not produced in every conditions or developmental stages (Dewick, 2009). However, it is believed that these compounds confer an adaptable advantage and result from a direct co-evolution of the plant with its environment (Bourgaud et al., 2001; Sottomayor and Ros Barceló, 2006). For ages, humans have taken advantage of plant secondary compounds, basically due to their bioactivity explored not only in the pharmaceutical field, but also as dyes, herbicides, flavours and scents, or as bioenergy sources (Hanson, 2003; Ragauskas et al., 2006). It is estimated that 34% of the new chemical entities explored since 1986 are natural products or their derivatives (Newman and Cragg, 2007). For all the above said, secondary compounds are invaluable sources of newly and unique bioactivities, and a complete understanding of their biosynthesis can only improve our capacity to develop new and better chemicals.

Plants, because of their sessile condition, need to avoid or survive to an extraordinary variety of biotic/abiotic stresses and they found in secondary metabolism a perfect mechanism of defence that gives them the plasticity to colonize almost any environment. In plants, secondary metabolites have been reported to confer protection from herbivores, pathogens and abiotic stresses, to function as both negative and positive allelochemicals, and to be involved in chemical signalling during many types of interaction with other organisms (Wink, 1993; Hartmann, 2007). Through a range of metabolic pathways, plants produce an incredible number of secondary metabolites estimated to be over 200 000, of which only ~15 % have been investigated. Likewise, plant secondary metabolism is still the major source of drugs as evidenced from the ~90 compounds or there derivatives tested in clinical trials per year (Saklani and Kutty, 2008; Wu and Chappell, 2008; Li and Vederas, 2009). Depending on the importance of the secondary compound, some of the biosynthetic pathways have been intensively investigated but, although many related enzymes and regulators have been characterized at protein and gene level, our knowledge is still scarce compared to the immense diversity of existing pathways. An important example of a plant where a secondary metabolism pathway has been intensively investigated is the medicinal plant *Catharanthus roseus.*

1.1 The plant *Catharanthus roseus*

Catharanthus roseus (L.) G. Don. (Fig.1) is a perennial semi-shrub known as the Madagascar periwinkle, highly appreciated as an ornamental plant. *C. roseus* belongs to the family Apocynaceae and it was first published by Linnaeus as *Vinca rosea*, in his "Systema Naturae" in 1759. This species was later published as *Catharanthus* by George Don in his "General System of Gardening and Botany" (1835). The genus *Catharanthus* was originated in Madagascar, except for the species *Catharanthus pusillus* that originated in India. Nonetheless, *C. roseus* has today a pantropical distribution, being naturalized in Africa, America's, Asia, Australia, Southern Europe, and in some islands in the Pacific Ocean (van der Heijden et al., 2004). *C. roseus* has been used for centuries in folk medicine to treat diabetes, and pursuing this hypoglycemic activity ultimately led to the discovery of an anticancer activity present in the leaves of the plant (Bennouna et al., 2005; Gomez et al., 2011). The high pharmaceutical importance of this anticancer activity stimulated an intensive research of *C. roseus,* which has become one of the most studied medicinal plants. The active principles of the cytostatic effect of *C. roseus* leaves were found to be two complex molecules classified as alkaloids.

Figure 1. Flowering plant of *Catharanthus roseus* cv. Little Bright Eye.

1.2 Alkaloids

Based on their biosynthetic origin, plant secondary compounds can be classified in terpenoids, glucosinolates and cyanoglucosides, phenylpropanoids and other phenolic compounds, and in our subject of study - the alkaloids (Giddings, 2011b). Alkaloids are among the most important groups of secondary metabolites: they are toxic, powerful hallucinogens and, above all, have important pharmacological activity, being used on a daily base, including examples such as morphine, codeine, nicotine or caffeine (Mano, 2006; Memelink and Gantet, 2007).

Alkaloids are a large chemical group of low molecular-weight molecules, containing one or more basic nitrogen, characteristically in a heterocyclic configuration. Due to their high bioactivity, intensive research has been done not only to characterize alkaloids, but also to discover novel and potentially more powerful bioactive alkaloids (De Luca and St Pierre, 2000; Facchini and De Luca, 2008). Alkaloids are produced by a large variety of organisms, including plants, animals, bacteria and fungi. Since the year 1804, when Friedrich Serturner isolated the first alkaloid – morphine, from opium, until our days, more than 12000 alkaloids were identified (Pollier et al., 2011). It is believed that alkaloids play an important role as herbivore deterrents in plants, with their frequent potent physiological activity in animal cells being a result of co-evolution designed to have a toxic effect, which eventually translates into a therapeutic effect in the appropriate dose (Hegnauer, 1988; Wink and Roberts, 1998; Wink, 1999). Alkaloids are rare in lower plants and are relatively common in the angiosperm orders, especially in the Solanaceae and Apocynaceae families where 60 to 70% of the species accumulate alkaloids (Facchini et al., 2004).

According to their structure, alkaloids can be organized in several groups, and contrasting with other secondary metabolites, there is no biosynthesis or phylogeny correlation between these groups. Research has focused essentially on tropane, pyrrolidine, purine, benzylisoquinoline and the indole alkaloids as a result of their high pharmaceutical interest (Fig. 2). These alkaloids have in common the limited number of species that produce them (Facchini, 2001)
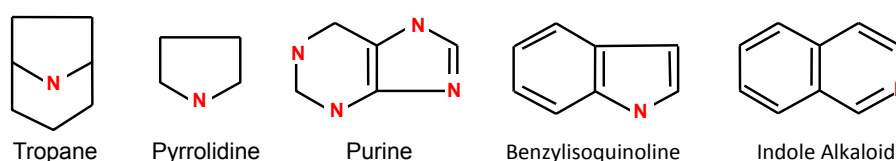
Figure 2. Basic chemical structure of the most studied groups of alkaloids. The heterocyclic nitrogen (N) is highlighted in red.

Human societies took advantage of the biological activity presented by the alkaloids since early times. In folk medicine, the records go back to 1200 years B.C., in the Middle East, where latex of opium poppy (*Papaver somniferum*) containing the alkaloid morphine was already used to treat several symptoms. Modern examples of the applicability of the biological activity of the alkaloids are the following: caffeine (*Coffea arabica* or *Camellia sinensis*) and nicotine (*Nicotiana tabacum*) - as stimulants; the opioid alkaloids (*Papaver somniferum)* - as sedative or analgesic; ajmalicine (*C. roseus* or *Rauvolfia serpentine*) – for hypertension; quinine from

FCUP 25

Unravelling the metabolism and transmembrane transport of the highly valuable medicinal alkaloids from *Catharanthus roseus*

(*Cinchona officinalis*) – treatment of malaria and lupus; sanguinarine (*Sanguinarea canadensis*) - as antibacterial; and cocaine (*Erythroxylun coca*) – as anesthethic (Wink, 1999; Mano, 2006; Zhao and Dixon, 2009). Finally, and among the most important pharmaceutically active alkaloids, are the antineoplastic principles of *C. roseus*, vinblastine and vincristine.

1.3 Bioactivity of the Vinca alkaloids

Since the 1960s, the interest in *C. roseus* by modern medicine has raised with the discovery of the antineoplastic effect of the plant leaves, followed by the isolation of the active principles, the alkaloids vinblastine (VLB) and vincristine (VCR; Fig. 3. Surprisingly, the isolation of VLB by Robert Noble and Charles Beer resulted from the effort to identify the compound responsible for the hypoglycemic effect of *C. roseus* leaf extracts used in folk medicine, which resulted in the observation of a marked antileukemic activity. Almost at the same time, Gordon Svoboda and his colleagues isolated VCR, also shown to have an important antileukemic effect (Noble et al., 1958; Svoboda et al., 1962). VLB and VCR became known as the "Vinca alkaloids", a designation that has remained until nowadays within the medical community, currently also including a number of anticancer semi-synthetic derivatives from VLB and VCR (Fig.3). Among the alkaloids later discovered to be produced by *C. roseus*, two more also have commercial use: serpentine, used as sedative, and ajmalicine, used in the treatment of hypertension. However, this last one is isolated from another member of the Apocynaceae family, *Rauwolfia serpentina*, where it is more abundant (van der Heijden et al., 2004; Memelink and Gantet, 2007).

The two anticancer alkaloids VCR and VLB are dimeric terpenoid indole alkaloids, resulting from the coupling of two subunits, the alkaloids catharanthine and vindoline by a single bond (Kingston, 2009). The two dimeric alkaloids only differ in a single chemical group: VLB has a methyl group where VCR has a formyl group, meaning that VCR is the oxidized form of VLB (Fig.3). In spite of this minor difference, these two compounds are quite distinct at activity level concerning their therapeutic applications. VLB is mainly used in the treatment of Hodgkin's disease, bladder and breast cancers, and VCR presents a higher reactivity, being used in a broader range of cancers, especially in the treatment of leukaemia, sarcomas, carcinomas, non-Hodgkin's lymphomas, etc. (Kingston, 2009; Sottomayor and Ros Barceló, 2006; Pollier et al., 2011). However, the high reactivity of VCR also results in more serious secondary effects, especially at the neurotoxic level.

The cytostatic effect of the Vinca alkaloids is due to inhibition of cell mitosis as a result from binding to tubulin and inducing tubulin self-association into spiral aggregates,

at the expense of microtubule growth. As a consequence, microtubule polymerization is deeply disturbed, impairing mitotic spindle organization in metaphase of the rapidly dividing cancer cells. This inhibits their malignant capacity of division and eventually leads to their death by apoptosis (van der Heijden et al., 2004; Gigant et al., 2005; Sottomayor and Ros Barceló, 2006; Loyola-Vargas et al., 2007).
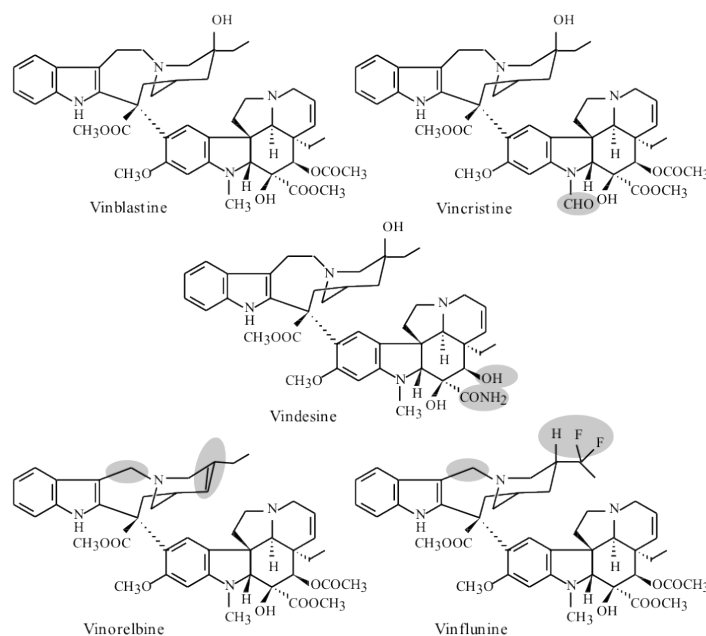
Figure 3. Structure of natural and semi synthetic Vinca alkaloids. Shaded areas indicate the structural differences from vinblastine.

Although many years have gone by since the 1960s, when VCR and VLB were first used in clinical chemotherapy, and in spite of the development of many new synthetic anticancer drugs, VLB and VCR still hold an important position in the treatment of cancer nowadays. Moreover, several semi-synthetic derivative drugs were developed, including vindesine, vinolrebine and vinflunine, which are also used in clinical chemotherapy (Fig.3). Vinolrebine was launched in 1989 for the treatment of non-metastatic breast cancer and non-small cell lung cancer (NSCLC) (Guéritte and Fahy, 2005). Initially, it was obtained from the conversion of vinblastine, but industrially it is now obtained from the plant monomeric precursors of VLB, catharanthine and vindoline (Mano, 2006). Vinflunine is a dihydrodifluoro derivative of vinolrebine that differs from VLB and vinorelbine in the way it interacts with tubulin. Likewise, vinflunine is being tested with success in a broader range of cancers, not only bladder cancer and NSCLC, but also hormone refractory prostate cancer, ovarian cancer and metastatic breast cancer (Bennouna et al., 2005). For all that, vinflunine is considered one of the most promising molecules originated from the Vinca alkaloids. Vindesine, one of the first Vinca

derivatives to be produced, has been recently introduced in the market as a high activity drug for lymphoid leukemia in children (Junaid Aslam et al., 2010).

1.4 Terpenoid indole alkaloids

When the chemical structure of VLB and VCR was resolved, it was discovered that they were dimeric terpenoid indole alkaloids, composed of two similar units, each containing a monoterpenoid and an indole moiety (Fig. 4). Terpenoid indole alkaloids (TIAs) were subsequently found to compose a large and structurally diverse group of alkaloids, including, once more, many constituents with pharmaceutical activity (Pollier et al., 2011). Among the ~2000 different TIAs isolated to date, many valuable bioactive molecules can be found, apart the anticancer VLB and VCR from *C. roseus*. Isolated from *Rauwolfia,* reserpine was used as an antihypertensive and antipsychotic before being abandoned by more recent drugs, ajmaline is used as an antiarrhythmic, yohimbine is a psychoactive drug used as stimulant and aphrodisiac, with its hydrochloride form used to treat erectile dysfunction, and ajmalicine is used in the treatment of hypertension (Drewes et al., 2003; Pollier et al., 2011*)*. Camptothecin, extracted from *Camptotheca acuminate,* and their derivatives topotecan hydrochloride and irinotecan hydrochloride are used in cancer therapy (Thomas et al., 2004). Quinine, extracted from *Cinchona* tree, is used as antipyretic, analgesic and is still the preferential drug used against malaria (Pollier et al., 2011). Conolidine, first extracted from *Tabernaemontana divaricate,* but common to the gender *Tabernaemontana,* was recently proved to have powerful analgesic properties and is believed to become a potential alternative to the known opiates as pain killer, without the side effects of these compounds (Tarselli et al., 2011). In spite of the diversity of pharmaceutical applications of TIAs, most of their actions are actually at the level of the nervous system, namely because of the similarity of TIAs structure with serotonin, resulting in interaction with serotonin receptors (Kochanowska-Karamyan and Hamann, 2010).

For the plant, TIAs are thought to be involved in defence responses, with a number of reports showing that physiological concentrations of TIAs can have antifeeding activity or can inhibit the growth of insect larvae, fungi and microbes (Aerts et al., 1991; Aerts et al., 1992; Luijendijk et al., 1996; Guirimand et al., 2010). As detailed below in secions 1.4.2, the TIA pathway is significantly induced by yeast elicitors and jasmonates, which supports an anti-fungal and anti-herbivore role. Moreover, the TIA strictosidine has been proposed to be involved in an ingenious inducible mechanism, a "nuclear time bomb", acting to protect the plant against herbivores (section 1.4.3). Most TIAs are produced by dicotyledones and are almost restricted to three plant families belonging to the order Gentianales - the Apocynaceae, Loganiaceae and Rubiaceae, with some species of

Nyssaceae also accumulating TIAs (Memelink and Gantet 2007).
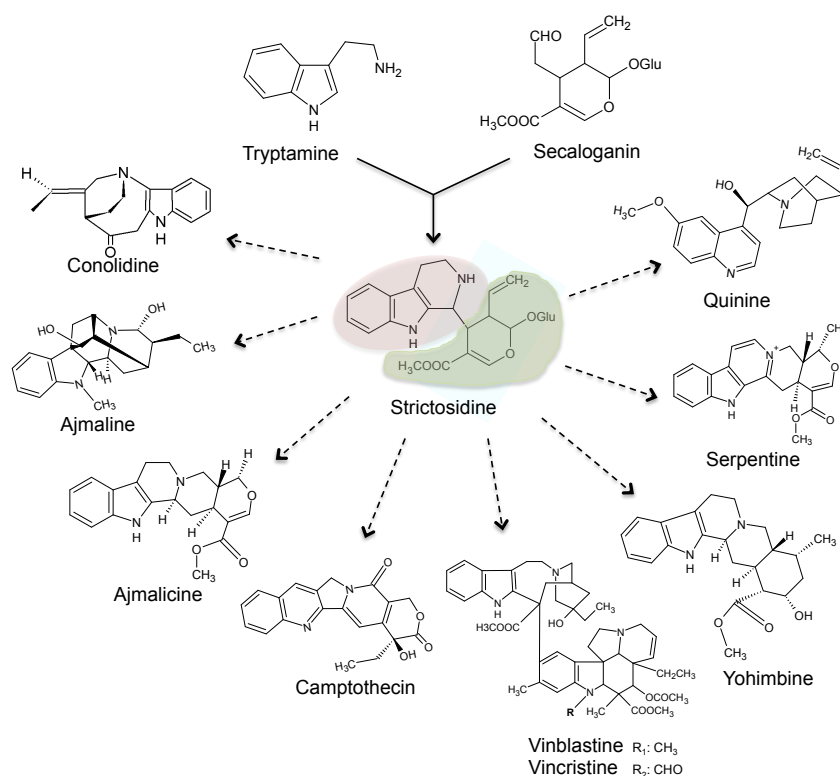
Figure 4. Chemical structure of TIAs with important pharmaceutical activity and of the common precursor of all TIAs, strictosidine. Highlighted in red is the indole moiety of strictosidine, resulting from the indole precursor tryptamine, and highlighted in green is the terpenoid moiety of strictosidine, resulting from the terpenoid precursor secaloganin. Solid arrow's represent single reactions. Dashed arrows represent multiple reactions.

1.4.1 Biosynthesis of terpenoid indole alkaloids in *C. roseus*

In *C. roseus*, as in all characterized plants producing TIAs, strictosidine is the first stone of the TIA pathway and the common precursor of all known TIAs (Fig. 5). Strictosidine is the result of a Pictet-Spengler coupling reaction of the monoamine alkaloid tryptamine, providing the indole moiety, with the monoterpene secologanin, providing the terpenoid moiety (O'Connor and Maresh, 2006). This coupling requires the combination of two metabolic pathways, the 2-*C*-methyl-D-erythritol 4-phospate pathway (MEP) through secaloganin, and the shikimate pathway through tryptamine (Fig. 5; van der Heijden et al., 2004; O'Connor and Maresh, 2006).

The shikimate pathway links carbohydrate metabolism, through the intermediates phosphoenolpyruvate and erythorose 4-phosphate, with the biosynthesis of aromatic aminoacids, phenylalanine, tyrosine and tryptophan, which function as precursors of many secondary metabolism pathways (Liu et al., 2007). Those two carbohydrate intermediates are converted into chorismate by a sequence of seven metabolic steps (Roberts et al., 1998), and the subsequent biosynthesis of tryptophan involves a number

FCUP | 29

Unravelling the metabolism and transmembrane transport of the highly valuable medicinal alkaloids from *Catharanthus roseus*

of steps for which one enzyme has been identified and characterized so far - anthranilate synthase (AS), responsible to convert chorismate into anthranilate, in a reaction downregulated by tryptophan (O'Connor and Maresh, 2006; Loyola-Vargas et al., 2007). The subsequent conversion of anthranilate into tryptophan remains unclear (Liu et al., 2007). Tryptophan is converted into tryptamine by the well characterized enzyme tryptophan decarboxylase (TDC), in a reaction that constitutes the switchover of primary metabolism (tryptophan) to secondary metabolism, with the production of the first indole alkaloid tryptamine (Loyola-Vargas et al., 2007; Verma et al., 2012).

The pathway that leads to the production of secaloganin (monoterpene secoiridoid pathway) involves seven putative enzymatic reactions starting with the monoterpene geraniol (Fig. 5). The first enzyme to be identified and characterized in this pathway was geraniol 10-hydroxylase (G10H), a cytochrome P450 monoxygenase (P450) enzyme that needs a P450 reductase to be active (Zhao and Verpoorte, 2007). The conversion of 10-hydroxygeraniol into loganin involves reactions of hemiacetylation, oxidation, glucosylation, hydroxylation and esterification, but the exact sequence of these enzymatic steps is not known (Giddings, 2011). A 10-hydroxygeraniol oxidoreductase (10HGO) activity has been detected, but the enzyme has not been characterized in *C. roseus* (Mahroug et al., 2007). Loganic acid O-methyltransferase (LAMT) catalyzes the penultimate step of this pathway and the last step is performed by another P450, secaloganin synthase (SLS) (Loyola-Vargas et al., 2007; Murata et al., 2008).

The coupling reaction of the indole alkaloid tryptamine with the monoterpenoid secaloganin is catalyzed by the enzyme strictosidine synthase (STR), constituting the first committed step of TIA biosynthesis (Fig. 5). From strictosidine, over 130 TIAs are produced in *C. roseus*, following different and complex pathways involving several specific / unspecific enzymatic reactions or spontaneous chemical reactions (Memelink et al., 2001). Due to the high diversity and complexity of these pathways, in most cases the enzymes involved are still unknown (Pollier et al., 2011).
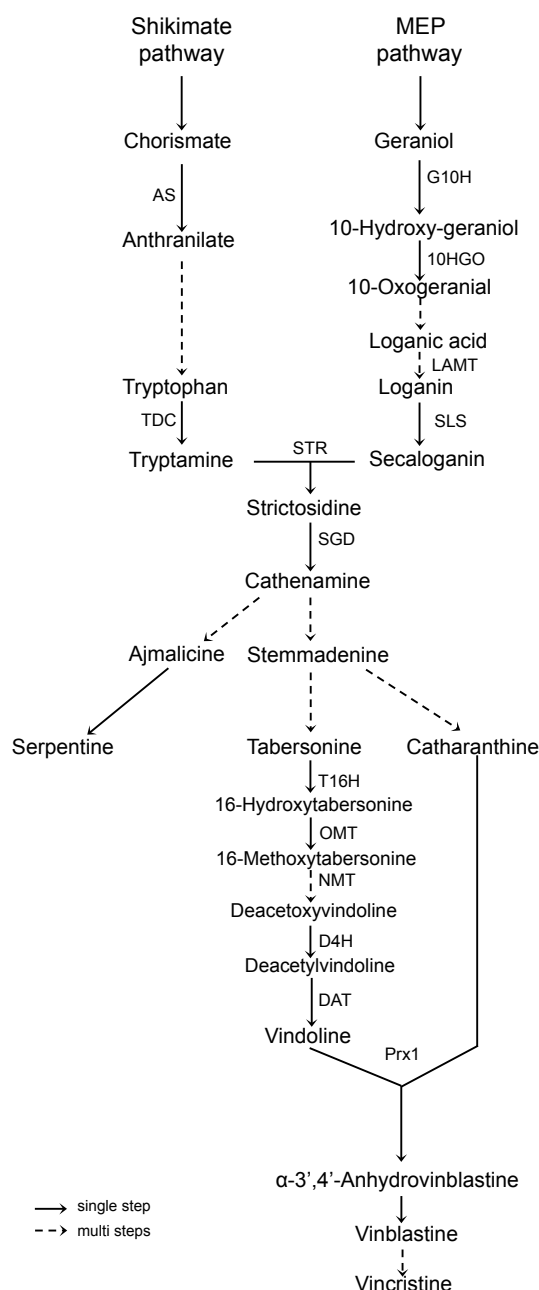
Figure 5. The TIA biosynthetic pathway in *C. roseus*. AS, anthranilate synthase; TDC, tryptophan decarboxylase; G10H, geraniol 10-hydroxilase; CPR, cytochrome P450-reductase; 10HGO, 10-hydroxygeraniol oxidoreductase; LAMT – loganic acid methyltransferase; SLS, secologanin synthase; STR - strictosidine synthase, SGD - strictosidine β-D-glucosidase, T16H - tabersonine 16-hydroxylase, OMT – 16-hydoxytabersonine 16-*O*-methyltransferase, NMT - *N*-methyltransferase, D4H - desacetoxyvindoline 4-hydroxylase, DAT - deacetylvindoline 4-*O*-acetyltransferase, Prx1 – peroxidase 1.

Strictosidine is deglucosylated by strictosidine β-D-glucosidase (SGD) to generate an unstable aglycon, that is rapidly converted into a dialdehyde intermediate and further into cathenamine (Fig. 5; Gomez et al., 2009; Guirimand et al., 2010). After cathenamine, the pathway eventually splits into different branches (Fig. 5). One of the branches leads to the production of ajmalicine, which is oxidized to serpentine, in a reaction proposed to be catalyzed by class III peroxidases (Sottomayor et al., 2004). Another two branches lead to the production of two important monomeric alkaloids,

vindoline and catharanthine, which are the leaf abundant monomeric precursors of VLB and VCR. The pathway to catharanthine remains uncharacterized, and the difficulty in the identification not only of the involved enzymes but even of the intermediates, suggest the possibility that most of these reaction intermediates may be unstable, spontaneous and/or highly toxic, and so rapidly converted to the final product catharanthine, which is significantly sequestered in the vacuole (Carqueijeiro et al., 2013). On the other hand, 5 out of the 6 last steps in the biosynthesis of vindoline were characterized (Fig. 5), namely the enzymes and genes of tabersonine 16-hydroxylase (T16H), 16-hydroxytabersonine 16-*O*-methyltransferase (OMT), N-methyltransferase (NMT), desacetoxyvindoline 4-hydroxylase (D4H) and deacetylvindoline 4-O-acetyltransferase (DAT). The only missing step is the hydration of 16-methoxytabersonine to 16-methoxy-2,3-dihydro-3-hydroxytabersonine, prior to methylation by NMT to form desacetoxyvindoline (Dethier and Deluca, 1993; Loyola-Vargas et al., 2007; Mahroug et al., 2007; Giddings et al. 2011).

Vindoline and catharanthine are coupled to form the first dimeric TIA, α-3',4'-anhydrovinblastine (AVLB), which is the common precursor of all dimeric TIAs in *C. roseus*, including the anticancer VLB and VCR (Fig. 6). Since early studies on the biosynthesis of VLB that the dimerization reaction attracted much attention due to its regulatory importance and potential application for the semi-synthetic production of the dimeric TIAs. In fact, the industrial production of the semi-synthetic Vinca alkaloids vinorelbine and vinflunine involves the chemical synthesis of AVLB from the plant extracted catharanthine and vindoline (Fig. 6), in a process with the production of toxic pollutants and high energy costs. The plant enzyme may therefore enable an attractive biotransformation alternative. The search for the dimerization enzyme in leaf tissue detected a single dimerization activity credited to the single class III plant peroxidase present in the leaves of the plant, in a study performed in our lab. The enzyme was purified to homogeneity, the correspondent gene was cloned, and a channeling mechanism was proposed for the peroxidase-mediated vacuolar synthesis of AVLB (Sottomayor et al., 1996; Sottomayor et al., 1998; Sottomayor and Barcelo, 2003; Costa et al., 2008). Finally, the biosynthetic steps from AVLB to the anticancer alkaloids VCR and VLB are still uncharacterized.
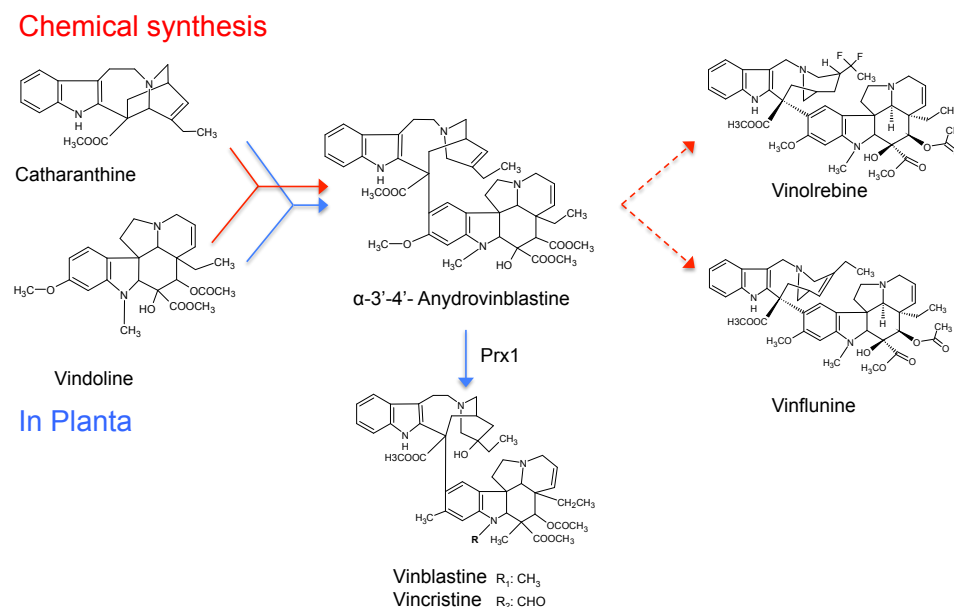
Figure 6. Coupling reaction of catharanthine and vindoline to yield AVLB. In planta AVLB is hydroxylated to VLB and then oxidised to VCR (blue pathway). During chemical synthesis AVLB is converted to the semi-synthetic vinolrebine and vinflunine (red pathway).

1.4.2 Regulation of the terpenoid indole alkaloid pathway in *C. roseus*

In *C. roseus,* the TIA biosynthetic pathway involves a high number of catalytic steps mediated by enzymes working under a strict molecular regulation. One of the most striking characteristics of the TIA pathway is the complex organ / tissue / cell-specific regulation that it presents, which is described in detail in section 1.4.4. The majority of the genes codifying TIA biosynthetic enzymes are also under developmental regulation, being expressed quite early during development, as both vindoline and catharanthine are accumulated a few days after germination (Vazquez-Flota et al., 1997; De Luca and St Pierre, 2000). In the developing seedlings, the enzymes TDC and STR are expressed 36-48h prior to D4H and DAT, whose developmental expression, together with vindoline accumulation, is totally dependent on the presence of light, and is restricted to the aerial parts of the plant. It was also observed that, during leaf development, the concentration of catharanthine and vindoline decreases concomitant with an increase in the levels of their coupling product, AVLB (Naaranlahti et al., 1991; Costa et al., 2008).

The study of the enzyme TDC (converts tryptophan into tryptamine; Fig. 5) has received special attention due to the fact that this enzyme is in the intersection between primary and secondary metabolism, suggesting it could be crucial to regulate the metabolic flux of the TIA pathway (Zhao and Verpoorte, 2007). In *C. roseus,* TDC is encoded by a single gene that has been shown to suffer developmental and inducible regulation (Eilert et al., 1987; Deluca et al., 1989; Goddijn et al., 1992; Pasquali et al., 1992). Intensive research showed that this enzyme is regulated by abiotic stresses such

as UV, and biotic stresses including treatment with yeast elicitors and jasmonates (Zhao and Verpoorte, 2007). However, the overexpression of TDC in *C. roseus* hairy roots or crown gall calluses did not result in increasing levels of tryptamine or other TIAs, and the dimeric TIAs were not detected in the roots (Goddijn et al., 1995; Hong et al., 2006).

TDC and STR have been shown to be often co-regulated, namely after auxin starvation, exposure to fungal elicitors and treatment with methyl jasmonate (MeJA) of cell suspension cultures (Goddijn et al., 1992; Pasquali et al., 1992; Roewer et al., 1992; Menke et al., 1999). In leaves, TDC and STR are also co-induced by a UV-B light pulse (Ouwerkerk and Memelink, 1999). On the other hand, D4H and DAT were shown to be induced by MeJA in cell cultures, indicating that this signal regulates both the early and the late TIA pathway (Van Der Fits and Memelink, 2000). Moreover, its has been shown that the induction of TDC and STR expression in response to yeast elicitors depends partially on jasmonates as a secondary signal (Menke et al., 1999).

According to Memelink and Gantet (2007), the major mechanism regulating alkaloid production in plant cells is the transcriptional control of the biosynthetic genes, which are regulated in a coordinate manner in response to developmental and environmental signals by specific transcription factors (TFs). Understanding the transcriptional regulation of a pathway may be extremely important, considering that this knowledge conveys a powerful tool for the manipulation of the pathway aiming at obtaining higher yields of its metabolites. This is particularly relevant for the TIA pathway in *C. roseus,* since the anticancer VLB and VCR are present in extremely low levels in the leaves of the plant. In fact, for pharmaceutical production, approximately half a ton of dry leaves is used to obtain 1 g of VLB (Noble, 1990). A good example of the power of TFs to manipulate a secondary metabolic pathway was the transformation of *Solanum lycopersicum* with two TFs that constitute true master switches of the anthocyanin pathway, inducing the expression not only of many biosynthetic genes, but also of genes codifying anthocyanin transporters (Butelli et al., 2008). It is conceivable that a similar architectural organization of the TIA pathway in *C. roseus* may exist.

To date, a number of genes encoding *C. roseus* transcriptional regulators of the TIA pathway have been isolated and characterized, including the TFs ORCA2, ORCA3, CrBPF1, CrWRKY1, CrMYC1 and CrMYC2, and the repressors ZCT1, ZCT2 and ZCT3 (Memelink and Gantet, 2007; Suttipanta et al., 2011). All these TFs respond in some way to jasmonic acid (JA), MeJA, and / or yeast elicitors. Both induction pathways may in fact intersect, as elicitors can induce JA / MeJA production.

A *cis*-acting element involved in JA and elicitor responses (jasmonate and elicitor responsive element, JERE) was identified in the promoter region of the STR gene, close to the TATA box (Menke et al., 1999; van der Fits and Memelink, 2001b). By using the

JERE element as bait in yeast one hybrid screening, two members of the AP2/ERF family of transcription factors were isolated and named ORCA1 and ORCA2 (octadecanoid-responsive Catharanthus AP2/ERF-domain). These two TFs bind to the JERE element of the STR promotor, and while ORCA2 responds to MeJA and elicitors, ORCA1 does not (van der Fits et al., 2001; van der Fits and Memelink, 2001b). ORCA3 is also an AP2/ERF TF that responds to JA and binds to the JERE element in the STR promoter, and overexpression studies in cell cultures resulted in increasing levels of AS, CPR, SLS, TDC, STR, and D4H (Fig. 5; van der Fits and Memelink, 2001b; Suttipanta, 2011b). However, both G10H and DAT did not respond to ORCA3, suggesting the involvement of other TFs inducible by JA (Memelink et al., 2001). Although ORCA3 plays an important role in regulating TIA biosynthesis, it is not sufficient by itself to regulate the complete pathway and increase the levels of TIAs.

The use of another JA- and elicitor-responsive region of the STR promoter as bait in a yeast one-hybrid screen resulted in the isolation of a MYB-like TF (CrBPF1), whose accumulation is induced by elicitor but not by MeJA, suggesting that elicitor induces STR gene expression via JA-dependent and independent pathways (Van Der Fits and Memelink, 2000). Another TF, CrMYC1, was isolated from *C. roseus* and characterized as a basic helix-loop-helix (bHLH) TF induced by fungal elicitor and MeJA, suggesting that CrMYC1 may be involved in the regulation of gene expression in response to these signals (Chatel et al., 2003).

Using an elicitor-responsive region of the TDC promoter in a yeast one hybrid screening, three members of the Cys2/His2-type zinc finger gene family were identified, ZCT1, ZCT2 and ZCT3 (Pauw et al., 2004). These proteins bind in a sequence-specific manner to the TDC and STR promoters in vitro and repress the activity of these promoters in trans-activation assays. In what concerns binding to the STR promoter, the ZCT proteins can repress the activating effect of the ORCAs without competing for the same binding sites. Curiously, the expression of ZCTs was induced by MeJA and yeast extracts, similarly to what happens with the ORCA activators. This paradox of the induction of both activators and repressors of STR and TDC gene expression by elicitor and MeJA was suggested by the authors to serve to fine tune the amplitude and timing of gene expression.

More recently, another bHLH TF, CrMYC2, was shown to be involved in the MeJA induction of TIA biosynthetic genes (Zhang et al., 2011). Knock-down of the CrMYC2 expression level caused a strong reduction in the level of MeJA-responsive ORCA3 and ORCA2 mRNA accumulation. Overall, the results showed that the MeJA-responsive expression of TIA biosynthesis genes in *C. roseus* is controlled by a TF cascade consisting of CrMYC2 regulating the expression of ORCA genes, which, in turn, regulate

FCUP 35

Unravelling the metabolism and transmembrane transport of the highly valuable medicinal alkaloids from *Catharanthus roseus*

a subset of TIA biosynthesis genes.

Finally a WRKY TF, CrWRKY1, was shown to up-regulate TDC, ZCT1, ZCT2, and ZCT3, and to repress the transcriptional activators ORCA2, ORCA3, and CrMYC2, resulting in up to 3-fold higher levels of serpentine in hairy roots (Suttipanta et al., 2011). It was proposed that CrWRKY1 may play a key role in determining the root-specific accumulation of serpentine in *C. roseus* plants.

In spite of the intense study of the events regulating the TIA pathway in *C. roseus*, it was not possible, to date, to isolate TFs leading to an increase of the levels of the anticancer TIAs, possibly because idioblast-specific TFs regulating the late, bottleneck part of the pathway were never identified (Memelink and Gantet, 2007; Zhang et al., 2011).

1.4.3 Sub-cellular compartmentation of the terpenoid indole alkaloid pathway in *C. roseus*

Studies of subcellular enzyme localization have shown that secondary metabolism takes place at quite different compartments inside plant cells, revealing a complex organization. In *C. roseus,* the spatial sequestration of several of the characterized enzymes of the pathway has been investigated and suggests the involvement of at least 4 different cell compartments, including the chloroplast, the cytosol, the nucleus and the vacuole (Guirimand et al., 2010; Guirimand et al., 2011a; Guirimand et al., 2011b). A summary of known and hypothetical localizations of the TIA enzymes in *C. roseus* plant cells is shown in fig. 7.

The shikimate pathway and the biosynthesis of tryptophan takes place in the chloroplast, as well as the MEP pathway leading to geraniol (Mahroug et al., 2007). TDC was shown to occur in the cytosol (De luca and Cutler, 1987), and G10H was initially reported to be localized in provacuole membranes (Madyastha et al., 1977), but recent work has indicated an ER membrane localization (Loyola-Vargas et al., 2007; Guirimand et al., 2009; Guirimand et al., 2011a). Recently, Guirimand et al. (2011a). demonstrated that LAMT and TDC form homodimers in the cytosol, preventing their passive diffusion to the nucleus, and that SLS is anchored to the cytosolic face of the ER membranes. Consequently, secologanin and tryptamine must be transported to the vacuole to become available to STR, which has been shown to be localized in the vacuole by cytochemical, density gradient and GFP imaging approaches (Mahroug et al., 2007; Guirimand et al., 2010).

Figure 7. Sub-cellular compartmentation of the TIA pathway in *C. roseus* leaves. RER - rough endoplasmatic reticulum, G10H - geraniol 10-hydroxylase, SLS - secologanin synthase, TDC - tryptophan decarboxylase, STR - strictosidine synthase, SGD - strictosidine β-D-glucosidade, T16H - tabersonine 16-hydroxylase, OMT - 16-hydoxytabersonine 16-*O*-methyltransferase; NMT - *N*-methyltransferase, D4H - desacetoxy vindoline 4-hydroxylase, DAT - deacetylvindoline 4-*O*-acetyltransferase; PRX– peroxidase .

The following enzyme of the pathway, SGD, was shown to accumulate as highly stable supramolecular aggregates within the nucleus and it was proposed that strictosidine is transported out of the vacuole to suffer deglucosylation in the nucleus (Guirimand et al., 2010). Interestingly, the same work shows that strictosidine levels are 10 fold induced by hormonal treatments mimicking insect attack, and that the strictosidine deglucosylation products are specifically responsible for in vitro protein cross-linking and precipitation. Therefore, the authors propose that the vacuolar strictosidine / nuclear SGD constitute a "nuclear time bomb" leading to activation of strictosidine into herbivore deterrent aglycons, upon enzyme-substrate reunion resulting from cell damage during herbivore feeding.

The next reactions of the TIA pathway towards vindoline and catharanthine are quite poorly characterized even at the intermediates level, and nothing is known about their subcellular localization. For the 5 out of 6 last steps of vindoline biosynthesis that have been characterized (Fig. 5), the subcellular localization of some of the enzymes has

been investigated. T16H, as expected being a P450, was shown to be anchored to the ER membrane, and OMT was shown to homodimerize in the cytosol, allowing its exclusion from the nucleus and thus facilitating the uptake of the T16H conversion product. However, no T16H/OMT interactions were found using bimolecular fluorescence complementation assays and yeast two-hybrid analysis (Schröder et al., 1999; St-Pierre et al., 1999; Guirimand et al., 2011b). The following enzyme, NMT, has been proposed to be plastidic, and D4H and DAT were shown to operate as monomers that reside in the nucleocytosolic compartment (De luca and Cutler, 1987; Guirimand et al., 2011b).

At this stage, vindoline and catharanthine are supposed to be transported to the vacuole again, where the vacuolar CrPrx1 is thought to mediate their coupling to yield AVLB, the direct precursor of VLB and VCR (Costa et al., 2008). Likely, it is possible that the hydroxylation of AVLB into VLB and its subsequent oxidation to VCR may happen within the vacuole.

A corollary of all the complex subcellular compartmentation observed for the TIA pathway is the existence of multiple steps of transmembrane transport of TIA intermediates (Fig. 7), namely in opposite direction across the same membrane, which must be very important for the metabolic fluxes of the pathway and will certainly be mediated by totally uncharacterized transporter proteins.

1.4.4 Organ, tissue and cell compartmentation of the terpenoid indole alkaloid pathway in *C. roseus*

The expression of different branches and stretches of the TIA pathway present organ, tissue and cell specificity. Vindoline catharanthine and AVLB are the main alkaloids present in the aerial parts of the plant, while catharanthine, ajmalicine and serpentine are the major TIAs present in the root, where vindoline is virtually absent (Arens et al., 1978; Westekemper et al., 1980; Deus-Neumann et al., 1987; Balsevich and Bishop, 1989; Naaranlahti et al., 1991; Sottomayor et al., 1998). Moreover, all TIA intermediates from tabersonine to vindoline were only detected in the aerial parts of differentiated *C. roseus* plants and never in roots (Murata and De Luca, 2005). Accordingly, *D4H* and *DAT*, the genes involved in the last two steps of vindoline biosynthesis, are not expressed in roots (Mahroug et al., 2007). Likewise, AVLB, VLB and VCR are only found in the aerial parts of the plant, especially in the leaves. Since catharanthine is present in the root in high levels, the question has been raised whether biosynthesis of catharanthine occurs independently in the leaf, or whether it is produced in the root and then transported to the aerial tissues, as observed for instance with nicotine in tobacco (Facchini and De Luca, 2008). However, this should not be the case

in *C. roseus*, since rootless shoot cultures are capable of producing both catharanthine and vindoline (Hirata et al., 1994).

In C. *roseus* leaves, the biosynthesis of VLB and VCR displays a remarkably elaborated tissue / cell organization, with at least four cell types involved in TIA production, including the parenchyma of internal phloem, epidermis, laticifers and idioblasts (Fig. 8; Mahroug et al., 2007; Guirimand et al., 2011a; Guirimand et al., 2011b). In order to better understand this complex organization, it must be clarified that *C. roseus* has simple, elliptical mesomorphic leaves (Fig. 1), with a typical anatomical organization including a single layer of elongated palisade parenchyma on the adaxial side, and a thicker multicellular spongy parenchyma on the abaxial side of the leaf, bordered by an upper and lower epidermis composed of thin-walled cells arranged in a single layer. In addition, *C. roseus* leaves also contain unbranched, nonarticulated laticifers associated with the veins, and idioblast cells dispersed along the palisade and spongy mesophyll (Fig. 8). Idioblasts are identified by their distinctive blue autofluorescence and by their larger size and lower chloroplast content than the surrounding mesophyll cells. TIAs have been seen to accumulate preferentially in laticifers and idioblasts, these being apparently enriched in vindoline and catharanthine, relative to other mesophyll cells, and presenting also a lower vacuolar pH as illustrated by their staining with neutral red (Yoder and Mahlberg, 1976; Mersey and Cutler, 1986). The strong blue fluorescence of laticifers and idioblasts has been credited to the TIA serpentine (Brown et al., 1984).

In a seminal report, St-Pierre et al. (1999) showed by in situ RNA hybridization and immunocytochemistry that TDC and STR1 are localized in the epidermis of stems, leaves and flower buds, whereas in roots, they appear in most protoderm and cortical cells around the apical tip meristem. D4H and DAT were associated with laticifers and idioblast cells of leaves, stems and flower buds. Subsequently, it was shown that the genes involved in the biosynthesis of the terpenoid precursor of TIAs (MEP pathway genes and G10H) are expressed in the internal (adaxial) phloem parenchyma of young aerial organs and that SLS is expressed in the epidermis (Irmler et al., 2000; Burlat et al., 2004). Murata and De Luca (2005) isolated *C. roseus* leaf cell types by laser-capture microdissection and showed that G10H, SLS, TDC, STR SGD and T16H were all detected preferentially in epidermal cells, showing that such a late step as the hydroxylation of tabesonine is also expressed in this cell type. Moreover, this work showed that epidermis-enriched leaf extracts did not contain vindoline or catharanthine, but were enriched in tabersonine, 16-methoxytabersonine and 16-hydroxytabersonine-16-*O*-methyltransferase, also placing OMT at the epidermis. More recently, Murata et al. (2008) identified the presence of LAMT in isolated epidermis of *C. roseus* leaf cells, a

localization confirmed by Guirimand et al. (2011a) using RNA in situ hybridization. The same group confirmed the localization of OMT in the epidermis by RNA in situ hybridization (Guirimand et al., 2011b).
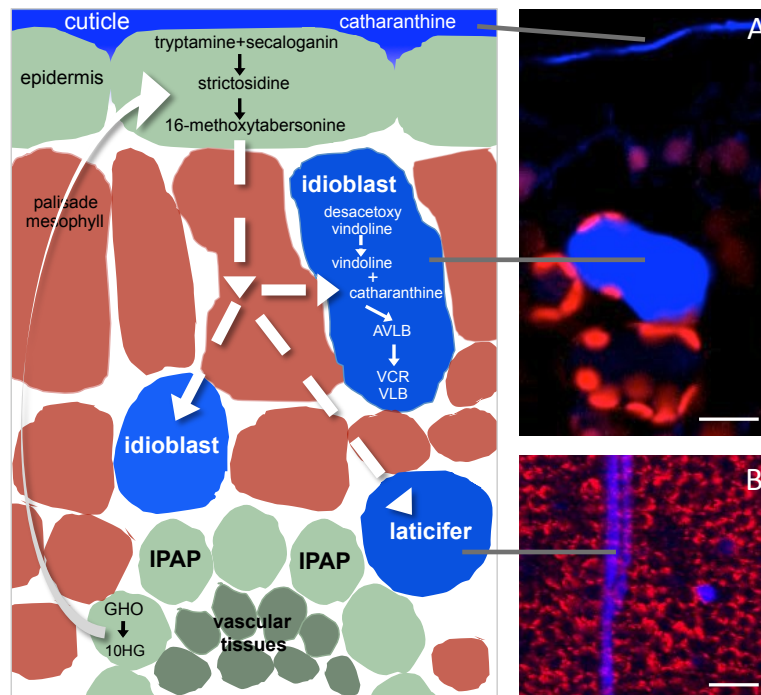
Figure 8. A predicted model for the multicellular compartmentation of the TIA pathway in *C. roseus* leaves (adapted from Facchini and De Luca, 2008), showing on the right idioblast and laticifer cells observed under the epifluorescence microscope. A, Epifluorescence microscopy image of a spongy parenchyma idioblast cell in a leaf cross section. B, Confocal microscopy tangential section of the palisade parenchyma showing two lacticifers and one idioblast. Red corresponds to chloroplast autofluorescence and blue fluorescence reveals alkaloid accumulating cells. IPAP - internal phloem associated parenchyma. G – geraniol, 10HGO – 10-hydroxygeraniol, AVLB – α-3',4'-anhydrovinblastine, VLB – vinblastine, VCR – vincristine. Scale bar - 20 μm in A and 100 μm in B.

In summary, the initial biosynthesis of the terpenoid precursor of TIAs takes place in the internal phloem parenchyma of leaves, the biosynthesis of the indole precursor tryptamine, the terpenoid precursor secologanin, and all TIA intermediates until at least 16-hydroxytabersonine-16-*O*-methyltransferase take place in leaf epidermal cells, and the two last steps of vindoline biosynthesis occur in laticifers and idioblast cells (Fig. 8). According to St-Pierre et al. (1999), the unique characteristics of idioblasts cells seem to be fitted to a specific function, sequestering the toxic dimers that could interfere with normal cellular processes. On top of the subcellular organization of the TIA pathway described in the previous section, this multi-cellular complexity adds further transmembrane transport steps to the TIA pathway, increasing the importance of addressing this aspect of TIA metabolism.

1.5 Transmembrane transport of secondary metabolites

The membrane transport of plant secondary metabolites is generally poorly characterized, but is emerging as a newly developing research area, due to their importance to understand metabolite fluxes, and for metabolic engineering aimed at increasing valuable secondary metabolites. As understood in the previous sections, secondary metabolism pathways may be extremely complex and involve many transmembrane transport events, across many different types of cellular rmembranes, about which very little is known. Generally, to achieve their function, such as protection against UV light, herbivores or pathogens, the toxic secondary metabolites are sequestered away of the cytosol, in the vacuole or the apoplast of specific cell types (Sirikantaramas et al., 2008). Moreover, quite often secondary metabolites are transported from source cells to neighboring cells, or even further to other tissues or remote organs, as is the case of the alkaloid nicotine, produced in the root and accumulated in the leaves of tobacco, and of the alkaloid berberine, produced in roots and accumulated in the rhizome of *Coptis japonica* (Shitan et al., 2003; Morita et al., 2009). In *C. roseus*, source cells are the epidermal cells, and the sink cells are idioblast cells (Fig. 8). Such translocations implicate at least three membrane transport events: efflux through the plasma membrane in source cells, influx at the plasma membrane in sink cells, and an additional transport step into the vacuoles, where final accumulation of many secondary metabolites, specially alkaloids is known to happen (Sirikantaramas et al., 2008).

In general, the transmembrane transport of secondary metabolites may be accomplished by one of three groups of mechanisms: i) by primary transport using directly the energy from ATP hydrolysis by means of ATP-binding cassette (ABC) transporters, ii) by secondary transport, where different types of transporters may use a concentration gradient generated by primary pumps to execute transport through a simport or antiport mechanism, and iii) by a variety of trapping mechanisms including ion or conformational trapping and formation of insoluble complexes (Fig.9; (Renaudin, 1989; Blom et al., 1991; Wink, 1993; Rea et al., 1998; Martinoia et al., 2012). There is also increasing evidence of vesicular transport of secondary compounds, namely for delivery to the vacuole of some alkaloids and anthocyanins (Grotewold, 2004; Yazaki, 2006; Poustka et al., 2007).
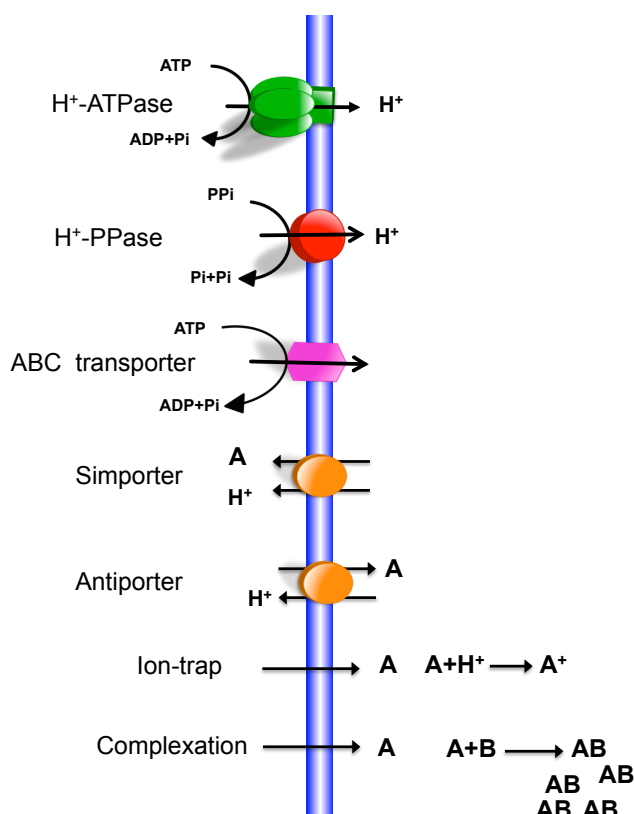
Figure 9. Mechanisms for transmembrane transport of secondary metabolites. Primary pumps exemplified by proton ATPases build a concentration gradient across a membrane that can be used for antiport or simport transport. Acidic compartments will sequester weak bases by an ion trap mechanism, and formation of complexes (AB) may also lead to sequestration. ABC - ATP-binding cassette, ATP - adenosine-5'-triphosphate, PPi – pyrophosphate, A – secondary metabolite.

So far, two main families of transporters have been implicated in the transport of secondary metabolites: ATP-binding cassette (ABC) transporters, using direct energization with ATP, and multidrug and toxic compound extrusion (MATE) transporters acting via an H^+-antiport. A third family of transporters that has also been implicated is the purine uptake permease family (PUP). Fig 10 shows a summary of all plasma membrane and tonoplast transporters identified so far for secondary metabolites. As can be seen, most belong to the ABC and MATE families of transporters, and are discussed below in dedicated sections. Concerning the PUP family, until now, only two were identified: AtPUP3 in Arabidopsis, transporting cytokinins, and NtPUP 1 in tobacco, which has high affinity for nicotine and is expressed in roots, the source organ of this alkaloid (Burkle et al., 2003; Hildreth et al., 2011).
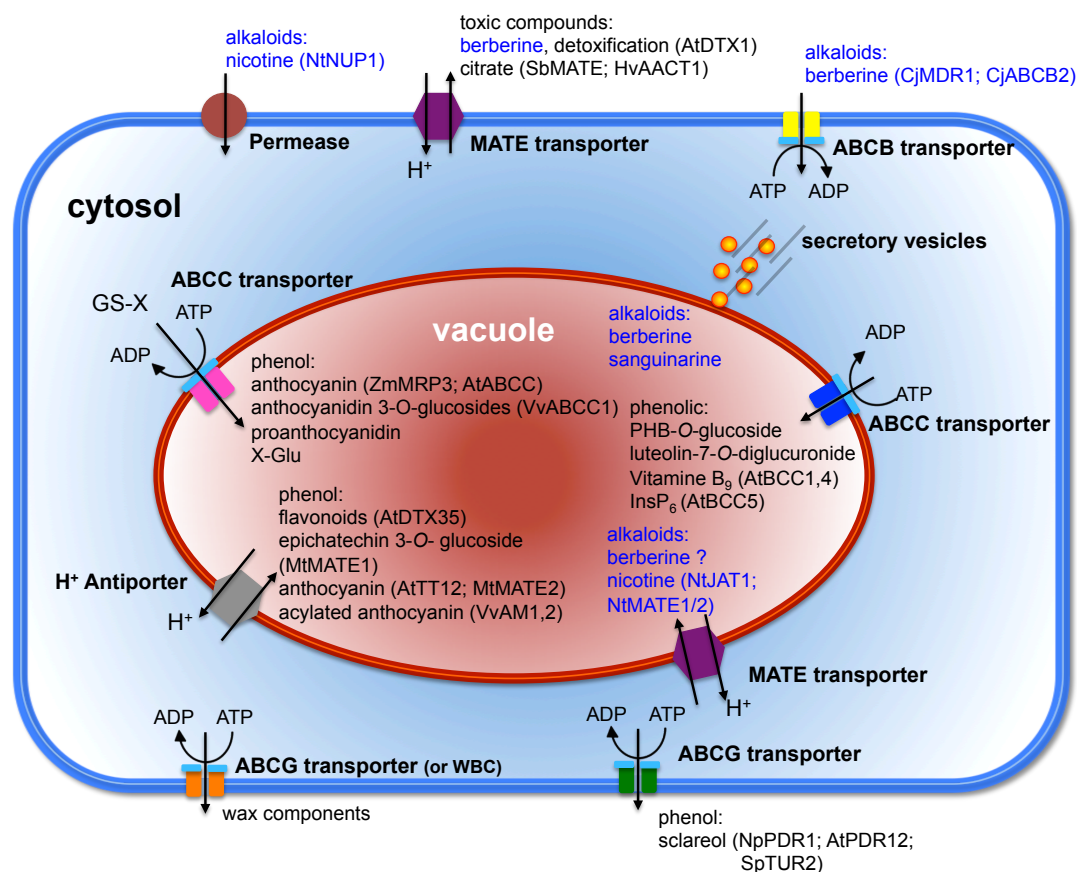
Figure 10. Membrane transporters of secondary metabolites identified in plant cells. Alkaloid substrates are highlighted in blue.

1.5.1 ABC transporters in plants

ABC transporters form a large superfamily of proteins and consist of multi-domain membrane proteins that mediate the transport of a diversity of substrates through direct energization by ATP (Sánchez-Fernández et al., 2001; Yazaki, 2005, 2006). Genome analyses of the model plants Arabidopsis and rice revealed the presence of more than 120 ABC protein genes in both plants, representing more than twice the number of ABC transporters in animals and insects (Yazaki et al., 2009). This diversity is believed to be related with the diversity of secondary metabolism in plants, with many members of this family possibly being involved in the complex compartmentation of this class of metabolites. So far, only a few ABC transporters have been characterized concerning the transported substrate(s) profile. Among the different ABC characterized, a variety of substrates was identified, including terpenoids, auxins, flavones, alkaloids, metal ions, malate, etc. (Klein et al., 2000; Jasinski et al., 2001; Goossens et al., 2003; Shitan et al., 2003; Otani et al., 2005; Terasaka et al., 2005; Rea, 2007) .

Structurally, ABC proteins consist of four subunits (full-size ABCs), with two transmembrane domains (TMD) and two nucleotide-binding domains (NBD) (Higgins,

FCUP 43

Unravelling the metabolism and transmembrane transport of the highly valuable medicinal alkaloids from *Catharanthus roseus*

1992), arranged in the "forward" (TMD-NBD-TMD2-NBD2) or in the "reverse" configuration (NBD-TMD-NBD2-TMD2; Table I). Some ABC transporters have only one TMD and one NBD domain and are called half-size. In plants, the full protein can be encoded by a single gene, or by two genes each coding for a TMD-NBD pair to form hetero- or homo-dimers. From phylogenetic analyses it was concluded that most eukaryotic ABC transporters could be grouped into 8 major subfamilies (from A to H). Members of the H subfamily have not been yet identified in plants (Verrier et al., 2008). Some characteristics of the plant ABC transporter subfamilies are shown in Table I.
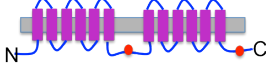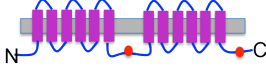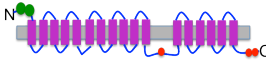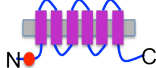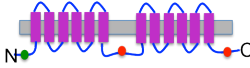
The ABC transporters that have been directly related with the transport of secondary compounds so far, belong to the subfamilies ABCB, ABCC and ABCG. An ABCB or MDR (multidrug resistance) localized at the plasma membrane of rhizome cells from *Coptis japonica* was the first alkaloid transporter identified - CjMDR1 (Shitan et al., 2003). CjMDR1 was shown to mediate the import of the alkaloid berberine into cells of the rhizome, the sink organ of berberine, which is produced in root cells. A second ABCB transporter of berberine was subsequently isolated, *CjABCB2*, which is expected to be a more specific transporter of berberine into the rhizome since it is expressed almost exclusively in this tissue, in contrast to the widely expressed *CjMDR1* (Shitan N, 2012).

All ABCC or MRP (multidrug resistance protein) implicated in the transport of secondary metabolites were localized at the tonoplasts membrane and several are suggested to be involved in the vacuolar sequestration of glucosides and gluthathione conjugates (Bartholomew et al., 2002; Frangne et al., 2002). AtMRP1 to 5, from Arabidopsis, seem to recognize GS-conjugates of secondary compounds, mainly phenolic compounds, like the anthocyanins (Tommasini et al., 1997; Lu et al., 1998; Tommasini et al., 1998). An ABCC transporter (ZmMRP3) was also identified in maize, localized in the tonoplast, and was shown to be essential for anthocyanin accumulation, as proven by the reduction of anthocyanin levels in the *mrp3* mutants (Goodman et al., 2004).

The ABCG transporters or PDR (pleiotropic drug resistance) that were implicated in the transport of secondary metabolites were localized at the plasma membrane and are associated with the cell efflux of substances, namely secretion of the defense terpenoid sclareol by NpPDR1 in *Nicotiana plumbaginifolia*, SpTUR2 in *Sprirodela polyrhiza*, and AtPDR1 in *Arabidopsis thaliana* (Jasinski et al., 2001; van den Brule et al., 2002; Campbell et al., 2003). Uncharacterized ABCG transporters were related with artemisinin yield in *Artemisia annua* (Zhang et al., 2012). ABCG transporters of the subtype WBC (white brown complex) have been associated with the plasma membrane

efflux of lipidic molecules that form cutin and wax layers in the epidermis, namely with the identification of AtWBC12 in Arabidopsis (Pighin et al., 2004).

Table I. Characterization of the main subfamilies of plant ABC transporters

Subfamily	Topology [a]	Remarks
ABCA	N —[TMD-NBD-TMD-NBD]— C	Also known as AOH (full-size) or ATH (half-size).
ABCB	N —[TMD-NBD-TMD-NBD]— C	Also known MDR (full-size), in humans are related to multidrug resistance are related to the mitochondria or the chloroplasts.
ABCC	N —[TMD0-TMD-NBD-TMD-NBD]— C	Also known as MRP. They have an N-terminal extension (green in the figure) called TMD0. The function of the TMD0 in plants is still unknown but probably is involved in protein targeting. Involved in the transport of glutathione conjugates.
ABCD	N —[TMD-NBD]— C	Half-size ABC transporter proteins associated with the peroxisomes.
ABCE, ABCF	N —[NBD-NBD]— C	Soluble proteins, only with NBD domains (in red).
ABCG	N —[NBD-TMD-NBD-TMD]— C	Also known as WBC (half-size) or PDR (full-size). This subfamily is particularly expanded in plants and its functions are highly diverse.

[a] *Adapted from* Rea (2007). Red - nucleotide-binding domains (NBDs), pink – trans membrane domains (TMDs), green - N-terminal extension (TMD0).

1.5.2 MATE transporters in plants

The MATE transporter family in plants is a comparatively large family, with 56 members identified in the Arabidopsis genome. As for ABC transporters, this family is much larger than in other organisms, e.g. the human genome has 2 MATE transporters, a diversity that is also putatively associated with the diversity of plant secondary metabolism. To date, the transport characteristics of only a few plant MATE transporters have been characterized (Moriyama et al., 2008).

MATE transporters are H^+ or Na^+ antiporters, with 9-12 transmembrane helices, and ranging in size from 400 to 700 amino acids. Like ABC transporters, MATE are also associated with the transport of a diversity of molecules, including polyaromatic and cationic substrates, and antibiotics and therapeutic drugs in bacteria and human cells (Omote et al., 2006; Lu et al., 2013).

In tobacco, three MATE transporters were associated with the vacuolar import of the alkaloid nicotine (Morita et al., 2009; Shoji et al., 2009). Nt-JAT1 was shown to be localized in the tonoplast of leaf cells and to function as a proton antiporter recognizing endogenous tobacco alkaloids, such as nicotine and anabasine, and other alkaloids, such as hyoscyamine and berberine, but not flavonoids (Morita et al. 2009). These findings strongly suggest that Nt-JAT1 plays an important role in nicotine accumulation

in the leaf vacuoles of tobacco. NtMATE1 and MtMATE2 were proposed to transport tobacco alkaloids from the cytosol into the vacuole in exchange for protons, in alkaloid-synthesizing root cells of tobacco (Shoji et al., 2009). Otani et al. (2005) showed that the alkaloid berberine is accumulated by a proton antiport mechanism in the vacuoles of high berberine-producing cell cultures of *Coptis japonica*, and already suggested that this transport could be mediated by a MATE transporter, since bacterial and Arabidopsis MATE transporters had been shown to recognize berberine as exogenous substrate.

In Arabidopsis, another MATE, transparent testa 12 (AtTT12), was associated with the vacuolar accumulation of flavonoids, and in *Medicago truncatula*, MtMATE1 was shown to recognize epicatechin 3'-O-glucoside, a precursor of protoanthocyanidins (Marinova et al., 2007; Zhao and Dixon, 2009). Two vacuolar MATE transporters that recognize acylated anthocyanins were still identified in *Vitis vinifera* (Gomez et al., 2009).

Investigation of MATE transporters in plants is in the very beginning, especially considering the high number of genes per plant.

1.5.3 Transmembrane transport of TIAs in *C. roseus*

In the case of the TIA pathway, the intricate subcellular and multicellular compartmentation of the pathway (section 1.4.3 and 1.4.4) predicts at least 7 different transmembrane transport events, of which virtually nothing is known, apart from preliminary work in their vacuolar accumulation mechanisms, during the 1980s. This early work suggested that vacuolar accumulation of TIAs and other alkaloids was mediated either by highly specific carriers (Deus-Neumann and Zenk, 1984, 1986; Wink, 1993) or by an unspecific ion-trap mechanism (Guern et al., 1987; Renaudin, 1989; Blom et al., 1991; Wink, 1993). The ion trap model implies that when several compartments exist, the alkaloid neutral base will diffuse across membranes and will be present at the same concentration in both the cytosol and the vacuole, while the alkaloid cation will remain trapped and will thus accumulate in the more acidic vacuolar compartment. This model was supported by a number of experiments performed mainly with ajmalicine and with some alkaloids not present in *C. roseus* (Guern et al., 1987; Renaudin, 1989; Blom et al., 1991). On the other hand, Deus-Neumann and Zenk (1984) observed that vacuolar uptake of vindoline was very specific for the endogenous TIAs in isolated vacuoles of *C. roseus* suspension cells, and that uptake was saturable and exhibited dependence on pH, indicating mediation by a specific transporter. Guern et al. (1987) tried to reconcile the two opposing concepts by proposing that the ion-trap and carrier models are not necessarily exclusive, but most likely coexist. However, all recent work suggests that alkaloids are accumulated in the vacuoles by a proton antiport, a

mechanism that is confirmed in this thesis for *C. roseus* TIAs (Carqueijeiro et al. 2013; Chapter II), indicating MATE transporters as likely candidates. To date, no TIA membrane transporter has been identified, but, curiously, overexpression of the above mentioned ABC transporter CjMDR1 of *Coptis japonica* in *C. roseus* cell cultures significantly enhanced the accumulation of ajmalicine and tetrahydroalastonine (Pomahacova et al., 2009).

FCUP 47

Unravelling the metabolism and transmembrane transport of the highly valuable medicinal alkaloids from *Catharanthus roseus*

2. MAIN OBJECTIVES OF THE THESIS

C. roseus accumulates in the leaves low levels of the important anticancer terpenoid indole alkaloids (TIAs) vinblastine (VLB) and vincristine (VCR), making of this plant one of the best characterized medicinal plants. However, although much is known about the biosynthesis and regulation of TIAs in *C. roseus*, gene / enzyme characterization is still lacking for many biosynthetic steps, the membrane transport mechanisms of TIAs are basically uncharacterized despite their importance for TIA accumulation, and no effective regulatory master switch of the TIA pathway has been identified to date. Therefore, the primary objectives of this thesis were:

i) to characterize the transmembrane transport mechanism responsible for the accumulation of TIAs in their final sequestration target, the vacuole;

ii) to identify putative candidate genes for a) the missing, bottleneck biosynthetic steps of VLB and VCR, b) the multiple transmembrane transport events of TIA intermediates during VLB biosynthesis, and c) the transcriptional regulation of the late, bottleneck steps of VLB biosynthesis.

In order to achieve these results, leaf isolated vacuoles and tonoplast membranes were used to investigate the vacuolar accumulation mechanism of TIAs, and two omic strategies were implemented to unravel new candidate genes involved in the TIA pathway. The first omic strategy implemented was the characterization of the proteome of the toxic vacuoles of *C. roseus* leaf cells, aiming to identify putative transtonoplast TIA transporters and missing TIA biosynthetic enzymes, at the same time the complexity of biological functions of the vacuoles were further investigated. The second omic strategy involved the optimization of a fluorescence activated cell sorting method for the isolation of specific leaf cells, idioblasts, where the late, bottleneck steps of VLB biosynthesis take place, followed by a differential transcription profiling of idioblasts by cDNA-AFLP. This approach was designed to unravel important candidate genes for the crucial part of the TIA pathway, including related biosynthetic enzymes, transporters and transcriptional regulators. This approach should also contribute to a deeper understanding of the specificities of idioblast cells.

LITERATURE CITED

Aerts RJ, Snoeijer W, Aertsteerlink O, Vandermeijden E, Verpoorte R (1991) Control and biological implications of alkaloid synthesis in Cinchona seedlings. Phytochemistry **30:** 3571-3577

Aerts RJ, Stoker A, Beishuizen M, Jaarsma I, Vandeheuvel M, Vandermeijden E, Verpoorte R (1992) Detrimental effects of Cinhona leaf alkaloids on larvae of the polyphagous insect spodoptera-exigua Journal of Chemical Ecology **18:** 1955-1964

Arens H, Stockigt J, Weiler EW, Zenk MH (1978) Radioimmunoassays for determination of indole alkaloids ajamlicine and serpentine in plants Planta Medica **34:** 37-46

Balsevich J, Bishop G (1989) Convenient preparation of iridodial by reduction of nepetalactone - corroboration for the role of iridodial as an indole alkaloid precursor in a Catharanthus roseus cell suspension Heterocycles **29:** 921-924

Bartholomew DM, Van Dyk DE, Lau SMC, O'Keefe DP, Rea PA, Viitanen PV (2002) Alternate energy-dependent pathways for the vacuolar uptake of glucose and glutathione conjugates. Plant Physiology **130:** 1562-1572

Bennouna J, Campone M, Delord J, Pinel M (2005) Vinflunine: a novel antitubulin agent in solid malignancies. Expert Opinion on Investigational Drugs **14**

Blom TJM, Sierra M, Van Vliet TB, Franke-Van Dijk MEI, De Koning P, Van Iren F, Verpoorte R, Libbenga KR (1991) Uptake and accumulation of ajmalicine into isolated vacuoles of cultured cells of *Catharanthus roseus* (L.) G. Don. and its conversion into serpentine. Planta **183:** 170-177

Bourgaud F, Gravot A, Milesi S, Gontier E (2001) Production of plant secondary metabolites: a historical perspective. Plant Science **161:** 839-851

Brown S, Renaudin JP, Prevot C, Guern J (1984) Flow-cytometry and sorting of plant-protoplasts-technical problems and physiological results from a study of pH and alkaoids in *Catharanthus roseus*. Physiologie Vegetale **22:** 541-554

Burkle L, Cedzich A, Dopke C, Stransky H, Okumoto S, Gillissen B, Kuhn C, Frommer WB (2003) Transport of cytokinins mediated by purine transporters of the PUP family expressed in phloem, hydathodes, and pollen of Arabidopsis. Plant Journal **34:** 13-26

Burlat V, Oudin A, Courtois M, Rideau M, St-Pierre B (2004) Co-expression of three MEP pathway genes and geraniol 10-hydroxylase in internal phloem parenchyma of Catharanthus roseus implicates multicellular translocation of intermediates

FCUP 49

Unravelling the metabolism and transmembrane transport of the highly valuable medicinal alkaloids from *Catharanthus roseus*

during the biosynthesis of monoterpene indole alkaloids and isoprenoid-derived primary metabolites. Plant Journal **38:** 131-141

Butelli E, Titta L, Giorgio M, Mock H-P, Matros A, Peterek S, Schijlen EGWM, Hall RD, Bovy AG, Luo J, Martin C (2008) Enrichment of tomato fruit with health-promoting anthocyanins by expression of select transcription factors. Nature Biotechnology **26:** 7

Campbell EJ, Schenk PM, Kazan K, Penninckx I, Anderson JP, Maclean DJ, Cammue BPA, Ebert PR, Manners JM (2003) Pathogen-responsive expression of a putative ATP-binding cassette transporter gene conferring resistance to the diterpenoid sclareol is regulated by multiple defense signaling pathways in Arabidopsis. Plant Physiology **133:** 1272-1284

Carqueijeiro I, Noronha H, Duarte P, Gerôs HV, Sottomayor M (2013) Vacuolar transport of the medicinal alkaloids from Catharanthus roseus is mediated by a proton driven antiport. Plant Physiology

Chatel G, Montiel G, Pre M, Memelink J, Thiersault M, Saint-Pierre B, Doireau P, Gantet P (2003) CrMYC1, a Catharanthus roseus elicitor- and jasmonate-responsive bHLH transcription factor that binds the G-box element of the strictosidine synthase gene promoter. Journal of Experimental Botany **54:** 2587-2588

Costa MMR, Hilliou F, Duarte P, Pereira LG, Almeida I, Leech M, Memelink J, Barcelo AR, Sottomayor M (2008) Molecular cloning and characterization of a vacuolar class III peroxidase involved in the metabolism of anticancer alkaloids in *Catharanthus roseus*. Plant Physiology **146:** 403-417

De luca V, Cutler AJ (1987) Subcellualr-localization of enzymes involved in indole alkaloid biosynthesis *Catharanthus roseus* Plant Physiology **85:** 1099-1102

De Luca V, St Pierre B (2000) The cell and developmental biology of alkaloid biosynthesis. Trends in Plant Science **5:** 168-173

Deluca V, Marineau C, Brisson N (1989) Molecular cloning and analysis of cDNA encoding a plant tryptophan decarboxylases - comparison with animal dopa decraboxylases Proceedings Of The National Academy Of Sciences Of The United States Of America **86:** 2582-2586

Dethier M, Deluca V (1993) Partial-purification of an N-Methyltransferase involved in vindoline biosynthesis in *Catharanthus roseus*. Phytochemistry **32:** 673-678

Deus-Neumann B, Stöckigt J, Zenk MH (1987) Radioimmunoassay for the Quantitative Determination of Catharanthine. Planta Med **53:** 184-188

Deus-Neumann B, Zenk MH (1984) A highly selective alkaloid uptake system in vacuoles of higher plants. Planta **162:** 250-260

Deus-Neumann B, Zenk MH (1986) Accumulation of alkaloids in plant vacuoles does not involve an ion-trap mechanism. Planta **167:** 44-53

Dewick PM (2009) Medicinal natural products: A biosynthetic approach. John Wiley & Sons, Ltd, West Susex

Drewes SE, George J, Khan F (2003) Recent findings on natural products with erectile-dysfunction activity. Phytochemistry **62:** 1019-1025

Eilert U, Deluca V, Constabel F, Kurz WGW (1987) Elicitor mediated induction of thryptophan deacarboxylase and strictosidine synthase activities in cell suspension cultures of Catharanthus roseus Archives of Biochemistry and Biophysics **254:** 491-497

Facchini PJ (2001) Alkaloid biosynthesis in plants: Biochemistry, cell biology, molecular regulation, and metabolic engineering applications. Annual Review of Plant Physiology and Plant Molecular Biology **52:** 29-66

Facchini PJ, Bird DA, St-Pierre B (2004) Can Arabidopsis make complex alkaloids? Trends in plant science **9:** 116-122

Facchini PJ, De Luca V (2008) Opium poppy and Madagascar periwinkle: Model non-model systems to investigate alkaloid biosynthesis in plants. Plant Journal **54:** 763-784

Frangne N, Eggmann T, Koblischke C, Weissenbock G, Martinoia E, Klein M (2002) Flavone glucoside uptake into barley mesophyll and arabidopsis cell culture vacuoles. Energization occurs by H^+-antiport and ATP-binding cassette-type mechanisms. Plant Physiology **128:** 726-733

Giddings L-A (2011b) Discovery, characterization, and rational design of the enzymes involved in monoterpene indole alkaloid biosynthesis in Madagascar periwinkle. Thesis (Ph. D.). Massachusetts Institute of Technology, Massachusetts Institute of Technology

Gigant B, Wang CG, Ravelli RBG, Roussi F, Steinmetz MO, Curmi PA, Sobel A, Knossow M (2005) Structural basis for the regulation of tubulin by vinblastine. Nature **435:** 519-522

Goddijn OJM, Dekam RJ, Zanetti A, Schilperoort RA, Hoge JHC (1992) Auxin rapidly down regulttes transcription of the tryptophan decarboxylase gene from *Catharanthus roseus* Plant Molecular Biology **18:** 1113-1120

Goddijn OM, Pennings EM, Helm P, Schilperoort R, Verpoorte R, Hoge JH (1995) Overexpression of a tryptophan decarboxylase cDNA inCatharanthus roseus crown gall calluses results in increased tryptamine levels but not in increased terpenoid indole alkaloid production. Transgenic Research **4:** 315-323

Gomez C, Conejero G, Torregrosa L, Cheynier V, Terrier N, Ageorges A (2011) In vivo grapevine anthocyanin transport involves vesicle-mediated trafficking and the contribution of anthoMATE transporters and GST. Plant Journal **67:** 960-970

Gomez C, Terrier N, Torregrosa L, Vialet S, Fournier-Level A, Verries C, Souquet J-M, Mazauric J-P, Klein M, Cheynier V, Ageorges A (2009) Grapevine MATE-Type Proteins Act as Vacuolar H+-Dependent Acylated Anthocyanin Transporters. Plant Physiology **150:** 402-415

Goodman CD, Casati P, Walbot V (2004) A multidrug resistance-associated protein involved in anthocyanin transport in *Zea mays*. Plant Cell **16:** 1812-1826

Goossens A, Häkkinen ST, Laakso I, Oksman-Caldentey K-M, Inzé D (2003) Secretion of Secondary Metabolites by ATP-Binding Cassette Transporters in Plant Cell Suspension Cultures. Plant Physiology **131:** 1161-1164

Grotewold E (2004) The challenges of moving chemicals within and out of cells: insights into the transport of plant natural products. Planta **219:** 906-909

Guéritte F, Fahy J (2005) The Vinca Alkaloids. *In* Anticancer Agents from Natural Products. CRC Press

Guern J, Renaudin JP, Brown SC (1987) The compartmentation of secondary metabolites in plant cell cultures. *In* F Constabel, IK Vasil, eds, Cell culture and somatic cell genetics of plants, Vol 4. Academic Press, San Diego, pp 43-76

Guirimand G, Burlat V, Oudin A, Lanoue A, St-Pierre B, Courdavault V (2009) Optimization of the transient transformation of Catharanthus roseus cells by particle bombardment and its application to the subcellular localization of hydroxymethylbutenyl 4-diphosphate synthase and geraniol 10-hydroxylase. Plant Cell Reports **28:** 1215-1234

Guirimand G, Courdavault V, Lanoue A, Mahroug S, Guihur A, Blanc N, Giglioli-Guivarc'h N, St-Pierre B, Burlat V (2010) Strictosidine activation in Apocynaceae: towards a "nuclear time bomb"? Bmc Plant Biology **10**

Guirimand G, Guihur A, Ginis O, Poutrain P, Héricourt F, Oudin A, Lanoue A, St-Pierre B, Burlat V, Courdavault V (2011a) The subcellular organization of strictosidine biosynthesis in Catharanthus roseus epidermis highlights several trans-tonoplast translocations of intermediate metabolites. FEBS Journal **278:** 749-763

Guirimand G, Guihur A, Poutrain P, Héricourt F, Mahroug S, St-Pierre B, Burlat V, Courdavault V (2011b) Spatial organization of the vindoline biosynthetic pathway in *Catharanthus roseus*. Journal of Plant Physiology **Volume 168:** 549-557

Hanson JR (2003) Naturalproducts: Secondary metabolites. The Royal Society of Chemistry, London

Hartmann T (2007) From waste products to ecochemicals: Fifty years research of plant secondary metabolism. Phytochemistry **68:** 2831-2846

Hegnauer R (1988) Biochemistry, distribution and taxonomic relevance of higher-plant alkaloids. Phytochemistry **27:** 2423-2427

Higgins CF (1992) ABC TRANSPORTERS - FROM MICROORGANISMS TO MAN. Annual Review of Cell Biology **8:** 67-113

Hildreth SB, Gehman EA, Yang H, Lu R-H, Ritesh KC, Harich KC, Yu S, Lin J, Sandoe JL, Okumoto S, Murphy AS, Jelesko JG (2011) Tobacco nicotine uptake permease (NUP1) affects alkaloid metabolism. Proceedings Of The National Academy Of Sciences Of The United States Of America **108:** 18179-18184

Hirata K, Miyamoto K, Miura Y (1994) Catharanthus roseus L. (Periwinkle): Production of Vindoline and Catharanthine in Multiple Shoot Cultures. *In* YPS Bajaj, ed, Medicinal and Aromatic Plants VI, Vol 26. Springer Berlin Heidelberg, pp 46-55

Hong S-B, Peebles CAM, Shanks JV, San K-Y, Gibson SI (2006) Expression of the Arabidopsis feedback-insensitive anthranilate synthase holoenzyme and tryptophan decarboxylase genes in Catharanthus roseus hairy roots. Journal of Biotechnology **122:** 28-38

Irmler S, Schroder G, St-Pierre B, Crouch NP, Hotze M, Schmidt J, Strack D, Matern U, Schroder J (2000) Indole alkaloid biosynthesis in Catharanthus roseus: new enzyme activities and identification of cytochrome P450CYP72A1 as secologanin synthase. Plant Journal **24:** 797-804

Jasinski M, Stukkens Y, Degand H, Purnelle B, Marchand-Brynaert J, Boutry M (2001) A plant plasma membrane ATP binding cassette-type transporter is involved in antifungal terpenoid secretion. Plant Cell **13:** 1095-1107

Junaid Aslam, Sheba Haque Khan, Zahid Hameed Siddiqui, Zohra Fatima, Mehpara Maqsood, Mukthar Ahmad Bhat, Sekh Abdul Nasim, Abdul Ilah, Iffat Zareen Ahmad, Saeed Ahmad Khan, Abdul Mujib, Sharma MP (2010) Catharanthus roseus (L.) G. Don. an important Drug: it's applications and production INTERNATIONAL JOURNAL OF COMPREHENSIVE PHARMACY **1:** 1-16

Kingston DGI (2009) Tubulin-Interactive Natural Products as Anticancer Agents. Journal of Natural Products **72:** 507-515

Klein M, Martinoia E, Hoffmann-Thoma G, Weissenbock G (2000) A membrane-potential dependent ABC-like transporter mediates the vacuolar uptake of rye

FCUP 53

Unravelling the metabolism and transmembrane transport of the highly valuable medicinal alkaloids from *Catharanthus roseus*

flavone glucuronides: regulation of glucuronide uptake by glutathione and its conjugates. Plant Journal **21:** 289-304

Kochanowska-Karamyan AJ, Hamann MT (2010) Marine Indole Alkaloids: Potential New Drug Leads for the Control of Depression and Anxiety. Chemical Reviews **110:** 4489-4497

Li JWH, Vederas JC (2009) Drug Discovery and Natural Products: End of an Era or an Endless Frontier? Science **325:** 161-165

Liu DH, Jin HB, Chen YH, Cui LJ, Ren WW, Gong YF, Tang KX (2007) Terpenoid indole alkaloids biosynthesis and metabolic engineering in Catharanthus roseus. Journal of Integrative Plant Biology **49:** 961-974

Loyola-Vargas VM, Galaz-Ávalos RM, Kú-Cauich R (2007) *Catharanthus* biosynthetic enzymes: the road ahead. Phytochemistry Reviews **6:** 307-339

Lu M, Symersky J, Radchenko M, Koide A, Guo Y, Nie R, Koide S (2013) Structures of a Na+-coupled, substrate-bound MATE multidrug transporter. Proceedings Of The National Academy Of Sciences Of The United States Of America **110:** 2099-2104

Lu YP, Li ZS, Drozdowicz YM, Hortensteiner S, Martinoia E, Rea PA (1998) AtMRP2, an Arabidopsis ATP binding cassette transporter able to transport glutathione S-conjugates and chlorophyll catabolites: Functional comparisons with AtMRP1. Plant Cell **10:** 267-282

Luijendijk TJC, vanderMeijden E, Verpoorte R (1996) Involvement of strictosidine as a defensive chemical in Catharanthus roseus. Journal of Chemical Ecology **22:** 1355-1366

Madyastha KM, Ridgway JE, Dwyer JG, Coscia CJ (1977) Subcellular localization of a cytochrome P-450-dependent monogenase in vesicles of the higher plant Catharanthus roseus. The Journal of Cell Biology **72:** 302-313

Mahroug S, Burlat V, St-Pierre B (2007) Cellular and sub-cellular organisation of the monoterpenoid indole alkaloid pathway in *Catharanthus roseus*. Phytochemistry Reviews **6:** 363-381

Mano M (2006) Vinorelbine in the management of breast cancer: New perspectives, revived role in the era of targeted therapy. Cancer treatment reviews **32:** 106-118

Marinova K, Pourcel L, Weder B, Schwarz M, Barron D, Routaboul JM, Debeaujon I, Klein M (2007) The Arabidopsis MATE transporter TT12 acts as a vacuolar flavonoid/H+-antiporter active in proanthocyanidin-accumulating cells of the seed coat. Plant Cell **19:** 2023-2038

Martinoia E, Meyer S, De Angeli A, Nagy R (2012) Vacuolar Transporters in Their Physiological Context. *In* SS Merchant, ed, Annual Review of Plant Biology, Vol 63, Vol 63, pp 183-213

Memelink J, Gantet P (2007) Transcription factors involved in terpenoid indole alkaloid biosynthesis in Catharanthus roseus. Phytochemistry Reviews **6:** 353-362

Memelink J, Verpoorte R, Kijne JW (2001) ORCAnization of jasmonate - responsive gene expression in alkaloid metabolism. Trends in plant science **6:** 212-219

Menke FLH, Champion A, Kijne JW, Memelink J (1999) A novel jasmonate- and elicitor-responsive element in the periwinkle secondary metabolite biosynthetic gene Str interacts with a jasmonate- and elicitor-inducible AP2-domain transcription factor, ORCA2. Embo Journal **18:** 4455-4463

Mersey BG, Cutler AJ (1986) Differential distribution of specific indole alkaloids in leaves of Catharanthus roseus Canadian Journal of Botany-Revue Canadienne De Botanique **64:** 1039-1045

Morita M, Shitan N, Sawada K, Van Montagu MCE, Inze D, Rischer H, Goossens A, Oksman-Caldentey K-M, Moriyama Y, Yazaki K (2009) Vacuolar transport of nicotine is mediated by a multidrug and toxic compound extrusion (MATE) transporter in Nicotiana tabacum. Proceedings Of The National Academy Of Sciences Of The United States Of America **106:** 2447-2452

Moriyama Y, Hiasa M, Matsumoto T, Omote H (2008) Multidrug and toxic compound extrusion (MATE)-type proteins as anchor transporters for the excretion of metabolic waste products and xenobiotics. Xenobiotica **38:** 1107-1118

Murata J, De Luca V (2005) Localization of tabersonine 16-hydroxylase and 16-OH tabersonine-16-O-methyltransferase to leaf epidermal cells defines them as a major site of precursor biosynthesis in the vindoline pathway in Catharanthus roseus. Plant Journal **44:** 581-594

Murata J, Roepke J, Gordon H, De Luca V (2008) The leaf epidermome of *Catharanthus roseus* reveals its biochemical specialization. Plant Cell **20:** 524-542

Naaranlahti T, Auriola S, Lapinjoki SP (1991) Growth-related dimerization of vindoline and catharanthine in *Catharanthus roseus* and effect of wounding on the process. Phytochemistry **30:** 1451-1453

Newman DJ, Cragg GM (2007) Natural Products as Sources of New Drugs over the Last 25 Years⊥. Journal of Natural Products **70:** 461-477

Noble RL (1990) The discovery of the vinca alkaloids - chemotherapeutic agents against cancer Biochemistry and Cell Biology-Biochimie Et Biologie Cellulaire **68:** 1344-1351

Noble RL, Beer CT, Cutts JH (1958) Role of chance observations in chemeotherapy - Vinca-rosea. Annals of the New York Academy of Sciences **76:** 882-894

O'Connor SE, Maresh JJ (2006) Chemistry and biology of monoterpene indole alkaloid biosynthesis. Natural Product Reports **23:** 532-547

Omote H, Hiasa M, Matsumoto T, Otsuka M, Moriyama Y (2006) The MATE proteins as fundamental transporters of metabolic and xenobiotic organic cations. Trends in Pharmacological Sciences **27:** 587-593

Otani M, Shitan N, Sakai K, Martinoia E, Sato F, Yazaki K (2005) Characterization of vacuolar transport of the endogenous alkaloid berberine in *Coptis japonica*. Plant Physiology **138:** 1939-1946

Ouwerkerk PF, Memelink J (1999) Elicitor-responsive promoter regions in the tryptophan decarboxylase gene from Catharanthus roseus. Plant Molecular Biology **39:** 129-136

Pasquali G, Goddijn OJM, Dewaal A, Verpoorte R, Schilperoort RA, Hoge JHC, Memelink J (1992) Coordinated regulation of 2 indole alkaloid biosynthetic genes from *Catharanthus roseus* by auxin and elicitors Plant Molecular Biology **18:** 1121-1131

Pauw B, Hilliou FAO, Martin VS, Chatel G, de Wolf CJF, Champion A, Pre M, van Duijn B, Kijne JW, van der Fits L, Memelink J (2004) Zinc finger proteins act as transcriptional repressors of alkaloid biosynthesis genes in *Catharanthus roseus*. Journal of Biological Chemistry **279:** 52940-52948

Pighin JA, Zheng HQ, Balakshin LJ, Goodman IP, Western TL, Jetter R, Kunst L, Samuels AL (2004) Plant cuticular lipid export requires an ABC transporter. Science **306:** 702-704

Pollier J, Moses T, Goossens A (2011) Combinatorial biosynthesis in plants: A (p)review on its potential and future exploitation. Natural Product Reports **28:** 1897-1916

Pomahacova B, Dusek J, Duskova J, Yazaki K, Roytrakul S, Verpoorte R (2009) Improved accumulation of ajmalicine and tetrahydroalstonine in Catharanthus cells expressing an ABC transporter. Journal of Plant Physiology **166:** 1405-1412

Poustka F, Irani NG, Feller A, Lu Y, Pourcel L, Frame K, Grotewold E (2007) A trafficking pathway for Anthocyanins overlaps with the endoplasmic reticulum-to-vacuole protein-sorting route in Arabidopsis and contributes to the formation of vacuolar inclusions. Plant Physiology **145:** 1323-1335

Ragauskas AJ, Williams CK, Davison BH, Britovsek G, Cairney J, Eckert CA, Frederick WJ, Hallett JP, Leak DJ, Liotta CL, Mielenz JR, Murphy R, Templer R, Tschaplinski T (2006) The path forward for biofuels and biomaterials. Science **311:** 484-489

Rea PA (2007) Plant ATP-Binding cassette transporters. *In* Annual Review of Plant Biology, Vol 58, pp 347-375

Rea PA (2007) Plant ATP-binding cassette transporters. Annu Rev Plant Biol **58:** 347-375

Rea PA, Li ZS, Lu YP, Drozdowicz YM, Martinoia E (1998) From vacuolar GS-X pumps to multispecific ABC transporters. Annual Review of Plant Physiology and Plant Molecular Biology **49:** 727-760

Renaudin JP (1989) Different mechanisms control the vacuolar compartmentation of ajmalicine in *Catharanthus roseus* cell cultures. Plant Physiol. Biochem. **27:** 613-621

Roberts F, Roberts CW, Johnson JJ, Kyle DE, Krell T, Coggins JR, Coombs GH, Milhous WK, Tzipori S, Ferguson DJP, Chakrabarti D, McLeod R (1998) Evidence for the shikimate pathway in apicomplexan parasites. Nature **393:** 801-805

Roewer IA, Cloutier N, Nessler CL, Luca V (1992) Transient induction of tryptophan decarboxylase (TDC) and strictosidine synthase (SS) genes in cell suspension cultures of Catharanthus roseus. Plant Cell **11:** 86-89

Saklani A, Kutty SK (2008) Plant-derived compounds in clinical trials. Drug Discovery Today **13:** 161-171

Sánchez-Fernández Ro, Davies TGE, Coleman JOD, Rea PA (2001) The Arabidopsis thaliana ABC Protein Superfamily, a Complete Inventory. Journal of Biological Chemistry **276:** 30231-30244

Schröder G, Unterbusch E, Kaltenbach M, Schmidt J, Strack D, De Luca V, Schröder J (1999) Light-induced cytochrome P450-dependent enzyme in indole alkaloid biosynthesis: tabersonine 16-hydroxylase. Febs Letters **458:** 97-102

Shitan N, Bazin I, Dan K, Obata K, Kigawa K, Ueda K, Sato F, Forestier C, Yazaki K (2003) Involvement of CjMDR1, a plant multidrug-resistance-type ATP-binding cassette protein, in alkaloid transport in Coptis japonica. Proceedings Of The National Academy Of Sciences Of The United States Of America **100:** 751-756

Shitan N DF, Dan K, Kato N, Ueda K, Sato F, Forestier C, Yazaki K (2012) Characterization of *Coptis japonica* CjABCB2, an ATP-binding cassette protein involved in alkaloid transport. Phytochemistry

Shoji T, Inai K, Yazaki Y, Sato Y, Takase H, Shitan N, Yazaki K, Goto Y, Toyooka K, Matsuoka K, Hashimoto T (2009) Multidrug and Toxic Compound Extrusion-Type Transporters Implicated in Vacuolar Sequestration of Nicotine in Tobacco Roots. Plant Physiology **149:** 708-718

Sirikantaramas S, Yamazaki M, Saito K (2008) Mechanisms of resistance to self-produced toxic secondary metabolites in plants. Phytochemistry Reviews **7:** 467-477

Sottomayor M, Barcelo AR (2003) Peroxidase from Catharanthus roseus (L.) G. Don and the biosynthesis of alpha-3 ',4 '-anhydrovinblastine: a specific role for a multifunctional enzyme. Protoplasma **222:** 97-105

Sottomayor M, dePinto MC, Salema R, DiCosmo F, Pedreno MA, Barcelo AR (1996) The vacuolar localization of a basic peroxidase isoenzyme responsible for the synthesis of alpha-3',4'-anhydrovinblastine in *Catharanthus roseus* (L) G. Don leaves. Plant Cell and Environment **19:** 761-767

Sottomayor M, Lopes Cardoso I, Pereira LG, Ros Barceló A (2004) Peroxidase and the biosynthesis of terpenoid indole alkaloids in the medicinal plant Catharanthus roseus (L.) G. Don. Phytochemistry Reviews **3:** 159-171

Sottomayor M, Lopez-Serrano M, DiCosmo F, Barcelo AR (1998) Purification and characterization of alpha-3 ',4 '-anhydrovinblastine synthase (peroxidase-like) from Catharanthus roseus (L) G. Don. Febs Letters **428:** 299-303

Sottomayor M, Ros Barceló A (2006) The Vinca Alkaloids: From Biosynthesis and Accumulation in Plant Cells, To Uptake, Activity and Metabolism in Animal Cells., Vol 33. Elsevier Science Publishers,, The Netherlands

St-Pierre B, Vazquez-Flota FA, De Luca V (1999) Multicellular compartmentation of Catharanthus roseus alkaloid biosynthesis predicts intercellular translocation of a pathway intermediate. Plant Cell **11:** 887-900

Suttipanta N (2011b) CHARACTERIZATION OF G10H PROMOTER AND ISOLATION OF WRKY TRANSCRIPTION FACTORS INVOLVED IN CATHARANTHUS TERPENOID INDOLE ALKALOID BIOSYNTHESIS PATHWAY. Kentucky

Suttipanta N, Pattanaik S, Kulshrestha M, Patra B, Singh SK, Yuan L (2011) The Transcription Factor CrWRKY1 Positively Regulates the Terpenoid Indole Alkaloid Biosynthesis in Catharanthus roseus. Plant Physiology **157:** 2081-2093

Svoboda GH, Gorman M, Neuss N, Johnson IS (1962) Current status of research on alkaloids of Vinca Rosea LINN (Catharanthus roseus G Don) Journal of Pharmaceutical Sciences **51:** 707-&

Tarselli MA, Raehal KM, Brasher AK, Streicher JM, Groer CE, Cameron MD, Bohn LM, Micalizio GC (2011) Synthesis of conolidine, a potent non-opioid analgesic for tonic and persistent pain. Nature Chemistry **3:** 5

Terasaka K, Blakeslee JJ, Titapiwatanakun B, Peer WA, Bandyopadhyay A, Makam SN, Lee OR, Richards EL, Murphy AS, Sato F, Yazaki K (2005) PGP4, an ATP binding cassette P-glycoprotein, catalyzes auxin transport in Arabidopsis thaliana roots. Plant Cell **17:** 2922-2939

Thomas CJ, Rahier NJ, Hecht SM (2004) Camptothecin: current perspectives. Bioorganic & Medicinal Chemistry **12:** 1585-1604

Tommasini R, Vogt E, Fromenteau M, Hortensteiner S, Matile P, Amrhein N, Martinoia E (1998) An ABC-transporter of Arabidopsis thaliana has both glutathione-conjugate and chlorophyll catabolite transport activity. Plant Journal **13:** 773-780

Tommasini R, Vogt E, Schmid J, Fromentau M, Amrhein N, Martinoia E (1997) Differential expression of genes coding for ABC transporters after treatment of Arabidopsis thaliana with xenobiotics. Febs Letters **411:** 206-210

van den Brule S, Muller A, Fleming AJ, Smart CC (2002) The ABC transporter SpTUR2 confers resistance to the antifungal diterpene sclareol. Plant Journal **30:** 649-662

van der Fits L, Hilliou F, Memelink J (2001) T-DNA activation tagging as a tool to isolate regulators of a metabolic pathway from a genetically non-tractable plant species. Transgenic Research **10:** 513-521

Van Der Fits L, Memelink J (2000) ORCA3, a jasmonate-responsive transcriptional regulator of plant primary and secondary metabolism. Science **289:** 295-297

van der Fits L, Memelink J (2001b) The jasmonate-inducible AP2/ERF-domain transcription factor ORCA3 activates gene expression via interaction with a jasmonate-responsive promoter element. Plant Journal **25:** 43-53

van der Heijden R, Jacobs DI, Snoeijer W, Hallared D, Verpoorte R (2004) The Catharanthus alkaloids: Pharmacognosy and biotechnology. Current Medicinal Chemistry **11:** 607-628

Vazquez-Flota F, DeCarolis E, Alarco AM, DeLuca V (1997) Molecular cloning and characterization of desacetoxyvindoline-4-hydroxylase, a 2-oxoglutarate dependent dioxygenase involved in the biosynthesis of vindoline in *Catharanthus roseus* (L) G. Don. Plant Molecular Biology **34:** 935-948

Verma P, Mathur AK, Srivastava A, Mathur A (2012) Emerging trends in research on spatial and temporal organization of terpenoid indole alkaloid pathway in Catharanthus roseus: a literature update. Protoplasma **249:** 255-268

Verrier PJ, Bird D, Burla B, Dassa E, Forestier C, Geisler M, Klein M, Kolukisaoglu U, Lee Y, Martinoia E, Murphy A, Rea PA, Samuels L, Schulz B, Spalding EJ, Yazaki K, Theodoulou FL (2008) Plant ABC proteins--a unified nomenclature and updated inventory. Trends Plant Sci **13:** 151-159

Westekemper P, Wieczorek U, Gueritte F, Langlois N, Langlois N, Langlois Y, Potier P, Zenk MH (1980) Radioimmunoassay for the determination of the indole alkaloid vindoline in Catharanthus Planta Medica **39:** 24-37

Wink M (1993) The plant vacuole: a multifunctional compartment. Journal of Experimental Botany **44:** 231-246

Wink M (1999) Plant Secondary Metabolism: biochemistry, function, and biotechnology. *In* W M, ed, Biochemstry of Plant Secondary Metabolism, Vol 2. Shefield Academic Press, pp 1-16

Wink M, Roberts MF (1998) Compartmentation of alkaloid biosynthesis, transport and storage. *In* MFaW Roberts, M., eds, ed, Alkaloids: Biochemistry, Ecologyand Medicinal Applications Plenum Press, pp 239–262,

Wu S, Chappell J (2008) Metabolic engineering of natural products in plants; tools of the trade and challenges for the future. Current Opinion in Biotechnology **19:** 145-152

Yazaki K (2005) Transporters of secondary metabolites. Current Opinion in Plant Biology **8:** 301-307

Yazaki K (2006) ABC transporters involved in the transport of plant secondary metabolites. Febs Letters **580:** 1183-1191

Yazaki K, Shitan N, Sugiyama A, Takanashi K (2009) Cell and Molecular Biology of ATP-binding cassette proteins in plants *In* KW Jeon, ed, International Review of Cell and Molecular Biology, Vol 276, Vol 276, pp 263-299

Yoder LR, Mahlberg PG (1976) Reactions of alkaloid and histochemical indicators in laticifers and specialized parenchyma cells of *Catharanthus roseus* (Apocynaceae). Amer. J. Bot. **63:** 1167-1173

Zhang H, Hedhili S, Montiel G, Zhang Y, Chatel G, Pre M, Gantet P, Memelink J (2011) The basic helix-loop-helix transcription factor CrMYC2 controls the jasmonate-responsive expression of the ORCA genes that regulate alkaloid biosynthesis in Catharanthus roseus. Plant Journal **67:** 61-71

Zhang L, Lu X, Shen Q, Chen Y, Wang T, Zhang F, Wu S, Jiang W, Liu P, Zhang L, Wang Y, Tang K (2012) Identification of Putative Artemisia annua ABCG Transporter Unigenes Related to Artemisinin Yield Following Expression Analysis in Different Plant Tissues and in Response to Methyl Jasmonate and Abscisic Acid Treatments. Plant Molecular Biology Reporter **30:** 838-847

Zhao J, Dixon RA (2009) MATE Transporters Facilitate Vacuolar Uptake of Epicatechin 3 '-O-Glucoside for Proanthocyanidin Biosynthesis in Medicago truncatula and Arabidopsis. Plant Cell **21:** 2323-2340

Zhao J, Verpoorte R (2007) Manipulating indole alkaloid production by Catharanthus roseus cell cultures in bioreactors: from biochemical processing to metabolic engineering. Phytochemistry Reviews **6:** 435-457

Chapter

II

Vacuolar transport of the medicinal alkaloids from *Catharanthus roseus* is mediated by a proton-driven antiport

Vacuolar transport of the medicinal alkaloids from *Catharanthus roseus* is mediated by a proton-driven antiport

Inês Carqueijeiro[1,2], Henrique Noronha[3,4], Patrícia Duarte[1], Hernâni Gerós[3,4], Mariana Sottomayor[1]*

[1]IBMC – Instituto de Biologia Molecular e Celular, Universidade do Porto, Rua do Campo Alegre, 823, 4150-180 Porto, Portugal;

[2]Departamento de Biologia, Faculdade de Ciências da Universidade do Porto, Rua do Campo Alegre s/n 4169-007 Porto, Portugal;

[3]Centro de Investigação e de Tecnologias Agro-Ambientais e Biológicas, quinta de Prados, 5001-801 Vila Real, Portugal;

[4]Departamento de Biologia, Universidade do Minho, Campus de Gualtar, 4710-057 Braga, Portugal;

* Corresponding author, e-mail: msottoma@ibmc.up.pt

Inês Carqueijeiro declares to have participated actively in this work, by contributing to the experimental design, performing all the experimental work, and by contributing to manuscript writing.

ABSTRACT

Catharanthus roseus is one of the most studied medicinal plants due to the interest of their dimeric terpenoid indole alkaloids (TIAs) vinblastine and vincristine, used in cancer chemotherapy. These TIAs are produced in very low levels in the leaves of the plant from the monomeric precursors vindoline and catharanthine and although TIA biosynthesis is reasonably well understood, much less is known about TIA membrane transport mechanisms. However, such knowledge is extremely important to understand TIA metabolic fluxes and to develop strategies aiming at increasing TIA production. In this study, the vacuolar transport mechanism of the main TIAs accumulated in *C. roseus* leaves, vindoline, catharanthine and α-3',4'-anhydrovinblastine, was characterized using a tonoplast vesicle system. Vindoline uptake was ATP-dependent and this transport activity was strongly inhibited by NH_4^+ and carbonyl cyanide m-chlorophenyl hydrazine, and was insensitive to the ABC transporter inhibitor vanadate. Spectrofluorimetry assays with a pH-sensitive fluorescent probe showed that vindoline and other TIAs indeed were able to dissipate a H^+ gradient preestablished across the tonoplast by either vacuolar H^+-ATPase or vacuolar H^+-pyrophosphatase. The initial rates of H^+ gradient dissipation followed Michaelis-Menten kinetics, suggesting the involvement of mediated transport, and this activity was species and alkaloid specific. Altogether, results strongly support that TIAs are actively taken up by *C. roseus* mesophyll vacuoles through a specific H^+ antiport system, and not by an ion trap mechanism or ABC transporters.

INTRODUCTION

Alkaloids form a very diverse and prominent family of plant natural products, including many compounds with important pharmaceutical applications. Paramount examples are taxol and vinblastine (VLB), used as anticancer drugs, and morphine, used as a painkiller. In plants, alkaloids play a key role in defense against pathogens and herbivores, with plant-herbivore coevolution possibly having determined the strong physiological activity of these compounds in animals. The metabolism of medically important alkaloids has been thoroughly investigated, and much is known about their biosynthetic pathways. However, little is known about the transport and accumulation mechanisms of alkaloids, in spite of their importance for the final output of metabolic fluxes.

A paradigmatic example of highly valuable alkaloids produced in very low levels in the plant are the anticancer terpenoid indole alkaloids (TIAs) of *Catharanthus roseus* (L.) G. Don – vinblastine (VLB) and vincristine (VCR) (Fig.1; Verpoorte et al., 2007). The great pharmacological importance of TIAs, associated with the low abundance in the plant (approximately 0.0005% fry weight), stimulated intense research on the TIA pathway, and *C. roseus* has become one of the most studied medicinal plants (van der Heijden et al., 2004; Verpoorte et al., 2007; Costa et al., 2008). TIA biosynthesis shows multi-cellular compartmentation in *C. roseus* leaves, with early steps occurring in epidermal cells, and late steps occurring in laticifer and mesophyll idioblast cells, predicting intercellular translocation of TIA intermediates (St-Pierre et al., 1999; Murata el al. 2008; Guirimand et al., 2011). Moreover, the TIA pathway also shows a complex subcellular organization, with different parts of the pathway being localized in the plastids, the vacuole, the cytosol and the endoplasmic reticulum (ER), predicting further transport events (Mahroug et al., 2007; Guirimand et al., 2011). In spite of the importance of all those TIA transmembrane transport steps as putative rate-limiting steps of the alkaloid metabolic fluxes, the knowledge about the transport mechanisms involved is still very poor.

Early work suggested that vacuolar accumulation of TIAs and other alkaloids was mediated either by highly specific carriers (Deus-Neumann and Zenk, 1984, 1986; Wink, 1993) or by an unspecific ion-trap mechanism in which the alkaloids, being weak bases, accumulate by diffusion in the acidic vacuole (Guern et al., 1987; Renaudin, 1989; Blom et al., 1991; Wink, 1993). However, recent work on alkaloid transmembrane transport has consistently supported the H^+/alkaloid antiport mechanism for the alkaloids berberine in *Coptis japonica* and nicotine in *Nicotiana tabacum* (Otani et al. 2005; Morita et al., 2009; Shoji et al., 2009. A plasma membrane influx permease functioning as a

proton symporter of nicotine has also been characterized in *N. tabacum*, and two ATP-binding cassette (ABC) transporters, CjMDR1 and CjABCB2, were implicated in plasma membrane influx in *C. japonica* (Hildreth et al., 2011; Shitan et al., 2003; Shitan et al., 2012). In *C. roseus,* nothing is known about TIA plasma membrane transport, and vacuolar transport remains poorly characterized.
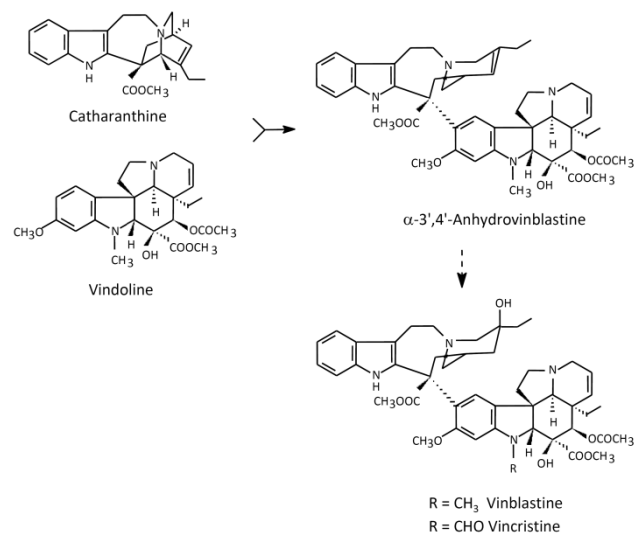
Figure 1. Biosynthesis of VLB and VCR from the monomeric precursors catharanthine and vindoline. AVLB is the product of the dimerization reaction and the direct precursor of the anticancer drugs.

Here, the vacuolar accumulation in *C. roseus* mesophyll cells of the main leaf TIAs vindoline, catharanthine and α-3',4'-anhydrovinblastine (AVLB) was characterized in highly pure tonoplast vesicles. Uptake of vindoline was dependent on ATP, with accumulation being strongly inhibited by H^+ gradient dissipators and unaffected by the ABC transporter inhibitor vanadate. Likewise, vindoline and other TIAs induced dissipation of a preestablished pH gradient across the tonoplast, with proton movements following a Michaelis-Menten kinetics, suggesting mediated transport. Overall, results indicate that TIAs are accumulated in the vacuole of *C. roseus* mesophyll cells through a specific proton antiport system.

MATERIAL AND METHODS

Plant material

Catharanthus roseus (L.) G. Don cv. 'Little Bright Eye' plants were grown at 25°C in a growth chamber, under a 16-h photoperiod, using white fluorescent light with a maximum intensity of 70 µmol m^{-2} s^{-1}. Seeds were acquired from AustraHort (Australia) and voucher specimens are deposited at the Herbarium of the Department of Biology of the Faculty of Sciences of the University of Porto (PO 61912). Plants used for protoplast and vacuole isolation were 6 to 8 months old.

Isolation of *C. roseus* mesophyll protoplasts

C. roseus mesophyll protoplasts were obtained using a protocol adapted from Zheng et al. (1997) and Sottomayor et al. (1996). Approximately eight to 10 leaves (approximately 1.5 to 2 g) of adult plants (usually second and third pairs from the tip) were cut into approximately 1 mm strips and transferred to a petri dish with 10 mL of digestion medium composed of 2% (w/v) cellulase (Onozuka R-10, DUCHEFA, The Netherlands), 0.3% (w/v) macerozyme (Onozuka R-10, SERVA, Germany) and 0.1% (v/v) pectinase (SIGMA) dissolved in MM buffer (0.4 M mannitol in 20 mM Mes pH 5.6-5.8). The medium was vacuum infiltrated for 15 min, and leaf strips were incubated for 3 h at 25°C in the dark. The suspension was then filtered through a 100-µm nylon mesh, and the filtrate was transferred into 15 mL Falcon tubes. The protoplast suspension was centrifuged at 65*g* for 5 min at 20°C, the supernatant was removed, and the protoplasts were washed four times in MM buffer. After the final wash, protoplasts were counted using a haemocytometer. The integrity of the isolated protoplasts was checked by observation under an optical microscope (OLYMPUS), and images were acquired by a coupled Olympus DP 25 digital camera and respective software (Cell B; OLYMPUS). To check the viability of the isolated protoplasts, these were stained with 5 µg mL^{-1} FDA and observed with the epifluorescence microscope (Leica Microsystems; DM-5000B, LEICA) using excitation and emission wavelengths of respectively 494 and 530 nm (Jones and Senft, 1985).

Isolation of *C. roseus* mesophyll vacuoles

Isolation of *C. roseus* mesophyll vacuoles was performed according to Fontes et al. (2010) with minor modifications. The isolated mesophyll protoplasts were centrifuged at 65*g* for 5 min at 20°C, and the protoplast pellets were chilled for at least 30 min on ice. Vacuoles were released following protoplast osmotic lysis at 42°C for 10 min in 9 mL of lysis buffer consisting of 150 µg mL^{-1} bovine serum albumin (BSA), 2 mM dithiothreitol (DTT), 0.2 M mannitol, 10% (w/v) Ficoll 400 and 15 mM EDTA in 10 mM MOPS, pH 8. The mixture was overlaid with 3 mL of 3% Ficoll in a 1:2 mixture of lysis and vacuole

buffers, and with 1 mL of vacuole buffer consisting of 2 mM DTT and 0.5 M mannitol in 10 mM MOPS pH 7.5. Isolated vacuoles were recovered in the vacuole buffer layer after centrifuging at 1000g for 17 min at room temperature. For visualization with the optical microscope, vacuoles were stained with neutral red and were counted using a haemocytometer. Vacuole integrity was tested using 10 µM FM1-43 (a membrane marker; Betz et al., 1996), and 3 µm Fluo-4 AM (an intracellular Ca^{2+} indicator). Labeling with the fluorescent probes was performed for 30 min at room temperature in the dark. FM1-43 and Fluo-4 AM fluorescence was examined using a SP2 AOBS SE confocal microscope (LEICA) equipped with a scan head with an argon laser. Visualization of the fluorescent probes was performed using an excitation wavelength of 488 nm and an emission wavelength window from 500 to 650 nm.

Isolation of tonoplast vesicles

Tonoplast vesicles from *C. roseus* leaves were isolated according to Façanha and de Meis (1998) and Queirós et al. (2009) with minor modifications. Approximately 15 g of leaves were homogenized using an Ultra-Turrax T25 apparatus (IKA, Janke & Kunkel, Germany), at 13,000 rpm, for 5 min at 4°C, in extraction buffer consisting of 1 mM phenylmethylsulphonyl fluoride, 0.1% (w/v) BSA, 2 mM DTT, 250 mM sucrose, 3 mM $MgCl_2$, 100 mM KCl and 2 mM EDTA in 70 mM Tris-HCl pH 8. The homogenate was filtered through four layers of cheesecloth and centrifuged for 10 min at 4°C, at 10,000g. The supernatant was centrifuged at 100,000g for 1h, the pellet was resuspended in 8 mL of resuspension buffer consisting of 1 mM DTT, 1 mM phenylmethylsulphonyl fluoride, 15% (v/v) glycerol and 1 mM EDTA in 20 mM Tris-HCl pH 7.5, homogenized with a glass potter homogenizer (40 mL vessel, tight pestle, WHEATON), overlaid on a 32/46% Suc step gradient in resuspension buffer, and centrifuged at 80,000g for 3 h at 4° C. The tonoplast fraction was obtained at the 0/32% interface, diluted in resuspension buffer, and centrifuged at 100,000g for 45 min at 4°C. The membrane pellet was resuspended in 0.3 to 1 mL of resuspension buffer, was frozen with liquid nitrogen and kept at -80°C until use. Tonoplast vesicles from grape (*Vitus vinifera*) cell cultures were isolated according to Queirós et al. (2009) with the modifications from Martins et al. (2012). Protein quantification was performed using the method described by Lowry et al. (1951).

Protein extraction and quantification

For protein extraction, protoplasts, vacuoles and tonoplast vesicles in the respective isolation buffers were frozen at -80°C and lyophilised for 2 d in a freeze–dry Edwards apparatus. Lyophilised samples were reconstituted in 50 mM Tris pH7.5, dialysed against the same buffer to remove mannitol and stored at -20°C until use.

Protein extraction from *C. roseus* leaves was described previously by Ferreres et al. (2011). Protein concentration of the dialyzed samples was determined according to the method described by Bradford (1976).

Western blot analysis

Protein samples obtained as described above were separated on 10% acrylamide gels as described by Laemmli (1970) and transferred to a nitrocellulose membrane. For the immuno-detection of soluble proteins, samples were boiled for 2 min prior to gel loading, while for the immunodetection of membrane proteins, protein samples were heated at 70°C for 10 min and immediately loaded onto the gel. The amount of protein loaded was 10 µg, except for the extract of tonoplast vesicles used for V-H$^+$-ATPase and V-H$^+$-PPase detection, where 1 µg was used. The following primary antibodies were used: an ER marker, rabbit anti-serum raised against calreticulin (a gift from J. Denecke, University of Leeds), at a 1:10,000 dilution; a chloroplast marker, rabbit antiserum raised against the chloroplast inner envelope TIC 40 protein (AS 10709-10; Agrisera), at a 1:2,500 dilution; two tonoplast markers, rabbit antisera raised against a V-H$^+$-ATPase (AS 07213, Agrisera) and a V-H$^+$-PPase (Maeshima and Yoshida, 1989), both at a 1:2000 dilution. The secondary antibody used was a peroxidase conjugated goat anti-rabbit (Santa Cruz Biotechnology, Inc) at 1:7500 dilutions and detection was performed with the chemiluminescent substrate ECL (GE Healthcare, Lifesciences**).**

Determination of ATP and PPi hydrolytic activities

Rates of ATP and PPi hydrolysis were determined by measuring the release of inorganic phosphate, according to Vera-Estrella et al. (2004) with some modifications. For protoplasts, vacuoles and tonoplast vesicles, ATP and PPi hydrolytic activities were assayed in fractions after freezing and thawing. For leaves, total protein extracts obtained as described by Ferreres et al. (2011) were used. Fifteen micrograms of total protein (in a maximum volume of 15 µL) were mixed with 300 µL of 3 mM ATP, 0.02% Triton X-100, 50 mM KCl, 1mM sodium molybdate, 6 mM MgSO4 in 30 mM Tris/Mes pH 8, and incubated for 30 min at 37ºC, with slow agitation. The reaction was stopped by the addition of 500 µL of cold 10% TCA, 4% perchloric acid, samples were kept 2 min on ice, centrifuged for 3 min at 2,400g, and 500 uL of the supernatant were mixed with 1.3 mL of Ames solution composed of 1 volume of 10% ascorbic acid mixed with 6 volumes of 4,2 g of ammonium molybdate and 28,6 mL of H$_2$SO$_4$ in 1L of water (Ames, 1966). After 15 min at room temperature in the dark, absorbance was read at 820 nm using a blank control performed without protein and NaH$_2$PO$_4$ as standard to build a calibration curve. For the determination of V-H$^+$-ATPase hydrolytic activity, two different inhibitors

FCUP 69

Unravelling the metabolism and transmembrane transport of the highly valuable medicinal alkaloids from *Catharanthus roseus*

were used, the F-H$^+$-ATPase inhibitor sodium azide at 0.5 mM, and the P-H$^+$-ATPase inhibitor vanadate at 0.1 mM. Thus, V-H$^+$-ATPase hydrolytic activity presented in supplemental Fig. S3 was estimated as the difference between the total hydrolytic activity and the activity in the presence of both inhibitors.

Proton transport assays

ATP and PPi proton-dependent transport across the tonoplast was measured as the initial rate of fluorescence quenching of ACMA, according to Façanha and de Meis (1998), with minor modifications. For intact vacuoles, 10^4 vacuoles were used in each reaction; for tonoplast vesicles, a volume corresponding to 50 µg of tonoplast proteins were used in each reaction. The reaction mixture (1 mL) was composed of 5 mM MgCl$_2$ and 2 µM ACMA in reaction buffer (30 mM KCl and 50 mM NaCl in 20 mM Hepes pH 7.2). When using intact vacuoles, the mixture was supplemented with 0.1% (w/v) BSA. For the V-H$^+$-ATPase activity assay, the reaction started with the addition of 0.05 to 1.5 mM ATP. For the V-H$^+$-PPase activity assay, the reaction started with the addition of 0.00125 to 0.1 mM PPi. The protonophore 1.5 mM NH$_4$Cl was added to confirm the establishment of a H$^+$ gradient. Fluorescence quenching was registered by a LS-5B fluorescence spectrophotometer (Perkin-Elmer) at excitation and emission wavelengths of 415 nm and 485 nm respectively. Reactions were performed at RT and the results were expressed as Δ Fluorescence in % min^{-1} µg^{-1} protein. Experimental data was analyzed with the GraphPad Prism software. For the determination of V-H$^+$-ATPase proton pump activity, three different inhibitors were used: the P-H$^+$-ATPase inhibitor vanadate (100 µM), the V-H$^+$-ATPase inhibitor nitrate (KNO$_3$ - 50 mM), and the V-H$^+$-ATPase inhibitor concanamycin A (0.1 µM).

Assay of proton antiport activities

For *C. roseus* tonoplast vesicles, the occurrence of transmembrane proton exchange activities with several ions and compounds was inferred by the dissipation of a pre-formed pH gradient established by the addition of 1 mM ATP, using the conditions described for the proton transport assays above. For *V. vinifera* tonoplast vesicles, a volume corresponding to 30 µg of tonoplast proteins was used, the reaction buffer was composed of 2µM ACMA, 100 mM KCl, 2 mM MgCl$_2$ and 0.1% BSA (w/v) in 10 mM MOPS-Tris pH 7.2, and energization was performed by addition of 50 µM PPi. After the fluorescence quenching of ACMA reached a steady state, different ions and compounds were added with the specified concentrations, and uptake was inferred by measuring the fluorescence recovery of the ACMA probe during the first 15 s of reaction. Results were expressed as Δ Fluorescence in % min^{-1} µg^{-1} protein. Experimental data was analyzed with the GraphPad Prism software.

Uptake assay

To assay the uptake of vindoline into tonoplast vesicles, membranes corresponding to 100 µg of proteins were incubated in reaction buffer in the presence of an ATP regenerator system (Marinova et al., 2007) consisting of 1 mM DTT, 5 mM $MgCl_2$, 10 mM of creatine phosphate and 10 µg mL^{-1} of creatine kinase (C9983-100UG; SIGMA), in a final volume of 1.2 mL. Energization of the tonoplast vesicles was initiated by the addition of 3 mM ATP, 1mM vindoline was added after 1 min, and the reaction proceeded for 15 min at RT with gently shacking. To stop the reaction, the assay was transferred to ice, and the vesicles were immediately isolated from the medium by centrifugation at 100,000*g* for 30 min at 4ºC. The supernatant was discarded, and the pellet was superficially washed with ice-cold reaction buffer and dried with N_2. The ABC inhibitor vanadate (1 mM) was added 5 min prior to ATP (Frangne et al., 2002), and the H^+ gradient dissipators NH_4Cl (1.5 mM) and CCCP (50 µM) were added to the reaction mixture after ATP and before vindoline addition. Control reactions were performed in the absence of ATP, inhibitors and creatine kinase, and subtracted from all other assays.

Alkaloid extraction and HPLC-DAD analysis

Alkaloid extraction and HPLC-DAD analysis were performed as described by Sottomayor et al., (1996), except for alkaloid extraction from tonoplast vesicles used in uptake assays, where alkaloids were directly extracted with HPLC grade methanol. In all cases, the biological material was always lyophilized prior to extraction.

RESULTS

TIAs are accumulated inside the vacuoles of *C. roseus* mesophyll cells

Vacuoles are considered the final accumulation target of alkaloids, where they are thought to function as a toxic defense and do not interfere with basic plant cell metabolism (Wink, 1993). Therefore, the transtonoplast transport mechanism is particularly important for alkaloid metabolic fluxes. In order to confirm the general assumption that alkaloids are accumulated in the vacuoles for *C. roseus* mesophyll cells, the alkaloid profile of leaves, isolated protoplasts, and vacuoles were investigated.

The protoplast suspension isolated from *C. roseus* leaves was highly pure, and the naked cells showed no apparent membrane damage or disintegration of the internal structure (Fig. 2A). The presence of protoplast idioblasts was confirmed by observation

of their conspicuous blue fluorescence under the fluorescence microscope (Fig. 2B). Protoplast viability was estimated by staining with fluorescein diacetate (FDA) as being 95 to 98% (Fig. 2C). Under the light microscope, the final vacuole fraction showed no noticeable protoplast or chloroplast contamination, and the accumulation of neutral red inside the vacuoles indicated that a transmembrane pH gradient was maintained inside the organelles, confirming the integrity of the tonoplast (Fig. 2D and E). Purified vacuoles exhibited intense fluorescence with Fluo 4-AM and FM1-43, indicating that the capacity to store high amounts of calcium and membrane integrity were preserved (Fig. 2F and G). The vacuole preparation was free of markers defining other endomembrane compartments, including the ER and chloroplasts, and was highly enriched in vacuolar markers (Fig. 2H). Furthermore, ATP hydrolytic activity was insensitive to the plasma membrane H^+-ATPase (P-H^+-ATPase) inhibitor vanadate and the mitochondria H^+-ATPase (F-H^+-ATPase) inhibitor azide, indicating respectively the absence of contamination with plasma membrane or mitochondrial membranes, and confirming the high purity of the vacuole fraction (Fig. 2I).
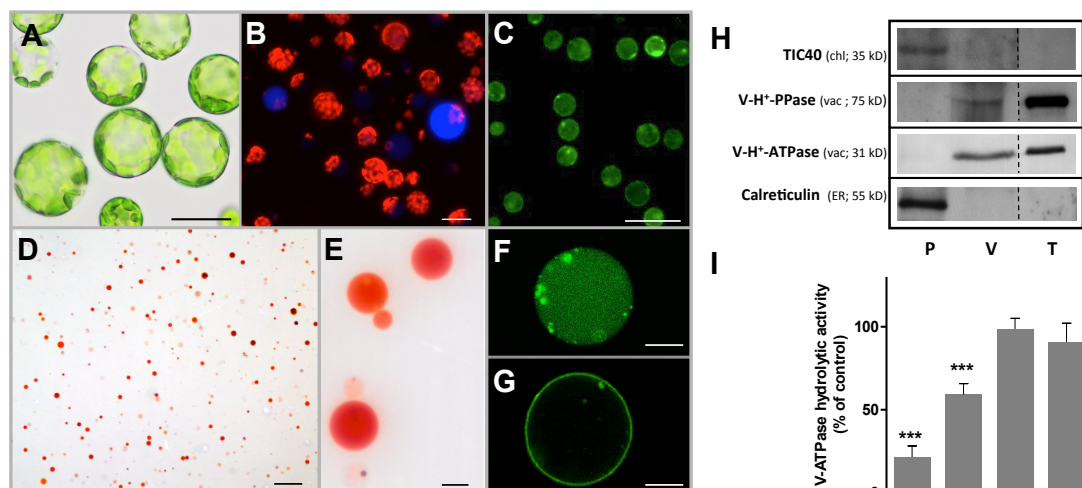
Figure 2. Characterization of the purity of protoplasts, vacuoles, and tonoplast vesicles isolated from *C. roseus* leaves. A to G, Optical microscopy images of protoplast and vacuole populations. A, Bright-field image of protoplasts. B, Fluorescence image of protoplasts with merging of the red and blue channels. Red corresponds to chloroplast autofluorescence, and blue fluorescence reveals alkaloid-accumulating idioblast cells. C, Fluorescence image of protoplasts labeled with FDA. D and E, Bright-field images of intact vacuoles stained with neutral red. F and G, Confocal images of intact vacuoles labeled with Fluo 4-AM (F) and FM1-43 (G). Bars = 20 μm (A and B), 100 μm (C and D), and 10 μm (E to G). H, Western blots of protein extracts from protoplasts (P), vacuoles (V) and tonoplast vesicles (T), using specific antibodies raised against the chloroplast inner envelope protein TIC40, the vacuole specific V-H^+-PPase and V-H^+-ATPase (subunit ε), and the ER-resident protein calreticulin. I, V-H^+-ATPase hydrolytic activity of protein extracts from leaves (L), protoplasts (P), vacuoles (V) and tonoplast vesicles (T). For each fraction, ATP hydrolytic activity was measured in the presence of 0.5 mM azide (mitochondrial ATPase inhibitor) and 100 μM vanadate (plasma membrane ATPase inhibitor) and expressed as the percentage of the total ATP hydrolytic activity in the absence of inhibitors (142, 304, 451, and 1839 nmol min^{-1} mg $prot^{-1}$ for L, P, V, T, respectively), revealing the residual percentage of activity corresponding to the V-H^+-ATPase present in each fraction. Statistical significance was evaluated using Student's *t* test

for pairwise comparison (*** P < 0.001). Data significantly different from control are indicated. Error bars indicate SD from three biological replicates with two biochemical replicates each.

HPLC-DAD analysis of alkaloid extracts from leaves showed that the main TIAs accumulated in *C. roseus* mesophyll cells are by far vindoline, catharanthine and AVLB (Supplemental Fig. S1), respectively the two monomeric and the first dimeric precursors of the anticancer TIAs (Fig.1). Analysis of protoplast and vacuole fractions showed the presence of high amounts of vindoline and catharanthine in both fractions, confirming the accumulation of these TIAs inside the vacuoles. AVLB was not found in isolated vacuoles but was present in the protoplasts (Table I).

Table I. TIA content estimated for leaves, protoplasts and vacuoles.
n.d. Not detected.

TIA	Leaves	Protoplasts		Vacuoles	
	$\mu mol\ g^{-1} fresh\ wt$	$nmol\ per\ 10^6$	$mg\ per\ 10^6$	$nmol\ per\ 10^6$	$mg\ per\ 10^6$
Vindoline	0.25±0.03	5.62±0.32	2.56±0.14	5.32±1.62	2.43±0.74
Catharanthine	0.24±0.02	9.56±1.85	3.56±0.69	4.67±1.47	1.74±0.55
AVLB	0.09±0.04	2.11±0.79	1.44±0.25	n.d.	n.d.

In order to measure uptake of vindoline by tonoplast vesicles, the transport reaction proceeded in the presence of an ATP-regenerating system, which enabled a continuous energization of the vesicles for periods up to 30 min (Supplemental Fig. S2). After incubation, tonoplast vesicles were immediately recovered at ice-cold temperature by ultracentrifugation and were submitted to TIA extraction and analysis by HPLC-DAD. A time course experiment revealed a rapid uptake of vindoline in the presence of ATP, whereas no uptake was observed in its absence, indicating that ATP is required for vindoline uptake (Fig. 3).
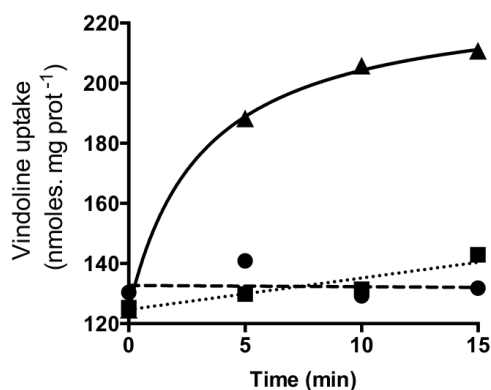
Figure 3. Time course of vindoline uptake into tonoplast vesicles from *C. roseus* leaves. Tonoplast vesicles were incubated in the presence of 1 mM vindoline (●), 1 mM vindoline, 1 mM ATP, 10 mM creatine phosphate and 10 μg mL^{-1}

creatine kinase (▲), or 1 mM vindoline, 1 mM ATP, 10 mM creatine phosphate,10 μg mL^{-1} creatine kinase and 1,5 mnM NH$_4$Cl (■). Values are the mean of two independent experiments.

In order to investigate if this was primary transport mediated by an ABC transporter, uptake was assayed in the presence of the specific inhibitor vanadate (Table II). This compound did not significantly affect vindoline uptake, ruling out direct transport by an ATP-dependent pump. On the other hand, the proton gradient dissipators NH$_4$Cl and CCCP (carbonyl cyanide *m*-chlorophenyl hydrazine) significantly compromised ATP-dependent vindoline uptake, indicating the involvement of an ATP-dependent transtonoplast pH gradient. To further clarify the importance of the proton gradient, the time-course experiment was also performed in the presence of NH$_4$Cl (Fig. 3), showing that dissipation of the proton gradient abolished the ATP-dependent vindoline uptake at all time points.

Table II. Characterization of ATP-dependent vindoline uptake.

Tonoplast vesicles were incubated with 1 mM of vindoline for 15 min under different conditions listed. SD values are from at least three biological replicates (*P < 0.05, **P < 0.01)

Condition	Uptake Vindoline
	%
+ 3mM ATP	100
+ 3 mM ATP + NH$_4$Cl (1,5 mM)	2.8 ± 1.6**
+ 3 mM ATP + CCCP (50 μM)	32.6 ± 0.07*
+ 3 mM ATP + Vanadate (1 mM)	113.8 ± 14.9

TIAs accumulation by *C. roseus* tonoplast vesicles is H$^+$ dependent

Following the indication that vindoline uptake could be dependent on a transtonoplast pH gradient, the capacity of ATP to generate a ΔpH across the membrane of the tonoplast vesicles was further studied using the pH-sensitive fluorescent probe 9-amino-6-chloro-2-methoxyacridine (ACMA; Fig. 4). Immediate fluorescence quenching signals were observed after addition of ATP, following Michaelis–Menten kinetics, and with fluorescence promptly recovering upon addition of NH$_4$Cl, all this demonstrating the generation of a transtonoplast pH gradient by an active vacuolar (V)-H$^+$-ATPase (Fig. 4A and B). The tonoplast specific V-H$^+$-pyrophosphatase (V-H$^+$-PPase) was also active in the isolated membranes (Supplemental Fig. S3A and B), which were also shown to present high ATP and pyrophosphate (PPi) hydrolytic activities (Supplemental Fig. S3C and D). The behaviour of both H$^+$ pumps in tonoplast

vesicles was comparable to that measured in isolated vacuoles (Supplemental Fig. S4). The generation of the transtonoplast pH gradient by ATP was insensitive to the P-H$^+$-ATPase inhibitor vanadate and was completely blocked by the tonoplast V-H$^+$-ATPase specific inhibitors concanamycin and KNO$_3$, further confirming the purity of the membrane fraction (Fig. 4C).
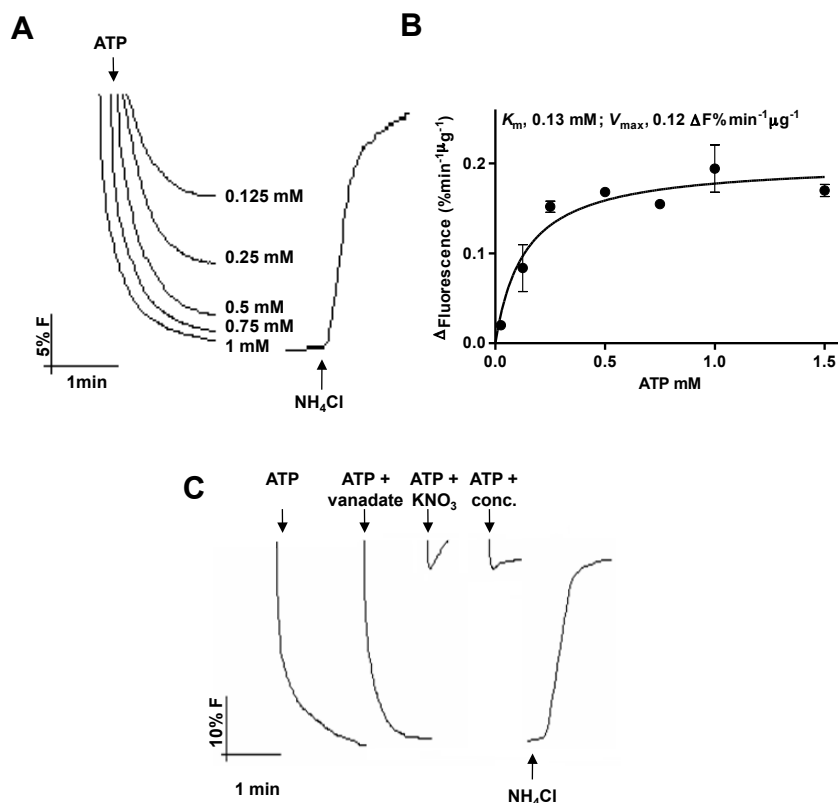
Figure 4. Pumping activities of V-H$^+$-ATPase in tonoplast vesicles isolated from *C. roseus* leaves measured by the fluorescence quenching of the pH-sensitive probe ACMA. A, H$^+$-pumping activity in tonoplast vesicles upon the addition of ATP. B, Michaelis-Menten plot of the initial rates of proton pumping in A. Values are the mean of three biological replicates. C, H$^+$ pumping activity in the presence of the P-H$^+$-ATPase inhibitor vanadate (100 μM) and the V-H$^+$-ATPase inhibitors KNO$_3$ (100 μM) and concanamycin (0.1 μM). Error bars indicate SD (n = 3).

Vindoline, catharanthine and AVLB, the main TIAs present in *C. roseus* mesophyll (Table I), promptly dissipated the proton gradient, indicating that catharanthine and AVLB are also incorporated into the vacuole by a H$^+$-dependent mechanism (Fig. 5A). A positive signal was also observed after addition of Ca^{2+} (Fig. 5A), in agreement with the known and observed capacity of the vacuoles to accumulate this cation (Fig. 2F; Hirschi 2001). On the contrary, the alkaloids atropine, ajmaline and papaverine, wich are not produced by *C. roseus,* did not dissipate the H$^+$ gradient (Fig. 5A). Significantly, vindoline did not affect the transtonoplast pH gradient of energized tonoplast vesicles isolated from grape (*Vitis vinifera*), a species that does not produce TIAs (Fig. 5B). The initial velocities of intravesicular alkalinisation upon addition of vindoline and AVLB

followed Michaelis-Menten kinetics, supporting the involvement of mediated transport for both substrates (Fig. 6A to D). Vindoline was shown to also induce fluorescence recovery in tonoplast vesicles energized with PPi (data not shown).
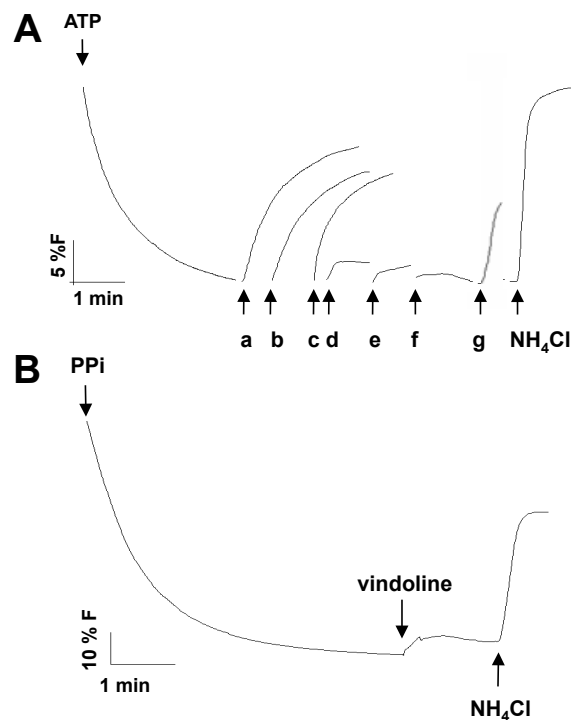
Figure 5. Effect of the addition of different solutes to a preestablished H^+ gradient measured by the fluorescence quenching of the pH-sensitive probe ACMA in tonoplast vesicles isolated from *C. roseus* leaves and grape cell cultures. A, Addition of different solutes to energized *C. roseus* tonoplast vesicles: 0.03 mM AVLB (a), 1 mM vindoline (b) and 0.075 mM catharanthine (c) from *C. roseus;* 1 mM atropine (d) from *Atropa belladonna*; 0.05 mM ajmaline (e) from *Rauwolfia serpentina*, 0.1 mM papaverine (f) from *Papaver somniferum*, and 0.15 mM $CaCl_2$ (g). B, Addition of 1 mM vindoline to energized grape tonoplast vesicles.

The hydrolytic activity of the V-H^+-ATPase in the presence of vindoline, catharanthine, or AVLB was also studied, to discard the possibility that the alkaloid-induced fluorescence recovery could be due to an alkaloid inhibition effect on the proton pump. The results showed that after a large incubation period (30 min) in the presence of high TIA concentrations (1 mM vindoline, 0.09 mM catharanthine, and 0.05 mM AVLB), there was a slight inhibition effect (11%, 28% and 6% respectively), by far not sufficient to explain the prompt and high fluorescence recovery observed (Fig. 5A and 6). Moreover, in proton transport assays, TIA addition prior to ATP did not significantly compromise the build up of a pH gradient across the tonoplast (data not shown), and the alkaloids atropine, ajmaline and papaverine did not cause any dissipation of the H^+ gradient, further indicating that alkaloids were not inhibitory under the conditions used in the spectrofluorimetry assays.

Altogether, results strongly indicated that TIAs dissipate the pH gradient in *C. roseus* vesicles due to the presence of a specific H^+/TIA antiport system.
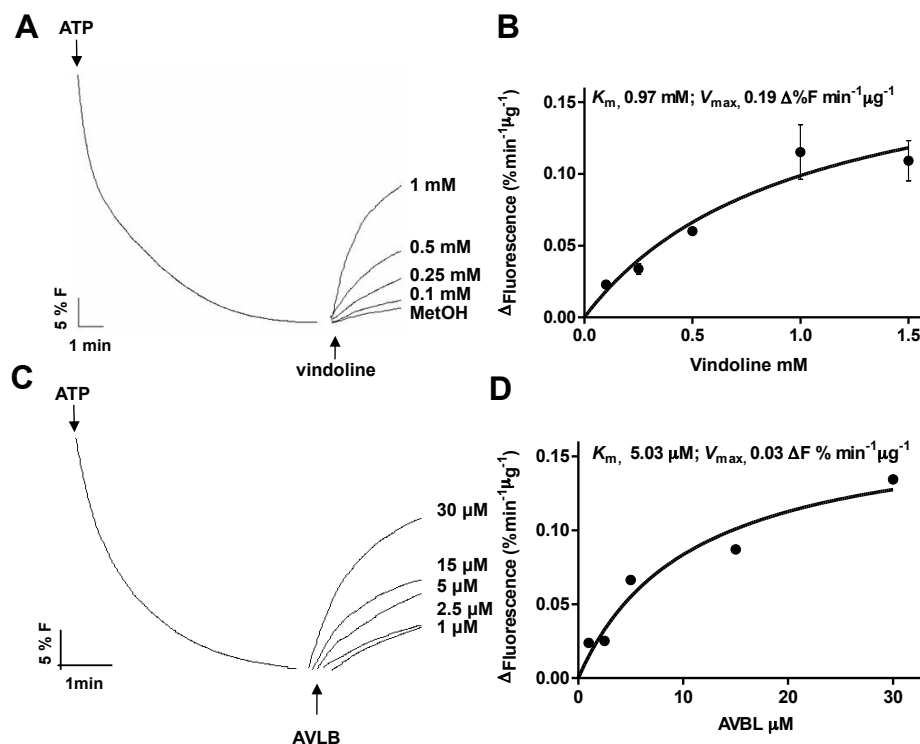
Figure 6. Proton-dependent transport of vindoline and AVLB in tonoplast vesicles isolated from *C. roseus* leaves. A, Dissipation of a preestablished H^+ gradient by different concentrations of vindoline, measured by the fluorescence recovery of the pH-sensitive probe ACMA. MetOH, Methanol. B, Michaelis-Menten plot of the initial rates of proton dissipation by vindoline in A. Error bars indicate S (n=3). C, Dissipation of a preestablished H^+ gradient by different concentrations of AVLB, measured by the fluorescence recovery of the pH-sensitive probe ACMA. D, Michaelis-Menten plot of the initial rates of proton dissipation by AVLB in C. Results in D are from one single experiment.

DISCUSSION

The membrane transport of plant secondary metabolites is still poorly characterized, but is emerging as a newly developing research area, due to their importance to understand metabolite fluxes and to implement metabolic engineering strategies aimed at increasing the levels of valuable secondary metabolites. In the case of alkaloids, their complex pathways involve several cell types and organelles, with a number of transmembrane steps being inferred (Shitan and Yazaki, 2007; Facchini and De Luca, 2008). Moreover, the final intracellular destination of most alkaloids is thought to be the vacuole, with the trans-tonoplast transport step putatively playing a key role for the final output of alkaloid metabolic fluxes. Here, a number of tools for the characterization of membrane transport of alkaloids in *C. roseus* were established, the vacuolar localization of the main TIAs accumulated in mesophyll cells was determined, and the vacuolar accumulation mechanism of those TIAs was elucidated.

In this study, protocols for the isolation of highly pure, functional vacuoles and tonoplast vesicles from *C. roseus* leaves were established. These methods may now be used for many studies concerning vacuolar functions in *C. roseus*. Both the vacuoles and the tonoplast vesicles samples isolated were shown to be highly pure, meeting the purity standards used in previous studies (Carter et al., 2004; Jaquinod et al., 2007). On the other hand, both isolated vacuoles and tonoplast vesicles were shown to be functionally active in what concerns transport activities, indicating the preservation of active membrane protein complexes and membrane integrity.

HPLC analysis of the alkaloids extracted from *C. roseus* leaves clearly shows that the main TIAs accumulated in *C. roseus* mesophyll cells are by far vindoline, catharanthine and AVLB (Supplemental Fig. S1). These are the direct precursors of the anticancer VLB and VCR (Fig. 1) and therefore their cellular accumulation mechanisms may be particularly important for the final levels of the anticancer TIAs. In *C. roseus*, TIAs have been shown to accumulate in the vacuoles by histochemical and cytological techniques (Yoder and Mahlberg, 1976; Neumann et al., 1983), the TIA serpentine was shown to accumulate mostly in the vacuoles of cell cultures (Deus-Neumann and Zenk, 1984), and immunocytochemical localization of vindoline indicated its major presence in the central vacuole and in small vesicles of mesophyll cells (Brisson et al., 1992). However, a thorough characterization of the subcellular accumulation of TIAs in the leaves of *C. roseus*, the only organ where the anticancer TIAs are accumulated, has not been performed. Our results here indicate that vindoline and catharanthine, two of the three main TIAs present in *C. roseus* leaves are localized mostly in the vacuoles (Table I). The third major TIA, AVLB, was not detected in isolated vacuoles but it is present in protoplasts, also suggesting vacuolar accumulation, since TIAs present in these naked cells can only be in the vacuole, sequestered away from the cytosol. This may suggest that, during vacuole isolation, AVLB is either lost by efflux or undergoes further metabolism or degradation, namely by the action of the vacuolar CrPrx1 (*Catharanthus roseus* peroxidase 1), which was shown to oxidate AVLB (Costa et al., 2008). Specific accumulation of AVLB in vesicles/peripheral small vacuoles, rather than in the central vacuole, cannot be discarded as well. The TIA contents observed for leaf isolated protoplasts and vacuoles are 5- to 10-fold higher than the content of the TIA serpentine quantified for isolated vacuoles of *C. roseus* cell cultures (Deus-Neumann and Zenk, 1984), and 13- to 17-fold lower than the nicotine content determined for tobacco mesophyll vacuoles (Saunders, 1979).

The primary localization of catharanthine in the vacuoles observed here contrasts with a previous study showing that catharanthine accumulates "exclusively" in leaf wax exudates (Roepke et al., 2010). According to these authors, this delocalization of

catharanthine relative to intracellular vindoline accounts for the low levels of the dimeric anticancer TIAs in *C. roseus* leaves. This is clearly not the case in the leaves of the *C. roseus* plants used in this study, since they accumulate high levels of AVLB (dimer), which can only result from co-localization of its monomeric precursors, catharanthine and vindoline. The differences observed in the two studies may result from the use of different cultivars, developmental stages and growth conditions, all factors that may likely affect the compartmentalization expression of the TIA pathway.

The observed vacuolar accumulation of vindoline together with previous localization studies indicating that the last biosynthetic step of vindoline occurs in the cytosol (Vazquez-Flota et al., 1997), suggest an intensive transport of vindoline across the tonoplast, which is most likely true for the other TIAs. The results obtained here strongly indicate that TIAs are accumulated in the vacuoles of *C. roseus* mesophyll cells by a specific proton antiport system, dependent on a trans-tonoplast pH gradient generated either by the V-H$^+$-ATPase or the V-H$^+$-PPase (Fig. 7).
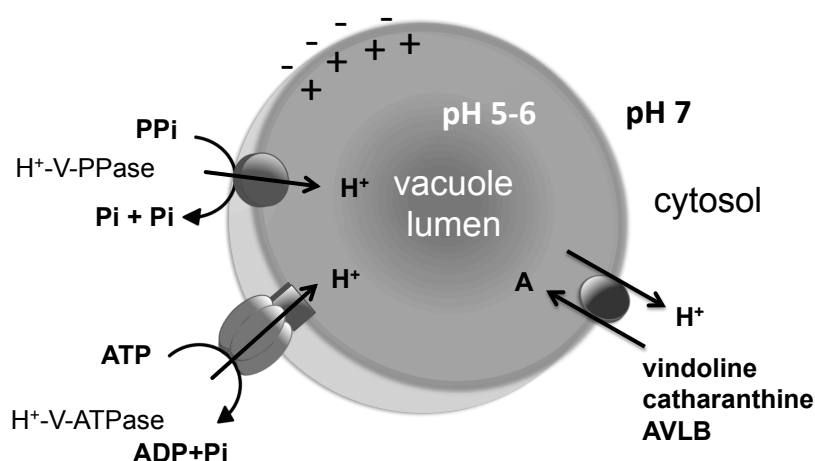
Figure 7. Model proposed for TIA vacuolar accumulation in *C. roseus* mesophyll cells. Cytosolic TIAs are actively transported into the vacuole by a proton antiport system dependent on the transtonoplast pH gradient generated by either of the two tonoplast vacuolar pumps, V-H$^+$-ATPase or V-H$^+$-PPase. Pi, Inorganic phosphate.

In fact, vindoline uptake was shown to be dependent on ATP (Fig. 3) and on the transtonoplast ΔpH, as supported by the observed inhibition with the H$^+$ gradient dissipators NH$_4$Cl and CCCP (Table II). In agreement, assays with the pH probe ACMA clearly indicated that several TIAs were capable of dissipating an ATP-dependent H$^+$ gradient and proton movements followed Michaelis-Menten kinetics (Fig. 5A and Fig. 6). Previously, TIAs have been suggested to accumulate in the vacuoles by an ion trap mechanism, in which the cytosolic neutral form of the basic alkaloid is capable of diffusing freely across the tonoplast to form a cation at the acidic vacuolar pH, becoming trapped inside this organelle (Guern et al., 1987; Renaudin, 1989; Blom et al., 1991).

FCUP 79

Unravelling the metabolism and transmembrane transport of the highly valuable medicinal alkaloids from *Catharanthus roseus*

Here, alkaloid uptake not only showed saturation (Fig. 6B and D), incompatible with this mechanism, but it was also alkaloid and species specific (Fig. 5), excluding the action of any unspecific mechanism such as ion trapping. The transmembrane transport of alkaloids may also be mediated by primary transport through ABC transporters, as in the case of berberine uptake across the plasma membrane of rhizome cells of *C. japonica*, where this alkaloid is accumulated upon translocation from the biosynthetic organ, the root (Shitan et al., 2003; Shitan et al., 2012). Vacuolar accumulation of other secondary metabolites such as anthocyanins was also shown to involve ABC transporters (Goodman et al., 2004). However, in the present study, vindoline accumulation by ATP energized tonoplast vesicles was clearly not affected by the ABC transporter inhibitor vanadate, and accumulation was also sustained by PPi energization, excluding the involvement of an ABC transporter as the principal tonoplast transporter for vindoline vacuolar accumulation.

The TIA transport assays indicate that the alkaloid transport system exhibits a higher affinity for AVLB and catharanthine than for vindoline (Fig. 5A and Fig. 6). Previous work from Deus Neumann & Zenk (1984) has actually estimated a K_m for vindoline in the range of the determined here for AVLB. However, the two studies are most likely not comparable, since those authors used vacuoles from cell suspension cultures, which do not produce vindoline, and seem to have determined reaction velocities at 90 min, possibly affecting K_m estimation. The concentration of vindoline *in planta*, estimated using the volume of protoplasts and vacuoles, is within the 1 mM range (Table I, r = 1,4 and 0.95 µm respectively). Yet, we have to take in consideration that only a fraction of cells should indeed accumulate vindoline (the idioblasts); thus its concentration must achieve much higher values, well above the vindoline K_m observed in this work. The dissimilar results for the different TIAs may be due to the involvement of different transport proteins, or of one protein type with different affinities for each substrate. On the other hand, the behavior of the transporters in isolated tonoplast vesicles may differ substantially from in vivo, where many factors may influence or actually regulate transporters activity. It must be stressed that the vacuolar transport activity determined here is not necessarily the single transport mode present in the diversity of *C. roseus* leaf cells.

Overall, the results gathered in this study are consistent with the early work from Deus Neumann & Zenk (1984) suggesting the involvement of an active, energy-requiring process with high specificity for the accumulation of ajmalicine and vindoline in the vacuoles of *C. roseus* cell cultures. Moreover, these results are consistent with the observed H^+-dependent vacuolar accumulation of the alkaloids berberine from *C. japonica* and nicotine from *N. tabacum* (Otani et al., 2005; Morita et al., 2009; Shoji et

al., 2009). In the case of nicotine, vacuolar transport was shown to be mediated by one of the three multidrug and toxic compound extrusion (MATE) transporters functioning as proton antiporters, which are differentially expressed in the root and the leaves of the plant (Morita et al., 2009; Shoji et al., 2009). Altogether, these results raise the question whether MATE transporters may be generally responsible for alkaloid vacuolar accumulation in plants. The plant MATE transporter subfamily is characterized by a high number of gene orthologs per species (58 in Arabidopsis), contrasting with bacterial and animal subfamilies (2 in humans), and suggesting an association with the highly diverse secondary metabolism found in plants (Omote et al., 2006).

CONCLUSION

In conclusion, this study strongly indicates that the important alkaloids from the medicinal plant *C. roseus*, namely vindoline, catharanthine and AVLB, are accumulated in the vacuoles of mesophyll cells by a specific proton antiport system, dependent on the transtonoplast pH gradient generated by V-H$^+$-ATPase and V-H$^+$-PPase (Fig. 7). This is in agreement with previous observations for the alkaloids berberine in *C. japonica* and nicotine in tobacco, and further supports a H$^+$ antiport mechanism as a general system for vacuolar accumulation of alkaloids in plants.

The approaches and results of this study open new perspectives to the search for vacuolar TIA transporter candidate genes, with MATE transporters being obvious targets. The question remains whether there is one vacuolar transporter with different affinities towards different TIAs, or there may exist an array of different vacuolar transporters with cell/organ differential localizations.

SUPPLEMENTAL MATERIAL

The following materials are presented in the end of the Chapter II.

Supplemental Figure S1. HPLC chromatogram of an alkaloid extract from *C. roseus* leaves.

Supplemental Figure S2. H$^+$ pumping activity in tonoplast vesicles upon addition of 1 mM of ATP in the presence (a) or in the absence (b) of an ATP regenerating system (10 mM of creatine phosphate plus 10 µg mL-1 of creatine kinase).

Supplemental Figure S3. Pumping activities of V-H$^+$-PPase in tonoplast vesicles and ATP and PPi hydrolytic activities in vacuoles and tonoplast vesicles isolated from C. roseus leaves.

Supplemental Figure S4. Pumping activity of V-H$^+$-PPase and V-H$^+$-ATPase in intact vacuoles from *C.roseus* leaves.

FCUP 81

Unravelling the metabolism and transmembrane transport of the highly valuable medicinal alkaloids from *Catharanthus roseus*

ACKNOWLEDGEMENTS

LITERATURE CITED

Ames BN (1966) Assay of inorganic phosphate, total phosphate and phosphatases. Methods Enzymol 8: 115–118.

Betz WJ, Mao F, Smith CB (1996) Imaging exocytosis and endocytosis. Curr Opin Neurobiol 6: 365-371.

Blom TJM, Sierra M, Van Vliet TB, Franke-Van Dijk MEI, De Koning P, Van Iren F, Verpoorte R, Libbenga KR (1991) Uptake and accumulation of ajmalicine into isolated vacuoles of cultured cells of Catharanthus roseus (L.) G. Don. and its conversion into serpentine. Planta 183: 170-177.

Bradford MM (1976) Rapid and Sensitive method for quantitation of microgram quantities of protein utilizing principle of protein-dye binding. Anal Biochem 72: 248-254.

Brisson L, Charest PM, De Luca V, Ibrahim RK (1992) Immunocytochemical localization of vindoline in mesophyll protoplasts of Catharanthus roseus. Phytochemistry 31: 465-470.

Carter C, Pan SQ, Jan ZH, Avila EL, Girke T, Raikhel NV (2004) The vegetative vacuole proteorne of Arabidopsis thaliana reveals predicted and unexpected proteins. Plant Cell 16: 3285-3303.

Costa MMR, Hilliou F, Duarte P, Pereira LG, Almeida I, Leech M, Memelink J, Barcelo AR, Sottomayor M (2008) Molecular cloning and characterization of a vacuolar class III peroxidase involved in the metabolism of anticancer alkaloids in Catharanthus roseus. Plant Physiol 146: 403-417.

Deus-Neumann B, Zenk MH (1984) A highly selective alkaloid uptake system in vacuoles of higher plants. Planta 162: 250-260.

Deus-Neumann B, Zenk MH (1986) Accumulation of alkaloids in plant vacuoles does not involve an ion-trap mechanism. Planta 167: 44-53.

Façanha AR, de Meis L (1998) Reversibility of H^+-ATPase and H^+-pyrophosphatase in tonoplast vesicles from maize coleoptiles and seeds. Plant Physiol 116: 1487-1495.

Facchini PJ, De Luca V (2008) Opium poppy and Madagascar periwinkle: Model non-model systems to investigate alkaloid biosynthesis in plants. Plant J 54: 763-784.

Ferreres F, Figueiredo R, Bettencourt S, Carqueijeiro I, Oliveira J, Gil-Izquierdo A, Pereira DM, Valentao P, Andrade PB, Duarte P, Barcelo AR, Sottomayor M (2011) Identification of phenolic compounds in isolated vacuoles of the medicinal plant Catharanthus roseus and their interaction with vacuolar class III peroxidase: an H_2O_2 affair? J Exp Bot 62: 2841-2854.

Fontes N, Silva R, Vignault C, Lecourieux F, Gerós H, Delrot S (2010) Purification and functional characterization of protoplasts and intact vacuoles from grape cells. BMC Res Notes 3:19.

Frangne N, Eggmann T, Koblischke C, Weissenbock G, Martinoia E, Klein M (2002) Flavone glucoside uptake into barley mesophyll and arabidopsis cell culture vacuoles. Energization occurs by H^+-antiport and ATP-binding cassette-type mechanisms. Plant Physiol 128: 726-733.

Goodman CD, Casati P, Walbot V (2004) A multidrug resistance-associated protein involved in anthocyanin transport in Zea mays. Plant Cell 16: 1812-1826.

Guern J, Renaudin JP, Brown SC (1987) The compartmentation of secondary metabolites in plant cell cultures. In F Constabel, IK Vasil, eds, Cell culture and somatic cell genetics of plants, Vol 4. Academic Press, San Diego, pp 43-76.

Guirimand G, Guihur A, Poutrain P, Héricourt F, Mahroug S, St-Pierre B, Burlat V, Courdavault V (2011) Spatial organization of the vindoline biosynthetic pathway in *Catharanthus roseus*. J Plant Physiol Volume 168: 549-557.

Hildreth SB, Gehman EA, Yang HB, Lu RH, Ritesh KC, Harich KC, Yu S, Lin JS, Sandoe JL, Okumoto S, Murphy AS, Jelesko JG (2011) Tobacco nicotine uptake permease (NUP1) affects alkaloid metabolism. Proc Natl Acad Sci USA 108: 18179-18184.

Hirschi KD (2001) Vacuolar H^+/Ca^{2+} transport: who's directing the traffic? Trends Plant Sci 6: 100–104.

Jaquinod M, Villiers F, Kieffer-Jaquinod S, Hugouvieu V, Bruley C, Garin J, Bourguignon J (2007) A proteomics dissection of Arabidopsis thaliana vacuoles isolated from cell culture. Mol Cell Proteomics 6: 394-412.

Jones KH, Senft JA (1985) An Improved Method to Determine Cell Viability by simnultaneous staining with fluorescein diacetate propidium iodide. J Histochem Cytochem 33: 77-79.

Laemmli UK (1970) Cleavage of strutural proteins during assembly of head of bacteriophage-T4. Nature 227: 680-685.

Lowry OH, Rosebrough NJ, Farr AL, Randall RJ (1951) Protein measurement with the folin phenol reagent. J Biol Chem 193: 265-275.

Maeshima M, Yoshida S (1989) Purification and properties of vacuolar membrane proton-translocating inorganic pyrophosphatase from mung bean. J Biol Chem 264: 20068-20073.

Mahroug S, Burlat V, St-Pierre B (2007) Cellular and sub-cellular organisation of the monoterpenoid indole alkaloid pathway in Catharanthus roseus. Phytochem Rev 6: 363-381.

Marinova K, Pourcel L, Weder B, Schwarz M, Barron D, Routaboul JM, Debeaujon I, Klein M (2007) The Arabidopsis MATE transporter TT12 acts as a vacuolar flavonoid/H+-antiporter active in proanthocyanidin-accumulating cells of the seed coat. Plant Cell 19: 2023-2038.

Martins V, Hanana M, Blumwald E, Gerós H (2012) Copper Transport and Compartmentation in Grape Cells. Plant Cell Physiol PMID: 22952251.

Morita M, Shitan N, Sawada K, Van Montagu MCE, Inzé D, Rischer H, Goossens A, Oksman-Caldentey KM, Moriyama Y, Yazaki K (2009) Vacuolar transport of nicotine is mediated by a multidrug and toxic compound extrusion (MATE) transporter in *Nicotiana tabacum*. Proc Natl Acad Sci USA 106: 2447-2452.

Murata J, Roepke J, Gordon H, De Luca V (2008) The leaf epidermome of Catharanthus roseus reveals its biochemical specialization. Plant Cell 20: 524-542.

Neumann D, Krauss G, Hieke M, Gröger D (1983) Indole alkaloid formation and storage in cell suspension cultures of *Catharanthus roseus*. Planta Med 48: 20-23.

Omote H, Hiasa M, Matsumoto T, Otsuka M, Moriyama Y (2006) The MATE proteins as fundamental transporters of metabolic and xenobiotic organic cations. Trends Pharmacol Sci 27: 587-593.

Otani M, Shitan N, Sakai K, Martinoia E, Sato F, Yazaki K (2005) Characterization of vacuolar transport of the endogenous alkaloid berberine in *Coptis japonica*. Plant Physiol 138: 1939-1946.

Queirós F, Fontes N, Silva P, Almeida D, Maeshima M, Gerós H, Fidalgo F (2009) Activity of tonoplast proton pumps and Na$^+$/H$^+$ exchange in potato cell cultures is modulated by salt. J Exp Bot 60: 1363-1374.

Renaudin JP (1989) Different mechanisms control the vacuolar compartmentation of ajmalicine in Catharanthus roseus cell cultures. Plant Physiol Biochem 27: 613-621.

Roepke J, Salim V, Wu M, Thamm AMK, Murata J, Ploss K, Boland W, De Luca V (2010) Vinca drug components accumulate exclusively in leaf exudates of Madagascar periwinkle. Proc Natl Acad Sci USA 107: 15287-15292.

Saunders JA (1979) Investigations of vacuoles isolated from Tobaco: I. Quantitation of Nicotine. Plant Physiol 64: 74-78.

Shitan N, Bazin I, Dan K, Obata K, Kigawa K, Ueda K, Sato F, Forestier C, Yazaki K (2003) Involvement of CjMDR1, a plant multidrug-resistance-type ATP-binding cassette protein, in alkaloid transport in *Coptis japonica*. Proc Natl Acad Sci USA 100: 751-756.

Shitan N DF, Dan K, Kato N, Ueda K, Sato F, Forestier C, Yazaki K (2012) Characterization of Coptis japonica CjABCB2, an ATP-binding cassette protein involved in alkaloid transport. Phytochemistry PMID: 22410351.

Shitan N, Yazaki K (2007) Accumulation and membrane transport of plant alkaloids. Curr Pharm Biotechnol 8: 244-252.

Shoji T, Inai K, Yazaki Y, Sato Y, Takase H, Shitan N, Yazaki K, Goto Y, Toyooka K, Matsuoka K, Hashimoto T (2009) Multidrug and Toxic Compound Extrusion-Type Transporters Implicated in Vacuolar Sequestration of Nicotine in Tobacco Roots. Plant Physiology 149: 708-718.

Sottomayor M, dePinto MC, Salema R, DiCosmo F, Pedreno MA, Barcelo AR (1996) The vacuolar localization of a basic peroxidase isoenzyme responsible for the synthesis of alpha-3',4'-anhydrovinblastine in *Catharanthus roseus* (L) G. Don leaves. Plant, Cell Environ 19: 761-767.

St-Pierre B, Vazquez-Flota FA, De Luca V (1999) Multicellular Compartmentation of Catharanthus roseus Alkaloid Biosynthesis Predicts Intercellular Translocation of a Pathway Intermediate. Plant Cell 11: 887–900.

van der Heijden R, Jacobs DI, Snoeijer W, Hallared D, Verpoorte R (2004) The Catharanthus alkaloids: Pharmacognosy and biotechnology. Curr Med Chem 11: 607-628.

Vazquez-Flota F, DeCarolis E, Alarco AM, DeLuca V (1997) Molecular cloning and characterization of desacetoxyvindoline-4-hydroxylase, a 2-oxoglutarate dependent dioxygenase involved in the biosynthesis of vindoline in *Catharanthus roseus* (L) G. Don. Plant Mol Biol 34: 935-948.

Vera-Estrella R, Barkla BJ, Higgins VJ, Blumwald E (1994) Plant defense response to fungal pathogens: activation of host-plasma membrane H^+-ATPase by elicitor-induced enzyme dephosphorylation. Plant Physiol 104: 209-215.

Verpoorte R, Lata B, Sadowska A, eds (2007) Biology and Biochemistry of Catharanthus roseus (L.) G. Don, Phytochemistry Reviews, Vol 6, Issue 2-3. Springer Verlag, The Netherlands.

Wink M (1993) The plant vacuole: a multifunctional compartment. J Exp Bot 44: 231-246.

Yoder LR, Mahlberg PG (1976) Reactions of alkaloid and histochemical indicators in laticifers and specialized parenchyma cells of *Catharanthus roseus* (Apocynaceae). Amer J Bot 63: 1167-1173.

Zheng HQ, Wang GL, Zhang L (1997) Alfalfa mosaic virus movement protein induces tubules in plant protoplasts. Mol Plant-Microbe Interact 10: 1010-1014.

SUPPLEMENTAL MATERIAL

Supplemental Figure S1. HPLC chromatogram of an alkaloid extract from *C. roseus* leaves.
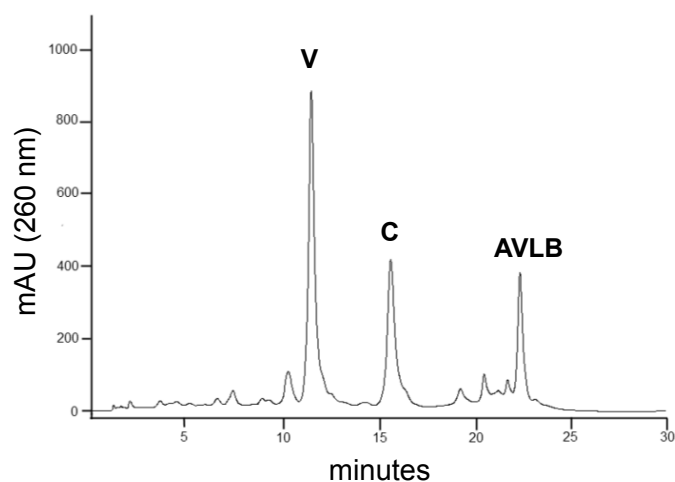
Figure S1. HPLC chromatogram of an alkaloid extract from *C. roseus* leaves showing the major presence of vindoline (V), catharanthine (C) and a-3',4'-anhydrovinblastine (AVLB).

Supplemental Figure S2. H^+ pumping activity in tonoplast vesicles upon addition of 1 mM of ATP in the presence (a) or in the absence (b) of an ATP regenerating system (10 mM of creatine phosphate plus 10 µg mL-1 of creatine kinase).
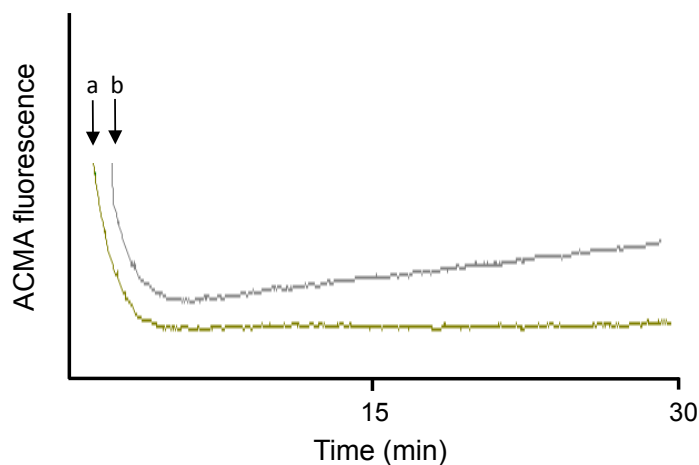
Figure S2. H^+ pumping activity in tonoplast vesicles upon addition of 1 mM of ATP in the presence (a) or in the absence (b) of an ATP regenerating system (10 mM of creatine phosphate plus 10 µg mL^{-1} of creatine kinase). In the absence of this regenerating system, after 1 min the system cannot maintain the H^+ gradient. The H^+ pumping activity was measured by the fluorescence quenching of the pH-sensitive probe ACMA.

FCUP | 87

Unravelling the metabolism and transmembrane transport of the highly valuable medicinal alkaloids from *Catharanthus roseus*

Supplemental Figure S3. Pumping activities of V-H$^+$-PPase in tonoplast vesicles and ATP and PPi hydrolytic activities in vacuoles and tonoplast vesicles isolated from C. roseus leaves.
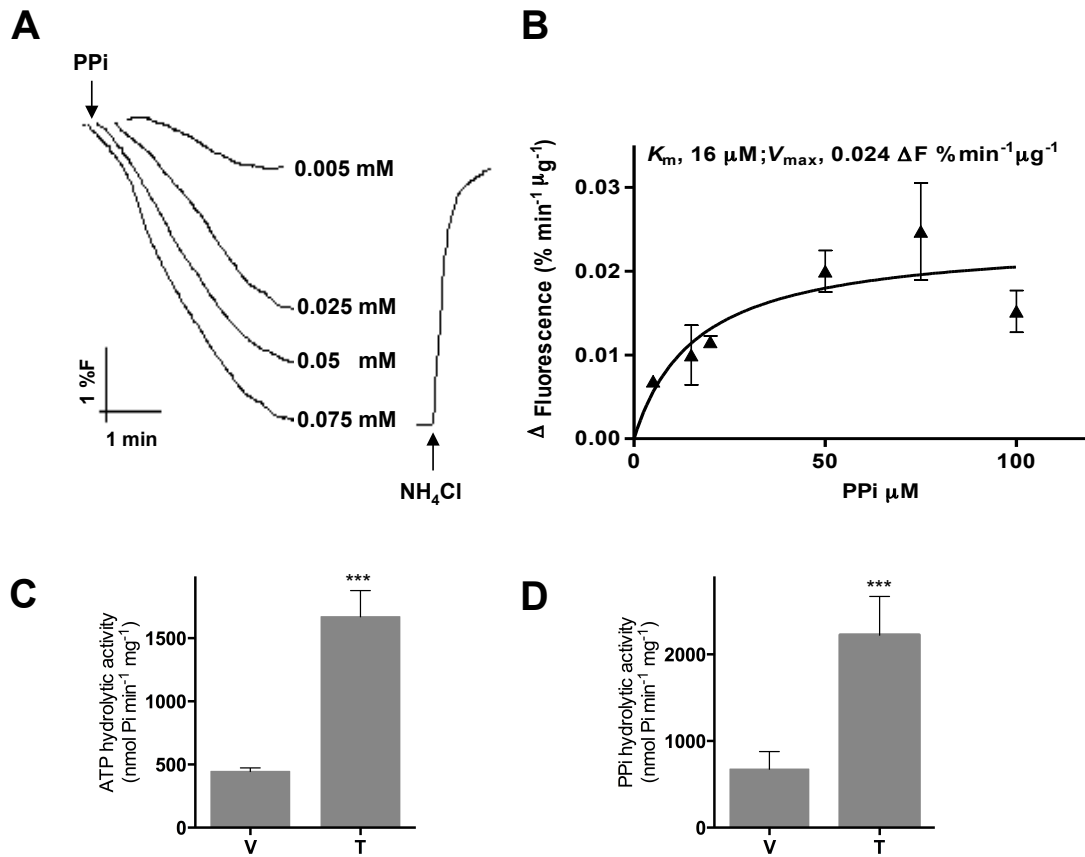
Figure S3. Pumping activities of V-H$^+$-PPase in tonoplast vesicles and ATP and PPi hydrolytic activities in vacuoles and tonoplast vesicles isolated from *C. roseus* leaves. A, H$^+$ pumping activity in tonoplast vesicles upon addition of PPi, measured by the fluorescence quenching of the pH-sensitive probe ACMA. B, Michaelis-Menten plot of the initial rates of proton pumping in A. Error bars indicate SD (n = 3). C, ATP hydrolytic activity of intact vacuoles (V) and tonoplast vesicles (T), in the presence of the P-H$^+$-ATPase inhibitor vanadate (100 μM) and the F-H$^+$-ATPase inhibitor azide (5 mM), to detect only the V-H$^+$-ATPase activity. D, PPi hydrolytic activity of intact vacuoles (V) and tonoplast vesicles (T). Statistical significance was evaluated using Student's *t* test for pairwise comparison (*** P < 0.001). Data significantly different are indicated. Error bars indicate SD (n = 3).

Supplemental Figure S4. Pumping activity of V-H$^+$-PPase and V-H$^+$-ATPase in intact vacuoles from *C.roseus* leaves.
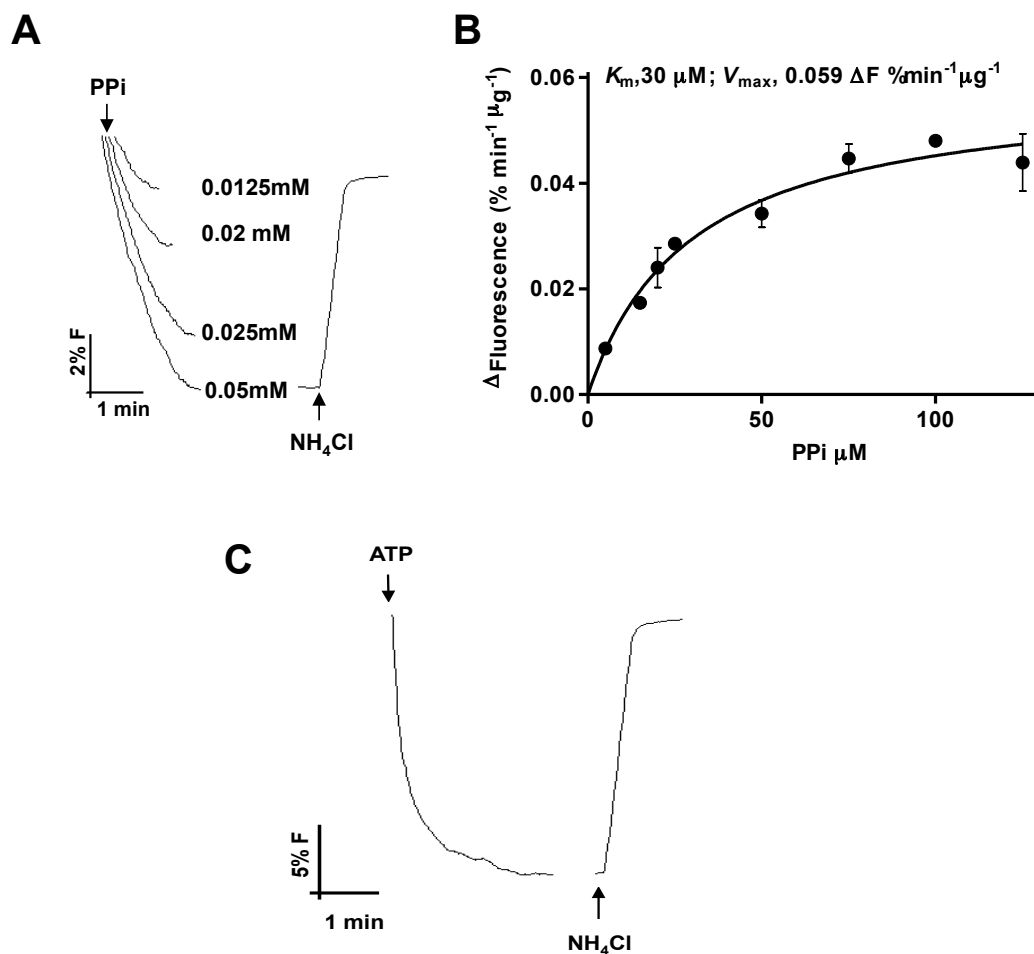
Figure S4. Pumping activity of V-H$^+$-PPase and V-H$^+$-ATPase in intact vacuoles from *C.roseus* leaves. A, H$^+$ pumping activity in intact vacuoles upon addition of PPi, measured by the fluorescence quenching of the pH-sensitive probe ACMA. B Michaelis-Menten plot of the initial rates of proton pumping in A. C, H$^+$ pumping activity in intact vacuoles upon addition of ATP, measured by the fluorescence quenching of the pH-sensitive probe ACMA. Error bars indicate SD (n = 3).

Chapter

III

The proteome of a toxic vacuole: analysis of the leaf vacuoles from the alkaloid producing plant *Catharanthus roseus*

The proteome of a toxic vacuole: analysis of the leaf vacuoles from the alkaloid producing plant *Catharanthus roseus*

Inês Carqueijeiro[1,2], Francisco Lima[1,2], Sara Bettencourt[1,2], Stephane Claverol[3], Marc Bonneu[3], Patrícia Duarte[1], Mariana Sottomayor[1,2]*

[1]IBMC – Instituto de Biologia Molecular e Celular, Universidade do Porto, Rua do Campo Alegre, 823, 4150-180 Porto, Portugal;

[2]Departamento de Biologia, Faculdade de Ciências da Universidade do Porto, Rua do Campo Alegre s/n 4169-007 Porto, Portugal;

[3]CGFB – Plateforme Protéome, Université Bordeaux Segalen, France.

Inês Carqueijeiro declares to have participated actively in this work, by contributing to the experimental design, performing most of the experiments, and by contributing to manuscript writing.

ABSTRACT

Vacuoles occupy most of the volume of plant cells and it is now clear that they play an array of key roles for plant cell physiology, still under debate. Among their functions, vacuoles are the accumulation target of many of the myriad of natural products produced by plants, providing a compartment where these compounds can exert their defence toxic effect without interfering with current cell physiology. Plant alkaloids are known by their characteristic toxicity often associated with pharmacological activity, and one of the best studied alkaloid accumulating plants is *Catharanthus roseus* (L.) G. Don. This plant has a particularly prolific alkaloid metabolism, producing over 130 different terpenoid indole alkaloids (TIAs), including the anticancer drugs vinblastine and vincristine, accumulated in very low levels in the plant leaf vacuoles. In spite of their importance for TIA metabolic fluxes, no tonoplast TIA transporters have been identified to date. In this work, the full proteome of the vacuole from *C. roseus* leaf cells was investigated, aiming to obtain the functional portrait of this alkaloid accumulating defence/toxic organelle and to identify candidate genes implicated in the transmembrane transport of the medicinal TIAs. Whole vacuoles and tonoplast membranes were isolated with high purity and a comprehensive characterization of the proteomic complement of these fractions was performed using state-of-the-art technologies. Running of the peptide sequence information obtained against the Medicinal Plant Genomics Resource transcriptomic database allowed the identification of 1886 putative proteins that indicate a high commitment of the *C. roseus* leaf vacuoles with secondary metabolism and defence, including the identification of several ABC and MATE transporters, and with redox homeostasis, including the identification of many key anti-oxidant enzymes. Apart from the well-known involvement in lytic reactions, it was shown that the *C. roseus* leaf vacuoles also present signs of a significant metabolic activity and of a possible association of innumerable transporters and signalling proteins in membrane microdomains, to form signalling platforms regulating trans-tonoplast fluxes. A significant presence of cytochrome P450 electron transfer chains was observed in the tonoplast, and the proteins Rubisco small chain and catalase were consistently detected, suggesting these may be "moonlighting" proteins, exhibiting activities distinct from their classically identified functions. Overall, the extensive proteome of the toxic vacuole from *C. roseus* leaves produced here constitutes an invaluable tool for current and future research on the multiple functions of this organelle.

INTRODUCTION

Contrary to old assumptions, plant vacuoles are much more than just a sink organelle. In the last decades, this large organelle that can occupy up to 90% of the cell volume has been implicated in diverse functions such as maintenance of the turgor pressure needed for support of the plant body and cell growth, storage and accumulation of inorganic ions, amino acids, proteins, sugars and secondary compounds, sequestration and inactivation of toxic compounds, cell homeostasis, signal transduction and plant development (Endler et al., 2006; Jaquinod et al., 2007; Zouhar and Rojo, 2009). Being big is also a quite important function of vacuoles, since this allows rapid cellular growth at a low cost, essential for plants to cope with the challenges of being a sessile organism.

The current view is that not all the above mentioned functions are accumulated by a single multifunctional vacuole, but are rather performed in a complementary way by two main different types of vacuoles, the lytic vacuole (LV) and the protein storage vacuole (PSV), who may fuse to yield a hybrid vacuole (Zouhar and Rojo, 2009). These two types of vacuoles are namely distinguishable by a different pH (acidic for LVs, neutral for PSVs), by the presence of proteases in the LVs and storage proteins in the PSVs, and by the differential presence of specific isoforms of aquaporins/tonoplast intrinsic proteins (TIPs) - α- and δ-TIPs in PSVs and γ-TIPs in LVs. However, this paradigm has recently been put in question by several authors (Hunter et al., 2007; Olbrich et al., 2007; Frigerio et al., 2008), who claim that the presence of two vacuole types may be an exception rather than the rule, with most plant cells possessing a single hybrid vacuole.

One of the important features of vacuoles is that they constitute the cellular accumulation target for most of the myriad of secondary metabolites that plants produce, including phenolics (e.g. anthocyanins), alkaloids, terpenoids, cyanogenic glucosides, glucosinolates, and betanins. These compounds have functions ranging from defence against herbivores, pathogens or UV light, to chemical signalling during many types of interaction with other organisms, but quite often their precise functions are unknown (Wink, 1993; Hartmann, 2007). Many of these secondary metabolites are toxic for cells, at least at the concentrations in which they are accumulated, and they are sequestered in the vacuole. How these compounds are transported across the tonoplast is an emerging field, with only in a few cases being characterized so far (Martinoia et al., 2012).

Catharanthus roseus is a paradigmatic example of a plant whose secondary metabolism has been extensively investigated, due to the pharmacological importance of its terpenoid indole alkaloids (TIAs), the anticancer vinblastine (VLB) and vincristine

(VCR), the antihypertensive ajmalicine, and the sedative serpentine (van der Heijden et al., 2004; Verpoorte et al., 2007). The great pharmacological importance of the anticancer alkaloids, allied to its low abundance in the plant leaves (around 0.0005% DW), stimulated intense research of the TIA pathway, and *C. roseus* has become a model species for many aspects of plant secondary metabolism. *C. roseus* was shown to accumulate more than 130 different TIAs, and VLB biosynthesis was shown to include at least 30 steps from primary metabolism, of which 13 have been characterized (Loyola-Vargas et al., 2007). Moreover, the TIA pathway was shown to have a complex subcellular compartmentation with intermediary steps localized in plastids, the cytosol and the vacuole, and a multi-cellular compartmentation, with early steps occurring in the leaf epidermal cells and late steps occurring in leaf laticifers and idioblast cells (Fig. 1; Mahroug et al., 2007; Guirimand et al., 2011a; 2011b). This complex organization predicts the involvement
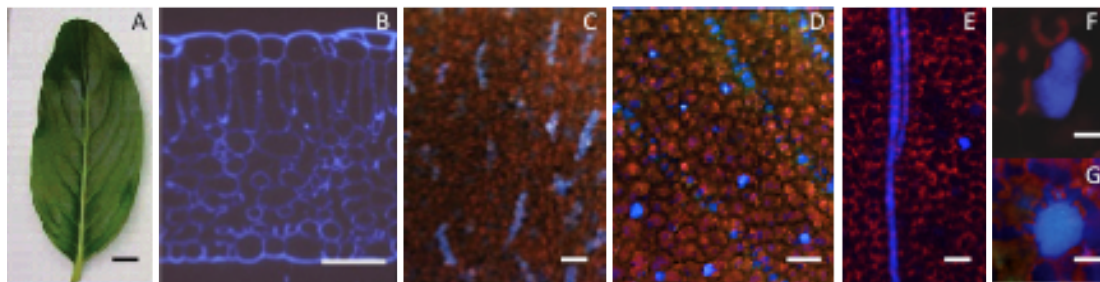
Figure 1. Different aspects of *C. roseus* leaves, the only plant organ producing and accumulating the anticancer VLB and VCR. A, Fully developed leaf. B, Leaf cross section showing the different leaf tissues. C, Epifluorescence microscopy image of the abaxial face of a whole mounted leaf. D, Epifluorescence microscopy image of the adaxial face of a whole mounted leaf. E, Confocal microscope tangential section of the palisade parenchyma showing two lacticifers. F and G, Epifluorescence microscopy images of idioblast cells in the adaxial face of a whole mounted leaf. Blue fluorescence is due to the alkaloid serpentine and reveals alkaloid containing idioblast and laticifer cells. Red fluorescence is due to chlorophyll. Bars = 0.5 cm (A), 100 μm (B to E), 20 μm (F,G).

of a significant number of transmembrane transport events along the TIA pathway with great importance for TIA metabolic fluxes. This stands true particularly in what concerns the vacuoles, since they are the final accumulation target of TIAs, where alkaloids are thought to function as a toxic defence, stored away from the basic plant cell metabolism with which they could interfere (Deus-Neumann and Zenk, 1984; Blom et al., 1991; Wink, 1993; Carqueijeiro et al., 2013; Chapter II). Recently, we have characterized the TIA vacuolar accumulation step, showing that the main TIAs from *C. roseus* leaves are accumulated in leaf vacuoles by a highly specific H^+ antiport system (Carqueijeiro et al., 2013; Chapter II), similarly to what has been observed for the alkaloid berberine in *Coptis japonica* (Otani et al., 2005) and the alkaloid nicotine in tobacco (Morita et al.,

2009). As has been characterized for nicotine, it was hypothesized that the vacuole accumulation of TIAs may be mediated by a MATE transporter.

Here, in order to investigate further the complexity of biological functions of the vacuoles, namely in what concerns their importance for secondary metabolism and respective compartmentation mechanisms, a strategy for the characterization of the proteome of the toxic vacuoles from *C. roseus* leaf cells was implemented. The detailed analysis of the identified complement of vacuolar proteins under the light of current knowledge, sets forth important new conclusions concerning the multiple roles of vacuoles.

MATERIAL AND METHODS

Plant material

Catharanthus roseus (L.) G. Don cv. Little Bright Eye plants were grown at 25 °C in a growth chamber, under a 16 h photoperiod, using white fluorescent light with a maximum intensity of 70 µmol m^{-2} s^{-1}. Seeds were acquired from AustraHort (Australia) and voucher specimens are deposited at the Herbarium of the Department of Biology of the Faculty of Sciences of the University of Porto (PO 61912). Plants used for vacuole/tonoplast membranes isolation were 6 to 8 months old.

Isolation of *C. roseus* leaf protoplasts

The isolation of leaf protoplasts was performed as described in Carqueijeiro et al. (2013;Chapter II). Visualization of the fluorescent probe FDA was performed using an excitation wavelength of 488 nm and an emission wavelength window from 500 to 650 nm.

Isolation of *C. roseus* leaf vacuoles

Isolation of *C. roseus* leaf vacuoles was performed according to Robert et al. (2007) with minor modifications. The isolated leaf protoplasts were centrifuged at 65 *g* for 5 min at RT, and the protoplast pellets were chilled for at least 30 min on ice. Vacuoles were released by resuspending the protoplasts in lysis buffer consisting of 0.2 M mannitol, 10 % (w/v) Ficoll 400, 10 mM EDTA and 5 mM sodium phosphate pH 8.0 at 37 °C, pipetting up and down 5-8 times with a serological pipette, and incubating at room temperature (RT) for 4 min. The lysed suspension was transferred into an ultra-clear centrifuge tube using a 5 mL micropipette and overlaid with 3 mL of 4% Ficoll in a 4.5:3 mixture of lysis and vacuole buffers at RT, and with 1 mL of ice-cold vacuole buffer consisting of 0.45 M mannitol, 2 mM EDTA, 2 mM DTT and 5 mM sodium phosphate pH 7.5. Isolated vacuoles were recovered in the upper layer of vacuole buffer after centrifugation at

71,000 *g*, for 1 h, at 10 ºC, in a Beckman ultracentrifuge Optima™ L80-XP with acceleration and deceleration in level 6. Vacuoles were stained with neutral red for visualization under the optical microscope and counted using a haemocytometer. Vacuoles were also visualized by labeling with the membrane marker FM1-43 (10 µM), for 30 min, at room temperature, in the dark (Betz et al., 1996), and fluorescence was examined using a SP2 AOBS SE confocal microscope (LEICA) equipped with a scan head with an argon laser, using an excitation wavelength of 488 nm and an emission wavelength window from 500 to 650 nm.

Isolation of *C. roseus* leaf tonoplast vesicles

Leaf tonoplast vesicles were isolated according to Carqueijeiro et al. (2013; Chapter II). After isolation, tonoplast vesicles were washed twice with ice-cold 1x PBS buffer by centrifugation at 100,000 *g* for 45 min at 4 ºC. The final pellet of tonoplast vesicles was resuspended in 1 mM DTT, 15 % (v/v) glycerol, 1 mM EDTA and 20 mM Tris-HCl pH 7.5, frozen with N_2 liquid and kept at -80 °C. Protein quantification was performed using the method described by Lowry et al. (1951).

Protein extraction and quantification

For protein extraction, protoplasts, vacuoles and tonoplast vesicles in the respective isolation buffers were frozen at -80 °C and lyophilised for 2 days in a freeze–dry Edwards apparatus. Lyophilised samples were reconstituted in 1 mM NaCl, 1 mM $CaCl_2$, 1mM $MgCl_2$, and 1 mM $MnCl_2.4H_2O$, dialysed against the same saline solution and stored at -20 °C until use. Protein extraction from *C. roseus* leaves was previously described by Ferreres et al. (2011). Protein concentration of the dialyzed samples was determined according to the method described by Bradford (1976).

Western blot analysis

Protein samples obtained as described above were separated on 10% acrylamide gels as described by Laemmli (1970). For the immuno-detection of soluble proteins, samples were boiled for 2 min prior to gel loading, while for the immuno-detection of membrane proteins, protein samples were heated at 70°C for 10 min and immediately loaded onto the gel. The amount of protein loaded was 10 µg, except for the extract of tonoplast vesicles used for V-H$^+$-ATPase and V-H$^+$-PPase detection, where 1 µg was used. Proteins were transferred to a nitrocellulose membrane for 1 h and 30 min at 100 V, according to the method described by Burnette (1981). For the immuno-detection of membrane proteins, the amount of SDS added to the transfer buffer was 0.03 %. Membranes were blocked for 1 h at RT in Tris-buffered saline (TBS) containing 0.1 %

(v/v) Tween-20 (TBS-T) with 5 % (w/v) skimmed milk powder, 1 % (w/v) BSA, 0.1 % (v/v) goat serum and 0.05 % (v/v) Tween-20. Membranes were probed against the different primary antibodies, at the appropriate dilutions (see below) for 1 h at RT in blocking solution, washed three times for 10 min with TBS-T, and incubated with a peroxidase conjugated goat anti-rabbit secondary antibody (Santa Cruz Biotechnology, Inc) at 1:7500 dilution in TBS-T for 45 min at RT. After washing three times for 10 min with TBS-T, the membranes were washed twice with ddH$_2$O and detection was performed with the *chemiluminescent substrate* ECL™ (GE Healthcare, Lifesciences), using manufacturer instructions. The following primary antibodies were used: an ER marker – rabbit anti-serum raised against calreticulin (a gift from J. Denecke, University of Leeds) at a 1:10000 dilution; a chloroplast marker – rabbit anti-serum raised against the chloroplast inner envelope TIC 40 protein (#AS 10709-10, AGRISERA, Germany) at a 1:2500 dilution; two tonoplast markers – rabbit anti-sera raised against a V-H$^+$-ATPase (#AS 07213, AGRISERA, Germany) and against a V-H$^+$-PPase (Maeshima and Yoshida, 1989) both at a 1:2000 dilution.

Determination of ATP and PPi hydrolytic activities

Rates of ATP and PPi hydrolysis were determined by measuring the release of inorganic phosphate (Pi) according to Vera-Estrella et al. (2004) with some modifications described in Carqueijeiro et al. (2013; Chapter II). For leaves, total protein extracts obtained as described by Ferreres et al. (2011) were used. For protoplasts, vacuoles and tonoplast vesicles, hydrolytic activities were assayed in fractions after freezing and thawing. Fifteen µg of total protein were used for each assay. For the determination of V-H$^+$-ATPase hydrolytic activity, two different inhibitors were used, the F-H$^+$-ATPase inhibitor sodium azide at 0.5 mM, and the P-H$^+$-ATPase inhibitor vanadate at 0.1 mM.

Proton transport assays

ATP and PPi proton-dependent transport across the tonoplast was measured as the initial rate of fluorescence quenching of ACMA, according to Façanha and de Meis (1998), with minor modifications described in Carqueijeiro et al. (2013; Chapter II). A volume of tonoplast vesicles corresponding to 100 µg of tonoplast proteins was used in each reaction. 1.5 mM NH$_4$Cl was added to confirm the establishment of a H$^+$ gradient. Fluorescence quenching was registered by a LS-5B fluorescence spectrophotometer (Perkin-Elmer) at excitation and emission wavelengths of 415 nm and 485 nm respectively. Reactions were performed at RT. Experimental data was analyzed with the GraphPad Prism software.

Alkaloid extraction and HPLC-DAD analysis

Alkaloid extraction and HPLC-DAD analysis were performed as described by Sottomayor et al. (1996). Biological material was always lyophilized prior to extraction.

Protein extraction from vacuoles and tonoplast vesicles for proteomic analysis

Vacuoles kept at -80 °C for at least one overnight were lyophilized for 2 days in a freeze–dry Edwards apparatus. Lyophilised vacuoles were reconstituted in PBS ice-cold buffer and defrost tonoplast membranes were diluted in the same buffer. Protein extraction was performed as described by Fontes (2010). In brief, 1 volume of SDS extraction buffer consisting of 2% SDS, 60 mM DTT and 40 mM Tris-HCl pH 6.8 was added to the samples. The mixture was vortexed, heated at 100 ºC for 5 min, and immediately changed to ice. Proteins were precipitated by adding half volume of 1:1 trichloroacetic acid/acetone with 60 mM DTT, vortexing and incubating at -20 °C for 1 h and 30 min. The samples were then centrifuged at 16,000 g for 20 min at 4 °C and the dried pellet was washed three times with 80 % acetone supplemented with 60 mM DTT. The final pellet was dried in a speed vacuum and kept at -80°C until use.

Sample preparation and protein digestion

Proteins samples were solubilized in Laemmli buffer and loaded onto 10% acrylamide SDS-PAGE. After colloidal blue staining, each lane was systematically cut in 8 slices of equal volume. Gel slices were destained in 25 mM ammonium bicarbonate and 50% acetonitrile (ACN), rinsed twice in ultrapure water and shrunk in ACN for 10 min. After ACN removal, gel slices were dried at room temperature, covered with the trypsin solution (10 ng/µL in 40 mM NH_4HCO_3 and 10% ACN), rehydrated at 4 °C for 10 min, and finally incubated overnight at 37 °C. After addition of 40 mM NH_4HCO_3 and 10% ACN, slices were incubated for 15 min at room temperature with rotary shaking. The supernatant was collected, and an H_2O/ACN/HCOOH (47.5:47.5:5) extraction solution was added onto gel slices for 15 min. The extraction step was repeated twice. All supernatants were pooled and concentrated in a vacuum centrifuge to a final volume of 45 µL. Digests were finally acidified by addition of 1.5 µL of formic acid (5 %, v/v) and stored at -20 °C.

nLC-MS/MS analysis

The peptide mixtures were analysed on an Ultimate 3000 nanoLC system (Dionex) coupled to a nanospray LTQ-Orbitrap XL mass spectrometer (ThermoFinnigan, San Jose, CA). Ten microliters of peptide digests were loaded onto a 300-µm-inner diameter

x 5-mm C18 PepMapTM trap column (LC Packings) at a flow rate of 30 µL/min. The peptides were eluted from the trap column onto an analytical 75-mm id x 15-cm C18 Pep-Map column (LC Packings) with a 5–40% linear gradient of solvent B in 35 min (solvent A was 0.1% formic acid in 5% ACN, and solvent B was 0.1% formic acid in 80% ACN). The separation flow rate was set at 200 nL/min. The mass spectrometer operated in positive ion mode at a 1.7-kV needle voltage and a 30-V capillary voltage. Data were acquired in a data-dependent mode, alternating an FTMS scan survey over the range *m/z* 300–1700 and six ion trap MS/MS scans with CID (Collision Induced Dissociation) as activation mode. MS/MS spectra were acquired using a 3-*m/z* unit ion isolation window and normalized collision energy of 35. Mono-charged ions and unassigned charge-state ions were rejected from fragmentation. Dynamic exclusion duration was set to 30s.

Database search and results processing

Data were searched by SEQUEST through Proteome Discoverer 1.4 (Thermo Fisher Scientific Inc.) against the protein database downloaded from MPGR (63,623 entries; http://medicinalplantgenomics.msu.edu/integrated_searches.shtml; Gongora-Castillo et al. 2012). Spectra from peptides higher than 5000 Da or lower than 350 Da were rejected. The search parameters were as follows: mass accuracy of the monoisotopic peptide precursor and peptide fragments was set to 10 ppm and 0.8 Da respectively. Only b- and y-ions were considered for mass calculation. Oxidation of methionines (+16 Da) was considered as variable modification. Two missed trypsin cleavages were allowed. Every eight LC-MS/MS run were searched together and peptide validation was performed using Percolator algorithm (Kall et al., 2007) and only "high confidence" peptides were retained corresponding to a 1% False Positive Rate at peptide level. Results are given as "grouped" listing so as to present the minimal number of proteins covering all detected peptides. Hits with score below 1.6 and identified by one peptide only were not included in the final list of proteins. Proteome Discoverer calculated the "Protein Area" by averaging peak area of the three most abundant distinct peptides identified for the protein (maximum three, minimum two, if only two were available), according to Silva et al. (2006). Relative abundance of each protein in the sample was then calculated as a percentage of the total sum of "Protein areas".

The grouped list of MPGR accessions and respectively assigned peptides was submitted to the Mercator programme of the MapMan platform (Usadel et al., 2005) to organize the predicted *C. roseus* proteins into functional categories. Mercator submitted the peptides to blast search against the following databases of plant proteins: TAIR 9; SwissProt / UniProt Plant Proteins; TIGR5 rice proteins. All blast hits with bitscore < 70

FCUP 99

Unravelling the metabolism and transmembrane transport of the highly valuable medicinal alkaloids from *Catharanthus roseus*

% were excluded and all sequences were scanned by MapMan for known motifs and families using Interproscan. The identified proteins were divided into functional categories using the MapMan software (version 3.5.1R2) based on similarities with *Arabidopsis* proteins (Thimm et al., 2004).

Construction of GFP Fusion Proteins and transient expression in *C. roseus* mesophyll protoplasts

The full coding sequence of CroMATE1 was isolated by RT-PCR using leaf mRNA extracted from protoplasts, which, in turn, were isolated from 7 months old plants. The following primers, already including extensions with the required restriction sites for cloning were used: for *MATE1-sGFP* fusion, 5'-AGCCGTCGACATGGGTTCCAAACAA AACTATGAAATAAACC-3' and 5'-GATGACATGTATCCTGAACCAGATTCATTGGACA AAGATTTTGGCTTG-3'; for *sGFP-MATE1* fusion, 5'-CAAGATCTCTATGGGTTCCAAA CAAAACTATGAAATAAACC-3' and 5'-CGCCTCGAGTTATTCATTGGACAAAGATTTT GGCTTGTCC-3'. In order to generate the construct *35S::MATE1-sGFP*, the adequate amplified product was cloned in frame in pTH-2 after the 35S promoter, and to generate the construct *35S::sGFP-MATE1,* the adequate amplified product was cloned in frame in pTH2-BN, after the 3' end of *GFP*.

The plant expression vector pMON999e35S obtained from Prof. Theodorus W. J. Gadella (University of Amsterdam) was used to clone the construct *35S::SP-sCFP4-AtAGP58,* with AtAGP58 corresponding to an arabinogalactan protein (AGP) anchored to the plasma membrane. sCFP4 (mTurquoise) (Goedhart et al., 2010) was amplified by PCR from a plasmid pMON999e35S already harboring sCFP4, also obtained from Prof. Theodorus W. J. Gadella, using the following primers adding the required restriction sites: *sCFP4Fw_EcoRI,* 5'-CGGAATTCATGGTGAGCAAGGGCGA-3' and *sCFP4Rv_SacI,* 5'-TTGAGCTCCTTGTACAGCTCGTCCA-3'. *AtAGP58* was amplified by PCR from the cDNA clone RAFL04-13-J15, n° pda00292, purchased from the Riken BioResource Center. The signal peptide (SP) sequence was predicted using SignalP (Emanuelsson et al., 2007) and amplified using the following primers adding the required restriction sites: *SP58Fw_BglII,* 5'-ATTAGATCTATGGCCTCTTCTTTCTCT-3' and *SP58Rv_EcoRI*, 5'- ATGAATTCAGC TTGAGCTAAAGAGAAAGG-3'. The *AtAGP58* sequence codifying only the AtAGP58 mature protein was amplified using the following primers adding the required restriction sites: *MP58Fw_SacI*, 5'-ATGAGCTCCAAGCT CCCATGATGGC-3') and *MP58Rv_BamHI*, 5'-ATGGATCCTCAAACGAGGAGAAAT GGG-3'. The amplified sCFP4 was cloned in pMON999e35S using EcoRI/SacI to generate the construct *35S::sCFP4*, which was used to clone *AtAGP58 SP* using *Bgl*II/*Eco*RI, to generate the construct 35S::SP-sCFP4. This latter was used to insert the

mature protein of *AtAGP58* at the 3' of CFP with *Sac*I/*Bam*HI, to generate the construct *35S::SP-sCFP4-AtAGP58*.

Transient expression in *C. roseus* leaf protoplasts was performed as described by Duarte et al. (2011).

RESULTS AND DISCUSSION

Isolation and purity of vacuole and tonoplast membrane fractions from *C. roseus* leaves

In order to investigate the vacuolar proteome of *C. roseus* leaf cells with a thorough coverage, namely of membrane proteins, vacuoles and tonoplast membranes were isolated from *C. roseus* leaves. Vacuole isolation involved first the optimization of a procedure to isolate leaf protoplasts. Isolated protoplasts showed no apparent membrane damage or disintegration of the internal structure when the optimized method was used (Fig. 2A), and presented 95 to 98% viability as validated by staining with fluorescein diacetate (FDA; Fig. 2B). After testing a number of different methods for high yield isolation of vacuoles from protoplasts, the method of Robert et al. (2007) with minor modifications was selected. Vacuoles were released through osmotic/temperature shock followed by purification in a Ficoll gradient to yield a preparation showing no detectable protoplast, chloroplast, or vesicles contamination (Fig. 2, C and D). The isolated vacuoles accumulated neutral red, indicating that a transmembrane pH gradient was maintained inside the organelles, confirming the integrity of the tonoplast (Fig. 2, C and D).

The purity of the vacuole fraction and of tonoplast membranes isolated by density gradient centrifugation was investigated by immunoblotting (Fig. 2E). Both preparations showed absence of labelling with antibodies raised against an ER-resident protein (calreticulin) and a chloroplast inner envelope protein (TIC 40). At the same time they showed a much more intensive labelling with antibodies raised against the vacuolar markers vacuolar H^+-ATPase (V-H^+-ATPase) and vacuolar H^+-pyrophosphatase (V-H^+-PPase), when compared to protoplasts (Fig. 2E). The absence of contamination with plasma membrane and mitochondria was confirmed measuring the ATP hydrolytic activity in the presence of the plasma membrane P-H^+-ATPase inhibitor orto-vanadate and the mitochondria F-H^+-ATPase inhibitor azide, since neither of the fractions showed any significant inhibition (Fig. 2F). All results indicated a high purity of the isolated vacuole and tonoplast fractions, with a level comparable to the purity of fractions used in previous vacuole proteomic studies (Carter et al., 2004; Jaquinod et al., 2007).
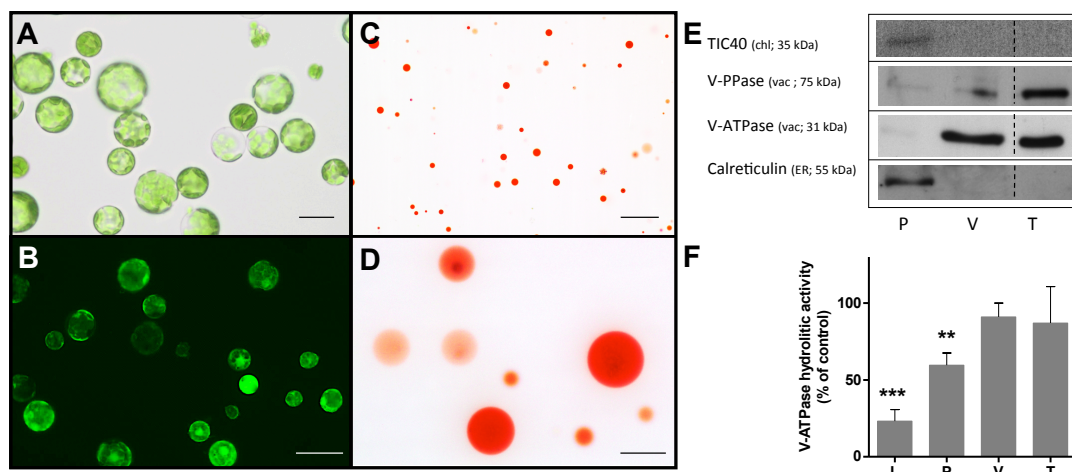
Figure 2. Characterization of the purity of protoplasts, vacuoles and tonoplast vesicles isolated from *C. roseus* leaves. A to D, Optical microscopy images of protoplast and vacuole populations. A, Bright field image of protoplasts. B, Fluorescence image of protoplasts labelled with FDA. C and D, Bright field images of intact vacuoles stained with neutral red. Bars = 20 µm (A and D), 50 µm (B), 100 µm (C). E, Western blots of protein extracts from protoplasts (P), vacuoles (V) and tonoplast vesicles (T) using specific antibodies raised against the chloroplast inner envelope protein TIC40, the vacuole specific V-H$^+$-PPase and V-H$^+$-ATPase (subunit epsilon), and the ER resident protein calreticulin. F, V-H$^+$-ATPase hydrolytic activity of protein extracts from leaves (L), protoplasts (P), vacuoles (V) and tonoplast vesicles (T). For each fraction, ATP hydrolytic activity was measured in the presence of 0.5 mM azide (mitochondrial ATPase inhibitor) and 100 µM vanadate (plasma membrane ATPase inhibitor) and expressed as the percentage of the total ATP hydrolytic activity in the absence of inhibitor revealing the residual % of activity corresponding to the V-H$^+$-ATPase present in each fraction. Statistical significance was evaluated using Student's *t* test for pairwise comparison (*** $P < 0.001$). Data significantly different from control are indicated. Error bars indicate SD from three biological replicates with two biochemical replicates each.

C.roseus leaf vacuoles are a reservoir of TIAs

Taking advantage of the isolation of a highly pure vacuole preparation, the level of accumulation of TIAs in the vacuoles of leaf cells was investigated. HPLC-DAD analysis of leaf extracts showed the major presence in leaves of the TIAs vindoline, catharanthine and α-3',4'-anhydrovinblastine (AVLB) (Fig. 3). Analysis of protoplast and vacuole extracts showed that the same TIAs were present in protoplasts and vacuoles, except AVLB, which was not present in isolated vacuoles.
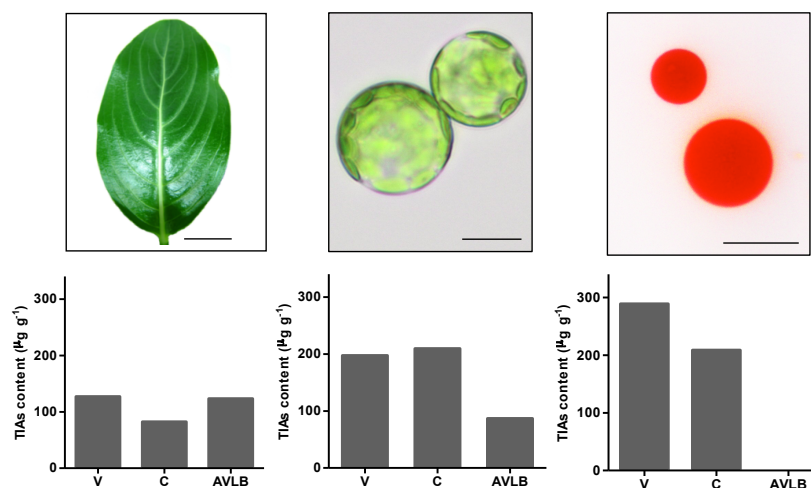
Figure 3. TIA content of leaves, isolated protoplasts and isolated vacuoles. V, vindoline; C, catharanthine and AVLB, α-3',4'-anhydrovinblastine. Bars = 1 cm (leaves), 25 µm (protoplasts and vacuoles). Values per g of FW were estimated by measuring the medium volume of protoplasts and converting mL to g using a density of 1. For vacuoles, the volume used was estimated as 80% of the protoplasts volume and not directly measured, since the isolated vacuoles are reduced by the high osmotic concentration of the buffer (contrary to the isotonic protoplast buffer).

Interestingly, estimation of concentrations to comparable values between leaves, protoplasts and vacuoles (Fig. 3) showed the detection of higher concentrations of vindoline and catharanthine in protoplasts than leaves, and even higher in vacuoles. This may result from the fact that extraction of TIAs is probably much more efficient from protoplasts than from whole leaves, and even more from isolated vacuoles. Alternatively, it can also result from an induction of the TIA pathway during protoplast isolation. On the other hand, AVLB shows a decreased concentration in protoplasts and is absent from vacuoles. This could indicate that AVLB is not localized in the big central vacuole but rather in vesicles or small vacuoles, or that it is further metabolized by CroPrx1 (*Catharanthus roseus* peroxidase 1) during protoplast and vacuole isolation, as has been previously shown by Costa et al. (2008). Another tempting explanation could be that AVLB is cleaved back to their monomeric precursors, vindoline and catharanthine, with the disappearance of AVLB leading to the observed increase of the correspondent monomeric precursors. However, nothing is known about the possibility of this reaction being reversible. In any case, it seems clear that, at least for catharanthine and vindoline, the vacuoles of *C. roseus* leaf cells are the single cell accumulation target, constituting reservoirs of TIAs.

Global analyses of the proteome of *C. roseus* leaf vacuoles

A single leaf vacuole proteome has been characterized before, for Arabidopsis (Carter et al., 2004), after which the sensitivity of MS apparatus has significantly

increased, now enabling a more thorough proteomic characterization of the vacuole from this central organ for plant life. In order to obtain a maximum coverage of vacuolar proteins, two independent samples for each vacuole and tonoplast membrane fraction were submitted to proteomic analysis following the workflow represented in Fig. 4.
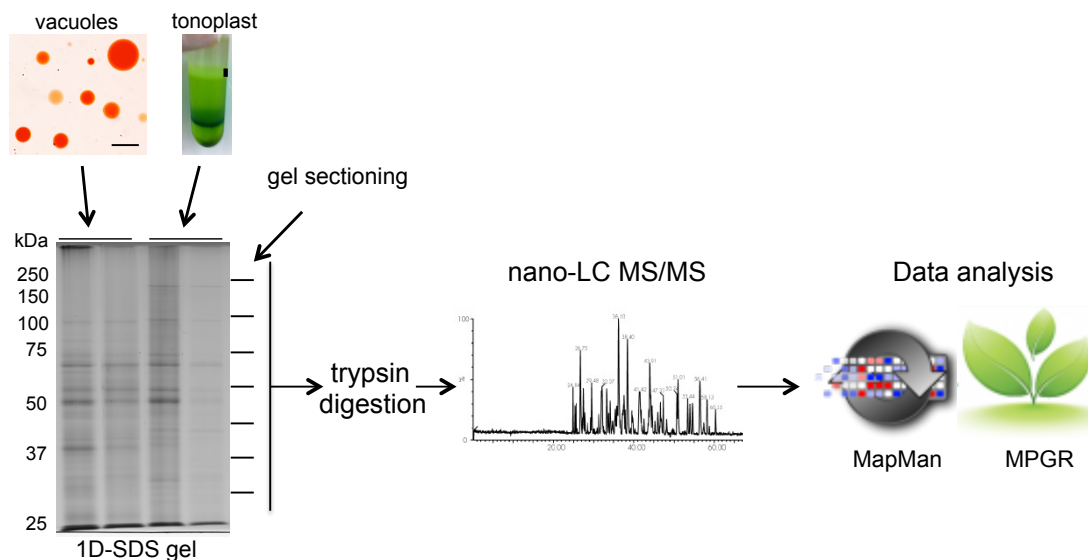
Figure 4. Workflow followed for the study of the proteome of *C. roseus* leaf vacuoles. Proteins from purified vacuoles and tonoplast membranes were separated by one-dimension SDS-PAGE, loading the following amounts of total protein by lane: 30 µg, 30 µg, 80 µg and 70 µg. Each gel lane was cut in 8 slices, proteins were submitted to in-gel trypsin digestion, and peptides were separated and analysed by nano-LC MS/MS Protein identification was performed using the MPGR database and protein organization and visualization was performed by MapMan software. Bar = 20 µm

The proteins identified using the *C. roseus* MPGR database were grouped to produce the minimal number of proteins covering all detected peptides, resulting in a non-redundant total identification of 1886 protein accessions of MPGR, corresponding to a maximum of 1886 different proteins (Supplemental Table SI). Due to the size of the initial list and the high sensitivity of the MS apparatus, only proteins identified with at least two peptides were considered. The MPGR database downloaded includes a collection of 63,623 entries of transcript assemblies for *C. roseus*, generated by the assembler Oases (Schulz et al., 2012). This assembly method identifies isoforms, which may correspond to alternative splice variants, alleles, or close paralogs, and therefore, the database was reported to include 32,607 unique transcripts or unigenes for *C. roseus* (Gongora-Castillo et al., 2012). In an effort to reduce the protein list obtained in this study, whenever there were accessions classified as isoforms, they were condensed into one single entry, represented by the common locus number of the database ID. However, it is still probable that the number of different proteins of the 1886 entries list is actually lower, since a number of MPGR accessions correspond to partial

sequences that, in some cases, may belong to the same protein. For simplicity, each MPGR entry identified will be addressed as corresponding to one protein, from now on.

The number of MPGR accessions identified for each sample is shown in Fig. 5. It is evident that duplicating samples has enabled to significantly increase the number of proteins identified. The use of multiple approaches for generating a comprehensive proteome list has been proposed to be important since some proteins may be found exclusively by a particular method (Whitelegge, 2002; Friso et al., 2004). Accordingly, some authors have used different methodologies that indeed have enabled the detection of different proteins (Carter et al., 2004). However, most authors use one single sample for each methodology or fraction type (Carter et al., 2004; Jaquinod et al., 2007). Our results indicate that even repeating the same methodology for equivalent samples results in the identification of more proteins, possibly as a result of erratic effects. Many steps of the experimental procedure may hinder in an erratic way the detection of proteins, such as solubilization prior to SDS-PAGE (possibly the cause of the low protein levels observed in the last lane of the gel in Fig. 4), migration during SDS-PAGE, gel sectioning, protein-protein interactions, trypsin digestion, elution from the gel, etc., and duplicating samples will compensate for some of those effects. In spite of the differences observed between duplications of samples, when the data was subjected to principal coordinate analysis (PCA), the areas covered by the four samples clearly clustered in two groups, corresponding to the duplications (Fig. 5B). Moreover, tonoplast and vacuole samples don't have a big distance between them, indicating their overlapping origin.

Recently, several methods for quantitative representation of MS/MS proteomic results have been reported (Blondeau et al., 2004; Silva et al., 2006). Some reports have used a "redundant peptide counting approach" that consists on calculating the percentage of total peptides assigned to a protein hit, as a means to calculate its relative abundance in the sample (Blondeau et al., 2004; Gilchrist et al., 2006). However, according to Silva et al. (2006), the number of observed peptides from one protein is useful within a narrow protein concentration range, whereby the observed peptides increase linearly as a function of the amount of protein, but the relationship deteriorates to an asymptotic limit after a certain concentration threshold.
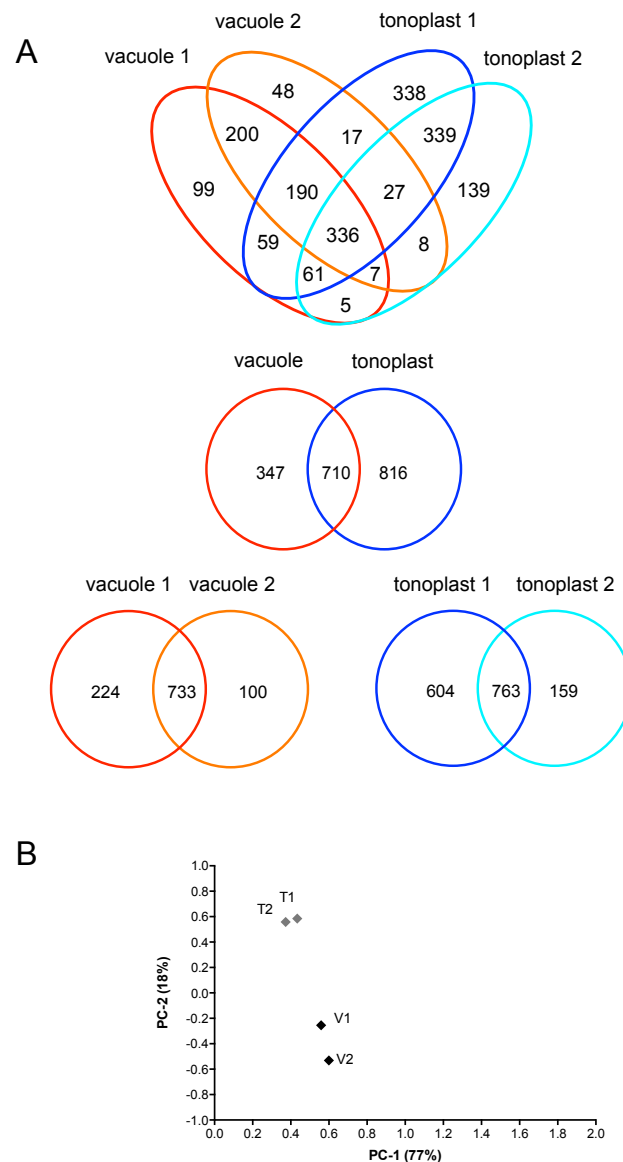
Figure 5. A, Distribution of identified proteins by the different samples, showing the overlap between the respective protein sets. B, Principal coordinate analysis (PCA) of the biological replicates. T1 and T2, tonoplast duplicates, V1 and V2, vacuole duplicates. Data are from Supplemental Table SI.

Accordingly, Zybailov et al. (2008) found that the 10-20 most abundant proteins in their study were underestimated when using a variant of this method. Silva et al. (2006), using 6 different standard proteins, showed that the pattern of intensity measurements of the detected peptides remains preserved throughout the dilution series of standards, with the average MS signal response for the three most intense tryptic fragments being constant per unit quantity of protein. Therefore, in this study, the relative abundance of proteins in each sample was estimated based on the ratio of the peak area intensity average obtained for the three more abundant peptides assigned to each protein (or two, when only two peptides were used to identify a protein), relative to the sum of the areas obtained for the total list of proteins.

The proteins identified in this proteomic study were first organized and visualized using the MapMan platform to generate the scheme represented in Fig. 6, which excluded all the proteins that had annotations relating them with other subcellular compartments. The presence of numerous transporters and the lytic nature of the vacuole were the most striking features observed.
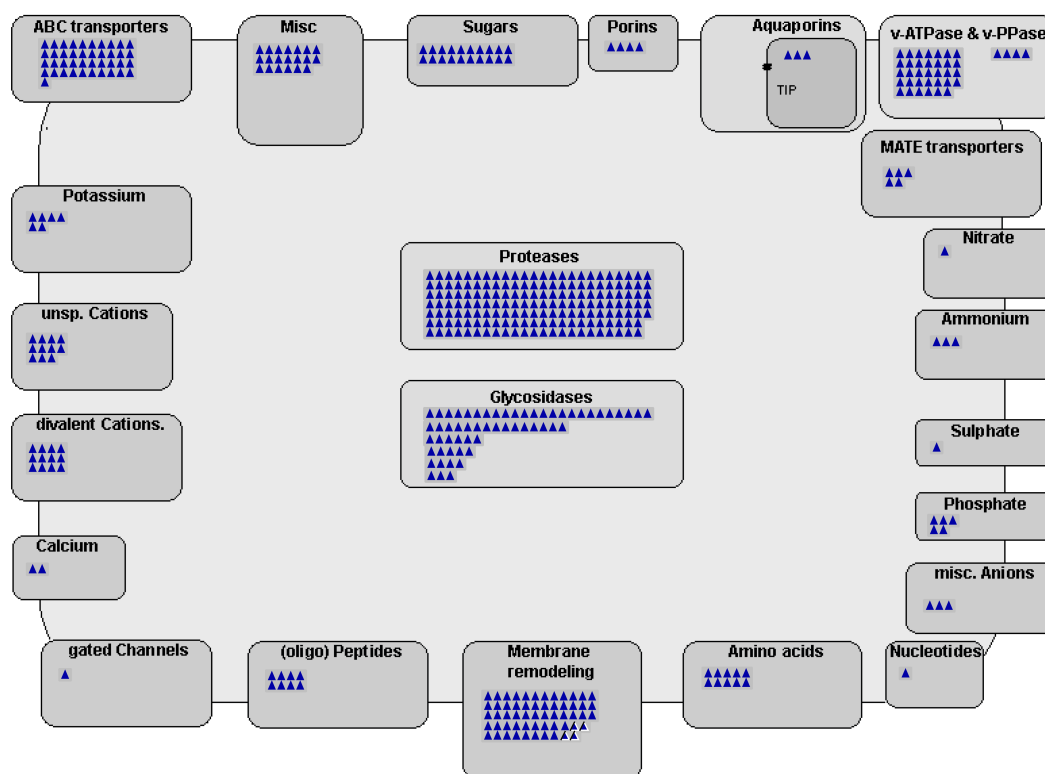
Figure 6. Localization and functional categorization of 427 selected proteins from the proteome of *C. roseus* leaf vacuoles using the MapMan platform. MapMan excluded all the proteins that had any annotation relating them with other subcellular compartments. Blue triangles represent the detected proteins.

In order to better classify and study the whole dataset generated, proteins were manually classified into 23 different categories, by combining the Gene Ontology information available in the most similar hits in the manually annotated UniProtKB / Swiss-Prot and in the Arabidopsis TAIR database (Fig. 7). Most categories correspond to functional classes, a few correspond to classes of enzymes or pathways, and some others correspond to subcellular localizations, when the proteins were clearly identified as being putatively located in organelles other than the vacuole, therefore potentially corresponding to contaminations (see discussion below). For possible double affiliation, or lack of information, decisions were made using the following criteria, very often inferred from the previous characterizations of vacuolar proteomes (Carter et al., 2004; Jaquinod et al., 2007): transporters were all included in the category "transport", regardless of the subcellular annotation of the most similar protein; proteins were

included in the category "stress response" only if they were associated with stress and had no annotation relating them with any other category (e.g. "redox metabolism", "signalling", etc.); proteins related with detoxification were included in the category "secondary metabolism"; cytochrome P450 monooxygenases (P450s) and the respective reductases were included in "secondary metabolism" since, in plants, most P450s are involved either in biosynthesis of secondary metabolites or detoxification (Bak et al., 2011); the category "catabolism and hydrolases", apart from hydrolase enzymes clearly related with catabolism, also include all proteins annotated as hydrolases and having no other clear annotation relating them with any other functional category; likewise, poorly annotated oxidoreductases were included under "redox metabolism".

Fig. 7 represents the total number of proteins identified for each category, together with the sum of the relative abundance of all the proteins in each category (sum of the means calculated for the duplicated samples; Supplemental Table SI). By far the category showing higher relative abundance of proteins, both in vacuole and tonoplast samples, is transport and ion homeostasis, including also a high number of proteins, as observed previously by Jaquinod et al. (2007). In the vacuole samples, secondary metabolism comes second in what concerns abundance, clearly supporting a strong engagement of the vacuole in this type of metabolism, which has been associated with a range of defence, adaptation and communication roles (Wink, 1993; Hartmann, 2007). Proteins predicted to belong to primary metabolism appear also with a significant abundance but, above all, with a very high number. As expected, proteins related with degradation processes are in high number and very abundant, with the protein and amino acid degradation coming as the third category in abundance for the vacuole fraction (Fig. 7A). Joining together all the catabolic categories (protein and amino acid degradation, glycosidases, catabolism and hydrolases) makes this group of proteins one of the most represented categories both in relative abundance and number of proteins. The categories redox metabolism and signalling are also significantly represented, especially in what concerns protein number, indicating an active and important role of vacuoles in redox homeostasis and signalling. There is still a significant number of proteins for which no annotation exists.
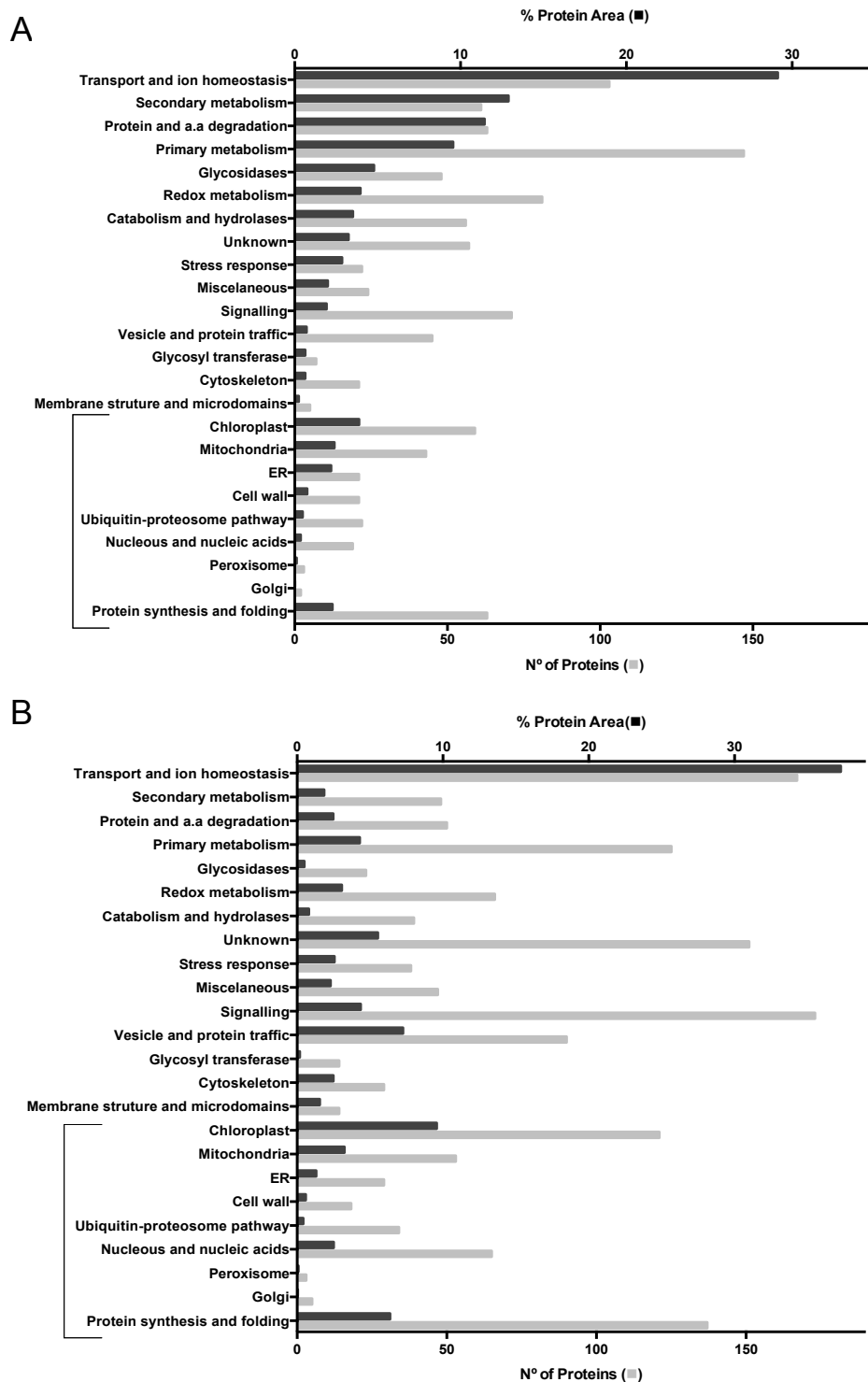
Figure 7. Cumulative relative abundance (% of protein area; black) and total number (grey) of the proteins assigned to each functional category. A, Vacuole fraction. B, Tonoplast fraction. Categories associated by a bracket are considered as potential contaminants. Relative abundances for each protein are the average of two biological replicates. Data are from Supplemental Table SI.

The main categories or groups of categories are described and discussed in more detail below, starting with the group of categories which were classified as potential contaminations (Fig. 7), following the same criteria of Carter et al. (2004).

Contamination or not contamination?

Until now it seems to be technically unfeasible to isolate an organelle fraction totally free from other cellular components and, on the other hand, the growing sensitivity of mass spectrometry allows detecting even minimal impurities. In this study, the vacuolar/tonoplast enrichment of the sampled fractions is clearly confirmed by the intense increase in the labelling of those fractions with the antibodies against the vacuolar $V-H^+-ATPase$ and $V-H^+-PPase$ (Fig. 2F), which are also among the proteins detected with higher relative abundance (Table I). Namely, one of the $V-H^+-ATPase$ subunits is the second protein with higher relative abundance in the vacuole fractions, and the first 5 proteins with higher relative abundance in the tonoplast fractions are 5 subunits of the $V-H^+-ATPase$. Overall, the two fraction types enabled the identification of 14 putatively different sequences corresponding to 9 different subunits out of 12 from the $V-H^+-ATPase$. Two different $V-H^+-PPase$ sequences were also identified. Almost all these sequences were among the 100 with higher relative abundance in the list of 1886 putative protein sequences detected, clearly indicating a strong enrichment of fractions in vacuole membranes. Carter et al. (2004) also identified 9 subunits from the $V-H^+-ATPase$ in the proteome of Arabidopsis rosette vacuoles. To our knowledge, only Endler et al. (2006) achieved the identification of the 12 subunits, in the tonoplast proteome of barley mesophyll, but their fraction was highly contaminated with plasma membrane.

In what concerns isolated vacuoles, it must be stressed that careful microscopic inspection of fractions did not detect the presence of any non- or partially-lysed protoplasts, nuclei, chloroplasts, or organelles/vesicles within the resolution limit of high magnification bright field microscopy, as can be seen in Fig. 2D and 8A. Moreover, observation under the fluorescence microscope detected no fluorescence related to chloroplasts, unlike Jaquinod et al. (2007), who saw "very few red-fluorescing chloroplasts or protoplasts" in their preparations used for vacuolar proteomics. Comparison of the vacuole preparations obtained here, by means of the vacuole isolation method used for proteomic analysis (Fig. 8A), with the vacuole preparations obtained using one of the methods initially tried and rejected (Fig. 8B), clearly shows the level of purity attained in the optimized method.

Table I. Selected proteins identified in the vacuolar proteome of *C.roseus* leaves (the five more abundant from each category, and the ones referred in the text). V, vacuole fraction and T, tonoplast fraction. Highlighted in bold are the proteins that fall in the range of the 100 more abundant proteins. * Average of two biological samples. Full data in Supplemental Table SI.

Accession number	Description	Relative abundance (%)	
		V*	T*
Transport and Ion homeostais			
cra_locus_7851_iso_2_len_1736_ver_3	**ABC transporter family C**	2.20	0.00
cra_locus_6707	ABC transporter family G	0.02	0.23
cra_locus_9964_iso_2_len_1107_ver_3	ABC transporter family protein	0.07	0.00
cra_locus_2817_iso_1_len_559_ver_3	**Aquaporin MIP family, γ-TIP**	1.02	0.46
cra_locus_435_iso_1_len_1283_ver_3	**Aquaporin, MIP family, α-TIP**	0.00	0.49
cra_locus_1952_iso_2_len_1572_ver_3	CroMATE1	0.06	0.25
cra_locus_5978_iso_1_len_2866_ver_3	Major facilitator superfamily protein	0.02	0.01
cra_locus_53644_iso_1_len_355_ver_3	**V-H$^+$-ATPase subunit A**	1.61	2.13
cra_locus_54	**V-H$^+$-ATPase subunit A1**	4.96	4.83
cra_locus_65117_iso_1_len_514_ver_3	**V-H+-ATPase subunit A1**	2.03	2.82
cra_locus_200	**V-H$^+$-ATPase subunit A3**	0.39	0.49
cra_locus_5984	**V-H$^+$-ATPase subunit B**	3.72	2.81
cra_locus_63502_iso_1_len_530_ver_3	**V-H$^+$-ATPase subunit B**	0.88	0.79
cra_locus_53534_iso_2_len_670_ver_3	**V-H$^+$-ATPase subunit C**	0.86	1.84
cra_locus_2357_iso_1_len_1646_ver_3	V-H$^+$-ATPase subunit c	0.00	0.02
cra_locus_3995_iso_2_len_1433_ver_3	**V-H$^+$-ATPase subunit d2 (AC39)**	2.99	3.75
cra_locus_50	**V-H$^+$-ATPase subunit E**	1.66	3.31
cra_locus_19417	**V-H$^+$-ATPase subunit G1**	0.32	0.69
cra_locus_1646	**V-H$^+$-ATPase subunit H**	0.28	0.31
cra_locus_10520_iso_8_len_2215_ver_3	**V-H$^+$-PPase**	0.98	0.48
cra_locus_1961	**V-H$^+$-PPase**	0.68	0.89
Secondary Metabolism			
cra_locus_3755_iso_6_len_1410_ver_3	**10-hydroxygeraniol oxidoreductase (10HGO)**	0.21	0.01
cra_locus_6243	10HGO	0.08	0.02
cra_locus_4319_iso_1_len_1221_ver_3	10HGO	0.17	0.11

Table I. (continued from previous page.)

Accession number	Description	Relative abundance (%)	
		V*	T*
cra_locus_2091	10HGO	0.05	0.11
cra_locus_1856	16-methoxy-2,3-dihydrotabersonine N-methyltransferase (NMT)	0.08	0.07
cra_locus_3558_iso_1_len_1647_ver_3	**Alliin lyase**	2.59	0.07
cra_locus_1734	NADPH cytochrome P450 reductase	0.00	0.04
cra_locus_2963_iso_1_len_2148_ver_3	NADPH cytochrome P450 reductase	0.00	0.004
cra_locus_1059	Deacetoxyvindoline 4-hydroxylase	0.01	0.01
cra_locus_2708	Geraniol 10-hydroxylase (G10H)	0.13	0.34
cra_locus_2336_iso_3_len_1241_ver_3	**Strictosidine synthase (STR)**	7.60	0.47
cra_locus_1596_iso_2_len_1463_ver_3	**STR**	0.58	0.02
cra_locus_2176_iso_5_len_1213_ver_3	STR	0.02	0.02
cra_locus_1560_iso_5_len_1420_ver_3	STR	0.01	0.00
cra_locus_2046_iso_5_len_1890_ver_3	Strictosidine-O-beta-D-glucosidase (SGD)	0.00	0.05
cra_locus_6962_iso_3_len_1689_ver_3	Vinorine synthase	0.03	0.00
Redox metabolism			
cra_locus_7752_iso_2_len_344_ver_3	**Ascorbate peroxidase**	0.37	0.03
cra_locus_9382_iso_1_len_318_ver_3	Ascorbate peroxidase	0.06	0.02
cra_locus_685_iso_1_len_1891_ver_3	Catalase	0.17	0.16
cra_locus_1674	Catalase	0.11	0.05
cra_locus_1237_iso_2_len_1797_ver_3	Glutathione reductase	0.04	0.01
cra_locus_2405_iso_4_len_2163_ver_3	Glutathione reductase	0.01	0.00
cra_locus_1383	Monodehydroascorbate reductase - putative	0.10	0.03
cra_locus_635_iso_2_len_1505_ver_3	Monodehydroascorbate reductase, putative	0.01	0.00
cra_locus_1009_iso_3_len_1775_ver_3	Monodehydroascorbate reductase, putative	0.01	0.05
cra_locus_1625_iso_1_len_1320_ver_3	**Peroxidase 1 (CroPRX1)**	1.12	0.11
cra_locus_3407_iso_1_len_1207_ver_3	Peroxidase 50 (CroPRX50)	0.08	0.00

Table I. (continued from previous page.)

Accession number	Description	Relative abundance (%)	
		V*	T*
cra_locus_2633_iso_4_len_1611_ver_3	Peroxidase 7 (CroPRX7)	0.15	0.18
cra_locus_8178	Superoxide dismutase (Fe), putative	0.00	0.16
cra_locus_10095	Superoxide dismutase Cu/Zn	0.05	0.01
cra_locus_2110_iso_3_len_915_ver_3	Superoxide dismutase Mn	0.03	0.00
Protein and a.a. degradation			
cra_locus_855	**Aspartic protease**	0.23	0.81
cra_locus_6663_iso_9_len_1563_ver_3	**Aspartic proteinase**	0.91	0.03
cra_locus_3253_iso_4_len_1097_ver_3	Aspartic proteinase nepenthesin-1	0.00	1.26
cra_locus_4949_iso_4_len_387_ver_3	**Cysteine protease Cp6**	2.17	0.06
cra_locus_4921_iso_1_len_758_ver_3	**Cysteine protease Cp1**	0.85	0.00
cra_locus_7770_iso_1_len_2462_ver_3	**Serine carboxypeptidase**	1.44	0.02
Glycosidades			
cra_locus_1243_iso_10_len_3398_ver_3	**Alpha-L-arabinofuranosidase**	0.54	0.01
cra_locus_2893	**Alpha-mannosidase**	0.52	0.06
cra_locus_2828_iso_3_len_2364_ver_3	**Beta-fructofuranosidase, isoform II**	0.43	0.00
cra_locus_3039_iso_2_len_2450_ver_3	**Vacuolar invertase**	1.05	0.03
Catabolism and hydrolases			
cra_locus_789_iso_8_len_2015_ver_3	**Acid phosphatase** 1	0.35	0.00
cra_locus_5635	**Carbon-nitrogen hydrolase family protein**	0.91	0.01
cra_locus_3512_iso_6_len_1718_ver_3	**Patatin 3**	0.35	0.30
cra_locus_2346_iso_5_len_666_ver_3	**RNase NGR3**	0.41	0.00
Primary metabolism			
cra_locus_5111	**Acetylornithine deacetylase**	1.42	0.05
cra_locus_949	**Serine hydroxymethyltransferase 5**	0.67	0.05
cra_locus_428	**Triosphosphate isomerase type II**	0.61	0.18
cra_locus_1347	**Glyceraldehyde-3-phosphate dehydrogenase B subunit**	0.27	0.46

Table 1. (continued from previous page.)

Accession number	Description	Relative abundance (%)	
		V*	T*
cra_locus_9604_iso_1_len_1317_ver_3	**Glyceraldehyde-3-phosphate dehydrogenase, cytosolic**	0.36	0.46
cra_locus_1129	**Malate dehydrogenase**	0.59	0.39
Signalling			
cra_locus_870_iso_2_len_839_ver_3	**Auxin-binding protein ABP20**	0.79	0.53
cra_locus_6940	Cell elongation protein diminuto	0.07	0.01
cra_locus_1297_iso_1_len_3928_ver_3	Kinase	0.06	0.03
cra_locus_5594_iso_3_len_2971_ver_3	Kinase	0.14	0.04
cra_locus_4473_iso_9_len_1152_ver_3	Ethylene-responsive small GTP-binding protein	0.01	0.14
cra_locus_11992_iso_1_len_1576_ver_3	**Fasciclin-like arabinogalactan protein (FLA)**	0.18	0.67
cra_locus_1847_iso_2_len_966_ver_3	FLA 1	0.00	0.02
cra_locus_6081_iso_1_len_1598_ver_3	FLA 10	0.01	0.04
cra_locus_439_iso_1_len_1952_ver_3	FLA 14	0.04	0.00
cra_locus_3390_iso_9_len_1387_ver_3	MRNA, clone: RTFL01-33-D01 (tobamovirus multiplication 2A)	0.00	0.29
Vesicle and protein traffic			
cra_locus_451_iso_3_len_516_ver_3	ADP-ribosylation factor	0.07	0.12
cra_locus_800_iso_6_len_1246_ver_3	Alpha-soluble NSF attachment protein	0.01	0.01
cra_locus_3527	GTP-binding 2 (Rab)	0.07	0.50
cra_locus_4051	N-ethylmaleimide sensitive fusion protein (v-SNARE SYP51)	0.01	0.01
cra_locus_8340	RAB7C	0.01	0.87
cra_locus_5837	RAB7D	0.01	0.58
cra_locus_2414_iso_2_len_1164_ver_3	RAB7A	0.05	0.51
cra_locus_5439_iso_3_len_1410_ver_3	Vesicle transport V-SNARE protein (VTI11)	0.02	0.04

Table 1. (continued from previous page.)

Accession number	Description	Relative abundance (%)	
		V*	T*
Glycosyl transferases			
cra_locus_811	Glycosyltransferase	0.09	0.01
cra_locus_2031	Ribophorin-protein N-linked glycosylation via asparagine	0.02	0.06
cra_locus_985_iso_3_len_1636_ver_3	Ribophorin	0.02	0.05
cra_locus_8313_iso_1_len_943_ver_3	**Transferase, transferring glycosyl groups**	0.46	0.00
Cytoskeleton			
cra_locus_1440	**Actin-1**	0.28	0.38
cra_locus_1440_iso_4_len_773_ver_3	**Actin 7**	0.06	0.23
cra_locus_1313	Centromeric protein E	0.00	0.82
cra_locus_357	Tubulin beta-1 chain	0.01	0.18
Stress Response			
cra_locus_504	**Band 7 family protein**	0.12	0.39
cra_locus_1913_iso_11_len_649_ver_3	**Dehydrin**	0.00	0.48
cra_locus_5305_iso_3_len_862_ver_3	**Germin subfamily 3 member 4**	0.62	0.60
cra_locus_3454	**Heat shock protein 70**	0.31	0.09
Unknown			
cra_locus_4857_iso_1_len_2434_ver_3	Conserved gene of unknown function	0.42	0.00
cra_locus_23	**Cyclase family protein**	0.25	0.04
cra_locus_1207_iso_3_len_1510_ver_3	**Heme-binding protein**	0.88	0.01
cra_locus_6904	**Patellin 1**	0.39	0.99
Miscellaneous			
cra_locus_7111	**Lectin**	0.84	0.07
cra_locus_11547_iso_6_len_1181_ver_3	**Embryo-specific protein 3**	0.55	0.14
cra_locus_18483	NAD-dependent epimerase/dehydratase	0.23	0.04
cra_locus_3329	Nicalin	0.04	0.09
cra_locus_2232	**Protein translocase**	0.00	1.25
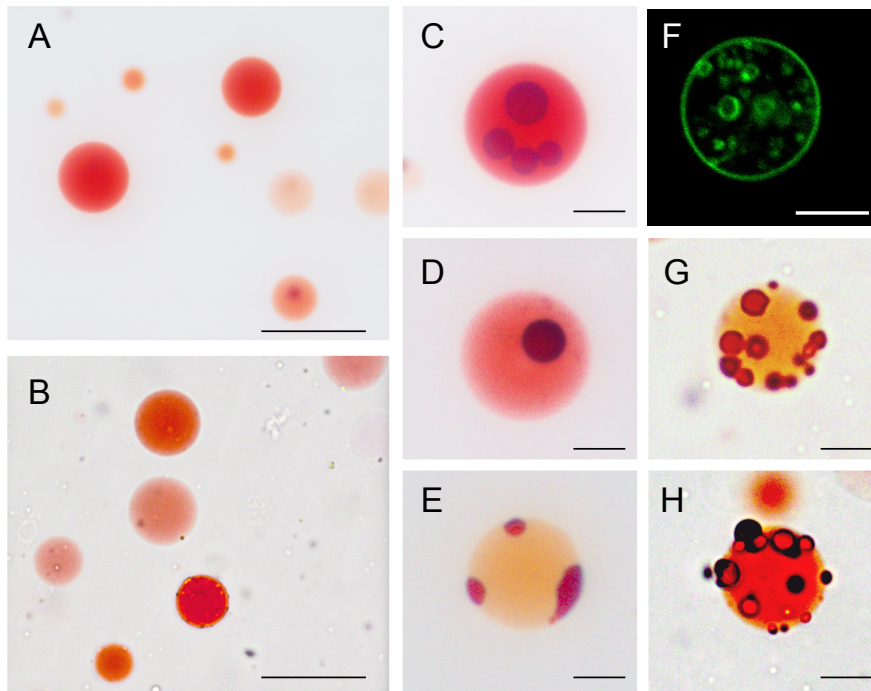
Figure 8. Observation of *C. roseus* leaf vacuoles under the optical microscope with selection of particular features observed. A, C to E, Bright field images of intact vacuoles used for proteomic analysis. B, G, H, Bright field images of intact vacuoles isolated using the method from Fontes et al. (2010). F, Confocal image of a selected intact vacuole labeled with FM1-43 (isolated as Fontes et al. (2010). Bars = 50 µm (A, B), 10 µm (C to H).

Vacuole purity came with one drawback, a great instability of the membranes, but this was not a problem for this proteomic study, since vacuoles were immediately frozen. However, it was not possible to perform assays of H^+ pumping activity with vacuoles, as for tonoplast vesicles (see below). Most vacuoles ranged from sizes between 14 - 23 µm, but there were also quite small vacuoles with 1 - 3 µm. These small vacuoles may not correspond to the central vacuole of differentiated cells, but rather to secondary vacuoles or to the small vacuoles of undifferentiated/meristematic cells. In any case, the vast majority seemed to be lytic vacuoles, since they stained with neutral red, even if with varying intensities, indicating that their lumen had an acid pH. Some vacuoles were observed (with a ~ 1 to 10 frequency), where one or more compartments with extremely acid pH were found inside the vacuoles, suggesting engulfment of small vacuoles or provacuoles (Fig. 8, C to F), while in other images, compartments staining intensely with neutral red seemed to be attached to the outside of the tonoplast of big vacuoles (Fig. 8, E, G and H). In principle, these compartments cannot result from an artifact of extraction, since vesicles formed from membrane burst during extraction would not have the availability of ATP or PPi in the medium necessary to build up the pH gradient they show. Therefore, it is possible that these compartments may correspond to prevacuoles/late endosomes attached to the vacuole. Shimaoka et al. (2004) also

reported the observation of small vesicles with acidic pH attached to the main vacuoles, which the authors presumed to be prevacuolar compartments. The compartments inside the vacuoles, in some cases (Fig. 8, E and F), have similarities with the "bulbs" described by Saito et al. (2002) and also reported by Bottanelli et al. (2012), but in other cases (Fig. 8, C and D) look to be completely independent from the tonoplast. One explanation for these compartments could be that the vacuoles are capable of undergoing a process similar to what happens to the prevacuoles, when they mature into multivesicular bodies, invaginating portions of their membranes to produce internal vesicles (Neuhaus and Martinoia, 2011). In conclusion, the only contamination that was possible to observe under the light microscope was possibly from prevacuoles.

According to Zybailov et al. (2008), contaminations in proteomic studies can be minimized by using multiple high quality MS/MS spectra and multiple unique peptide sequences in multiple independent preparations. Here, only proteins identified by more than one peptide and at least one unique peptide were used, but they were selected for the final list independently of being present in all the samples. In fact, for instance, vacuolar proteins such as the subunit F from V-H$^+$-ATPase appear only in one of the vacuolar samples, and with a significant relative abundance (Table I). Therefore, here, the list generated includes all the proteins detected with high confidence MS data in any of the duplicate samples, favouring the compensation of erratic effects during the experimental procedures that may lead to loss of proteins, even if this may also favour the detection of contaminants. In any case, the information of the presence of all the 1886 proteins in the different samples is made available for future analysis (Supplemental Table SI).

The biological preparations analysed in this study contained a number of proteins putatively considered contaminants, namely the ones included in the categories chloroplast, mitochondria, ER, Golgi, nuclei and peroxisomes, cell wall, ubiquitin and proteasome pathway, and protein synthesis and folding (Fig. 7). In vacuole samples, these categories account for a total of 12 % in relative protein abundance and 13 % in what concerns the number of putative proteins, while in tonoplast samples those values are 24 % and 25 % respectively. These values are within the values reported in other vacuole or tonoplast proteomic studies, in which the contamination values are given or may be calculated using the information available, based on the number of proteins: in Carter et al. (2004) contamination values are 15 % for the vacuole study as a whole, and 17 % for the tonoplast fraction; in Shimaoka et al. (2004) contamination values are 21 % in a tonoplast proteome characterization. When considering contamination of vacuolar fractions, Endler et al. (2006) highlights that the protein content of the vacuolar membrane constitutes less than 1 % of the total cellular protein, and therefore, low

contaminations in the range of 2 % to 4 % will have a significant impact on the proteins detected. Moreover, in mesophyll cells, the surface area of chloroplastic membranes exceeds by far that of the vacuole, and have a much higher content of proteins, having as consequence that a contamination of 2 % with chloroplasts would result in the presence of about 20 % plastid proteins in the vacuolar fraction (Endler et al., 2006). Likewise, the highest contamination category in this study is chloroplasts (Fig. 7). However, the most abundant polypeptide in mesophyll cells, the Rubisco large subunit (RbCL) (Zybailov et al., 2008), is not represented by a single peptide in the present study. This indicates the absolute absence of intact chloroplasts from our vacuole fractions and hence their high purity. Curiously, and opposite to RbCL, the Rubisco small subunit (RbCS) is represented with a high and similar relative abundance in all samples (~1 %) (Supplemental Table SI). RbCS was also detected in the vacuole proteome of Arabidopsis by Carter et al. (2004), also both in vacuoles and tonoplast membranes. Since RbCS is a soluble polypeptide, its presence in the tonoplast membrane fraction in similar levels to the organelle fraction, suggests that this contamination may result from a high capacity of unspecific binding of RbCS to membranes or membrane proteins. Meaningfully, RbCS has been shown to interact with several virus proteins (Zhao et al., 2013). Another more speculative possibility is that RbCS may be a "moonlighting" protein, a multifunctional protein exhibiting activities distinct from their classically identified functions, as discovered for many enzymes of the glycolytic pathway (Sirover, 2011).

The presence of proteins from the ER and Golgi, and therefore from ribosomes, may also result from recent vesicle trafficking from these compartments to the vacuoles (Garin et al., 2001; Carter et al., 2004). Monoubiquitinylation of membrane proteins has been reported to tag them for transport and degradation in the animal lysosome, and the existence of such a mechanism in plant cells would explain the presence of the members of the ubiquitin pathway detected here. Finally, the vacuole is a lytic organelle where many processes of degradation happen, including the degradation of organelles and portions of cytosol that are autophagocyted and targeted to the vacuole for degradation being possible that their proteins are transiently detected during the course of this process (De, 2000; Schmidt et al., 2007). The high amount of proteins involved in the categories protein degradation, catabolism and hydrolases, and glycosidases that were identified here, confirms the lytic role of the vacuole (Fig. 7). Moreover, when submitted to stress conditions, plant cells have been reported to intensify the phagocytosis of organelles and their targeting to the vacuole for degradation, to recycle nutrients (He and Klionsky, 2009). This situation may have happened in the stressed

protoplast cells used for vacuole isolation, leading to the presence of the proteins considered here as contaminants.

Contamination or not contamination, it will be interesting to follow who will stand the test of time, but it is likely that many proteins now considered contaminants are just suffering degradation inside the vacuole, while others may be true functionally active vacuolar proteins on their own right.

Transport and ion homeostasis – within and without

As a big compartment inside the plant cell, working as a temporary storage target for many ions and low molecular weight compounds, and having a major role in cell expansion and support of the plant body through the building of turgor pressure, the vacuole membrane has an intense transport activity mediated by many transporters. Moreover, being a sink organ, degradation products such as amino acids should also be recycled back to the cytosol by mediated transport. Therefore, it is not a surprise that one of the most represented categories of proteins in this proteomic study is transport and ion homeostasis, with 176 putative proteins corresponding to a total relative abundance of 29.13 and 37.28 % for vacuole and tonoplast fractions respectively (Fig. 7). By far the most abundant proteins in this category are several subunits of the V-H$^+$-ATPase, with the subunits A1 reaching a cumulative relative abundance around 7 % in both characterized fractions, being the most abundant protein detected in this proteomic study together with strictosidine synthase (Table I).

In fact, most transport processes across the tonoplast membrane depend on the proton motive force generated across the membrane by the proton pumps V-H$^+$-ATPase and V-H$^+$-PPase (Martinoia et al., 2012). Accordingly, two V-H$^+$-PPases were also detected, with a cumulative relative abundance of 1.66 and 1.36 % in vacuole and tonoplast fractions. To further characterize these pumps in *C. roseus* leaf cells, their activity was quantified by measuring their ATP / PPi hydrolytic activity (Table II) and by measuring their proton pumping activity as the fluorescence quenching of the pH-sensitive probe ACMA (Fig. 9). Both intact vacuoles and tonoplast membranes presented high ATP and PPi specific hydrolytic activities (Table II), although it must be referred that the PPase activity measured may have a contribution from other soluble and membrane inorganic pyrophosphatases (Maeshima, 2000). The proton pumping activity was measured only for the tonoplast fraction, due to the short life and instability

Table II. ATP and PPi hydrolytic activities of the vacuole and tonoplast fractions used for the proteomic study. *in the presence of the P-H$^+$-ATPase inhibitor vanadate (100 μM) and the F-H$^+$-ATPase inhibitor azide (5 mM), to detect only the V-H$^+$-ATPase activity.

	ATP hydrolytic activity (nmol Pi min^{-1} mg^{-1})	ATP hydrolytic activity in the presence of inhibitors* (nmol Pi min^{-1} mg^{-1})	PPi hydrolytic activity (nmol Pi min^{-1} mg^{-1})
Intact vacuoles	679.81 ± 133.8	596.58 ± 81.00	675.59 ± 201.86
Tonoplast membranes	968.24 ± 90.14	875.32 ± 95.17	2223.10 ± 445.66

of intactvacuoles used in this study. As can be seen in Fig. 9, immediate fluorescence quenching signals were observed after addition of either ATP or PPi to tonoplast vesicles, with fluorescence promptly recovering upon addition of NH$_4$Cl, demonstrating the generation of a transtonoplast pH gradient by the V-H$^+$-ATPase and the V-H$^+$-PPase, respectively.
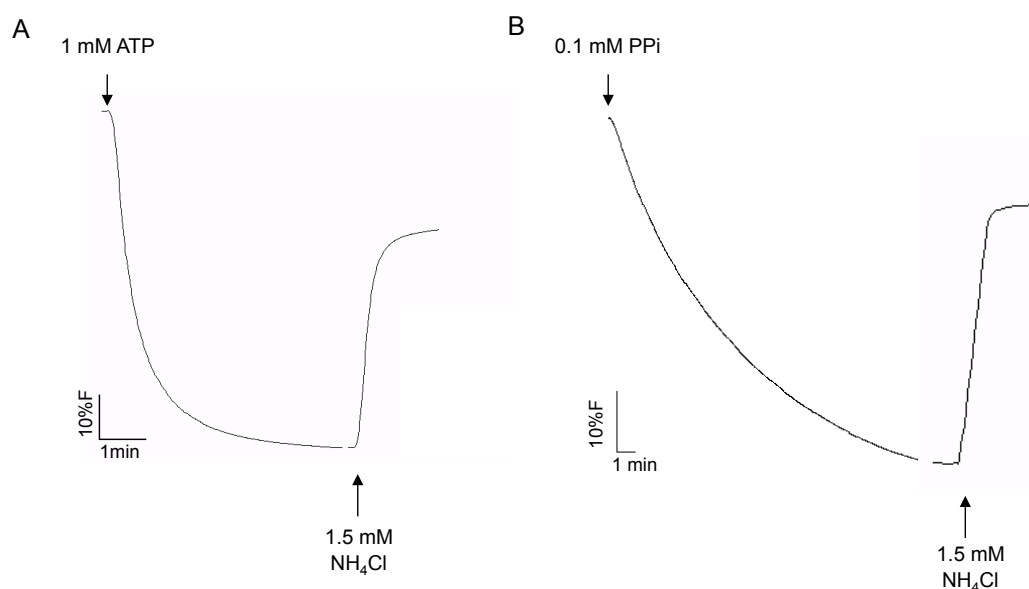
Figure 9. Pumping activities of the V-H$^+$-ATPase and the V-H$^+$-PPase in tonoplast vesicles isolated from *C. roseus* leaves measured by the fluorescence quenching of the pH-sensitive probe ACMA. A, H$^+$-pumping activity in tonoplast vesicles upon the addition of 1 mM ATP. B, H$^+$-pumping activity in tonoplast vesicles upon the addition of 0.1 mM of PPi.

The concentration range of PPi used for measurements was lower than for ATP, since higher concentration of PPi were inhibitory. Interestingly, when the Michaelis-Menten constants were determined for both pumps (Table III), it was found that the V-H$^+$-PPase has a lower K_m than the V-H$^+$-ATPase, being capable of sustaining significant activity under lower concentrations of substrate. This fits with the estimated cytosolic concentrations of ATP and PPi, reported to be lower for PPi: 0.2 mM for PPi and 0.5 to 1 mM or above for ATP (Gout et al., 1992; Maeshima, 2000; Borisjuk et al.,

120 | FCUP

Unravelling the metabolism and transmembrane transport of the highly valuable medicinal alkaloids from *Catharanthus roseus*

2003). The K_m values determined for the *C. roseus* tonoplast proton pumps fit well with previous values reported in the literature, where the apparent K_{ms} for the V-H$^+$-ATPase are always higher than for the V-H$^+$-PPase, respectively from 0.3 to 0.8 mM, and from 5 to 30 µM, as expected from the relative cytosolic concentrations of ATP and PPi (White et al., 1990; Gout et al., 1992; Costa dos Santos et al., 2003; Rienmueller et al., 2012). In spite of the lower affinity for its substrate, the V-H$^+$-ATPase seems to have a higher turnover capacity than the V-H$^+$-PPase (higher V_{max}), and it has been reported to have a coupling ratio of 2 to 4 protons pumped for each hydrolyzed ATP molecule, while the H$^+$/ PPi stoichiometry of the V-H$^+$-PPase has been determined to be 1 (Maeshima, 2000; Rienmueller et al., 2012). According to White et al. (1990), in mesophyll cells the V-H$^+$-PPase may act as an ancillary enzyme that maintains the proton-motive force across the vacuolar membrane when the activity of the tonoplast H$^+$-ATPase is restricted by substrate availability. This might explain the lower abundance of V-H$^+$-PPases relative to V-H$^+$-ATPases detected in this study. In fact, although generally V-H$^+$-PPase activity is high in young tissues, V-H$^+$-ATPase activity seems to be otherwise predominant (Martinoia et al., 2007).

Table III. Michaelis–Menten constants estimated for the two proton pumps present in isolated tonoplast membranes.

	K_m (µM)	V_{max} (%F min^{-1} µg^{-1})
V-H$^+$-ATPase	130	0.120
V-H$^+$-PPase	16	0.024

As expected, several aquaporins were detected, with a γ-TIP, reported as typical from LVs, being the more abundant (Table I). An α-TIP was also significantly abundant in the tonoplast fraction but was absent from intact vacuoles, maybe suggesting that membranes from PSVs were more represented in isolated tonoplast membranes than in the isolated vacuole fractions. The presence of an α-TIP in *C. roseus* leaves is different from what happens in Arabidopsis, where the single α-TIP seems to be restricted to the seed (Frigerio et al., 2008).

The role of the vacuole in ion homeostasis and Ca^{2+} signalling is evident by the identification of 5 Ca^{2+}, 5 K$^+$ and 5 Na$^+$ transporters, 2 anion channels, and 15 transporters putatively involved in the transport of diverse ions, including 4 dedicated to heavy metals (Supplemental Table SI). One calcineurin B-like protein and an iron binding protein putatively involved in ion homeostasis were also identified.

Eleven proteins associated with sugar transport were identified, highlighting the importance of vacuoles in carbohydrate metabolism and storage, and also in the

regulation of the cytosolic sugar concentration (Martinoia et al., 2012). Seven transporters are annotated as involved in amino acid / peptide transport, related with the protein/peptide degradation role of the vacuoles. There is evidence suggesting that hormone pools may exist inside the vacuole, being released during signalling (Martinoia et al., 2012) and vacuolar auxin transport has been implicated in auxin signalling (Ranocha et al., 2010). Interestingly, two auxin efflux carrier components were identified here (Supplemental Table SI).

Last, but definitely not the least, 42 proteins potentially involved in the transport of secondary metabolites were identified: 34 ATP-binding cassette (ABC) transporters, 6 multidrug and toxic compound extrusion (MATE) transporters and two anthocyanin permeases. This reveals a huge investment of *C. roseus* in this type of metabolism that has no parallel with previous vacuole proteomes characterized (Carter et al., 2004; Jaquinod et al., 2007; Schmidt et al., 2007). Both the ABC and MATE gene families have a high diversity in plants, which has been related precisely with the diversity of plant secondary metabolism (Omote et al., 2006; Yazaki, 2006). It has been shown that ABC transporters play a major role in the transport of secondary metabolites in plants, including alkaloids. For instance, in *Coptis japonica*, several ABCB transporters have been implicated in the cellular import of the alkaloid berberine in the rhizome and other tissues (Shitan et al., 2003; Shitan N, 2012). In particular, the ABCC subfamily has been implicated in the vacuolar accumulation of several compounds and ions, including glucosylated anthocyanidin, glucuronide flavones, xenobiotic-glutathione conjugates, Cd^{2+} and Hg^{2+}, folate, phytate, etc. (Li et al., 1997; Klein et al., 2000; Liu et al., 2001; Goodman et al., 2004; Nagy et al., 2009; Raichaudhuri et al., 2009; Park et al., 2012). To date, only ABC transporters from the subfamily C were proven to be localized in the vacuole. However, although ABCC transporters are the main subfamily identified in this study (11), there are also two other families significantly represented, the ABCB with 7 transporters identified, most annotated as "pheromone exporter", and the ABCG, with 5 proteins (Supplemental Table SI). Meaningfully, the subcellular organization of the biosynthesis of TIAs in *Catharanthus roseus* predicts several trans-tonoplast translocations of intermediate metabolites, some of which could be mediated by ABC transporters (Guirimand et al., 2011b).

The identification of 6 MATE transporters is particularly interesting, since we have recently shown that the major TIAs present in the leaves of *C. roseus* are accumulated in leaf vacuoles by a proton-driven antiport possibly operated by a MATE protein (Carqueijeiro et al., 2013; Chapter II). Vacuolar accumulation of the alkaloid nicotine in tobacco leaves has been shown to be mediated by a MATE transporter also functioning as a proton antiport (Morita et al., 2009), and the benzylisoquinoline alkaloid berberine is

also transported across the tonoplast of *Coptis japonica* via a specific H$^+$/berberine antiport mechanism (Otani et al., 2005). All this strongly suggests that vacuolar accumulation of alkaloids in general and of the *C. roseus* TIAs in particular may be mediated by a MATE transporter, with this study providing strong candidate genes for this function. One of the MATE transporters, CroMATE1, is particularly abundant and is, therefore, the most likely candidate to TIA vacuolar accumulation (Table I). In order to confirm the vacuolar localization of CroMATE1 before proceeding to functional characterization, its subcellular localization was investigated by GFP-tagging. As can be seen in Fig. 10, both GFP-CroMATE1 and CroMATE1-GFP fusions appeared clearly localized in the tonoplast, supporting its choice as a primary candidate for TIA vacuolar accumulation, and further supporting the vacuolar / tonoplast nature of our fractions.

Secondary metabolism and the TIA pathway – a defence landmine

Plants produce a variety of secondary metabolites with deterrent / repellent or toxic properties against microorganisms, viruses, and/or herbivores from which they cannot escape, being sessile organisms. Some of these compounds also influence the growth of neighbouring plants. These allelochemicals can be constitutively expressed, they may be activated by wounding - e.g. cyanogenic glycosides, glucosinolates, coumaryl glycosides, alliin, ranunculin, etc., or they may be produced *de novo,* induced by elicitors, infection or herbivory – phytoalexins (Wink, 1993; Hartmann, 2007). Many of these metabolites are also toxic to the producing cells and a range of specific self-resistance mechanisms exist in plants, with sequestering in the vacuole being one of the most important (Sirikantaramas et al., 2008). Moreover, some of the reactions involved in the biosynthesis of these compounds have also been shown to occur in the vacuole (Verma et al., 2012).
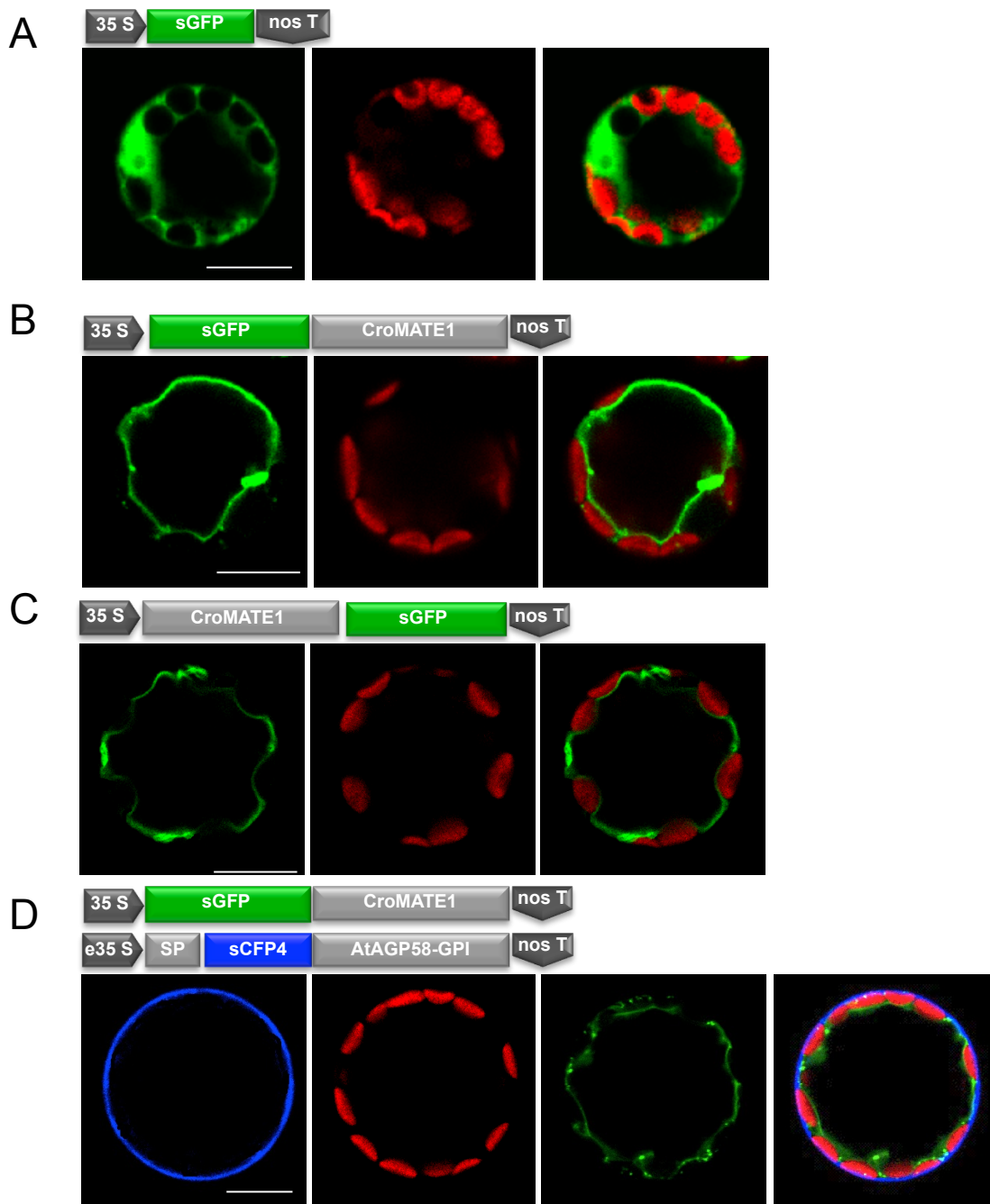
Figure 10. Confocal microscopy images from transient transformation of *C. roseus* leaf protoplasts with GFP- CroMATE1 fusions, for the validation of the tonoplast localization of the membrane protein CroMATE1, identified in the vacuolar proteome. The schematic representation of the construct(s) used for transformation is depicted right above the respective set of confocal images. A, GFP fluorescence pattern observed with the *35S::sGFP* construct. B, GFP fluorescence observed with the N-terminal construct 35S::sGFP-MATE1. C, GFP fluorescence observed with the C-terminal construct 35S::MATE1-sGFP. D, Co-tranformation of *C. roseus* protoplasts with the constructs 35S::sGFP-MATE1 and 35S::SP-CFP-AtAGP58-GPI, which codifies a plasma membrane marker. A and B, Left column – GFP channel; middle column – red channel showing chloroplast autofluorescence; right column – merged images. C, Left column – CFP channel; second column – GFP channel; third column – red channel showing chloroplast autofluorescence; fourth column – merged images. Bars = 10 μm.

Here, 70 entries assigned as potentially involved in secondary metabolism were identified in the vacuolar proteome of *C. roseus* leaf cells (Supplemental Table SI). Fig. 11A shows the distribution of MPGR entries assigned by MapMan to different secondary metabolic pathways, totalizing 218 entries (all the MPGR entries identified by the Proteome Discoverer 1.4 search irrespective of the score and number of peptides were uploaded to MapMan, corresponding to a number of entries significantly higher than the 1886 considered for most of this study). The most represented pathway is the phenylpropanoid, suggesting that many of their reactions may take place in the vacuole. This fact and the presence of several entries related with flavonoid metabolism relates well with the recent detection of a diversity of these compounds in *C. roseus* leaves, and a high concentration of a few of them precisely in the vacuoles (Ferreres et al., 2008; Ferreres et al., 2011).
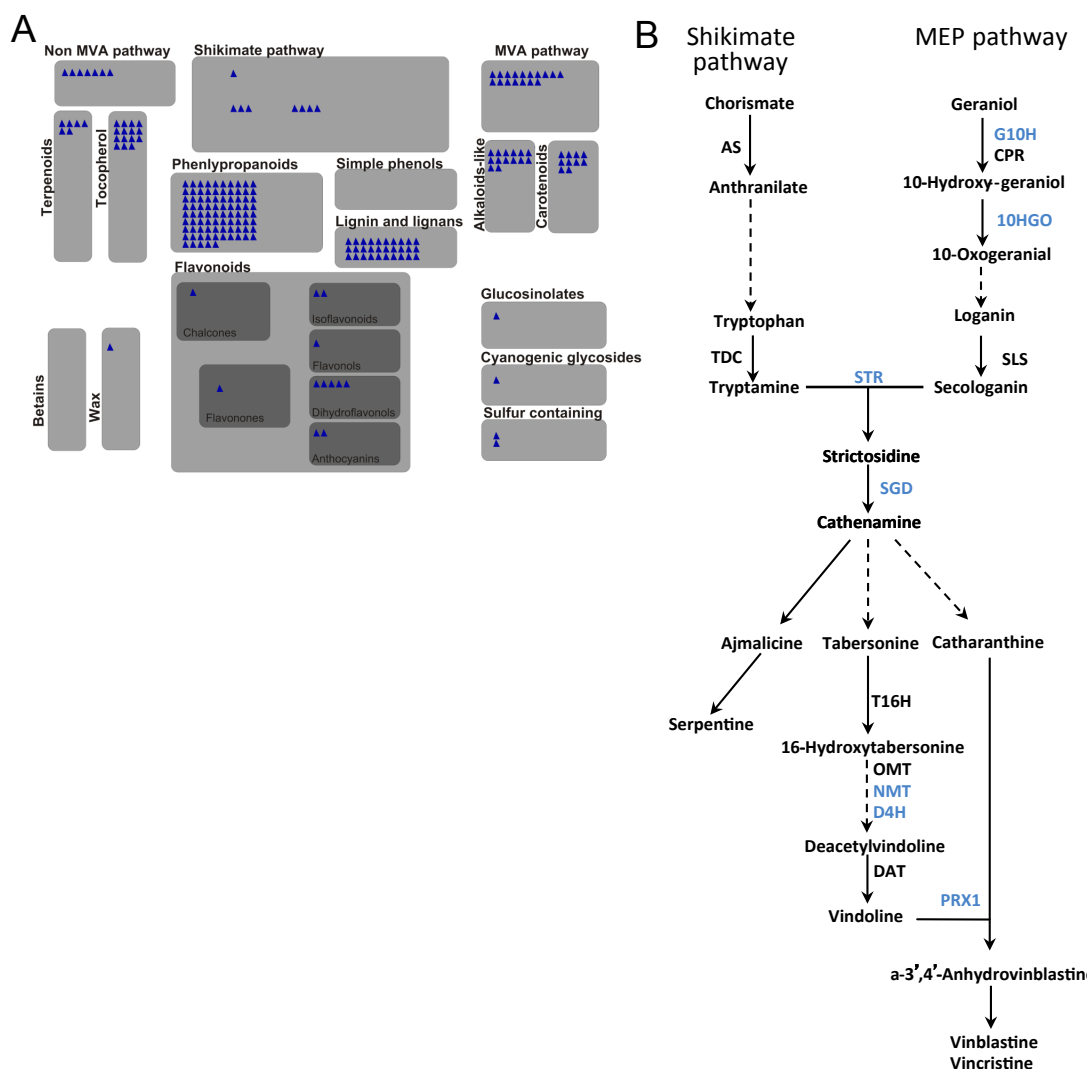
Figure 11. A, Image generated by the MapMan visualization platform of the proteins from the *C. roseus* vacuole proteome assigned to different secondary metabolism pathways. Blue triangles represent each detected protein. B, The *C. roseus* TIA pathway. The enzymes detected in this study are represented in blue. G10H - Geraniol 10- hydroxylase, 10HGO - 10-hydroxygeraniol oxidoreductase, SLS - secologanin synthase, STR - strictosidine synthase, SGD - strictosidine β-D-

glucosidase, T16H - tabersonine 16-hydroxylase, OMT - 2,3-dihydro-3-hydroxytabersonine *O*-methyltransferase, NMT - 16-metoxy-2,3-dihydro-3-hydroxytabersonine *N*-methyltransferase, D4H- desacetoxy vindoline 4-hydroxylase, DAT- deacetylvindoline 4-*O*-acetyltransferase, PRX1 – peroxidase 1.

Importantly, the single entry with higher relative abundance in the entire proteome is one strictosidine synthase (STR) isoenzyme – 7.60 % in the vacuole fraction, with 3 more isoenzymes also present but with lower abundances (sum of 0.61 %). STR is the central enzyme of TIA metabolism, catalyzing the condensation of secologanin (monoterpenoid precursor) with tryptamine (indole precursor) to yield strictosidine, the first terpenoid indole alkaloid of the pathway and the precursor of all TIAs (Fig. 11B; Loyola-Vargas et al., 2007). This indicates the strong investment of *C. roseus* leaves in TIA production and the central role of the vacuole in the pathway. Other enzymes of TIA biosynthesis were also detected in the vacuole proteome and are highlighted in Fig. 11B representing the TIA pathway. The cytochrome P450 geraniol 10-hydroxylase (G10H), catalysing the first committed step of the biosynthesis of the monoterpenoid precursor secologanin, was detected with relative high abundance both in the vacuole and the tonoplast fractions. This enzyme was initially reported to be localized in provacuole membranes (Madyastha et al., 1977), but recent work has indicated an ER membrane localization (Loyola-Vargas et al., 2007; Guirimand et al., 2009; Guirimand et al., 2011a). Our results re-open the possibility that this enzyme may also be indeed present in the tonoplast. The next enzyme in the secologanin pathway is 10-hydroxygeraniol oxidoreductase (10-HGO), and 5 of their isoenzymes were identified in the *C.roseus* vacuole proteome, all with significant relative abundances. 10-HGO was significantly present in both the vacuole and tonoplast samples, suggesting a membrane localization of this enzyme (Table I). After its synthesis, strictosidine is deglycosylated to yield an unstable aglycone that is rapidly converted into a highly reactive dialdehyde, from which more than 2,000 TIAs are derived. This reaction is catalysed by strictosidine-β-D-glucosidase (SGD), which has been initially associated with the vacuoles (Stevens et al., 1993), then with the ER (Geerlings et al., 2000), and finally SGD-GFP fusions were shown to accumulate in the nucleus, using constructs under the control of the 35S promoter expressed in *C. roseus* cell suspensions (Guirimand et al., 2010). Closing the circle, SGD has been detected in the tonoplast fractions in this study, reopening again the vacuolar localization discussion (Table I). The last steps of the biosynthesis of one of the TIA monomeric precursors from VLB and VCR, vindoline, has been well characterized, and here, two enzymes from this TIA branch have been identified: 2,3-dihydro-3-hydroxytabersonine *N*-methyltransferase (NMT) and desacetoxyvindoline 4-hydroxylase (D4H). D4H has been reported to be cytosolic, while NMT has been

proposed to be associated with thylakoid membranes (Mahroug et al., 2007; Guirimand et al., 2011b). Particularly NMT is present in all the vacuole / tonoplast samples with a significant relative abundance, strongly supporting a tonoplast localization. Vindoline is transported to the vacuole (Carqueijeiro et al., 2013; Chapter II) and is coupled with catharanthine to yield AVLB, the precursor of the anticancer VLB and VCR and of all dimeric TIAs. The major class III peroxidase (Prx) from *C. roseus* leaves, CroPRX1, has been implicated in this coupling reaction, and its vacuolar localization has been demonstrated by biochemical, cytochemical and molecular methods (Sottomayor et al., 1996; Costa et al., 2008; Ferreres et al., 2011). Predictably, CroPrx1 was indeed detected in this study, with one of the highest relative abundances in the vacuole fraction (1.12 %, 14th highest), further indicating the vacuolar identity of our fractions. The relevance of the presence of this enzyme with such high abundance may relate with the importance of the biosynthesis of TIA dimers, but may also relate with the proposed role of CroPrx1 in H_2O_2 scavenging (Ferreres et al., 2011), which is discussed in more detail in the section redox metabolism below. Surprisingly, this study detected the presence of an enzyme annotated as vinorine synthase, an acetyltransferase that leads to the formation of the alkaloid, which is the direct precursor of ajmalin, an antiarrhythmic drug from *Rauvolfia serpentine* (Bayer et al., 2004). Vinorine synthase has 31 % of similarity with deacetylvindoline-4-O-acetyltransferase (DAT), a cytosolic acetyltransferase enzyme responsible for the last biosynthetic step of vindoline in *C. roseus.* It is possible that the detected vinorine synthase may catalyse an alternative reaction, since, to our knowledge *C. roseus* does not produce ajmaline, and it is the first time that this enzyme is reported in Catharanthus.

Counting with G10H, a total of 17 P450s were detected in the vacuole/tonoplast fractions, a few of them with a significant relative abundance (Supplemental Table SI). Moreover, two NADPH cytochrome P450 reductases and one cytochrome b5 plus the respective NADH cytochrome b5 reductase (P450 electron donors), were also identified, although in lower levels and only in the tonoplast fraction. The question whether there are P450s in the vacuole has been raised by De Luca (2003), who speculated whether secologanin synthase (SLS; CYP72A1; Fig. 11B) could be localized in the vacuole, handily delivering secologanin to STR. However, ER P450s are anchored to the cytosolic face of the ER membranes, and since all the endomembrane system shares a common topology, tonoplast P450s, if they exist, should also catalyse cytosolic reactions. This may, however, indicate the existence of specifically located metabolic channels for the synthesis of certain vacuolar metabolites, guaranteeing their immediate transport into the vacuole after synthesis.

The second protein with higher relative abundance in the category secondary metabolism (2.58 %) was an alliin lyase or alliinase. In plants of the genus *Allium*, such as garlic and onions, alliinases are responsible for catalyzing chemical reactions that produce the volatile chemicals that give these foods their flavors, odors, and tear-inducing properties (Lancaster et al., 2000). This manifestation is part of the plant's defence against herbivores - when the plant is damaged by a feeding animal, the alliinase is released from the vacuoles where it is stored and reacts with substrates released from vesicles to catalyze the production of the pungent chemicals with deterrent effects. The finding of an alliinase with such a high concentration in *C. roseus* leaves, suggests that they might also have a similar defence system, which, to our knowledge, has never been reported. The presence of similar compounds to the known S-alk(en)yl-lCys sulfoxide substrates of allinase, or of its products pyruvate, ammonia, and sulfur-containing volatiles (Lancaster et al., 2000) were not detected in recent phytochemical surveys of *C. roseus* (Ferreres et al., 2008; De Pinho et al., 2009; Pereira et al., 2009). Strikingly, alliinase is present in *Allium cepa* bulbs at high levels, representing up to 6 % by weight of the soluble protein in the bulb (Nock and Mazelis, 1987). This high abundance of a vacuolar protein in a tissue, may relate with the finding of Carter et al. (2004) in the Arabidopsis leaf vacuole proteome of a single protein that represented the bulk of vacuolar protein content. This protein was identified as being a myrosinase-associated protein (MAP; At3g14210) and the authors related its high levels with the high abundance of proteins that act as buffer to changes in osmotic pressure in animal systems, suggesting that this MAP could play a role in controlling drastic osmotic fluctuations within the vacuole. The possibility that this MAP could also be involved in modulating the enzyme activity of myrosinase was also referred. Curiously, myrosinase, similarly to alliinase, is an enzyme involved in plant defence against herbivores, catalysing the hydrolysis of glucosinolates to generate sulphur defence toxic products, forming the so called "mustard oil bomb" glucosinolate-myrosinase defence system in Brassicaceae such as Arabidopsis (Kissen et al., 2009). All these results seem to converge into a strong commitment of the vacuoles with defence secondary metabolism.

Redox metabolism – the ultimate defence against reactive oxygen species

Among the proteins identified in the vacuole and tonoplast of *C. roseus* leaves, a group of enzymes involved in redox reactions appeared with a quite significant representation in relative abundance and protein number (Fig. 7). In particular CroPrx1, already mentioned above as being involved in TIA metabolism, appeared with a very high relative abundance of 1.12 %, corroborating its high activity in intact vacuoles reported by Ferreres et al. (2011). This high abundance of CroPrx1 gives further

strength to our previous proposal that vacuolar Prxs, in association with a range of vacuolar secondary metabolites potentially acting as their reducing substrates, represent an important sink/buffer of H_2O_2 in green plant cells, namely during high light conditions (Fig. 12; Ferreres et al. 2011) Like-minded, Zipor and Oren-Shamir (2013) propose that vacuolar Prxs are key players in the adaptation of plants to change, and serve as plant caretakers, namely controlling the quality and quantity of light reaching the photosynthetic apparatus, depending on the peroxidase mediated degradation of anthocyanins, since these vacuolar pigments act as a light shield. Related to this, two anthocyanins were identified in *C. roseus* vacuoles (Ferreres et al. 2011), and two anthocyanin permeases were identified here.
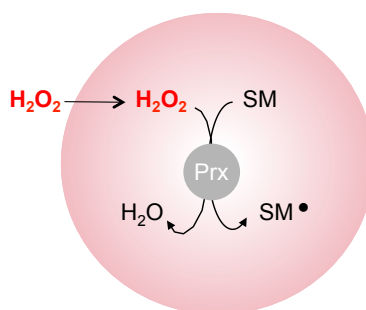
Figure 12. Scheme representing the H_2O_2 scavenging activity of vacuolar peroxidases (Prx) at the expenses of the oxidation of vacuolar secondary metabolites (SM).

Two more Prxs were detected in this study, CroPrx7 and CroPrx50 (according to PeroxiBase nomenclature; (Passardi et al., 2007), and their alignment with CroPrx1 and a well characterized cell wall peroxidase, peanut PNC1 (Fig. 13), highlights the presence of a C-terminal extension (CTE) in all the *C. roseus* Prxs detected in the vacuolar proteome. In CroPrx1, this CTE has been shown to determine the vacuolar sorting of CroPrx1 (Costa et al., 2008) and the presence of CTEs in CroPrx7 and CroPrx50 further supports their vacuolar localization.

```
PNC1      280 NAATFNTDFGNAMIKMGNLSPLTGTSGQIRTNCRKTN--------------------------
CroPrx1   296 NQTLFFEKFVYAMIKMSQLNVLTGNQGEIRSNCSLRNAAAMGRSSSSLLGSVVEEAAEIGLSMF
CroPrx7   294 NETLFFEKFVIGMIKMGQMNVLTGTQGEIRAKCSVRNRDNSMI------STVVDEIEDIGLSMF
CroPrx50  281 DENEFFKAFVQGMLKMGDLQ--SGRPGEIRRNCRMVNRRPVDF----LLEDXSKEEDEVHN---
```

Figure 13. Alignment of the C-terminal sequence of the three Prx proteins identified in the vacuole proteome of *C. roseus* leaf cells with the well characterized cell wall peanut Prx PNC1. The regions highlighted in black correspond to conserved amino acid residues in at least two of the proteins and in red is the last conserved cysteine of Prxs. A C-terminal extension (CTE) is visible in the three identified Prxs, which constitutes a confirmed vacuolar sorting determinant for CrPrx1 (Costa et al. 2008) and putative vacuolar sorting determinants for CroPrx7 and 50.

Unexpectedly, key enzymes of plant cell antioxidant defences including ascorbate peroxidase, catalase, and superoxide dismutase were detected both in vacuole and tonoplast fractions (Table I). In total, were identified two isoenzymes for ascorbate peroxidase, one with very high relative abundance (0.37 %) in vacuoles, two isoenzymes for catalase with relatively high abundance, and three isoenzymes for superoxide dismutase, one Cu/Zn, one Fe and one Mn (Table I). Even more striking, three isoenzymes of monodehydroascorbate reductase and two isoenzymes of glutathione reductase were also identified, almost fulfilling the conditions to accomplish the glutathione-ascorbate cycle in the vacuole (Fig. 14). The only missing link is dehydroascorbate reductase, which was actually detected by Carter et al. (2004) in the vacuole proteome of Arabidopsis leaves, together with catalase 3, ascorbate peroxidase and superoxide dismutase. Ascorbate peroxidase was also detected by Jaquinod et al. (2007) in vacuoles of Arabidopsis suspension cells, and by Schmidt et al. (2007) in vacuoles of cauliflower buds. The possibility that the glutathione-ascorbate cycle may operate in the vacuole would be just further dependent on the presence of ascorbate, which we have previously shown to be present in *C. roseus* vacuoles in significant amounts (Ferreres et al., 2011), and on the presence of $NADP^+$ / NADPH. Although the presence of $NADP^+$ / NADPH in the vacuoles has not been detected in previous metabolomic studies (Tohge et al. 2011), it is not impossible that some may end up in the vacuole, from autophagocytosis or from multivesicular bodies having entrapped cytosolic $NADP^+$ / NADPH during the vesiculation process. The identification of a putative glutamate/malate translocator in this study suggests that the existence of a membrane shuttle guaranteeing $NADP^+$ energization inside the vacuole is a possibility.

The presence of catalase deserves special mentioning. Contrary to the other antioxidant enzymes, for which a range of different subcellular localizations are known, catalase is considered to be localized in the peroxisome (Mhamdi et al., 2012) although some indications of possible cytosolic and mitochondrial localization have been reported (Mhamdi et al., 2010). Curiously, as found for RbCS, catalase presents a similar relative abundance in the two fractions / four samples analysed and has also been shown to bind to viral proteins, which, in the case of catalase, changed it localization from cytosolic to nucleus (Inaba et al., 2011). This curious resemblance with what happens for RbCS also raises the speculation whether catalase can also be a "moonlighting" protein.

Other antioxidant enzymes detected in the vacuole and tonoplast fractions include glutathione peroxidase, 3 peroxiredoxins and thioredoxin-dependent peroxidase. The presence of all those antioxidant enzymes and isoenzymes, often in high levels, in vacuole and tonoplast fractions having many signs of high purity and enrichment can

hardly be explained as contamination. Therefore, this study indicates an extremely important role of vacuoles in reactive oxygen species (ROS) scavenging and redox homeostasis in plant cells.
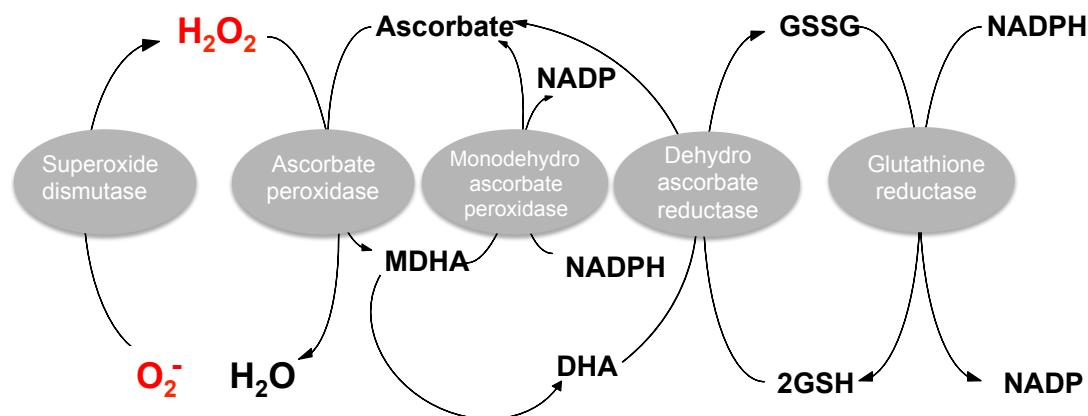
Figure 14. The ascorbate–glutathione cycle involved in scavenging of H_2O_2 in plant cells. This cycle has been shown to operate in chloroplasts, peroxisomes, mitochondria and the cytosol. MDHA (monodehydroascorbate reductase); NADP (nicotinamide adenine dinucleotide); GSSG (oxidized glutathione); 2GSH (glutathione); NADPH (Nicotinamide adenine dinucleotide phosphate); DHA (dehydrascorbate).

Catabolism categories – a recycling factory

Vacuoles are the lytic compartment of plant cells and the categories considered here that are involved in lytic activities are three: protein and amino acid degradation, glycosidases, and catabolism and hydrolases. Together, the proteins of these categories are second to transport in abundance (19.75 %), and the first in number of proteins (167) in what concerns the vacuole fractions (Fig. 7A). Since most of these enzymes are soluble, they are not so significantly represented in the tonoplast fractions (Fig. 7B). The most abundant catabolic category is protein degradation, with a high number of proteases and peptidases detected (79), including 7 aspartic, 6 cysteine and 11 serine proteases. The three most abundant proteases in the vacuole fraction are a cysteine protease Cp6, a serine carboxypeptidase and an aspartic proteinase, with 2.17 %, 1.44 % and 0.91 % relative abundance respectively. There is also a membrane aspartic proteinase nepenthesin-1 with a very high abundance of 1.26 %.

Another highly represented catabolic category was glycosidases, including a total of 56 proteins. The more abundants were an invertase, α-L-arabinofuranosidase and α-mannosidase, with 1.05 %, 0.54 % and 0.52 % relative abundance respectively. Several chitinases were present, again confirming the defence importance of the vacuole. Interestingly, several amylases were also identified, suggesting a role of the vacuole in starch degradation.

Finally, all other hydrolases were joined in the category catabolism and hydrolases, which includes, namely, a number of lipases, esterases, phosphatases and a

chlorophyllase. The most abundant proteins in this category were a carbon-nitrogen hydrolase family protein, RNase NGR3 and acid phosphatase 1, with 0.91 %, 0.41 % and 0.35 % relative abundance respectively. It is known that the vacuole has high levels of RNase activity due to the detection of RNA-oligonucleotides in vacuoles (Abel et al., 1990), but almost nothing is known about this vacuolar RNA degradation activity (Martinoia et al., 2012). Previous proteomic characterizations of the vacuole have not detected the presence of RNases (Carter et al., 2004; Jaquinod et al., 2007; Schmidt et al., 2007), therefore, the detection of an RNase NGR3 here opens the way to the study of the role of the vacuole in RNA degradation.

In summary, the most significant catabolic activity of the vacuoles is undoubtedly proteolysis, indicative of the intense turnover that proteins suffer in cells. This is immediately followed by glycosidases, also indicating that carbohydrate metabolism is highly important and active in plant cells.

Primary metabolism and glycosyl transferases

Unlike previous proteomic studies of the plant cell vacuole, we have detected a significant number of enzymes that could be related with primary metabolism, justifying the formation of this category. In fact, this category had the highest number of proteins of all categories in the vacuole fraction (188), corresponding to the fourth in terms of relative abundance (Fig. 7A). Around 22 % of those proteins appear only in tonoplast fractions (42/188), suggesting that part of them (the soluble ones) may be a contamination resulting from adhesion of cytosolic proteins to the membranes. However, this does not have a significant impact in total protein relative abundance of this category, due to the very low abundance of these proteins in the tonoplast samples. Primary metabolism, namely of carbohydrates, has been associated with the vacuoles (Pollock and Kingston-Smith, 1997), and accordingly a high number of glycosyl transferases was identified here. Since this organelle has been shown to accumulate many amino acids, sugars, organic acids, fatty acids, etc. (Tohge et al., 2011), it is likely that it also participates in the metabolism of those compounds. Martinoia et al. (2012), acknowledges that the vacuole also contains metabolic enzymes that use compounds transported into the vacuole to produce new metabolites. Examples of this are fructans, which are produced within the vacuole from sucrose (Pollock and Cairns, 1991), chain elongation of the raffinose sugar family (Bachmann et al., 1994), and acylation of some compounds (Hause et al., 2002). The three most abundant proteins identified in primary metabolism were acetylornithine deacetylase, serine hydroxymethyltransferase 5 and triosphosphate isomerase type II with 1.42 %, 0.67 % and 0.61 % relative abundance

respectively, while the three most abundant glycosyl transferases had 0.46 %, 0.09 % and 0.03 % relative abundance, all in the vacuole fraction.

Signalling and membrane structure and microdomains

The highest number of proteins assigned into a category, in each fraction, corresponds to the category signalling in the tonoplast fraction – 173 (Fig. 7 and Supplemental Table SI). This result establishes the tonoplast as a highly active signalling platform. As discussed throughout this study, the vacuole is extremely important for cell homeostasis, namely by storing or releasing ions, metabolites, hormones, etc., or regulating turgor pressure, according to the cell needs. This means that all the myriad of tonoplast transporters (see above) working in both ways have to be regulated with a high precision. Therefore, it is logical that the tonoplast presents such a high number of proteins involved in signalling as detected here. These include many protein kinases from a number of different families, many putative receptor proteins, phospholipases, etc. The most abundant proteins in this category, in the vacuole fraction, were auxin-binding protein ABP20 (0.79 %), a kinase (0.14 %) and cell elongation protein DIMINUTO (0.07 %) (Table I). This last protein was also identified in the Arabidopsis vacuole proteomes characterized by Carter et al. (2004) and Jaquinod et al. (2007). Moreover, Jaquinod et al. (2007) have proven the tonoplast localization of this protein using a GFP fusion.

Related with signalling, a small number of proteins associated with membrane structure and microdomains were identified, namely several fasciclin-like arabinogalactan proteins (FLAs), that have also been detected in the previous vacuole proteomes published (Carter et al., 2004; Jaquinod et al., 2007; Schmidt et al., 2007). FLAs are a large class of chimeric arabinogalactan proteins (AGPs) that contain one or two fasciclin domains, thought to be important for protein-protein interactions, and one or two AGP domains (Ellis et al., 2010). AGPs and FLAs have been considered as plasma membrane proteins, but we have previously detected abundant immuno-labelling of AGPs in the vacuole suggesting their localization in membrane microdomains of the tonoplast, evocative of lipid rafts (Sottomayor et al., 2008; Figueiredo, 2011). In fact, most FLAs are attached to the membrane by a GPI-anchor and are thought to be important for the formation of membrane microdomains (rafts), facilitating signalling (Johnson et al., 2003). Meaningfully, it was proposed that an FLA, SOS5/FLA4, is a ligand of two members of the Leu-rich repeat receptor-like kinase family in Arabidopsis (Xu et al., 2008). Very recently, the presence of detergent-resistant membrane microdomains, interpreted as lipid rafts, was detected for the first time in tonoplast membranes (Ozolina et al., 2013). This data, together with the results of this study,

suggest that microdomains associating particular sets of signalling proteins and transporters may act in the tonoplast to regulate the multiple functions of the vacuole.

Vesicle and protein traffic and cytoskeleton

The vacuole is a major component of the plant endomembrane system, which is characterized by an intensive vesicle and protein traffic among its components. On the other hand, vesicle traffic and organelle positioning is dependent on interaction with the cytoskeleton. Therefore, it is not surprising that *C. roseus* leaf vacuoles, specially the tonoplast, presents here 95 proteins identified as associated with vesicle and protein traffic, and 29 classified in the category cytoskeleton (Supplemental Table SI). Noticeably, 6 Rabs are the most abundant proteins in the vesicle and protein traffic category, with three different Rab7 heading the list. This further supports the involvement of Rab 7 in vacuolar delivery of the 'late prevacuolar compartment' as proposed recently by Bottanelli et al. (2012). Several proteins identified by Carter et al. (2004) have also been identified in this study, including N-ethylmaleimide-sensitive factor attachment protein receptor v-SNARE SYP51, a VTI11 protein, and a α-soluble NSF attachment protein.

The main proteins under the category cytoskeleton are actin and tubulin subunits, with several dynamin isoenzymes and kinesin being also present (Supplemental Table SI). The presence of these proteins may be due to their involvement in anchoring vesicles to the vacuole or in membrane dynamics of the tonoplast itself, for instance to form the intracellular vesicles observed in Fig. 8 or the intracellular bulbs mentioned by Saito et al. (2002) and Bottanelli et al. (2012). Previous proteomic studies in arabidopsis and cauliflower leaf vacuoles also reported the presence of cytoskeleton proteins (Carter et al., 2004; Shimaoka et al., 2004; Endler et al., 2006; Jaquinod et al., 2007).

Miscellaneous

For a number of proteins, the related annotations did not enable to assign them to a defined category and were included under miscellaneous. The most abundant protein in this list is a lectin with a high relative abundance of 1.572 %. Plant lectins are considered storage proteins that have also been reported to have an important defence role against fungi, bacteria, and insects, as well as during abiotic stresses (Candido et al., 2011). So it is possible that this lectin may have a dual function of storage and defence, in any case with importance due to its high abundance. It should be noted that this was the single case detected of a protein with a storage function.

Unknwon

For 168 proteins it was not possible to find any functional annotation, which is not synonymous of low importance, since some of them presented very high relative abundances, near 1% (Supplemental Table SI). The identification of these proteins in the plant vacuole may aid future research to discover their functions.

A model for the multifunctional vacuole

The analysis of the proteome of the toxic vacuole from *C. roseus* leaf cells enabled the identification of 1886 putative proteins that allow new insights into vacuole functions. The main aspects of vacuole function highlighted with this study are gathered in the model represented in Fig. 15.

C. roseus leaf vacuoles are definitely deeply engaged in secondary metabolism, with the TIA central enzyme strictosidine synthase being the most abundant protein detected, and a very high number of proteins being assigned to secondary metabolism (Fig. 7A and 11A). A **defence** role of the vacuole was therefore clearly diagnosed. Related to this, an unparalleled number of **ABC transporters** was identified (42), together with a few MATE transporters (6), potentially involved in the active traffic across the tonoplast of different TIA intermediates and other secondary metabolites such as the also highly represented phenylpropanoid pathway (Fig. 11A).

The high number and diversity of **transporters** detected underlines the role of the vacuole in cell homeostasis including ion levels, signalling and recycling of cell components, with the big investment in this last role of recycling being also clearly indicated by the presence of a high number of **lytic** enzymes (protein degradation, glycosidases and hydrolases in Fig. 7A and Supplemental Table SI).

The very significant vacuolar representation of CroPrx1, which has been shown to be capable of using a range of vacuolar alkaloids and phenolics as substrates to reduce H_2O_2 to water (Sottomayor et al., 1998; Ferreres et al., 2011), together with the unexpected detection of some of the enzymes considered among the most important systems in cellular antioxidant defences, clearly indicate to an important role of vacuoles in **ROS scavenging** and therefore in redox homeostasis of plant cells.

The proteins identified further point to the vacuole as a highly regulated organelle, through a vast array of membrane signalling molecules potentially involved in the regulation of the transporters mediated fluxes essential for all vacuolar functions. Accordingly, the presence of several FLAs suggests the presence of membrane microdomains (rafts) in the tonoplast, which may constitute **signalling platforms** where particular sets of signalling proteins and transporters may interact to fulfil precise functions.

Finally, this proteomic study suggests the existence of an active **metabolism** inside this organelle, as well as the presence in the tonoplast of short electron transference chains constituted by P450s and the associated reductases.
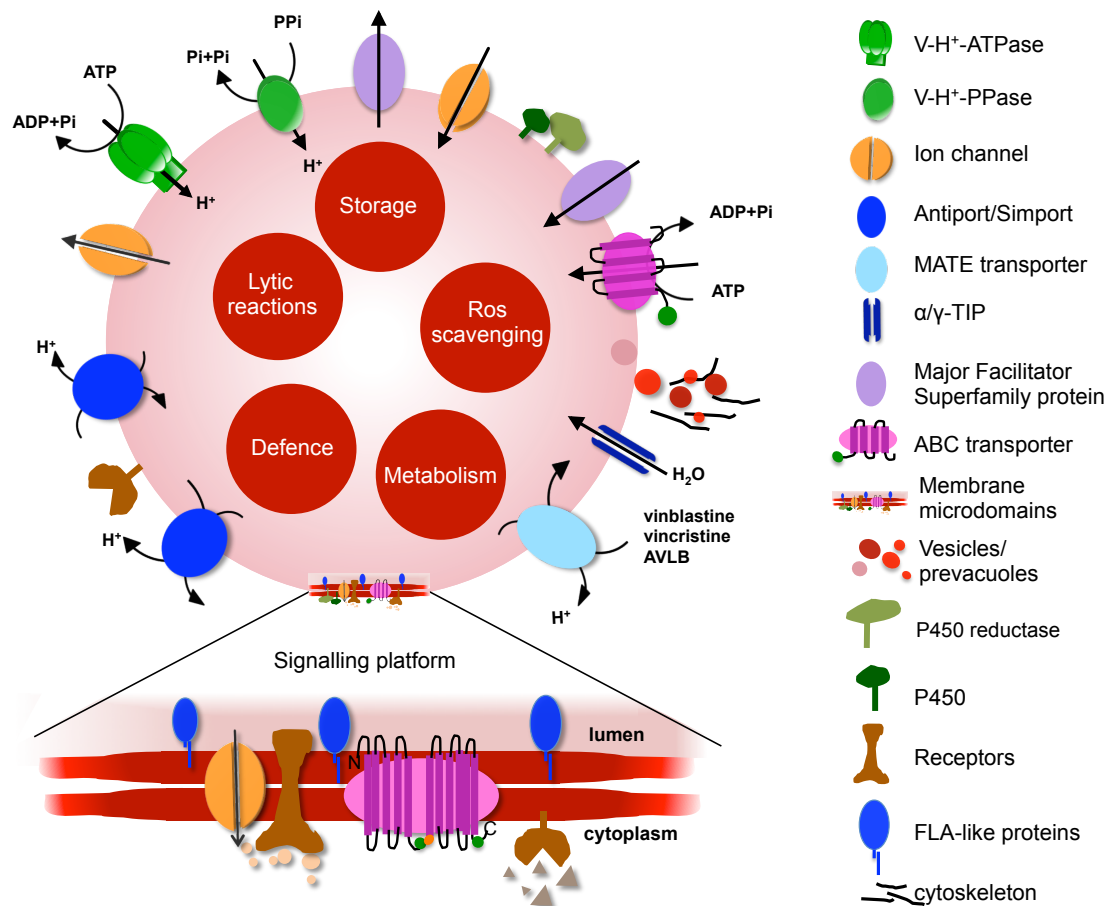
Figure 15. Model proposed for the multifunctional vacuole in *C. roseus* leaf cells including the main classes of membrane proteins detected and reference to the main functions diagnosed. The amplified insert represents the structure of a putative membrane microdomain (raft).

The question remains whether all these functions, suggested by the vacuolar complement of proteins detected in this study, are joined together in a single vacuole or are segregated in different types of vacuoles, or in vacuoles from the different types of cells present in the leaves of *C. roseus*, namely mesophyll, epidermal, idioblast, or stomata guard cells (Fig. 1). Interestingly, in this vacuolar proteomic study, almost all isolated vacuoles presented an acidic lumen typical of LVs, and very few markers of PSVs were identified - a lectin and a α-TIP. It is conceivable that PSVs may have a different density from LVs, having as consequence that they will not be recovered with the gradient centrifugation used to purify the isolated vacuoles. α-TIP, considered to be a PSV marker, was detected in isolated tonoplast membranes and not in isolated vacuoles, supporting this hypothesis. It would be interesting, in the future, to isolate

vacuoles having LVs and PSVs labelled with different FP markers to try to characterize the two populations.

CONCLUSIONS

As an immense organelle enclosed inside the plant cell, the vacuole has an extraordinary potential to act as a buffering compartment, with major importance for cell homeostasis in plants. This is well known, and was confirmed here, namely in what concerns ion and sugar homeostasis, but a very significant role in redox homeostasis should now be added to this list. As a whole, the proteome of the toxic vacuoles from *C. roseus* leaves further indicates, apart from the well-known involvement in lytic reactions, a high commitment of this organelle with secondary metabolism and defence, the presence of a significant metabolic activity, and the possible association of innumerable transporters and signalling proteins in membrane microdomains, with a special reference to the presence of many ABC transporters. The extensive list of 1886 putative proteins identified here stands as an invaluable tool for future studies of vacuole and protein function. An exciting clue raised, is whether RbCS and catalase may be "moonlighting" proteins, multifunctional proteins exhibiting activities distinct from their classically identified functions, as discovered for many enzymes of the glycolytic pathway, including glyceraldehyde-3-phosphate dehydrogenase (Sirover, 2011). Further supporting this hypothesis, glyceraldehyde-3-phosphate dehydrogenase itself has also been identified in this study, with a very high relative abundance and with similar values for both vacuole and tonoplast fractions, exactly as observed for RbCS and catalase.

SUPPLEMENTAL MATERIAL

The following materials are attached in digital format.

Supplemental Table SI.

ACKNOWLEDGEMENTS

LITERATURE CITED

Abel S, Blume B, Glund K (1990) Evidence for RNA-oligonucleotides in plant vacuoles isolated from cultured tomato cells Plant Physiology **94:** 1163-1171

Bachmann M, Matile P, Keller F (1994) Metabolism of the Raffinose Family Oligosaccharides in Leaves of Ajuga reptans L. (Cold Acclimation, Translocation, and Sink to Source Transition: Discovery of Chain Elongation Enzyme). Plant Physiology **105:** 1335-1345

Bak S, Beisson F, Bishop G, Hamberger B, Höfer R, Paquette S, D W-R (2011) Cytochromes P450. The Arabidopsis Book, **9**

Bayer A, Ma XY, Stockigt J (2004) Acetyltransfer in natural product biosynthesis - functional cloning and molecular analysis of vinorine synthase. Bioorganic & Medicinal Chemistry **12:** 2787-2795

Betz WJ, Mao F, Smith CB (1996) Imaging exocytosis and endocytosis. Current Opinion in Neurobiology **6:** 365-371

Blom TJM, Sierra M, Van Vliet TB, Franke-Van Dijk MEI, De Koning P, Van Iren F, Verpoorte R, Libbenga KR (1991) Uptake and accumulation of ajmalicine into isolated vacuoles of cultured cells of *Catharanthus roseus* (L.) G. Don. and its conversion into serpentine. Planta **183:** 170-177

Blondeau F, Ritter B, Allaire PD, Wasiak S, Girard M, Hussain NK, Angers A, Legendre-Guillemin V, Roy L, Boismenu D, Kearney RE, Bell AW, Bergeron JJM, McPherson PS (2004) Tandem MS analysis of brain clathrin-coated vesicles reveals their critical involvement in synaptic vesicle recycling. Proceedings Of The National Academy Of Sciences Of The United States Of America **101:** 3833-3838

Borisjuk L, Rolletschek H, Walenta S, Panitz R, Wobus U, Weber H (2003) Energy status and its control on embryogenesis of legumes: ATP distribution within Vicia faba embryos is developmentally regulated and correlated with photosynthetic capacity. Plant Journal **36:** 318-329

Bottanelli F, Gershlick DC, Denecke J (2012) Evidence for Sequential Action of Rab5 and Rab7 GTPases in Prevacuolar Organelle Partitioning. Traffic **13:** 338-354

Bradford MM (1976) Rapid and Sensitive method for quantitation of microgram quantities of protein utilizing principle of protein-dye binding. Analytical Biochemistry **72:** 248-254

Burnette WN (1981) Western Blotting - Electrophoretic Transfer of proteins from sodium dodecyl sulfate-polycrylamide gels to unmodified nitrocellulose and radiographic detection with antibody and radioiodinated protein-A. Analytical Biochemistry **112:** 195-203

Candido EdS, Soares Pinto MF, Pelegrini PB, Lima TB, Silva ON, Pogue R, Grossi-de-Sa MF, Franco OL (2011) Plant storage proteins with antimicrobial activity: novel insights into plant defense mechanisms. Faseb Journal **25:** 3290-3305

Carqueijeiro I, Noronha H, Duarte P, Gerôs HV, Sottomayor M (2013) Vacuolar transport of the medicinal alkaloids from Catharanthus roseus is mediated by a proton driven antiport. Plant Physiology

Carter C, Pan SQ, Jan ZH, Avila EL, Girke T, Raikhel NV (2004) The vegetative vacuole proteorne of Arabidopsis thaliana reveals predicted and unexpected proteins. Plant Cell **16:** 3285-3303

Costa dos Santos A, Seixas da-Silva W, de Meis L, Galina A (2003) Proton Transport in Maize Tonoplasts Supported by Fructose-1,6-Bisphosphate Cleavage. Pyrophosphate-Dependent Phosphofructokinase as a Pyrophosphate-Regenerating System. Plant Physiology **133:** 885-892

Costa MMR, Hilliou F, Duarte P, Pereira LG, Almeida I, Leech M, Memelink J, Barcelo AR, Sottomayor M (2008) Molecular cloning and characterization of a vacuolar class III peroxidase involved in the metabolism of anticancer alkaloids in *Catharanthus roseus*. Plant Physiology **146:** 403-417

De D (2000) Plant Cell Vacuoles :An Introduction. CSIRO Publication, Collingwood, Australia.

De Pinho PG, Goncalves RF, Valentao P, Pereira DM, Seabra RM, Andrade PB, Sottomayor M (2009) Volatile composition of Catharanthus roseus (L.) G. Don using solid-phase microextraction and gas chromatography/mass spectrometry. Journal of Pharmaceutical and Biomedical Analysis **49:** 674-685

Deus-Neumann B, Zenk MH (1984) A highly selective alkaloid uptake system in vacuoles of higher plants. Planta **162:** 250-260

Duarte P., Ribeiro D., Henriques G., Hilliou F. RAS, Lima F., Amorim I., M. S (2011) Cloning and Characterization of a Candidate Gene from the Medicinal Plant Catharanthus roseus Through Transient Expression in Mesophyll Protoplasts. *In* Molecular Cloning-Selected applications in Medicine and Biology. Intech, pp 291-308

FCUP 139

Unravelling the metabolism and transmembrane transport of the highly valuable medicinal alkaloids from *Catharanthus roseus*

Ellis M, Egelund J, Schultz CJ, Bacic A (2010) Arabinogalactan-proteins (AGPs): Key regulators at the cell surface? Plant Physiology

Emanuelsson O, Brunak S, von Heijne G, Nielsen H (2007) Locating proteins in the cell using TargetP, SignalP and related tools. Nature Protocols **2:** 18

Endler A, Meyer S, Schelbert S, Schneider T, Weschke W, Peters SW, Keller F, Baginsky S, Martinoia E, Schmidt UG (2006) Identification of a vacuolar sucrose transporter in barley and arabidopsis mesophyll cells by a tonoplast proteomic approach. Plant Physiology **141:** 196-207

Ferreres F, Figueiredo R, Bettencourt S, Carqueijeiro I, Oliveira J, Gil-Izquierdo A, Pereira DM, Valentao P, Andrade PB, Duarte P, Barcelo AR, Sottomayor M (2011) Identification of phenolic compounds in isolated vacuoles of the medicinal plant *Catharanthus roseus* and their interaction with vacuolar class III peroxidase: an H2O2 affair? Journal of Experimental Botany **62:** 2841-2854

Ferreres F, Pereira DM, Valentão Pc, Andrade PB, Seabra RM, Sottomayor M (2008) New Phenolic Compounds and Antioxidant Potential of Catharanthus roseus. Journal of Agricultural and Food Chemistry **56:** 9967-9974

Figueiredo R (2011) Functions of Class III Peroxidases in higher plants: multiple approaches using the medicinal plant Catharanthus roseus and the model plant Arabidopsis thaliana. Universidade do Porto, Porto

Fontes N, Silva R, Vignault C, Lecourieux F, Geros H, Delrot S (2010) Purification and functional characterization of protoplasts and intact vacuoles from grape cells. BMC research notes **3:** 19

Frigerio L, Hinz G, Robinson DG (2008) Multiple vacuoles in plant cells: Rule or exception? Traffic **9:** 1564-1570

Friso G, Giacomelli L, Ytterberg AJ, Peltier J-B, Rudella A, Sun Q, Wijk KJv (2004) In-Depth Analysis of the Thylakoid Membrane Proteome of Arabidopsis thaliana Chloroplasts: New Proteins, New Functions, and a Plastid Proteome Database. The Plant Cell Online **16:** 478-499

Garin J, Diez R, Kieffer S, Dermine JF, Duclos S, Gagnon E, Sadoul R, Rondeau C, Desjardins M (2001) The phagosome proteome: Insight into phagosome functions. Journal of Cell Biology **152:** 165-180

Geerlings A, Ibañez MM-L, Memelink J, van der Heijden R, Verpoorte R (2000) Molecular Cloning and Analysis of Strictosidine β-d-Glucosidase, an Enzyme in Terpenoid Indole Alkaloid Biosynthesis in Catharanthus roseus. Journal of Biological Chemistry **275:** 3051-3056

Gilchrist A, Au CE, Hiding J, Bell AW, Fernandez-Rodriguez J, Lesimple S, Nagaya H, Roy L, Gosline SJC, Hallett M, Paiement J, Kearney Robert E, Nilsson T,

Bergeron JJM (2006) Quantitative Proteomics Analysis of the Secretory Pathway. Cell **127:** 1265-1281

Goedhart J, van Weeren L, Hink MA, Vischer NOE, Jalink K, Gadella TWJ (2010) Bright cyan fluorescent protein variants identified by fluorescence lifetime screening. Nature Methods **7:** 2

Gongora-Castillo E, Childs KL, Fedewa G, Hamilton JP, Liscombe DK, Magallanes-Lundback M, Mandadi KK, Nims E, Runguphan W, Vaillancourt B, Varbanova-Herde M, DellaPenna D, McKnight TD, O'Connor S, Buell CR (2012) Development of Transcriptomic Resources for Interrogating the Biosynthesis of Monoterpene Indole Alkaloids in Medicinal Plant Species. Plos One **7**

Goodman CD, Casati P, Walbot V (2004) A multidrug resistance-associated protein involved in anthocyanin transport in Zea mays. Plant Cell **16:** 1812-1826

Gout E, Bligny R, Douce R (1992) Regulation of intracellular pH values in higher-plant cells C13 and P31 nuclear magnetic resinance studies Journal of Biological Chemistry **267:** 13903-13909

Guirimand G, Burlat V, Oudin A, Lanoue A, St-Pierre B, Courdavault V (2009) Optimization of the transient transformation of Catharanthus roseus cells by particle bombardment and its application to the subcellular localization of hydroxymethylbutenyl 4-diphosphate synthase and geraniol 10-hydroxylase. Plant Cell Reports **28:** 1215-1234

Guirimand G, Courdavault V, Lanoue A, Mahroug S, Guihur A, Blanc N, Giglioli-Guivarc'h N, St-Pierre B, Burlat V (2010) Strictosidine activation in Apocynaceae: towards a "nuclear time bomb"? Bmc Plant Biology **10**

Guirimand G, Guihur A, Ginis O, Poutrain P, Héricourt F, Oudin A, Lanoue A, St-Pierre B, Burlat V, Courdavault V (2011) The subcellular organization of strictosidine biosynthesis in Catharanthus roseus epidermis highlights several trans-tonoplast translocations of intermediate metabolites. FEBS Journal **278:** 749-763 **(a)**

Guirimand G, Guihur A, Poutrain P, Héricourt F, Mahroug S, St-Pierre B, Burlat V, Courdavault V (2011) Spatial organization of the vindoline biosynthetic pathway in *Catharanthus roseus*. Journal of Plant Physiology **Volume 168:** 549-557 **(b)**

Hartmann T (2007) From waste products to ecochemicals: Fifty years research of plant secondary metabolism. Phytochemistry **68:** 2831-2846

Hause B, Meyer K, Viitanen P, Chapple C, Strack D (2002) Immunolocalization of 1-O-sinapoylglucose:malate sinapoyltransferase in Arabidopsis thaliana. Planta **215:** 26-32

He CC, Klionsky DJ (2009) Regulation Mechanisms and Signaling Pathways of Autophagy. *In* Annual Review of Genetics, Vol 43. Annual Reviews, Palo Alto, pp 67-93

Hunter PR, Craddock CP, Di Benedetto S, Roberts LM, Frigerio L (2007) Fluorescent Reporter Proteins for the Tonoplast and the Vacuolar Lumen Identify a Single Vacuolar Compartment in Arabidopsis Cells. Plant Physiology **145:** 1371-1382

Inaba J-i, Kim BM, Shimura H, Masuta C (2011) Virus-Induced Necrosis Is a Consequence of Direct Protein-Protein Interaction between a Viral RNA-Silencing Suppressor and a Host Catalase. Plant Physiology **156:** 2026-2036

Jaquinod M, Villiers F, Kieffer-Jaquinod S, Hugouvieu V, Bruley C, Garin J, Bourguignon J (2007) A proteomics dissection of Arabidopsis thaliana vacuoles isolated from cell culture. Molecular & Cellular Proteomics **6:** 394-412

Jaquinod M, Villiers F, Kieffer-Jaquinod S, Hugouvieux V, Bruley C, Garin J, Bourguignon J (2007) A Proteomics Approach Highlights a Myriad of Transporters in the Arabidopsis thaliana Vacuolar Membrane. Plant signaling & behavior **2:** 413-415

Johnson KL, Jones BJ, Bacic A, Schultz CJ (2003) The fasciclin-like arabinogalactan proteins of arabidopsis. A multigene family of putative cell adhesion molecules. Plant Physiology **133:** 1911-1925

Kall L, Canterbury JD, Weston J, Noble WS, MacCoss MJ (2007) Semi-supervised learning for peptide identification from shotgun proteomics datasets. Nature Methods **4:** 923-925

Kissen R, Rossiter JT, Bones AM (2009) The 'mustard oil bomb': not so easy to assemble?! Localization, expression and distribution of the components of the myrosinase enzyme system. Phytochemistry Reviews **8:** 69-86

Klein M, Martinoia E, Hoffmann-Thoma G, Weissenbock G (2000) A membrane-potential dependent ABC-like transporter mediates the vacuolar uptake of rye flavone glucuronides: regulation of glucuronide uptake by glutathione and its conjugates. Plant Journal **21:** 289-304

Laemmli UK (1970) Cleavage of strutural proteins during assembly of head of bacteriophage-T4. Nature **227:** 680-&

Lancaster JE, Shaw ML, Joyce MDP, McCallum JA, McManus MT (2000) A Novel Alliinase from Onion Roots. Biochemical Characterization and cDNA Cloning. Plant Physiology **122:** 1269-1280

Li Z-S, Lu Y-P, Zhen R-G, Szczypka M, Thiele DJ, Rea PA (1997) A new pathway for vacuolar cadmium sequestration in Saccharomyces cerevisiae: YCF1-catalyzed

transport of bis(glutathionato)cadmium. Proceedings of the National Academy of Sciences **94:** 42-47

Liu GS, Sanchez-Fernandez R, Li ZS, Rea PA (2001) Enhanced multispecificity of Arabidopsis vacuolar multidrug resistance-associated protein-type ATP-binding cassette transporter, AtMRP2. Journal of Biological Chemistry **276:** 8648-8656

Lowry OH, Rosebrough NJ, Farr AL, Randall RJ (1951) Protein measurement with the folin phenol reagent. Journal of Biological Chemistry **193:** 265-275

Loyola-Vargas VM, Galaz-Ávalos RM, Kú-Cauich R (2007) *Catharanthus* biosynthetic enzymes: the road ahead. Phytochemistry Reviews **6:** 307-339

Luca VD (2003) Chapter eight Biochemistry and molecular biology of indole alkaloid biosynthesis: The implication of recent discoveries. *In* TR John, ed, Recent Advances in Phytochemistry, Vol Volume 37. Elsevier, pp 181-202

Madyastha KM, Ridgway JE, Dwyer JG, Coscia CJ (1977) Subcellular localization of a cytochrome P-450-dependent monogenase in vesicles of the higher plant Catharanthus roseus. The Journal of Cell Biology **72:** 302-313

Maeshima M (2000) Vacuolar H+-pyrophosphatase. Biochimica Et Biophysica Acta-Biomembranes **1465:** 37-51

Maeshima M, Yoshida S (1989) Purification and Properties of vacuolar membrane Uproton-tramslcating inorganic pyrophosphate from mung bean. Journal of Biological Chemistry **264:** 20068-20073

Mahroug S, Burlat V, St-Pierre B (2007) Cellular and sub-cellular organisation of the monoterpenoid indole alkaloid pathway in *Catharanthus roseus*. Phytochemistry Reviews **6:** 363-381

Martinoia E, Maeshima M, Neuhaus HE (2007) Vacuolar transporters and their essential role in plant metabolism. Journal of Experimental Botany **58:** 83-102

Martinoia E, Meyer S, De Angeli A, Nagy R (2012) Vacuolar Transporters in Their Physiological Context. *In* SS Merchant, ed, Annual Review of Plant Biology, Vol 63, Vol 63, pp 183-213

Mhamdi A, Noctor G, Baker A (2012) Plant catalases: Peroxisomal redox guardians. Archives of Biochemistry and Biophysics **525:** 181-194

Mhamdi A, Queval G, Chaouch S, Vanderauwera S, Van Breusegem F, Noctor G (2010) Catalase function in plants: a focus on Arabidopsis mutants as stress-mimic models. Journal of Experimental Botany **61:** 4197-4220

Morita M, Shitan N, Sawada K, Van Montagu MCE, Inze D, Rischer H, Goossens A, Oksman-Caldentey K-M, Moriyama Y, Yazaki K (2009) Vacuolar transport of nicotine is mediated by a multidrug and toxic compound extrusion (MATE)

FCUP 143

Unravelling the metabolism and transmembrane transport of the highly valuable medicinal alkaloids from *Catharanthus roseus*

transporter in Nicotiana tabacum. Proceedings Of The National Academy Of Sciences Of The United States Of America **106:** 2447-2452

Nagy R, Grob H, Weder B, Green P, Klein M, Frelet-Barrand A, Schjoerring JK, Brearley C, Martinoia E (2009) The Arabidopsis ATP-binding Cassette Protein AtMRP5/AtABCC5 Is a High Affinity Inositol Hexakisphosphate Transporter Involved in Guard Cell Signaling and Phytate Storage. Journal of Biological Chemistry **284:** 33614-33622

Neuhaus J-M, Martinoia E (2011) Plant Vacuoles. *In* eLS. John Wiley & Sons, Ltd

Nock LP, Mazelis M (1987) The C-S Lyases of higher-plants – direct comparison of the physical-properties of homologeneous alliin lyase of garlic (*Allium sativum*) and onoin (*Allium cepa*). Plant Physiology **85:** 1079-1083

Olbrich A, Hillmer S, Hinz G, Oliviusson P, Robinson DG (2007) Newly Formed Vacuoles in Root Meristems of Barley and Pea Seedlings Have Characteristics of Both Protein Storage and Lytic Vacuoles. Plant Physiology **145:** 1383-1394

Omote H, Hiasa M, Matsumoto T, Otsuka M, Moriyama Y (2006) The MATE proteins as fundamental transporters of metabolic and xenobiotic organic cations. Trends in Pharmacological Sciences **27:** 587-593

Otani M, Shitan N, Sakai K, Martinoia E, Sato F, Yazaki K (2005) Characterization of vacuolar transport of the endogenous alkaloid berberine in *Coptis japonica*. Plant Physiology **138:** 1939-1946

Ozolina NV, Nesterkina IS, Kolesnikova EV, Salyaev RK, Nurminsky VN, Rakevich AL, Martynovich EF, Chernyshov MY (2013) Tonoplast of Beta vulgaris L. contains detergent-resistant membrane microdomains. Planta **237:** 859-871

Park J, Song W-Y, Ko D, Eom Y, Hansen TH, Schiller M, Lee TG, Martinoia E, Lee Y (2012) The phytochelatin transporters AtABCC1 and AtABCC2 mediate tolerance to cadmium and mercury. The Plant Journal **69:** 278-288

Passardi F, Theiler G, Zamocky M, Cosio C, Rouhier N, Teixera F, Margis-Pinheiro M, Ioannidis V, Penel C, Falquet L, Dunand C (2007) PeroxiBase: The peroxidase database. Phytochemistry **68:** 1605-1611

Pereira DM, Ferreres F, Oliveira J, Valentao P, Andrade PB, Sottomayor M (2009) Targeted metabolite analysis of Catharanthus roseus and its biological potential. Food and Chemical Toxicology **47:** 1349-1354

Pollock CJ, Cairns AJ (1991) Fructan metabolism in grasses and cereals. Annual Review of Plant Physiology and Plant Molecular Biology **42:** 77-101

Pollock CJ, Kingston-Smith AH (1997) The Vacuole and Carbohydrate Metabolism. *In* DS R.A. Leigh, JA Callow, eds, Advances in Botanical Research, Vol Volume 25. Academic Press, pp 195-215

Raichaudhuri A, Peng M, Naponelli V, Chen S, Sánchez-Fernández R, Gu H, Gregory JF, Hanson AD, Rea PA (2009) Plant Vacuolar ATP-binding Cassette Transporters That Translocate Folates and Antifolates in Vitro and Contribute to Antifolate Tolerance in Vivo. Journal of Biological Chemistry **284:** 8449-8460

Ranocha P, Denance N, Vanholme R, Freydier A, Martinez Y, Hoffmann L, Koehler L, Pouzet C, Renou J-P, Sundberg B, Boerjan W, Goffner D (2010) Walls are thin 1 (WAT1), an Arabidopsis homolog of Medicago truncatula NODULIN21, is a tonoplast-localized protein required for secondary wall formation in fibers. Plant Journal **63:** 469-483

Rienmueller F, Dreyer I, Schoenknecht G, Schulz A, Schumacher K, Nagy R, Martinoia E, Marten I, Hedrich R (2012) Luminal and Cytosolic pH Feedback on Proton Pump Activity and ATP Affinity of V-type ATPase from Arabidopsis. Journal of Biological Chemistry **287:** 8986-8993

Robert S, Zouhar J, Carter C, Raikhel N (2007) Isolation of intact vacuoles from Arabidopsis rosette leaf-derived protoplasts. Nature Protocols **2:** 259-262

Saito C, Ueda T, Abe H, Wada Y, Kuroiwa T, Hisada A, Furuya M, Nakano A (2002) A complex and mobile structure forms a distinct subregion within the continuous vacuolar membrane in young cotyledons of Arabidopsis. Plant Journal **29:** 245-255

Schmidt UG, Endler A, Schelbert S, Brunner A, Schnell M, Neuhaus HE, Marty-Mazars D, Marty F, Baginsky S, Martinoia E (2007) Novel tonoplast transporters identified using a proteomic approach with vacuoles isolated from cauliflower buds. Plant Physiology **145:** 216-229

Schulz MH, Zerbino DR, Vingron M, Birney E (2012) Oases: robust de novo RNA-seq assembly across the dynamic range of expression levels. Bioinformatics **28:** 1086-1092

Shimaoka T, Ohnishi M, Sazuka T, Mitsuhashi N, Hara-Nishimura I, Shimazaki KI, Maeshima M, Yokota A, Tomizawa KI, Mimura T (2004) Isolation of intact vacuoles and proteomic analysis of tonoplast from suspension-cultured cells of Arabidopsis thaliana. Plant and Cell Physiology **45:** 672-683

Shitan N, Bazin I, Dan K, Obata K, Kigawa K, Ueda K, Sato F, Forestier C, Yazaki K (2003) Involvement of CjMDR1, a plant multidrug-resistance-type ATP-binding cassette protein, in alkaloid transport in Coptis japonica. Proceedings Of The National Academy Of Sciences Of The United States Of America **100:** 751-756

Shitan N DF, Dan K, Kato N, Ueda K, Sato F, Forestier C, Yazaki K (2012) Characterization of *Coptis japonica* CjABCB2, an ATP-binding cassette protein involved in alkaloid transport. Phytochemistry

Silva JC, Gorenstein MV, Li GZ, Vissers JPC, Geromanos SJ (2006) Absolute quantification of proteins by LCMSE - A virtue of parallel MS acquisition. Molecular & Cellular Proteomics **5:** 144-156

Sirikantaramas S, Yamazaki M, Saito K (2008) Mechanisms of resistance to self-produced toxic secondary metabolites in plants. Phytochemistry Reviews **7:** 467-477

Sirover MA (2011) On the functional diversity of glyceraldehyde-3-phosphate dehydrogenase: Biochemical mechanisms and regulatory control. Biochimica Et Biophysica Acta-General Subjects **1810:** 741-751

Sottomayor M, dePinto MC, Salema R, DiCosmo F, Pedreno MA, Barcelo AR (1996) The vacuolar localization of a basic peroxidase isoenzyme responsible for the synthesis of alpha-3',4'-anhydrovinblastine in *Catharanthus roseus* (L) G. Don leaves. Plant Cell and Environment **19:** 761-767

Sottomayor M, Duarte P, Figueiredo R, Ros Barcelo A (2008) A vacuolar class III peroxidase and the metabolism of anticancer indole alkaloids in Catharanthus roseus: Can peroxidases, secondary metabolites and arabinogalactan proteins be partners in microcompartmentation of cellular reactions? Plant signaling & behavior **3:** 899-901

Sottomayor M, Lopez-Serrano M, DiCosmo F, Barcelo AR (1998) Purification and characterization of alpha-3 ',4 '-anhydrovinblastine synthase (peroxidase-like) from Catharanthus roseus (L) G. Don. Febs Letters **428:** 299-303

Stevens LH, Blom TJM, Verpoorte R (1993) Subcellular-localization of tryptophan decarboxylase, strictosidine synthase and strictosidine glucosidase in suspension-cultured cells of *Catharanthus roseus* and *Tabernaemontana divaricata* Plant Cell Report **12:** 573-576

Thimm O, Blasing O, Gibon Y, Nagel A, Meyer S, Kruger P, Selbig J, Muller LA, Rhee SY, Stitt M (2004) MAPMAN: a user-driven tool to display genomics data sets onto diagrams of metabolic pathways and other biological processes. Plant Journal **37:** 914-939

Tohge T, Ramos MS, Nunes-Nesi A, Mutwil M, Giavalisco P, Steinhauser D, Schellenberg M, Willmitzer L, Persson S, Martinoia E, Fernie AR (2011) Toward the Storage Metabolome: Profiling the Barley Vacuole. Plant Physiology **157:** 1469-1482

Usadel B, Nagel A, Thimm O, Redestig H, Blaesing OE, Palacios-Rojas N, Selbig J, Hannemann J, Piques MC, Steinhauser D, Scheible WR, Gibon Y, Morcuende R, Weicht D, Meyer S, Stitt M (2005) Extension of the visualization

tool MapMan to allow statistical analysis of arrays, display of coresponding genes, and comparison with known responses. Plant Physiology **138:** 1195-1204

van der Heijden R, Jacobs DI, Snoeijer W, Hallared D, Verpoorte R (2004) The Catharanthus alkaloids: Pharmacognosy and biotechnology. Current Medicinal Chemistry **11:** 607-628

Vera-Estrella R, Barkla BJ, Bohnert HJ, Pantoja O (2004) Novel regulation of aquaporins during osmotic stress. Plant Physiology **135:** 2318-2329

Verma P, Mathur AK, Srivastava A, Mathur A (2012) Emerging trends in research on spatial and temporal organization of terpenoid indole alkaloid pathway in Catharanthus roseus: a literature update. Protoplasma **249:** 255-268

Verpoorte R, Lata B, Sadowska A, eds (2007) Biology and Biochemistry of *Catharanthus roseus* (L.) G. Don Vol 2-3. Springer Verlag

White PJ, Marshall J, Smith JAC (1990) Substrate Kinetics of the Tonoplast H^+-Translocating Inorganic Pyrophosphatase and Its Activation by Free Mg^{2+}. Plant Physiology **93:** 1063-1070

Whitelegge JP (2002) Plant proteomics: blasting out of a MudPIT. Proceedings of the National Academy of Sciences **99:** 11564-11566

Wink M (1993) The plant vacuole: a multifunctional compartment. Journal of Experimental Botany **44:** 231-246

Xu S-L, Rahman A, Baskin TI, Kieber JJ (2008) Two Leucine-Rich Repeat Receptor Kinases Mediate Signaling, Linking Cell Wall Biosynthesis and ACC Synthase in Arabidopsis. Plant Cell **20:** 3065-3079

Yazaki K (2006) ABC transporters involved in the transport of plant secondary metabolites. Febs Letters **580:** 1183-1191

Zhao J, Liu Q, Zhang H, Jia Q, Hong Y, Liu Y (2013) The rubisco small subunit is involved in tobamovirus movement and Tm-2(2)-mediated extreme resistance. Plant Physiology **161:** 374-383

Zipor G, Oren-Shamir M (2013) Do vacuolar peroxidases act as plant caretakers? Plant Science **199:** 41-47

Zouhar J, Rojo E (2009) Plant vacuoles: where did they come from and where are they heading? Current Opinion in Plant Biology **12:** 677-684

Zybailov B, Rutschow H, Friso G, Rudella A, Emanuelsson O, Sun Q, van Wijk KJ (2008) Sorting Signals, N-Terminal Modifications and Abundance of the Chloroplast Proteome. Plos One **3:** e1994

Chapter
IV

A fluorescence activated cell sorting method for isolation of *Catharanthus roseus* leaf cells accumulating medicinal alkaloids

A fluorescence activated cell sorting method for isolation of *Catharanthus roseus* leaf cells accumulating medicinal alkaloids

Inês Carqueijeiro[1,2], Rui Gardner[3], Telma Lopes[3], Francisco Lima[1,2], Patricia Duarte[1], Mariana Sottomayor[1,2]*

[1]IBMC – Instituto de Biologia Molecular e Celular, Universidade do Porto, Rua do Campo Alegre, 823, 4150-180 Porto, Portugal;

[2]Departamento de Biologia, Faculdade de Ciências da Universidade do Porto, Rua do Campo Alegre s/n 4169-007 Porto, Portugal;

[3]Instituto Gulbenkian de Ciência, Rua da Quinta Grande 6, 2780-156 Oeiras, Portugal.

Inês Carqueijeiro declares to have participated actively in this work, by contributing to the experimental design, performing most of the experiments, and by contributing to manuscript writing.

FCUP 151

Unravelling the metabolism and transmembrane transport of the highly valuable medicinal alkaloids from *Catharanthus roseus*

ABSTRACT

Plant secondary metabolism presents often a complex cell-specific compartmentation essential to accomplish the biosynthesis of many valuable plant natural products. Hence, the characterization and potential manipulation of those pathways will depend on the capacity to isolate specific cell types to perform their differential characterization. *Catharanthus roseus* accumulates in low levels the terpenoid indole alkaloids (TIAs) vinblastine and vincristine, used in cancer chemotherapy, ajmalicine, used as an antihypertensive, and serpentine, used as sedative. Although much is known about the TIA pathway, a number of biosynthetic steps remain unknown, no master regulators have been identified, and the mechanisms of TIAs transport and accumulation inside the cells are poorly characterized. In *C. roseus* leaves, the late steps of the biosynthetic pathway leading to the anticancer TIAs have been shown to occur in specialized mesophyll cells called idioblasts, which accumulate high levels of TIAs and are characterized by a conspicuous blue fluorescence credited to the TIA serpentine. In order to be able to characterize the differential transcriptome of these important cells, a methodology for the isolation of idioblasts by means of fluorescence activated cell sorting (FACS) of leaf protoplasts was established here. This methodology takes advantage of the distinctive autofluorescence of idioblasts and includes a procedure for highly efficient isolation of stable leaf protoplasts, followed by FACS using an optimized buffer to culminate in the isolation of a highly pure and viable population of idioblast protoplasts. This achievement represents a crucial step for further development of differential omic strategies leading to the identification of important candidate genes putatively involved in the biosynthesis, regulation and transport of the anticancer alkaloids from *C. roseus*.

INTRODUCTION

A major breakthrough in plant secondary metabolism was the discovery that many pathways present highly specific inter-cellular compartmentation (Ziegler and Facchini, 2008). Being so, it becomes crucial to separate different types of plant cells present in the same tissue, one approach that is already highly explored in animal models. The isolation of different cell organelles has long been achieved with major success by a number of different protocols and approaches, but a harder field to explore is the separation of different types of cells from a single tissue. Two major techniques are available: Laser Capture Microdissection (LCM) and Fluorescence Activating Cell Sorting (FACS), with the latter producing more easily a high number of cells, provided a differential fluorescence exists. This is often the case for cells accumulating specific plant secondary metabolites, since these compounds frequently present autofluorescence.

A paradigmatic example of cell-specific compartmentalization involving autofluorescence is the terpenoid indole alkaloid (TIA) pathway from the medicinal plant *Catharanthus roseus*. *C. roseus* is known for the production of the TIAs vinblastine (VLB) and vincristine (VCR), which were the first natural anticancer products to be clinically used, and are still among the most valuable agents used in cancer chemotherapy. The production of these valuable anticancer alkaloids is restricted to the leaves of the plant, where they accumulate in very low levels (Verpoorte et al., 2007). Along with VLB and VCR, *C. roseus* also accumulates other alkaloids with medicinal interest, including ajmalicine, used as an antihypertensive, and serpentine, used as sedative (van der Heijden et al., 2004). Previous studies showed that the TIA pathway presents multi-cellular compartmentation in *C. roseus* leaves, with early steps being expressed in the epidermis of the leaf, and late steps being expressed in laticifers and idioblast cells (Mahroug et al., 2007; Murata et al., 2008). Idioblasts were shown to specifically accumulate catharanthine and vindoline (VLB precursors) and are characterized by a conspicuous blue fluorescence that has been credited to the accumulation of the TIA serpentine (Brown et al., 1984; Mersey and Cutler, 1986). Noteworthy, VLB and VCR were never detected in other plant cell/tissues/organs but leaf laticifers and idioblasts, and were neither detected in cell cultures. Thus, leaf idioblasts seem to be a hot spot of TIA accumulation and, together with laticifers, are possibly the single site in the plant where the biosynthesis of VLB is completed. Accomplishing the isolation of those cells may be decisive to fully unravel the TIA pathway, since this will enable the use of differential transcriptomic approaches leading to the identification of the crucial genes involved in the bottleneck steps of the pathway.

FCUP 153

Unravelling the metabolism and transmembrane transport of the highly valuable medicinal alkaloids from *Catharanthus roseus*

In fact, although much is known about the biosynthesis and regulation of TIAs, many biosynthetic steps remain unknown, no master regulators have been identified, and the mechanisms of TIAs transport and accumulation inside the cells are largely uncharacterized.———

In this study, a procedure to isolate alkaloid-accumulating idioblast cells without the need to use reporter genes is described. This strategy involves the isolation of protoplasts from leaves and the use of optimized FACS conditions that allow the separation of autofluorescent idioblast protoplasts from those of common mesophyll cells. The amount / quality of cells sorted and the buffer composition makes the sorting methodology developed here compatible with the implementation of subsequent transcriptomic, metabolomic and proteomic studies.

MATERIAL AND METHODS
Plant material

Catharanthus roseus (L.) G. Don cv. Little Bright Eye plants were grown at 25°C, in a growth chamber, under a 16 h photoperiod, using white fluorescent light with a maximum intensity of 70 μmol m^{-2} s^{-1}. Seeds were acquired from AustraHort (Australia) and voucher specimens are deposited at the Herbarium of the Department of Biology of the Faculty of Sciences of the University of Porto (PO 61912). Plants used for protoplast isolation were 6 to 8 months old.

Isolation of *C. roseus* mesophyll protoplasts

Two methodologies were tested in order to obtain an optimized protocol for the isolation of *C. roseus* mesophyll protoplasts. The first method tested was adapted from Duarte et al. (2008) and Sottomayor et al. (1996) with a number of modifications. Briefly, 8 to 10 leaves from the 2nd and 3rd pairs from the tip of flowering plants (~1.5 to 2 g) were cut into ~1 mm wide strips and transferred to a Petri dish with 10 mL of digestion medium composed of 2 % (w/v) cellulase Onozuka R10 (Duchefa, The Netherlands), 0.3 % (w/v) macerozyme Onozuka R10 (Serva, Germany) and 0.1 % pectinase (Sigma, UK) dissolved in a medium (TEX) containing 3.2 g L^{-1} Gamborg's B5 medium (Duchefa, The Netherlands), 5.1 mM CaCl$_2$.2H$_2$O, 0.4 M sucrose and 2.6 mM Mes, pH 5.6–5.8, and incubated overnight, in the dark, at 25 °C. Protoplasts were released by orbital shaking at low speed for 15 min, the suspension was filtered through a 100 μm nylon mesh and the living/floating protoplast fraction was obtained by centrifugation at 100 *g*, for 10 min, at RT, and washed once in the above medium without enzymes. The protoplast fraction was then gently mixed with two-three volumes of mannitol/W5 containing 0.32 M D(-)-mannitol, 1 mM D(+)-glucose, 30.8 mM NaCl, 25 mM CaCl$_2$, 1 mM KCl, 0.3 mM Mes, pH

5.6–5.8, and protoplasts were pelleted at 100 *g* for 5 min at RT, counted and resuspended in FACS buffer to obtain 4×10^5 protoplasts mL^{-1}. The second method for protoplast isolation is described in Chapter III.

The integrity of the isolated protoplasts was checked by observation under an optical microscope (Olympus, Japan) and colour images were acquired by a coupled Olympus DP 25 Digital Camera and respective software (Cell B, Olympus, Japan). Protoplasts were also observed under the confocal microscope (Leica SP2 AOBS SE) using an excitation wavelength of 405 nm and an emission wavelength window of 420-520 nm for visualization of idioblasts and of 600-700 nm for visualization of chlorophyll. Protoplasts were stained with 5 µg mL^{-1} FDA to check viability, and were observed under the epifluorescence microscope (Leica Microsystems DM-5000B, Leica, Germany) using excitation / emission wavelengths of 494 / 530 nm (Jones and Senft, 1985).

Fluorescence Activated Cell Sorting (FACS) of *C. roseus* protoplasts

Mesophyll protoplasts resuspended in different buffers (Table 1) were run in a MoFlo (Beckman Coulter, Fort Collins, USA), at 4ºC, immediately after isolation, and with no further filtration. Protoplasts were sorted using either mannitol/W5 medium or PBS as sheath, at a constant pressure of 200 kPa (~30 psi), using a 100 µm nozzle, and a drop drive frequency of 40 kHz (~40,000 drops / sec). For alkaloid blue fluorescence detection, a water-cooled I90-C Coherent argon laser operating at multiline UV wavelengths (330-360 nm), with 100 mW output and a 455/30 nm bandpass filter was used. For scatter measurements and chlorophyll autofluorescence detection, a 488 nm laser line from a Coherent Sapphire 488-200 CDRH laser, with 140 mW output and a 670/40 nm bandpass filter was used. Calibration was performed using SPHERO Ultra Rainbow Fluorescent Particles (Spherotech Inc.) with 3 to 3.4 µm. Sorting rates of events were < 8,000 events / sec. MU-fluorescing protoplasts were collected in microcentrifuge tubes containing mannitol/W5, and quantified logarithmically with data collected and analysed using FACS software (Summit version 4.0). Sorted cells/idioblasts were observed under the epifluorescence microscope (DMIRE2, Leica) and were also stained with neutral red and observed under an optical microscope (Olympus).

RNA isolation and RT-PCR

Extraction of RNA was performed using the RNeasy Plant Mini Kit (Qiagen) according to the manufacturer's instructions with the modifications described by Birnbaum et al. (2005) plus some additional modifications. A volume of 500 L of sorted cells was mixed with an equal volume of RLT buffer from the RNeasy Plant Mini Kit

(Qiagen) supplemented with 5 L of 0.05% (v/v) -mercaptoethanol and immediately frozen at -80°C for storage. Samples were thawed on ice, were added 1 mL of RLT buffer with 10 L of -mercaptoethanol, mixed with a vortex, added 1 mL of 100% ethanol RNase Free, and mixed immediately. The 3 mL of sample were passed through a single RNeasy spin column and the kit protocol was followed for the remainder of the extraction, eliminating the optional spin. For elution, 30 L of RNase-free water were added to the column, which was left to stand at RT for 2 min prior to centrifugation. Approximately 6 µg of total RNA were obtained from roughly 400 000 idioblast cells, which was a much lower yield than the one obtained for whole mesophyll protoplasts, suggesting that the idioblast secondary metabolites probably affect RNA stability. cDNA was synthesized using the iScript™ Select cDNA Synthesis Kit (BioRad) according to manufacture instructions, using an amount of RNA normalized by in gel quantification. 35 PCR cycles were performed using the following primers: 5'-GTGCGTATCCGTTGGTTTCT-3' and 5'-TGACGATGGAATTGAGTTCG-3' for deacetylvindoline-4-O-acetyltransferase (*DAT*) (Genebank accession number AF053307.1; (Murata et al., 2006) and for the housekeeping 40S ribosomal protein S9 (RSP9) 5'-GAGCGTTTGGATGCTGAGTT-3' and 5'-TCATCTCCATCACCACCGA-3' (Genebank accession number AJ749993;(Menke et al., 1999).

RESULTS

Isolation of mesophyll protoplasts

One crucial step in the establishment of a method for isolation of *C. roseus* leaf idioblast cells (Fig. 1B) by FACS was the optimization of an efficient technique for the preparation of leaf protoplasts. It was necessary to obtain a high yield of stable protoplasts to minimize and face the losses during FACS, at the same time a minimum disturbance was assured in order to maintain as much as possible the expression profile of the leaf cells. The initial method used was adapted from Duarte et al. (2008) and Sottomayor et al. (1996) and resulted in a high yield of protoplasts. However, the naked cells were fragile and bursted easily during manipulation of the suspension. When NH_4NO_3 was removed from the TEX medium used for digestion, protoplasts became much more stable and resistant to manipulation, leading also to much cleaner suspensions with almost no cellular debris. Under the optical microscope, protoplasts were spherical, indicating full digestion of the cell wall, and showed no apparent membrane damage or disintegration of the internal structure (Fig. 1 C). The viability of the isolated protoplasts was tested with the fluorescent dye fluorescein diacetate (FDA) and ranged from 95-98% (Fig. 1E and F).
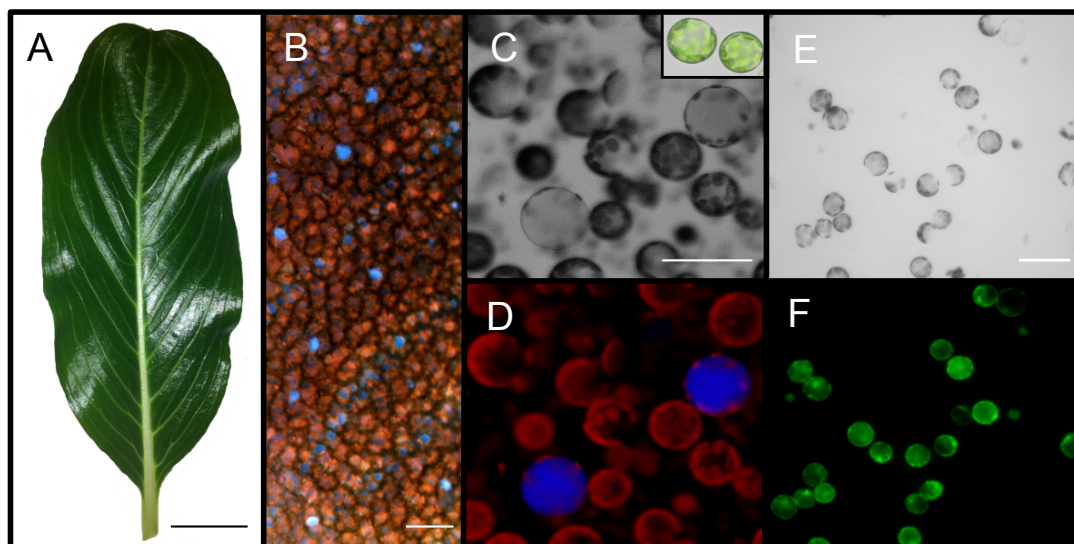
Figure 1. A, Fully developed leaf of *C. roseus*. B, Epifluorescence microscopy image of the adaxial face of a whole mounted *C. roseus* leaf. C to F, Optical microscopy images of leaf protoplasts. C, Phase contrast image of protoplasts (acquired with a one channel camera); in set - bright field colour image of protoplasts. D, Confocal image of C with merging of the red and blue channels; red corresponds to chloroplast autofluorescence and blue fluorescence reveals alkaloid-accumulating idioblast cells. E, Bright field image of protoplasts stained with FDA (acquired with a one channel camera). F, Fluorescence image of E showing the viable protoplasts stained by FDA, presenting green fluorescence. Bars = 1 cm (A), 100 μm (B), 50 μm (C) and 30 μm (D).

Under the fluorescence microscope, a small number of protoplasts showed intense blue fluorescence in their vacuoles, enabling their identification as idioblasts (Fig. 1D). It was noticeable that idioblasts presented a lower content in chloroplasts than other mesophyll cells (Fig. 1C and D). The proportion of idioblasts present in the protoplast suspension was similar to the one observed in the leaves (Fig. 1B), indicating that these cells are amenable to protoplast isolation in a similar way to common mesophyll cells, and retain their distinctive alkaloid accumulating character. The medium size of protoplasts was 31 μm, ranging from 15 to 40 μm, with idioblasts being usually big cells, above 30 μm (Fig. 1C to F).

Purification of idioblast protoplasts by FACS

In *C. roseus* leaves, idioblast cells with high TIA accumulation are slightly larger than common mesophyll cells, depict a conspicuous blue fluorescence in their vacuoles assigned to the TIA serpentine, and present a lower number of chloroplasts (Fig. 1B and D). After protoplast isolation, these characteristics allow a subtle differentiation of idioblasts (Fig.1C and D), which can, nevertheless, be explored for their separation by FACS, taking advantage of the differences in the blue fluorescence of the vacuoles and the red fluorescence of chloroplasts.

FCUP 157

Unravelling the metabolism and transmembrane transport of the highly valuable medicinal alkaloids from *Catharanthus roseus*

To sort idioblasts relying only on intrinsic fluorescence, the PMT (photomultiplier tube) detector voltages of the FACS apparatus were set in the first experiment to maximize differences between the minimum and maximum fluorescence of *C. roseus* mesophyll protoplast populations, for both the blue and red channels. Target values for calibration beads were set based on these PMT gains, which were used in all subsequent experiments. Due to the size of *C. roseus* mesophyll protoplasts, the biggest nozzle with 100 µm was used, with adaptation of the pressure to 30 psi, of the cell flow rate to below 8,000 events / sec and of the drop frequency to ~40,000 drops / sec, in order to obtain a viable population of sorted idioblasts. To avoid clogging, the maximum cell concentration used was $4x10^5$ protoplasts mL^{-1} and only 500 µL of protoplast suspension were loaded each time in the sorter.

Initially, the final protoplast re-suspension buffer, mannitol/W5, was used as FACS sheath buffer. However, the FACS apparatus is usually run with PBS and using mannitol/W5 as sheath is not only expensive but also demands time-consuming calibrations. Re-suspension of protoplasts in PBS was not possible since they burst in this buffer. Therefore, the use of PBS as sheath together with mannitol/W5 as cell re-suspension medium was considered. Initially, the possibility of occurrence of optical interferences resulting from fluidic instabilities at the interrogation point was assessed, using a suspension of beads with 2 fluorescence peaks corresponding to the two fluorescences measured for *C. roseus* protoplasts. No differences were observed between beads suspended in PBS or mannitol/W5, confirming the lack of interference of any possible buffer interactions. The use of PBS as sheath revealed to work well for *C. roseus* protoplasts sorting as well. However, it lowered the stability of the sorted protoplast populations and, thus, it was only used when further manipulation of cells was not needed.

The most relevant event populations based on the two intrinsic fluorescence signals, blue and red, are shown in Fig. 2A. These four populations were identified by sorting drops directly onto a microscope slide followed by direct visualization under a fluorescence microscope (Fig. 2). Population I showed the highest blue fluorescence signal associated with low red fluorescence, and was constituted by cells with very low numbers of chloroplasts and vacuolar intense blue fluorescence, which were identified as idioblasts (Fig. 2F to H). Population II showed the highest red fluorescence signal and was constituted by cells with a high content in chloroplasts and no vacuolar blue fluorescence (Fig. 2I to K), seemingly corresponding to protoplasts of common mesophyll cells. Population III showed a very low red fluorescence signal, and was constituted by what seemed isolated vacuoles and cell debris (Fig. 2L to M). Population

IV showed a high red fluorescence signal associated to a very low blue fluorescence and was constituted mainly by free chloroplasts (Fig. 2O to R).
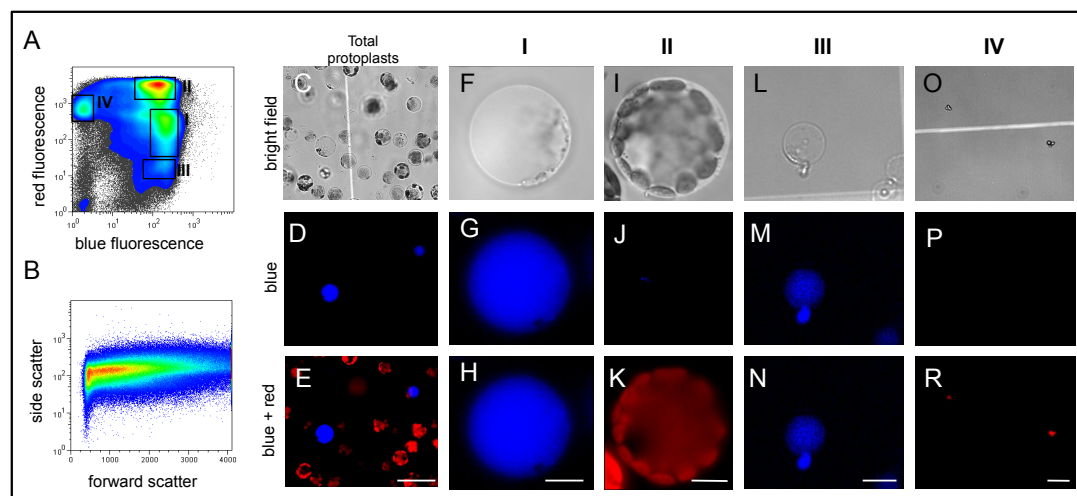
Figure 2. Isolation of idioblast cells from *C.roseus* leaf protoplasts by FACS. A, Cell populations detected in the filtrate pre-sorting. All populations were sorted and characterized under the epifluorescence microscope (I to R). The high blue fluorescence / low red fluorescence population I was selected for sorting idioblast cells. B, Scatter plot of the initial protoplast population. C to E, Pre-sort protoplast population under the epifluorescence microscope. F to H, Typical example of a sorted protoplast observed in population I from A, identified as an idioblast protoplast. I to K, Typical example of a sorted protoplast observed in population II from A, identified as a mesophyll protoplast. L to N, Example of the structures observed in population III from A, identified as vacuoles and cell debris. O to R, Example of the structures observed in population IIV from A, identified as free chloroplasts. Blue fluorescence is due to the alkaloid serpentine and reveals alkaloid containing idioblast cells. Red fluorescence is due to chlorophyll. Scale bar = 20 μm (E), 10 μm (H, K N and R).

Sorted idioblast cells accumulated neutral red inside their vacuoles indicating that cells maintained a physiological acidic vacuole (data not shown), and purity of the sorted cells was assessed by re-analyzing aliquots of the idioblast fraction sorted into collection tubes containing mannitol/W5 (Fig.3). Resorting the idioblast fraction produced 4 populations (Fig. 3A) including whole idioblasts in sorting gate I as before (Fig 3B to D), and three more populations that showed to include only material resulting from cell disruption: population V consisted of aggregated chloroplasts (Fig. 3E to G) while populations VI and VII consisted of undetermined debris (Fig. 3H to M). Using as sheath phase either PBS or M/W5, the purity of the sorted cells achieved 92-97%, considering only the presence of events corresponding to cells, and neglecting all the events corresponding to cell debris / organelles, likely resulting from disruption of idioblast cells during resorting.

Typically ca. 100,000 idioblast cells were obtained from 1,000,000 mesophyll protoplasts (10%), with a total of about 6×10^5 idioblast cells being recovered during one operation day. For RNA isolation, PBS was used as sheath and idioblast cells were sorted directly to extraction buffer, with about $4,9 \times 10^6$ cells yielding 2 μg de RNA. This

yield was 10 times lower than the one obtained for the mother population of mesophyll protoplasts, possibly due to the presence of high concentration of TIAs and other secondary metabolites in these cells.
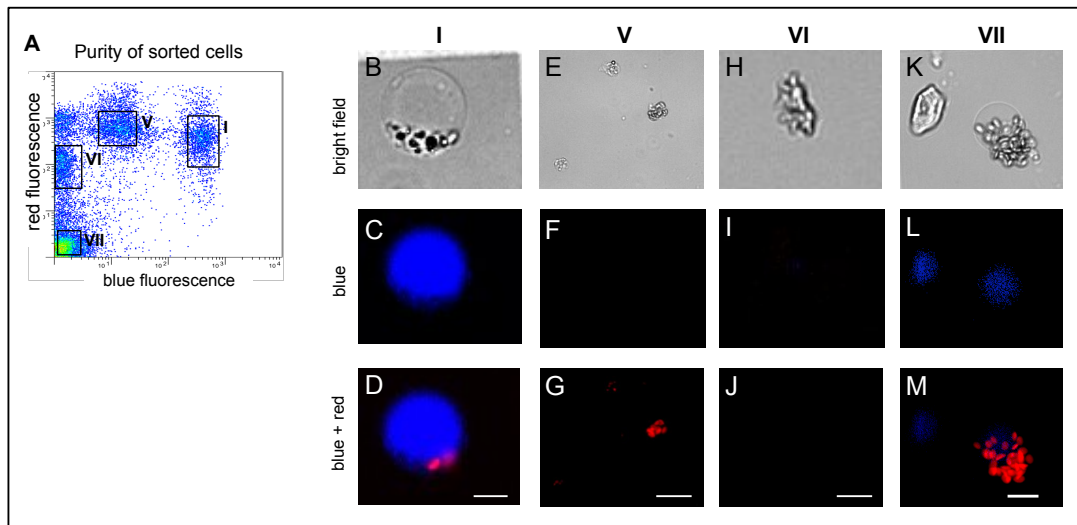
Figure 3. Purity of the sorted fraction of idioblast protoplasts. A, Cell populations detected in the filtrate pre-sorting. All populations were sorted and characterized under the epifluorescence microscope (B to L). B to D, Typical example of a sorted protoplast observed in population I from A, identified as an idioblast protoplast. E to G, Example of the structures observed in population V from A, identified as aggregates of chloroplasts. H to J, Example of the structures observed in population VI from A, corresponding to miscellaneous debris. K to M, Example of the structures observed in population VII from A, corresponding to miscellaneous debris. Blue fluorescence is due to the alkaloid serpentine and reveals alkaloid containing idioblast cells. Red fluorescence is due to chlorophyll. Scale bar = 15 µm.

DISCUSSION

Plant organs are built by an array of different tissues and cell types with specialized functions that are highly problematic to study due to the difficulty in working exclusively with one tissue or cell type. In plants, this may be achieved by digestion of the cell wall to obtain protoplasts, followed by separation of the free cells by FACS. More than 20 years ago, FACS of mesophyll protoplasts based on chlorophyll autofluorescence or FDA has been performed in Arabidopsis and *Nicotiana tabacum* (Jones and Senft, 1985; Harkins et al., 1990), and FACS of protoplasts from suspension cells was reported for *C. roseus*, based on their capacity to accumulate the blue fluorescing serpentine (Brown et al., 1984). No equivalent FACS procedure has been reported for *C. roseus* leaf idioblasts, but Murata et al. (2005) has used the technique of Laser Capture Microdissection (LCM) on paraffin sections of *C. roseus* leaves to obtain individual epidermal, vascular, idioblast, laticifer, and mesophyll cells, which were used for RNA extraction followed by RT-PCR. However, the number of cells recovered was relatively low (2500-5000), limiting subsequent characterization studies. More recently, FACS has been used, in plants, mainly to sort fluorescent cell lines resulting from GFP expression

driven by cell-specific promoters, and to isolate pollen cells and microspores (Galbraith et al., 1999; Galbraith et al., 2002; Birnbaum et al., 2003; Galbraith, 2003; Borges et al., 2012; Gronlund et al., 2012).

In *C. roseus*, the specific expression of the late, bottleneck steps of the TIA pathway in idioblast cells embedded in the leaf mesophyll (Fig. 1B) constitutes a difficult challenge, but it also delivers an invaluable comparative tool to investigate the pathway, provided it is possible to isolate these cells. Here, we developed a FACS method that allows the selective sorting of the *C. roseus* leaf idioblast protoplasts, merely taking advantage the autofluorescence properties of these cells (Fig. 2). Unlike previous work using fluorescent cell lines resulting from GFP expression driven by cell-specific promoters (Galbraith et al., 1999; Birnbaum et al., 2003; Gronlund et al., 2012), we showed here that FACS is a reliable and efficient technique allowing isolation of protoplast cells based only on their autoflourescence characteristics, without the need of using fluorescent protein reporter genes and plant transformation, or other dyes that could interfere with downstream analysis. Moreover, we also proved that independently of the ressuspension buffer of the protoplasts, PBS can be used as sheath buffer without significantly compromising the stability of the protoplasts during sorting, as far as pre-sort cells are suspended in an osmotically protector buffer, which is also used to collect sorted cells. Finally, the FACS procedure optimized here enables the isolation of a high number of cells, 100,000 idioblast cells per operation day, highly exceeding the 2500-5000 idioblast cells isolated by Murata et al. (2005) using LCM. The idioblast cell fraction obtained was highly pure and may now be used for the implementation of differential transcriptomic, metabolomic and proteomic studies, enabling to uncover the differentiation status and functions of idioblast cells, as well as novel candidate genes involved in the biosynthesis, transport and regulation of TIAs. This FACS method allows the isolation of intact leaf protoplast populations according to their autofluorescence, and is likely applicable to many other situations involving specific cell types.

ACKNOWLEDGEMENTS

LITERATURE CITED

Birnbaum K, Shasha DE, Wang JY, Jung JW, Lambert GM, Galbraith DW, Benfey PN (2003) A gene expression map of the Arabidopsis root. Science **302:** 1956-1960

Borges F, Gardner R, Lopes T, Calarco JP, Boavida LC, Slotkin RK, Martienssen RA, Becker JD (2012) FACS-based purification of Arabidopsis microspores, sperm cells and vegetative nuclei. Plant Method **8:** 4

Brown S, Renaudin JP, Prevot C, Guern J (1984) Flow-cytometry and sorting of plant-protoplasts-technical problems and physiological results from a study of pH and alkaoids in *Catharanthus roseus*. Physiologie Vegetale **22:** 541-554

Duarte P, Pissarra J, Moore I (2008) Processing and trafficking of a single isoform of the aspartic proteinase cardosin a on the vacuolar pathway. Planta **227:** 1255-1268

Galbraith D, Lambert G, Macas J, Doležel J (2002) Analysis of nuclear DNA content and ploidy in higher plants. *In* J Robinson, Z Darzynkiewicz, P Dean, A Hibbs, A Orfão, P Rabinovitch, L Wheeless, eds, Current protocols in cytometry. John Wiley & Sons, Inc., New York

Galbraith DW (2003) Global analysis of cell type-specific gene expression. Comparative and Functional Genomics **4:** 208-215

Galbraith DW, Anderson MT, Herzenberg LA (1999) Flow cytometric analysis and FACS sorting of cells based on GFP accumulation. Methods in Cell Biology, Vol 58 **58:** 315-341

Gronlund JT, Eyres A, Kumar S, Buchanan-Wollaston V, Gifford ML (2012) Cell specific analysis of Arabidopsis leaves using fluorescence activated cell sorting. Journal of visualized experiments : JoVE

Harkins KR, Jefferson RA, Kavanagh TA, Bevan MW, Galbraith DW (1990) Expression of photosynthesis-related gene fusion is restricted by cell type in transgenic plants and in transfected protoplasts Proceedings Of The National Academy Of Sciences Of The United States Of America **87:** 816-820

Jones KH, Senft JA (1985) An Improved Method to Determine Cell Viability by simnultaneous staining with fluorescein diacetate propidium iodide. Journal of Histochemistry & Cytochemistry **33:** 77-79

Mahroug S, Burlat V, St-Pierre B (2007) Cellular and sub-cellular organisation of the monoterpenoid indole alkaloid pathway in *Catharanthus roseus*. Phytochemistry Reviews **6:** 363-381

Menke FLH, Champion A, Kijne JW, Memelink J (1999) A novel jasmonate- and elicitor-responsive element in the periwinkle secondary metabolite biosynthetic gene Str interacts with a jasmonate- and elicitor-inducible AP2-domain transcription factor, ORCA2. Embo Journal **18:** 4455-4463

Mersey BG, Cutler AJ (1986) Differential distribution of specific indole alkaloids in leaves of Catharanthus roseus Canadian Journal of Botany-Revue Canadienne De Botanique **64:** 1039-1045

Murata J, Bienzle D, Brandle JE, Sensen CW, De Luca V (2006) Expressed sequence tags from Madagascar periwinkle (Catharanthus roseus). Febs Letters **580:** 4501-4507

Murata J, De Luca V (2005) Localization of tabersonine 16-hydroxylase and 16-OH tabersonine-16-O-methyltransferase to leaf epidermal cells defines them as a major site of precursor biosynthesis in the vindoline pathway in Catharanthus roseus. Plant Journal **44:** 581-594

Murata J, Roepke J, Gordon H, De Luca V (2008) The leaf epidermome of *Catharanthus roseus* reveals its biochemical specialization. Plant Cell **20:** 524-542

Sottomayor M, dePinto MC, Salema R, DiCosmo F, Pedreno MA, Barcelo AR (1996) The vacuolar localization of a basic peroxidase isoenzyme responsible for the synthesis of alpha-3',4'-anhydrovinblastine in *Catharanthus roseus* (L) G. Don leaves. Plant Cell and Environment **19:** 761-767

van der Heijden R, Jacobs DI, Snoeijer W, Hallared D, Verpoorte R (2004) The Catharanthus alkaloids: Pharmacognosy and biotechnology. Current Medicinal Chemistry **11:** 607-628

Verpoorte R, Lata B, Sadowska A, eds (2007) Biology and Biochemistry of *Catharanthus roseus* (L.) G. Don Vol 2-3. Springer Verlag

Ziegler J, Facchini PJ (2008) Alkaloid Biosynthesis: Metabolism and Trafficking. Annual Review of Plant Biology **59:** 735-769

Chapter
V

A targeted transcriptomic approach to unravel the metabolism of the highly valuable medicinal alkaloids from *Catharanthus roseus*

A targeted transcriptomic approach to unravel the metabolism of the highly valuable medicinal alkaloids from *Catharanthus roseus*

Inês Carqueijeiro[1,2], Jacob Poiller[3], Rui Gardner[4], Telma Lopes[4], Francisco Lima[1,2], Patrícia Duarte[1], Alain Goossens[3], Mariana Sottomayor[1,2]

[1]IBMC – Instituto de Biologia Molecular e Celular, Universidade do Porto, Rua do Campo Alegre, 823, 4150-180 Porto, Portugal;

[2]Departamento de Biologia, Faculdade de Ciências da Universidade do Porto, Rua do Campo Alegre, s/n, 4169-007 Porto, Portugal;

[3]Department of Plant Systems Biology, Flanders Institute for Biotechnology (VIB) and Department of Plant Biotechnology and Genetics, Ghent University, Belgium;

[4]IGC – Instituto Gulbenkian de Ciência, Rua da Quinta Grande, 6 P-2780-156 Oeiras, Portugal.

Inês Carqueijeiro declares to have participated actively in this work, by contributing to the experimental design, performing most of the experiments, and by contributing to manuscript writing.

ABSTRACT

The leaves of *Catharanthus roseus* accumulate in low levels the terpenoid indole alkaloids (TIAs) vinblastine and vincristine, widely used in anticancer treatments. The TIA pathway is highly complex, involving more than 30 biosynthetic steps and several subcellular compartments and cell types, with various transmembrane transport steps being predicted. In spite of intense research, and although much is known about the biosynthesis and regulation of TIAs, gene/enzyme characterization is still lacking for many biosynthetic steps, the membrane transport mechanisms of TIAs are basically uncharacterized, despite their importance for TIA accumulation, and no effective master switch of the TIA pathway has been identified.

The late, bottleneck steps of the TIA pathway take place in specialized mesophyll cells, the idioblasts, that seem to be accumulation targets of TIAs. In this study, a targeted strategy involving the isolation of idioblast protoplasts by Fluorescence Activation Cell Sorting and their differential transcriptomic analysis by cDNA - amplified fragment length polymorphism enabled the identification of a set of 98 genes showing significant up-regulation in idioblasts and a set of 49 genes showing significant down-regulation in idioblasts. Among them, one cytochrome P450, 3 ABC transporters and 13 transcription factors are good candidates, respectively, to the biosynthesis of VLB, tonoplast / plasma membrane TIA transport, and regulation of the late TIA pathway in idioblast cells. Conversely, 3 other ABC transporters and 4 other transcription factors are good candidates to plasma membrane TIA transport and regulation of the early TIA pathway in epidermal cells. These findings open exciting new avenues of research on TIA metabolism.

INTRODUCTION

Catharanthus roseus (L.) G. Don (formerly *Vinca rosea* L.) accumulates in the leaves the dimeric terpenoid indole alkaloids (TIAs) vinblastine (VLB) and vincristine (VCR), which were the first natural anticancer products to be clinically used. Together with a number of semisynthetic derivatives, these TIAs are universally known as the Vinca alkaloids, which are still among the most valuable agents used in the treatment of cancer. Two other TIAs with important pharmacological activity have also been isolated from *C. roseus*: ajmalicine, used as an antihypertensive, and serpentine, used as sedative (van der Heijden et al., 2004).

The great pharmacological importance of the TIAs, associated with the low abundance of the anticancer drugs in the plant (around 0.0005% DW), stimulated intense research on the TIA pathway, and *C. roseus* has become one of the most extensively studied medicinal plants (van der Heijden et al., 2004; Verpoorte et al., 2007). Nowadays, about 130 TIAs have been isolated from *C. roseus*, and it has been shown that the biosynthesis of VLB is highly complex, involving at least 30 steps from the amino acid tryptophan and the monoterpenoid geraniol (Fig. 1). All the TIAs of *C. roseus* derive from the common precursor strictosidine, after which the TIA pathway splits into several branches including a short one leading to ajmalicine, and two long branches leading to vindoline and catharanthine, the leaf abundant monomeric precursors of VLB and VCR (Loyola-Vargas et al., 2007). Thirteen steps of the TIA pathway have been characterized at the enzyme and/or gene level and several transcription factors regulating the expression of sets of TIA biosynthetic genes have also been identified, but their overexpression on cell cultures failed to induce TIA levels (Memelink and Gantet, 2007).

TIA biosynthesis presents a complex subcellular organization, with different parts of the pathway taking place in the plastids, the vacuole, the cytosol and the ER (Mahroug et al., 2007; Guirimand et al., 2011a). Furthermore, the TIA pathway shows multi-cellular compartmentation in *C. roseus* leaves, with early steps being expressed in leaf phloem parenchyma and epidermal cells, and the two last steps of vindoline biosynthesis being expressed in laticifers and idioblast cells (St-Pierre et al., 1999; Mahroug et al., 2007; Murata et al., 2008; Guirimand et al., 2011b). This indicates that the dimeric VLB and VCR possibly occur only in leaf idioblasts / laticifers. Idioblasts are specialized parenchyma cells that, in *C. roseus* leaves, are slightly larger than other mesophyll cells, present a conspicuous blue fluorescence, few chloroplasts, and are involved in TIA accumulation. It is noteworthy that, together with vindoline, none of the 36 known *C. roseus* dimeric TIAs has ever been extracted from roots, hairy roots, callus or cell cultures (Mahroug et al., 2007), what correlates with the above mentioned need for a

specific organ / cell differentiation to express this part of the TIA pathway. On the other hand, early work using a leaf cell fraction enriched in idioblasts indicated the specific accumulation of catharanthine and vindoline in these cells, and the idioblast characteristic blue fluorescence has been credited to the accumulation of serpentine (Brown et al., 1984; Mersey and Cutler, 1986). Thus, leaf idioblasts seem to be a hot spot of TIA accumulation and, together with leaf laticifers, possibly the single site in the plant where the biosynthesis of VLB is completed.

The sub-cellular and multicellular complexity of the TIA pathway predicts several transmembrane transport events important for the metabolic flux of the pathway, specially the ones occurring at the final accumulation target, the idioblasts. Recently, the involvement of ATP-binding cassette (ABC) transporters in TIA accumulation has been suggested (Pomahacova et al., 2009), and we have shown that the vacuolar accumulation of TIAs in *C. roseus* leaf cells is mediated by a proton driven antiport mechanism suggesting involvement of a multidrug and toxic compound extrusion (MATE) transporter (Carqueijeiro et al., 2013; chapter II). In recent years, genomic / transcriptomic / proteomic / metabolomic approaches have also gathered much information in the global *C. roseus* metabolism, network organization and the TIA pathway (Jacobs et al., 2005; Rischer et al., 2006; Shukla et al., 2006; Murata et al., 2008). For instance, the analysis of the epidermome, where early steps of the pathway occur, has enabled the identification of two new genes involved in TIA biosynthesis (Murata et al., 2008). However, although much is known about the biosynthesis and regulation of TIAs, gene/enzyme characterization is still lacking for many biosynthetic steps, no membrane transporter of TIAs has been isolated, and no effective master switch of the pathway has been identified. Idioblast cells are an accumulation target of TIAs and are, by all odds, the site where the late, bottleneck steps of VLB biosynthesis take place. Therefore, these cells are the ideal system to look for all the missing parts cooperating to generate VLB and VCR accumulation.

The aim of this work was the implementation of a targeted strategy involving the isolation of idioblast protoplasts from those of common mesophyll cells by Fluorescence Activation Cell Sorting (FACS), followed by differential transcriptomic analysis of idioblast protoplasts by cDNA - amplified fragment length polymorphism (AFLP), in order to identify/characterize novel candidate genes involved in the biosynthesis, transport and regulation of the TIA pathway. Most down regulated genes in idioblast cells are related to photosynthesis, and among the up regulated genes a number of highly interesting novel candidate genes concerning the TIA pathway were identified, including several enzyme, transporter and transcription factor genes.
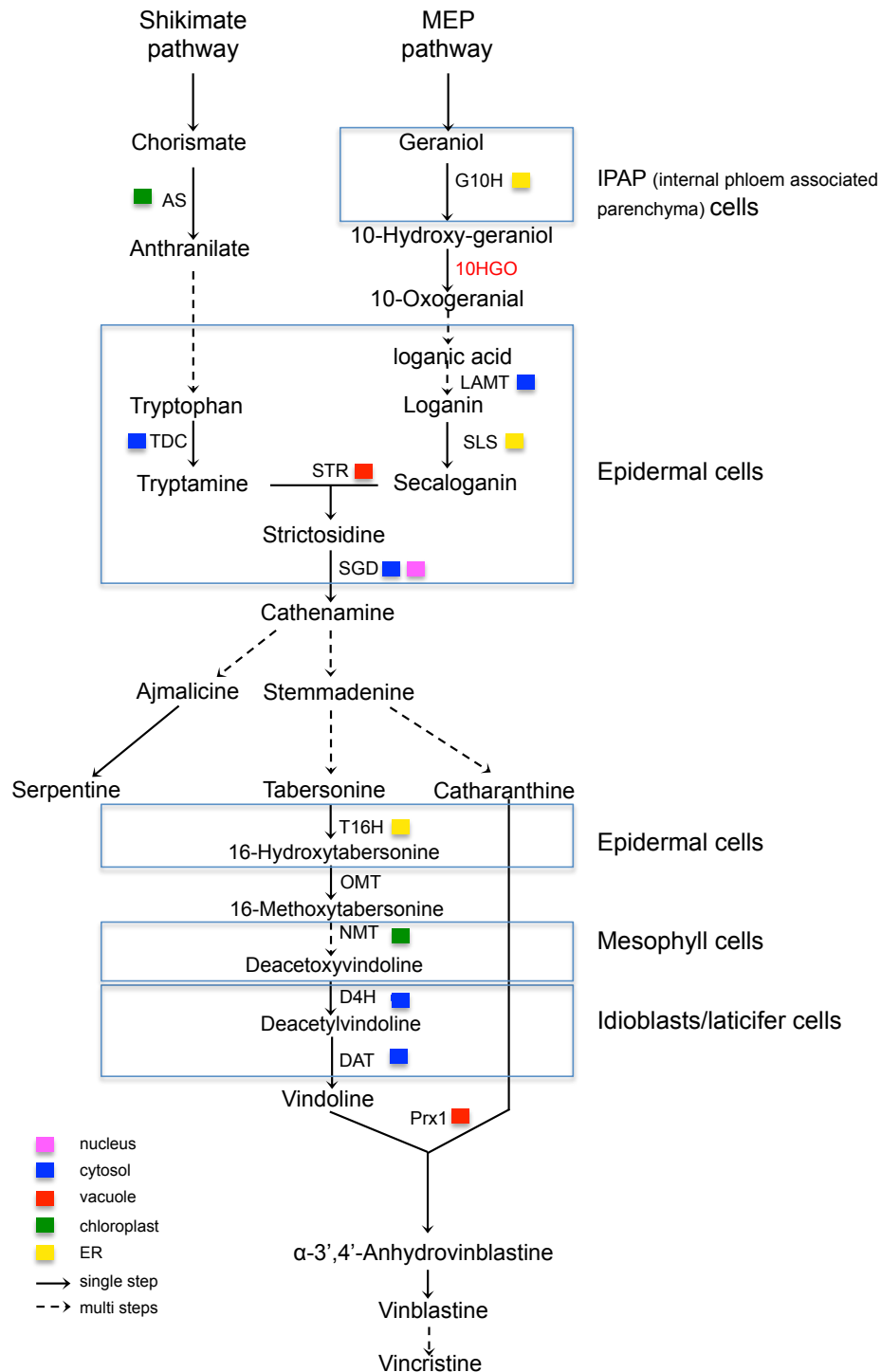
Figure 1. The TIA biosynthetic pathway in *C. roseus*. Enzymes written in red were identified as up-regulated in idioblasts in the present study. Blue rectangles highlight the cellular localization of TIA enzymes in leaves. Colour of solid boxes indicates the subcellular localization of the respective enzymes. AS – anthranilate synthase, TDC – tryptophan decarboxylase, G10H - Geraniol 10-hydroxylase, 10HGO - 10-hydroxygeraniol oxidoreductase, LAMT – loganic acid methyltransferase, SLS - secologanin synthase, STR - strictosidine synthase, SGD - strictosidine β-D-glucosidase, T16H - tabersonine 16-hydroxylase, OMT – 16-hydoxytabersonine 16-*O*-methyltransferase, NMT - *N*-methyltransferase, D4H - desacetoxyvindoline 4-hydroxylase, DAT - deacetylvindoline 4-*O*-acetyltransferase, Prx1 – peroxidase 1.

MATERIAL AND METHODS

Plant material

Catharanthus roseus (L.) G. Don cv. Little Bright Eye plants were grown at 25 °C in a growth chamber, under a 16 h photoperiod, using white fluorescent light with a maximum intensity of 70 µmol m^{-2} s^{-1}. Seeds were acquired from AustraHort (Australia) and voucher specimens are deposited at the Herbarium of the Department of Biology of the Faculty of Sciences of the University of Porto (PO 61912). Plants used for protoplast isolation were 6 to 8 months old.

Isolation of *C. roseus* leaf protoplasts

Leaf protoplasts were isolated using the first method described in chapter IV. The integrity of the isolated protoplasts was checked by observation under an optical microscope (Cell B, OLYMPUS, Japan, equipped with an Olympus DP 25 Digital Camera and respective software). Epifluorescence microscopy of protoplasts was performed in a LEICA DMLB microscope (Leica, Heerbrugg, Switzerland), using a 340 - 380 nm excitation filter combined with a 430 nm barrier filter. The viability of the isolated protoplasts was evaluated by staining with 5 µg mL^{-1} FDA and observation under an epifluorescence microscope (Leica Microsystems DM-5000B, LEICA, Germany) using excitation and emission wavelengths of respectively 494 and 530 nm (Jones and Senft, 1985).

FACS of *C. roseus* protoplasts

C. roseus protoplasts were used for FACS of idioblasts, taking advantage of their blue autofluorescence and lower red autofluorescence from chlorophyll. Protoplasts were sorted as described by Birnbaum et al. (2005) with some modifications, as described in Chapter IV.

RNA extraction from protoplasts

Extraction of RNA from the *C. roseus* idioblast protoplast enriched population was performed as described by Birbaum et al. (2005) with some modifications, as described in Chapter IV. RNA was cleaned by precipitation upon addition of 50 µL of 7.5 M ammonium acetate, 0.5 µL of RNase free glycogen and 250 µL of absolute ethanol (at -20 ºC) to 100 µL of RNA followed by vortexing. The RNA was allowed to precipitate overnight at -20 ºC, was centrifuged at 12,000 *g* at 4 ºC for 30 min, and washed twice with 0.5 mL of 80 % ethanol (at -20 ºC). The final pellet was air dried and ressuspended in the appropriate volume of RNase free water. RNA concentration and purity was

determined by spectrophotometry (NanoDrop 2000c/2000 UV-Vis Spectrophotometers, Thermo, USA).

RNA extraction from leaves and roots

RNA from leaves and roots was extracted using the RNeasy Plant Mini kit (Qiagen), according to the manufacturer's instructions, and cleaned as described above.

RT-PCR

For the synthesis of cDNA, 1 mg of the isolated RNA was first treated with DNaseI (Thermo Scientific), followed by enzyme inactivation by heating at 65 °C for 10 min in the presence of 20 mM EDTA. First-strand cDNA was synthesized from total RNA using the iScript™ cDNA Synthesis Kit (BioRad) and oligo(dT), according to manufacturer's instructions. The following primers were used for PCR amplification: *DAT* - Fw, 5'-GTGCGTATCCGTTGGTTTCT-3' and Rev, 5'-CGAACTCAATT CCATCGTCA-3'; *RPS9* - Fw, 5'-GAGCGTTTGGATGCTGAGTT-3' and Rev 5'-TCATCTCCATCACCACCAGA-3' used in 35 PCR cycles.

cDNA-AFLP analysis and data processing

Sample preparation and cDNA-AFLP based transcript profiling were performed as described by Vuylsteke et al. (2007a). Approximately 500 ng of double stranded cDNA was synthetized from 1.5 μg of total RNA. All 128 possible *Bst*YI + 1/*Mse*I + 2 primer combinations (New England Biolabs) were used. [33]P - labeled amplification products were separated on 5% polyacrylamide gels using the Sequigel system (Biorad). Dried gels were exposed to Kodak Biomax films and scanned with a PhosphorImager (Amersham Biosciences, Little Chalfont, UK). Band intensities were analyzed by the gel image analysis software QuantarPro (Keygene products N.V.). Gene tags displaying expression values in the idioblast sample corresponding to a 4 fold increase or decrease relative to the average expression value of the four samples (leaves, leaf protoplasts and roots) were selected by QuantarPro. Automatic selection was controlled by visual inspection, which allowed further selection of 29 tags. The selected tags were cut from the dried gel and reamplified through a two-step PCR, as described. To characterize the isolated cDNA-AFLP fragments, the sequences directly obtained from the reamplified PCR product were compared against nucleotide and protein sequences in several publicly available databases by BLAST sequence alignments. For the final compilation of results, BLAST analysis was performed against the Medicinal Plant Genomics Resource transcriptomic data base (MPGR; http://medicinalplantgenomics.msu.edu/).

Hierarchical clustering co-expression analysis

Expression levels of idioblast up- and down-regulated genes together with known TIA biosynthetic genes, for different organs and treatment situations, were subjected to hierarchical clustering analysis using MeV v4.8.1 for Windows (MultiExperiment Viewer, TM4; Saeed et al., 2003). The clustering analysis was performed using the HCL logarithmic factor with a Pearson correlation distance and average linkage clustering. The expression mapping data used for the cluster analysis was downloaded from MPGR and is reported in the supplemental data. The original data was converted using a root mean square factor (RMS) before clustering analysis.

RESULTS

Isolation of a highly pure idioblast population

To perform a differential transcriptomic profiling of *C. roseus* leaf idioblast cells, where the late, bottleneck biosynthetic steps of VLB take place, it is necessary to isolate these cells from the leaf tissue where they are embedded (Fig. 2B). In order to do that, the cell wall of leaf cells was first digested to produce a complex population of protoplasts where idioblast cells preserved their identity, as indicated by their conspicuous blue fluorescence under UV light (Fig. 2D). The isolated protoplasts
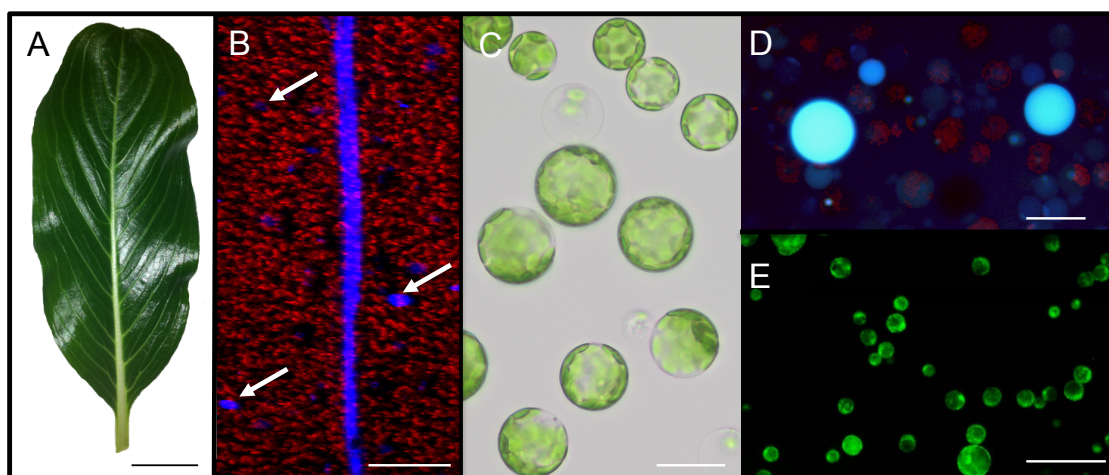
Figure 2. Images of *C. roseus* leaves and leaf protoplasts. A, Fully developed leaf representative of leaves used for protoplast isolation. B, Confocal microscopy image stack of several optical sections from a whole mounted leaf with the adaxial face up. C, Bright field image of isolated leaf protoplasts. D, Epifluorescence microscopy image of isolated leaf protoplasts. E, Epifluorescence microscopy image of isolated leaf protoplasts labelled with FDA. Blue fluorescence is due to the alkaloid serpentine and reveals alkaloid containing idioblast and laticifer cells. Red fluorescence is due to chlorophyll. White arrows indicate idioblasts. Bars = 1 cm (A), 600 μm (B), 25 μm (C), 50 μm (D) and 100 μm (E).

showed no apparent membrane damage or disintegration of the internal structure damage, and their viability was confirmed by staining with fluorescein diacetate (FDA) (Fig. 2E).

A FACS method was then developed to isolate idioblasts from all other leaf protoplasts, taking advantage of their blue fluorescence and lower red fluorescence from chlorophyll – idioblasts present a low number of chloroplasts (Fig. 2C and 3E). The optimized FACS method is described in Chapter IV and enabled the isolation of a highly enriched population of idioblasts cells (Fig. 3).
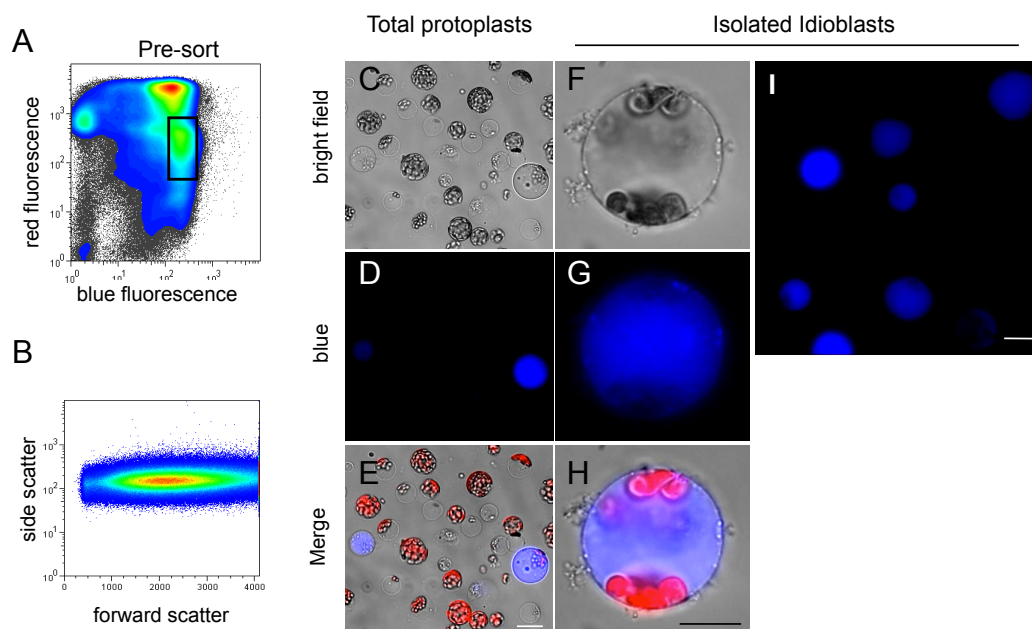
Figure 3. Purification of blue fluorescing idioblast protoplasts by FACS. A, Cell populations detected in the filtrate pre-sorting. The high blue fluorescence / low red fluorescence population marked by the black box was selected for sorting. B, Scatter plot of the initial protoplast population. C to I, Epifluorescence microscopy images of pre-sort leaf protoplasts (C to E) and sorted idioblast protoplasts (F to H). E and H are merged images of C and D, and F and G, respectively. Blue fluorescence is due to the alkaloid serpentine and reveals alkaloid containing idioblasts. Red fluorescence is due to chlorophyll. Scale bar = 20 μm (E and I) and 10 μm (H).

The identity of the isolated idioblast cells was further accessed through evaluation of the expression level by semi-quantitative RT-PCR of deacetylvindoline 4-O-acetyltransferase (DAT), previously shown to be specifically expressed in idioblasts and laticifers (St-Pierre et al., 1999). Strikingly, when the commonly used housekeeping gene 40S ribosomal protein S9 (*RPS9*) (Menke et al., 1999) was used as control for the RT-PCR, it was found that this gene was not expressed at all in the idioblast cell fraction (Fig. 4A). This revealed a very distinctive character for the idioblast cell fraction in comparison with the total leaf protoplast population, suggesting a quite different regulation also of primary metabolism in these cells. mRNA levels were then determined by in gel quantification and it was possible to conclude that DAT expression levels were significantly higher in the idioblast cell fraction than in the total leaf protoplast population (Fig. 4A). All results indicated that a highly enriched and high quality idioblast cell

fraction was obtained by the optimized FACS method, suitable for differential transcript profiling.
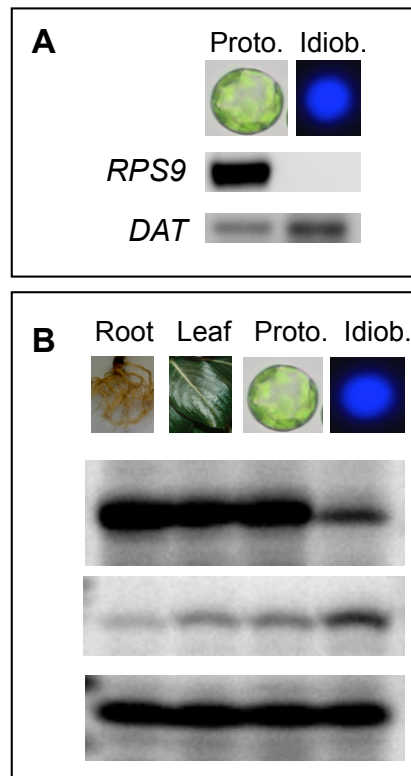
Figure 4. A, Semi-quantitative RT-PCR of deacetylvindoline 4-O-acetyltransferase (*DAT*) and of the housekeeping gene 40S ribosomal protein S9 (*RPS9*). B. Examples of the P[33]-PAGE results for the cDNA-AFLP screening showing an idioblast down-regulated tag (top row), an idioblast up-regulated tag (central row) and a potential housekeeping tag (bottom row). Proto., total leaf protoplast population; Idiob. sorted idioblast protoplasts.

Differential transcript profiling of idioblast cells

With the aim of identifying new candidate genes potentially involved in TIA biosynthesis, TIA transport and TIA pathway regulation, a genomewide transcript profiling by cDNA-amplified fragment-length polymorphism (cDNA-AFLP) was performed, using high quality mRNA extracted from roots, leaves, leaf protoplasts, and idioblast protoplasts isolated by FACS. Undigested leaves were included in this study to be able to distinguish the possible effects in expression levels resulting from the stress inflicted by the protoplast isolation technique. The inclusion of roots was to guarantee the identification of inhibition situations. The goal was to detect both up- and down-regulated genes in idioblasts since the first may be involved in the late steps of the TIA pathway, known to be specifically expressed in these cells, while the second may enable to detect genes involved in the early steps of the TIA pathway, known to be specifically expressed in epidermal cells (St-Pierre et al., 1999; Mahroug et al., 2007; Murata et al., 2008; Guirimand et al., 2011b).

The cDNA-AFLP 128 BstY1+1/MseI+2 primer combinations previously used by (Rischer et al., 2006) to determine gene-to-metabolite networks for TIA biosynthesis in *C. roseus* cells enabled here the detection of the quantitative accumulation patterns of over 15,000 transcript tags. Typical results for an idioblast down-regulated tag, an idioblast up-regulated tag and a potential housekeeping tag are shown in Fig. 4B. Computer aided analysis of the results complemented with manual analysis enabled the selection of 265 tags with expression levels significantly up- or down-regulated in idioblasts (Fig. 5). These tags were isolated and PCR amplification / sequencing enabled the generation of good-quality sequences for 189 tags. These sequences were then analysed using the Medicinal Plant Genomics Resource transcriptomic data base (MPGR; http://medicinalplantgenomics.msu.edu/), which includes a collection of 63,623 entries of transcript assemblies for *C. roseus*, generated by the assembler Oases (Schulz et al., 2012). A substantial number of the MPGR assembled transcripts is full or near-full length and, according to Góngora-Castillo et al. (2012), the representation of known genes from the TIA biosynthetic pathway is robust. Screening of the 189 tag sequences against MPGR enabled the detection of 171 matches to MPGR identified genes, with only 10% of the sequences having no similarities to any identified plant gene (Fig. 5).
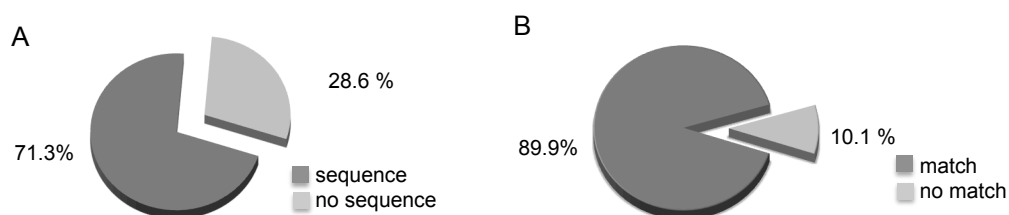
Figure 5. Net identification efficiency of the cDNA-AFLP tags selected as being up- or down-regulated in idioblasts. A, Amplification / sequencing efficiency of the selected tags. B, Database identification of the sequences obtained in A.

The initial characterization of the isolated idioblast cells showed that they did not express at all the housekeeping gene usually used for *C. roseus*, RPS9 (Fig. 4A). Therefore, the cDNA-AFLP profiling was also used to select tags corresponding to potential housekeeping genes, presenting an identical expression level in all the four organ / cells investigated (roots, leaves, leaf protoplasts and idioblast protoplasts). This enabled the identification of 21 tags with a null discrepancy in the expression levels, for which 20 good-quality sequences were obtained. Screening against MPGR enabled the detection of matches for all the 20 sequences (Table I) and 5 were selected for evaluation as housekeeping genes (bold in Table I). For four of these genes, 40S ribosomal protein S28, glyceraldehyde-3-phosphate dehydrogenase, 60S ribosomal protein L24 and ADP-ribosylation factor 2 (underlined in Table I), it was possible to design highly specific

primers generating a single and abundant PCR product. These genes are now being evaluated by qPCR for their real quality as housekeeping genes for *C. roseus*.

Table I. List of putative housekeeping genes for *C. roseus* selected from the cDNA-AFLP analysis ween roots, leaves, leaf protoplasts and idioblast protoplasts. Genes in bold were selected for aracterization and underlined genes were successfully amplified and are under assessment. MPGR – dicinal Plant Genomic Resource (http://medicinalplantgenomics.msu.edu/).

MPGR accession number	Functional category	Description
cra_locus_535_iso_3_len_1176_ver_3	Vesicle and protein traffic	Tetraspanin7
cra_locus_28666_iso_1_len_683_ver_3	Protein synthesis and folding	**40S ribosomal protein S28**
cra_locus_3431_iso_3_len_2859_ver_3	Signalling	LRR receptor kinase
cra_locus_1931_iso_1_len_1430_ver_2	Stress response	Chilling-responsive protein
cra_locus_9604_iso_1_len_1317_ver_3	Primary metabolism	**Glyceraldehyde-3-phosphate dehydrogenase, cytosolic**
cra_locus_2367_iso_5_len_2330_ver_3	Unknown	Unknown
cra_locus_2225_iso_10_len_1584_ver_3	Nucleus and nucleic acids	XPA-binding protein
cra_locus_526_iso_4_len_2747_ver_3	Vesicle and protein traffic	Endosomal P24A protein
cra_locus_920_iso_5_len_1724_ver_3	Primary metabolism	Phosphatidic acid phosphatase
cra_locus_3020_iso_2_len_1454_ver_3	Unknown	Phosducin - Thioredoxin superfamily protein
cra_locus_2570_iso_3_len_1598_ver_3	Protein synthesis and folding	**60S ribosomal protein L24**
cra_locus_11139_iso_1_len_1139_ver_3	Membrane structure and microdomains	Steroid binding protein
cra_locus_1915_iso_4_len_804_ver_3	Unknown	Hypothetical protein
cra_locus_3931_iso_9_len_1479_ver_3	Signalling	Calmodulin-7
cra_locus_493_iso_5_len_1087_ver_3	Signalling	LRR receptor kinase 1
cra_locus_850_iso_2_len_751_ver_3	Transporter	Bax inhibitor 1
cra_locus_15446_iso_1_len_500_ver_3	Protein synthesis and folding	Protein disulfide isomerase-like 1
cra_locus_9888_iso_8_len_1434_ver_3	Unknown	Conserved gene of unknown function
cra_locus_11407_iso_3_len_322_ver_3	Ubiquitin-proteasome pathway	**Polyubiquitine**
cra_locus_11407_iso_3_len_322_ver_3	Signallling GTP-binding proteins ,	**ADP-ribosylation factor 2**

From the total 171 tags with a differential expression in idioblasts, 112 tags corresponding to 98 genes in the MPGR data base showed up-regulation in idioblasts and 59 tags corresponding to 49 genes showed down-regulation (Table II). This decrease from number of tags to number of genes suggests that the cDNA-AFLP

technique not always yields the claimed one gene / one tag ratio. Hierarchical cluster analysis of the differential expression levels of the 98 idioblast up-regulated genes and of the 49 idioblast down-regulated genes is presented in Fig. 6 and 7 as heat maps.

In Fig. 6 it can be seen that all the genes selected as up-regulated indeed present a significantly higher expression in idioblasts than in leaves and leaf protoplasts. In some cases, the expression levels seem to be induced by the protoplast treatment, while for other cases (bottom clusters) expression levels are lower in protoplasts than in the source leaves, but in any case still significantly higher in idioblasts. Interestingly, most of the leaf transcripts that are down-regulated in protoplasts are highly expressed in roots. A similar phenomenon can be observed in cluster analysis of the idioblast down-regulated genes (Fig. 7), where a set of transcripts highly abundant in roots is clearly repressed in protoplasts relative to leaves. This suggests that the functions of all these genes become less needed during the protoplast state, where the cell activates stress responses and possibly invests intensely in producing a new cell wall, with a part of them being important for idioblasts and others not. This shows that idioblast cells have a very distinctive character from other leaf cells, namely in their response to protoplasting, which is also clearly indicated in Fig. 7 by the cluster of transcripts that are strongly induced by the protoplast treatment in the whole population of leaf protoplasts, but are present in low levels in idioblast protoplasts.

Table II. *C. roseus* genes up- and down-regulated in idioblasts (I) in comparison with leaves (L) and leaf protoplasts (P). Genes were grouped in functional categories and separated in up- and down-regulated in each category. Genes referred in the text are highlighted in bold, and genes codifying proteins identified in the *C.roseus* leaf vacuole proteome (Chapter III) are underlined.

MPGR accession number	Description	Relative expression level		
		L	P	I
***Nucleus and nucleic acids* – up-regulated**				
cra_locus_11320_iso_5_len_1045_ver_3	ATP-dependent RNA helicase	1.48	0.50	1.23
cra_locus_11973_iso_3_len_1075_ver_3	Chromodomain helicase DNA	0.50	1.60	2.94
cra_locus_12897_iso_3_len_1813_ver_3	DEAD-box ATP-dependent RNA helicase	0.65	1.26	2.69
cra_locus_5773_iso_1_len_746_ver_3	DNA polymerase alpha subunit	0.50	0.68	2.70
cra_locus_2032_iso_2_len_4257_ver_3	nuclear matrix constituent protein 1	0.50	0.95	2.73
cra_locus_9424_iso_2_len_3381_ver_3	nuclear (Nop14)	0.50	0.92	2.78
cra_locus_39011_iso_1_len_431_ver_3	Putative polyprotein	0.50	0.51	1.23
cra_locus_115540_iso_1_len_286_ver_3	Putative retroelement polyprotein	0.52	0.50	2.39
cra_locus_118948_iso_2_len_379_ver_3	Putative retroelement polyprotein	1.72	0.50	2.60
cra_locus_595_iso_7_len_2043_ver_3	RNA-binding protein	0.50	1.85	2.89
cra_locus_4462_iso_7_len_1090_ver_3	Serine/arginine rich splicing factor	0.50	0.86	2.71
cra_locus_1913_iso_2_len_1847_ver_3	Splicing factor U2af large subunit B	0.50	2.60	0.75
cra_locus_4594_iso_2_len_2637_ver_3	**TF1up-bHLH13**	0.50	0.65	2.56
cra_locus_517_iso_1_len_3280_ver_3	**TF2up-DNA binding**	0.71	0.50	2.51
cra_locus_45433_iso_1_len_858_ver_3	**TF3up-DNA binding**	0	0.5	1.91
cra_locus_13911_iso_5_len_1494_ver_3	**TF4up-GTE6**	0.66	1.73	2.64
cra_locus_5262_iso_1_len_2814_ver_3	**TF5up-homeobox ML1**	0.84	0.50	2.72
cra_locus_3966_iso_4_len_1476_ver_3	**TF6up-HSFB2a**	0.50	1.48	2.67
cra_locus_4787_iso_1_len_2989_ver_3	**TF7up-MYB**	2.76	0.50	2.38
cra_locus_117794_iso_1_len_322_ver_3	**TF8up-MYB**	0.59	0.50	1.67
cra_locus_7437_iso_1_len_359_ver_3	**TF9up-MYB**	0.56	0.67	2.57
cra_locus_86047_iso_1_len_516_ver_3	**TF10up-MYB**	0.59	0.50	1.47
cra_locus_16332_iso_5_len_1539_ver_3	**TF11up-NAC**	0.53	1.25	2.64
cra_locus_12026_iso_2_len_974_ver_3	**TF12up-NAC**	0.50	1.26	2.62
cra_locus_23016_iso_2_len_1374_ver_3	**TF13up-UNE10**	0.99	0.55	2.63

Table II. (continued from previous page.)

MPGR accession number	Description	Relative expression level		
		L	P	I
***Nucleus and nucleic acids** – down-regulated*				
cra_locus_5773_iso_2_len_2494_ver_3	DNA polymerase alpha	0.50	2.62	1.05
cra_locus_11919_iso_1_len_602_ver_3	Putative DNA repair protein RAD23	0.50	2.57	1.78
cra_locus_40994_iso_1_len_1061_ver_3	Putative retroelement polyprotein	1.52	0.91	0.50
cra_locus_726_iso_7_len_2263_ver_3	Splicing factor, arginine/serine-rich	2.67	0.70	0.50
cra_locus_13911_iso_1_len_878_ver_3	TF1down-GTE6	1.97	0.79	0.59
cra_locus_115540_iso_1_len_286_ver_3	TF2down-MYB	0.5	2.58	0.51
cra_locus_11431_iso_1_len_999_ver_3	TF3down-NAC	0.70	2.64	1.81
cra_locus_5366_iso_3_len_1889_ver_3	TF4down-NAC	0.57	2.62	0.89
***Unknown** – up-regulated*				
cra_locus_148_iso_4_len_3157_ver_3	Hypothetical protein	0.58	0.50	1.07
cra_locus_2239_iso_4_len_818_ver_3	Hypothetical protein	0.53	1.07	2.63
cra_locus_3927_iso_9_len_2065_ver_3	Hypothetical protein	0.96	0.50	0.79
cra_locus_4075_iso_5_len_1308_ver_3	Hypothetical protein	0.88	0.64	2.65
cra_locus_5223_iso_7_len_945_ver_3	Hypothetical protein	0.00	0.50	1.91
cra_locus_5314_iso_1_len_2884_ver_3	Hypothetical protein	0.61	0.50	1.79
cra_locus_8026_iso_1_len_990_ver_3	Hypothetical protein	0.70	0.50	2.64
cra_locus_8546_iso_1_len_371_ver_3	Hypothetical protein (Ycf68-like)	0.50	1.25	1.85
cra_locus_9489_iso_10_len_1330_ver_3	Hypothetical protein	0.63	1.89	2.57
cra_locus_9489_iso_10_len_1330_ver_3	Hypothetical protein	0.50	1.02	2.64
cra_locus_10052_iso_1_len_1530_ver_3	Hypothetical protein	0.50	0.99	2.70
cra_locus_13604_iso_2_len_2662_ver_3	Hypothetical protein	0.50	0.62	2.67
cra_locus_14965_iso_1_len_1147_ver_3	Hypothetical protein	0.54	0.50	2.25
cra_locus_120423_iso_1_len_623_ver_3	Hypothetical protein	0.50	0.57	2.64
cra_locus_123761_iso_1_len_304_ver_3	Hypothetical protein	0.50	0.58	0.89
cra_locus_25758_iso_1_len_469_ver_3	Hypothetical protein	0.50	1.60	2.50
cra_locus_2697_iso_9_len_1136_ver_3	MtN19-like protein	0.50	0.77	2.62

Table II. (continued from previous page)

MPGR accession number	Description	Relative expression level		
		L	P	I
***Unknown* – up-regulated (cont.)**				
cra_locus_115540_iso_1_len_286_ver_3	Putative retroelement polyprotein	0.89	0.50	1.02
***Unknown* – down-regulated**				
cra_locus_8546_iso_7_len_468_ver_3	Hypothetical protein	0.50	2.70	1.51
cra_locus_9489_iso_10_len_1330_ver_3	Hypothetical protein	2.73	0.77	0.50
cra_locus_10502_iso_3_len_1437_ver_3	Hypothetical protein	1.99	0.87	0.50
cra_locus_51352_iso_1_len_357_ver_3	Hypothetical protein	2.43	1.00	0.50
***Signalling* – up-regulated**				
cra_locus_6111_iso_1_len_1838_ver_3	BCL-2-associated athanogene	0.50	1.00	2.65
cra_locus_10830_iso_1_len_1294_ver_3	Calmodulin binding protein	0.50	0.81	2.74
cra_locus_11884_iso_3_len_2216_ver_3	CASP-like protein	2.68	0.62	1.22
cra_locus_470_iso_4_len_1013_ver_3	Cell number regulator 8-like (SAT5)	0.50	1.18	2.86
cra_locus_11366_iso_1_len_1441_ver_3	Nodulation protein	0.50	0.00	2.39
cra_locus_11114_iso_2_len_2253_ver_3	Lectin-receptor like protein kinase	0.66	1.39	2.69
cra_locus_110261_iso_1_len_323_ver_3	Serine/threonine-protein phosphatase	0.50	1.12	2.46
cra_locus_17177_iso_1_len_2408_ver_3	Serine/threonine protein kinase SAPK	1.34	0.50	2.73
cra_locus_7121_iso_4_len_1540_ver_3	Serine/threonine-protein kinase	0.72	0.50	2.69
cra_locus_7842_iso_1_len_2596_ver_3	Serine/threonine-protein kinase	0.50	1.56	2.50
cra_locus_9177_iso_3_len_3548_ver_3	Serine/threonine-protein kinase	0.50	1.54	2.86
cra_locus_13185_iso_3_len_1469_ver_3	Tyrosine-protein phosphatase	1.71	0.62	2.62
cra_locus_1962_iso_7_len_985_ver_3	Upstream activation factor (spp27-like)	0.50	0.54	2.52
***Signalling* – down-regulated**				
cra_locus_19_iso_3_len_1427_ver_3	serine/threonine protein kinase SAPK	2.74	0.96	0.50
***Primary Metabolism* – up-regulated**				
cra_locus_1375_iso_4_len_3323_ver_3	Arogenate dehydrogenase 1	0.88	0.50	2.14
cra_locus_14737_iso_4_len_2704_ver_3	CRAL/TRIO domain containing protein	0.93	0.50	2.61
cra_locus_2315_iso_1_len_372_ver_3	Glutamine synthetase	1.14	0.55	2.64

Table II. (continued from previous page)

MPGR accession number	Description	Relative expression level		
		L	P	I
Primary Metabolism – up-regulated (contn.)				
cra_locus_8687_iso_5_len_1090_ver_3	Pyruvate decarboxylase	0.69	1.34	2.71
cra_locus_2934_iso_1_len_1354_ver_3	S-2-hydroxy-acid oxidase GLO4	0.50	1.98	2.74
cra_locus_5891_iso_1_len_642_ver_3	S-adenosyl-L-homocysteine hydrolase	0.50	0.71	1.17
cra_locus_5010_iso_4_len_830_ver_3	Threonine aldolase	0.50	1.04	2.73
cra_locus_4673_iso_10_len_2043_ver_3	Xylose isomerase	2.52	0.50	2.41
Primary Metabolism – down-regulated				
cra_locus_9224_iso_6_len_2188_ver_3	β-1,3-galactosyltransferase 14	0.50	2.75	1.01
cra_locus_18077_iso_1_len_1084_ver_3	1-aminocyclopropane-1-carboxylate oxidase	0.68	2.58	0.59
cra_locus_2315_iso_1_len_372_ver_3	Glutamine synthetase	0.58	2.63	0.92
cra_locus_2315_iso_1_len_372_ver_3	Glutamine synthetase	0.87	2.52	0.50
cra_locus_10329_iso_4_len_1269_ver_3	Phosphoglycolate phosphatase	1.18	2.84	0.50
cra_locus_2288_iso_3_len_2751_ver_3	Long chain acyl-CoA synthetase 4	0.50	2.61	0.90
cra_locus_13793_iso_1_len_2581_ver_3	Sucrose synthase	0.53	2.52	0.50
Transport – up-regulated				
cra_locus_6597_iso_4_len_2355_ver_3	**ABCA1**	0.85	0.50	2.42
cra_locus_3692_iso_7_len_2056_ver_3	**ABCC1**	0.50	1.04	2.64
cra_locus_1810_iso_7_len_4881_ver_3	**ABCC2**	0.50	0.86	2.68
cra_locus_9464_iso_1_len_4509_ver_3	**ABCG1**	0.50	1.77	2.78
cra_locus_7628_iso_3_len_2346_ver_3	Graves disease carrier protein 1	0.50	0.50	2.54
cra_locus_16643_iso_1_len_1469_ver_3	Vacuolar membrane protein YML018C	0.50	1.00	2.66
Transport – down-regulated				
cra_locus_12286_iso_3_len_2300_ver_3	**ABCB1**	2.46	1.08	0.50
cra_locus_14396_iso_4_len_2840_ver_3	**ABCG2**	0.79	2.74	1.15
cra_locus_23607_iso_1_len_1405_ver_3	**ABCG3**	2.82	0.97	0.50
cra_locus_1366_iso_9_len_2662_ver_3	ATP synthase subunit beta	2.66	0.96	0.50

Table II. (continued from previous page)

MPGR accession number	Description	Relative expression level		
		L	P	I
Secondary Metabolism – up-regulated				
cra_locus_2091_iso_3_len_1101_ver_3	**10-hydroxygeraniol oxidoreductase** (10HGO)	0.50	0.51	2.54
cra_locus_16113_iso_1_len_1085_ver_3	**10HGO**	0.5	0.69	2.61
cra_locus_4293_iso_2_len_2076_ver_3	**Cytochrome P450**	0.53	1.54	2.42
cra_locus_3366_iso_1_len_934_ver_3	**Resveratrol/hydroxycinnamic acid O-glucosyltransferase**	0.50	1.07	2.67
Secondary Metabolism – down-regulated				
cra_locus_3558_iso_1_len_1647_ver_3	**Alliin lyase**	0.50	2.65	0.91
cra_locus_14774_iso_4_len_1241_ver_3	Glutathione s-transferase	2.69	2.11	1.01
cra_locus_71018_iso_1_len_510_ver_3	Glutathione S-transferase	0.56	2.65	1.18
Miscellaneous – up-regulated				
cra_locus_86537_iso_1_len_482_ver_3	2S albumin	0.74	0.86	2.68
cra_locus_61387_iso_1_len_468_ver_3	Miraculin	0.55	1.13	2.64
cra_locus_6695_iso_2_len_1987_ver_3	No exine formation	0.50	1.79	1.93
cra_locus_1477_iso_4_len_2200_ver_3	Zinc finger CCHC domain	0.97	0.50	2.81
cra_locus_16564_iso_1_len_281_ver_3	Zinc finger CCHC domain	1.38	1.27	2.89
cra_locus_4353_iso_6_len_2431_ver_3	Zinc finger CCCH domain	0.50	0.96	2.61
Miscellaneous – down-regulated				
cra_locus_2137_iso_7_len_1240_ver_3	S-adenosylmethionine-dependent methyltransferase	1.59	2.81	0.50
cra_locus_23004_iso_1_len_868_ver_3	Miraculin-like protein	0.50	2.57	0.74
cra_locus_48050_iso_1_len_297_ver_3	Miraculin	0.50	2.70	1.79
Protein synthesis and folding - up-regulated				
cra_locus_2315_iso_1_len_372_ver_3	Putative translation factor	0.57	1.48	2.64
cra_locus_3628_iso_3_len_1244_ver_3	Putative translation factor	0.74	1.30	2.73
cra_locus_10159_iso_4_len_850_ver_3	Ribosome biogenesis protein BOP1	1.24	0.50	1.31
Protein synthesis and folding - down-regulated				
cra_locus_7983_iso_10_len_910_ver_3	Eukaryotic initiation factor 4A	2.68	2.34	0.50

Table II. (continued from previous page)

MPGR accession number	Description	Relative expression level		
		L	P	I
Protein synthesis and folding - down-regulated (cont.)				
cra_locus_7187_iso_1_len_2099_ver_3	Glutamyl-tRNA reductase	0.77	2.74	1.36
cra_locus_323_iso_279_len_5998_ver_3	Ribosomal protein S4	2.55	2.17	0.83
Ubiquitin-proteosome pathway - up-regulated				
cra_locus_12796_iso_1_len_1590_ver_3	F-box protein	0.50	0.61	1.85
cra_locus_4614_iso_6_len_2324_ver_3	Protein FAM188A-like	0.50	0.60	2.35
cra_locus_3260_iso_10_len_2095_ver_3	Ubiquitin carboxyl-terminal hydrolase	0.50	0.80	2.68
cra_locus_2424_iso_1_len_1820_ver_3	Ubiquitin fusion degradaton protein	0.50	1.46	2.61
cra_locus_2503_iso_7_len_2805_ver_3	Ubiquitin-protein ligase	0.96	0.50	0.93
Catabolism and hydrolases - down-regulated				
cra_locus_12978_iso_3_len_1933_ver_3	Abhydrolase domain	0.50	1.32	2.66
cra_locus_22456_iso_1_len_817_ver_3	Phospholipase Dp1	0.50	0.92	2.69
Protein degradation – up-regulated				
cra_locus_2024_iso_4_len_922_ver_3	Peptidase domain	0.52	1.35	2.62
cra_locus_3183_iso_11_len_876_ver_3	Protease, putative	1.37	0.50	2.91
Glycosidases - up-regulated				
cra_locus_10215_iso_3_len_2750_ver_3	Alkaline alpha galactosidase I	0.50	0.72	1.23
Redox metabolism - up-regulated				
cra_locus_11519_iso_3_len_1225_ver_3	CroPrx5	0.53	1.43	2.62
Redox metabolism - down-regulated				
cra_locus_4912_iso_1_len_998_ver_3	Bifunctional monodehydroascorbate reductase	0.50	2.59	0.88
cra_locus_12587_iso_3_len_2077_ver_3	NADP-dependent malic enzyme	0.50	2.70	1.28
cra_locus_4644_iso_3_len_2087_ver_3	NADP-dependent malic enzyme-like	0.58	2.66	1.24
cra_locus_8537_iso_2_len_1182_ver_3	Oxidoreductase, putative	0.50	2.66	0.78
Stress response - up-regulated				
cra_locus_8467_iso_3_len_2142_ver_3	ERD (early-responsive to dehydration stress)	0.50	0.82	2.76

Table II. (continued from previous page)

MPGR accession number	Description	Relative expression level		
		L	P	I
Stress response - down-regulated				
cra_locus_7117_iso_7_len_1351_ver_3	PTI1-like tyrosine-protein kinase	1.91	0.64	0.50
Vesicle and protein traffic - up-regulated				
cra_locus_16863_iso_1_len_2142_ver_3	CASP-like protein	2.68	0.62	1.22
Vesicle and protein traffic - up-regulated				
cra_locus_4345_iso_1_len_1001_ver_3	GTP binding protein	0.50	2.67	1.18
Cytoskeleton - up-regulated				
cra_locus_34876_iso_1_len_501_ver_3	Myosin	0.50	0.68	2.67
Chloroplast - down-regulated				
cra_locus_73250_iso_1_len_453_ver_3	Chlorophyll a/b binding protein	2.52	0.57	0.50
cra_locus_1910_iso_3_len_936_ver_3	Cytochrome c	2.60	1.73	0.54
cra_locus_1953_iso_3_len_3606_ver_3	NADH-plastoquinone oxidoreductase	2.50	1.39	0.50
cra_locus_323_iso_11_len_1227_ver_3	Photosystem I P700 apoprotein A2	2.08	2.44	0.60
cra_locus_1910_iso_5_len_4791_ver_3	Photosystem II CP47 chlorophyll apoprotein	2.22	2.28	0.86
cra_locus_1910_iso_7_len_3247_ver_3	Photosystem II phosphoprotein	1.08	2.82	1.82
cra_locus_2142_iso_2_len_1209_ver_3	Photosystem II protein K	2.55	0.89	0.50
cra_locus_2142_iso_7_len_4140_ver_3	Photosystem Q	2.54	1.90	0.50
cra_locus_11283_iso_5_len_1333_ver_3	Thioredoxin-like 2	0.50	2.60	0.75

Figure 6. cDNA-AFLP transcriptome analysis of *C. roseus* roots, leaves, leaf protoplasts (Ppt) and idioblasts (Idio), showing average linkage hierarchical clustering of selected genes **up-regulated** in idioblasts, according to their expression pattern in the four samples assayed. The heat map grey scale reflects expression levels relative to the average expression level of all samples. Underlined in red are genes discussed in the text.
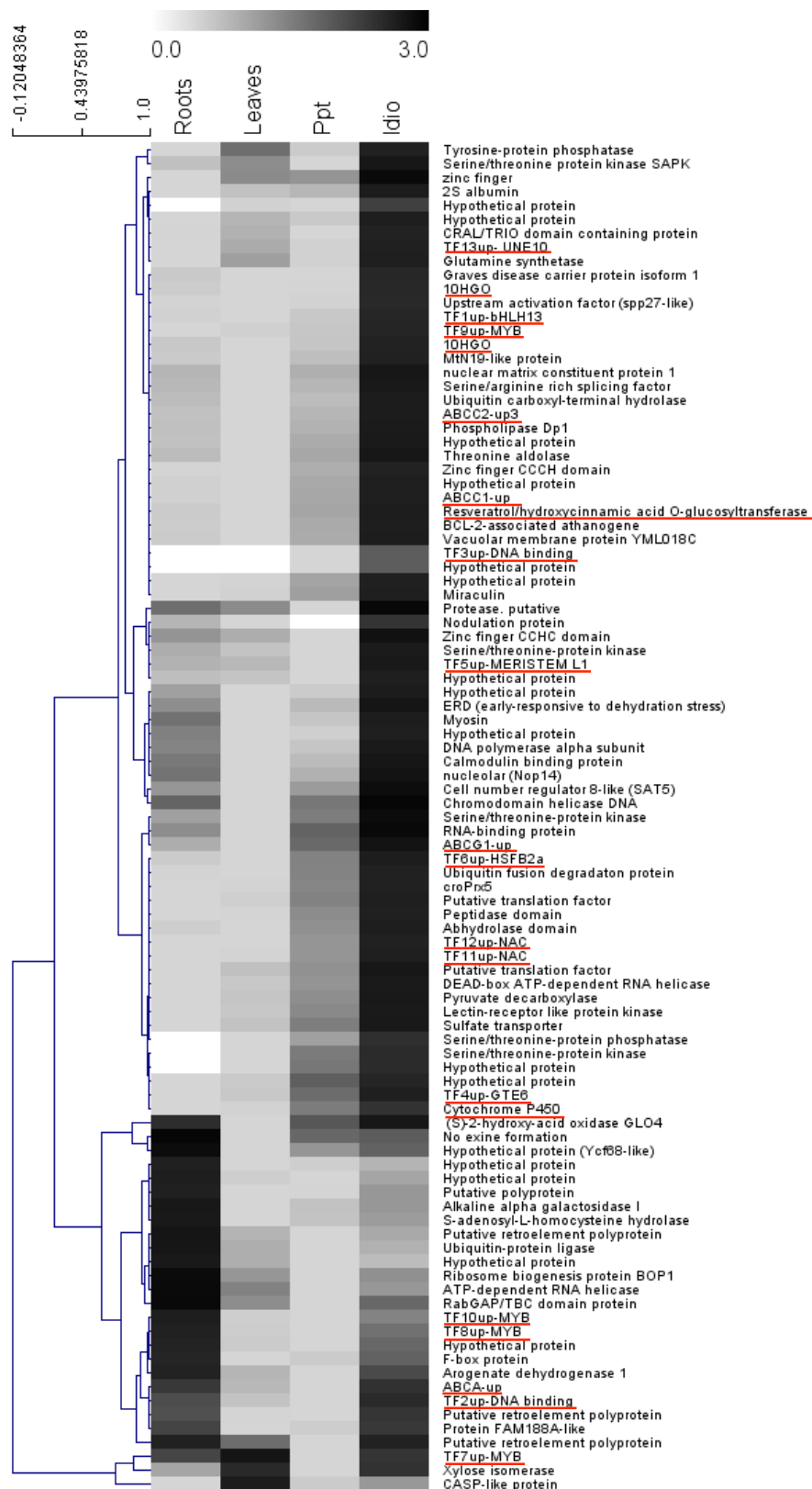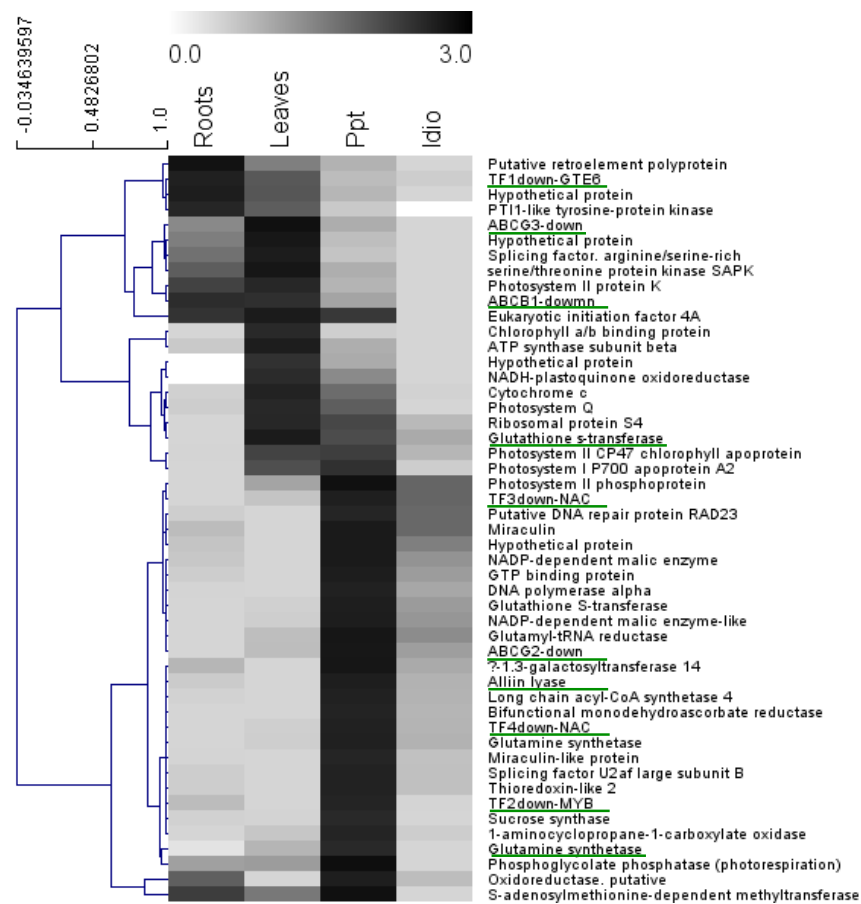
Figure 7. cDNA-AFLP transcriptome analysis of *C. roseus* roots, leaves, leaf protoplasts (Ppt) and idioblasts (Idio), showing average linkage hierarchical clustering of selected genes **down-regulated** in idioblasts, according to their expression pattern in the four samples assayed. The heat map grey scale reflects expression levels relative to the average expression level of all samples. Underlined in green are genes discussed in the text.

The distribution of the idioblast up- and down-regulated genes by functional categories is shown in Fig. 8. The more represented functional category in both groups is nucleus and nucleic acids, including 13 up- and 4 down-regulated transcription factors, clearly indicating a significant genetic reprogramming of idioblast cells, in comparison with leaf or protoplast cells. Possibly related with this, the expression activation in idioblasts of a significant number of signalling proteins is observed, which may be involved in the determination of the differential metabolism of these cells. Eighteen unknown genes are also up-regulated and should be monitored in the future since they may be important for TIA metabolism. Genes codifying chloroplast proteins are the second category of down-regulated genes (after nucleus and nucleic acids), and are completely absent from the up-regulated group, consistent with the observation that idioblast cells have a much lower or even absent population of chloroplasts than common mesophyll cells (Fig. 2D and 3E).
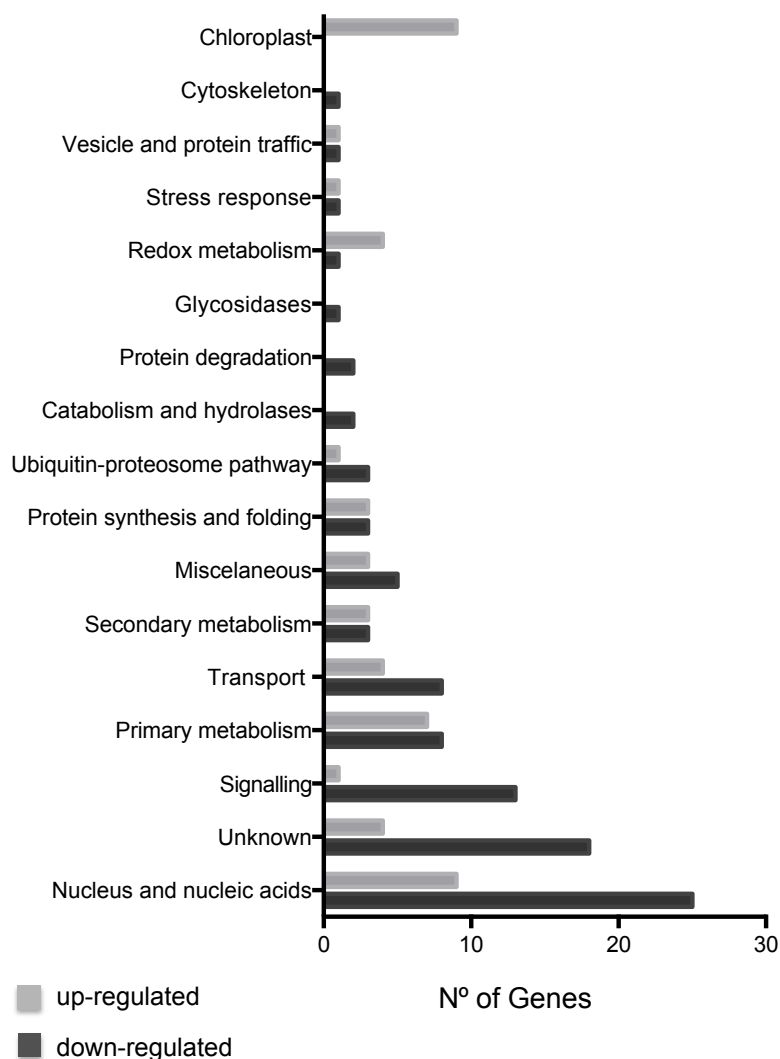
Figure 8. Distribution by functional categories of the *C. roseus* up- and down-regulated genes in idioblasts.

The main target categories of this study, enzymes of secondary metabolism, transporters and transcription factors are described and discussed in more detail below. For this discussion, the transcript abundances provided by MPGR for a number of organ/tissues were used to perform hierarchical cluster co-expression analysis of the idioblast up- and down-regulated genes together with the MPGR genes identified as codifying enzymes from the TIA pathway, as performed by Giddings et al. (2011) to identify a novel gene involved in TIA biosynthesis. The results of hierarchical clustering are visualized as a heat map (Fig. 9). MPGR provides transcript abundances for the tissues and treatments used to generate their transcriptome data, estimated by mapping the reads from all experimental libraries to the assembled transcripts using TopHat and quantifying expression abundances using Cufflinks (Gongora-Castillo et al., 2012). Expression levels are represented as fragments per kilobase of transcript per million mapped reads (FPKM).

Secondary metabolism

Curiously, the number of idioblast up- and down-regulated genes confirmedly related with secondary metabolism is low: two isoforms of 10-hydroxygeraniol oxidoreductase (*10HGO*), a resveratrol/hydroxycinnamic acid glucosyltransferase and a P450 are up-regulated, and two isoforms of glutathione S-transferase and an alliin lyase are down-regulated (Table II, Fig. 6 and 7). The two last genes involved in vindoline biosynthesis, desacetoxyvindoline 4-hydroxylase (*D4H*) and deacetylvindoline 4-O-acetyltransferase (*DAT*), which were shown to be specifically expressed in idioblasts (St-Pierre et al., 1999) were not detected in this screening. However, semi-quantitative RT-PCR showed that *DAT* transcripts were indeed present in the idioblast samples, in higher levels than in the total leaf protoplast population (Fig. 4A). Their absence from this screening may result from the incomplete coverage of the transcriptome by cDNA-AFLP or from a deficient separation / detection in the electrophoresis gel. On the other hand, the presence of *10HGO* in higher levels in idioblasts contrasts with the current view that the early TIA pathway is expressed only in the internal phloem associated parenchyma and in the leaf epidermis (Fig. 1; St-Pierre et al., 1999; Guirimand et al., 2010). 10HGO is located in the monoterpenoid precursor pathway, between geraniol 10-hydroxylase (*G10H*), expressed in phloem parenchyma cells, and loganic acid methyltransferase (*LAMT*), expressed in epidermal cells (Fig. 1), and would therefore be expected to be expressed in one of these cell types. In any case, it would not be expected in the idioblasts, where only *D4H* and *DAT* expression was detected so far. However, it is anticipated that this simple view of the TIA pathway may be challenged in the future, since the MPGR database has enabled the detection of many isoforms for the TIA biosynthesis enzymes, being possible that they may have differential expression profiles, and that the TIA pathway is expressed more broadly in leaf tissues, just using different genes from the same family. In fact, cluster analysis of the transcription levels data available at MPGR for those isoforms clearly shows that many of the different isoforms have very different organ and methyl jasmonate responsive expression profiles (Fig. 9). The intense up-regulation in idioblasts of resveratrol/hydroxycinnamic acid glucosyltransferase may indicate that some of the glycosylated phenolic compounds that have been shown to be present in *C. roseus* leaves (Ferreres et al., 2011) may also be particularly accumulated in idioblasts.

So far, four P450s were shown to mediate TIA biosynthetic steps, including G10H, secologanin synthase (SLS), tabersonine 16-hydroxylase (T16H) and tabersonine 19-hydroxylase (T19H; Loyola-Vargas et al., 2007; Giddings et al., 2011), with three of these steps corresponding to hydroxylations. Therefore, it is tempting to hypothesize that the up-regulated *P450* in idioblasts may correspond to the enzyme catalysing the

bottleneck hydroxylation of α-3',4'-anhydrovinblastine (AVLB) into VLB, since this reaction is thought to occur in idioblasts. Moreover, this P450 protein has been detected in the vacuole proteome of *C. roseus* leaves (Chapter III), and this organelle is the subcellular location where this reaction is also predicted to happen. Finally, the expression profile of this *P450* falls in a cluster of TIA biosynthesis genes that are induced by methyl jasmonate (Fig. 9), further reinforcing its putative involvement in the TIA pathway. In fact, induction of TIA levels by methyl jasmonate is well documented (Memelink and Gantet, 2007), and association of the *T19H P450* gene with the above mentioned cluster was the strategy used by Giddings et al. (2011) to uncover this TIA gene. Therefore, the idioblast up-regulated *P450* gene is now under study in our group.

Two glutathione S-transferases are down-regulated in idioblasts (Fig. 7). These enzymes are involved in detoxification and have also been involved in vacuole sequestration of several secondary metabolites such as phenolics and flavonoids (Yazaki, 2006; Dixon and Hassoun, 2010). These two enzymes may be involved for instance in detoxification at the level of the epidermal cells, being in low levels in idioblasts. One of them is strongly induced by protoplasting (Fig. 7), and is possibly involved in the response to the stress endured by protoplasts. The same is true for alliin lyase, the other secondary metabolism gene down-regulated in idioblasts. Alliin lyases or alliinases are responsible for catalyzing chemical reactions that produce the volatile chemicals that give to plants of the genus *Allium*, such as garlic and onions, their flavors, odors, and tear-inducing properties (Lancaster et al., 2000). This system is a defence against herbivores, where the damage of plant cells by a feeding animal releases the vacuolar alliinase, which reacts with cytosolic substrates to catalyse the production of pungent chemicals with deterrent effects. It is possible that the digestion of the cell wall may be perceived as a herbivore attack, inducing the up-regulation observed for the alliinase in protoplasts. In Fig. 9, it can be seen that this gene is induced by methyl jasmonate in seedlings, indicating a defence role of the alliinase during this developmental stage. This alliinase has also been detected in the vacuole proteome of *C. roseus* leaves, strengthening the hypothesis that *C. roseus* may indeed have such a defence system, which, to our knowledge, has never been reported for *C. roseus*.
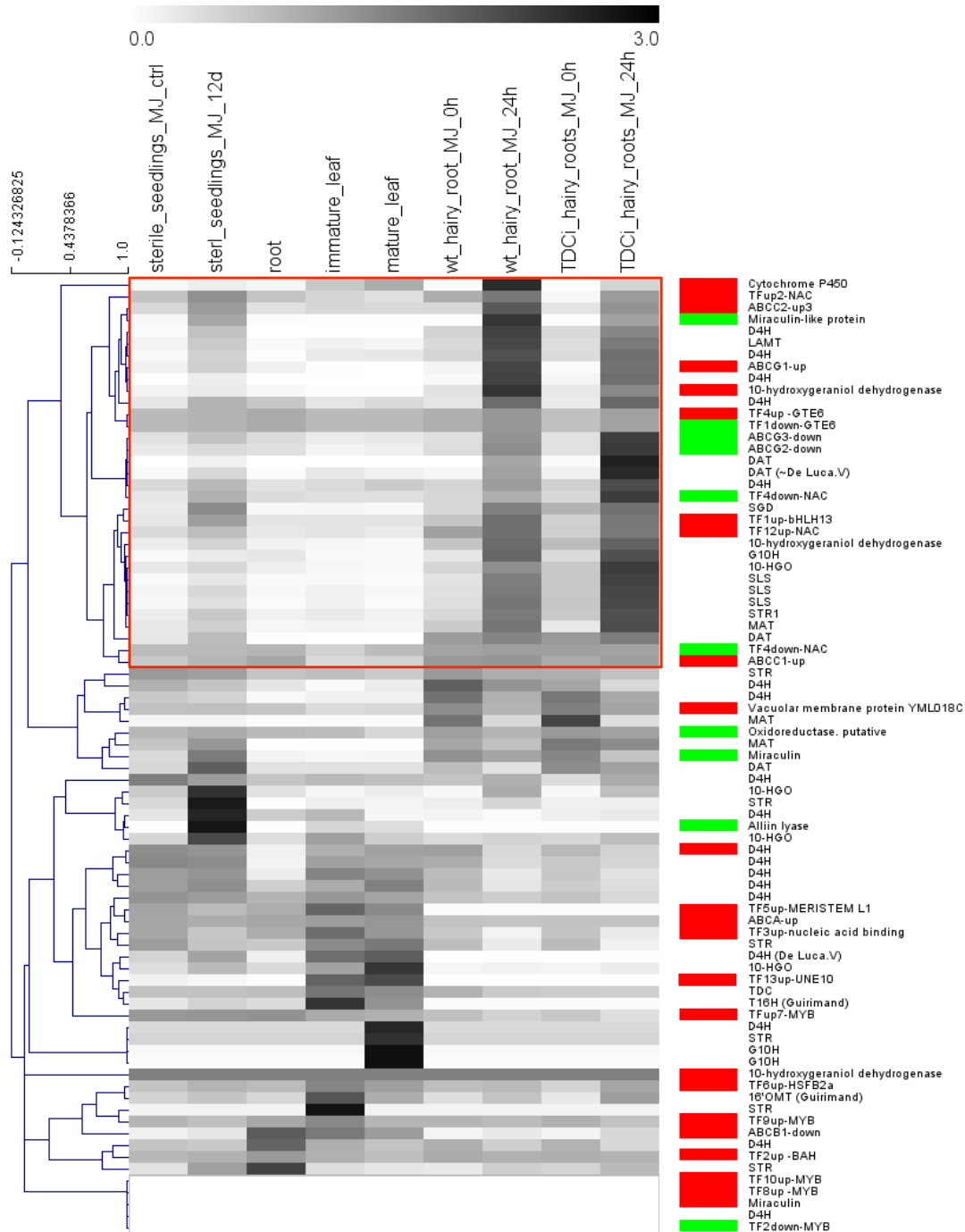
Figure 9. Hierarchical co-expression clustering analysis of up- and down-regulated genes in idioblasts together with known TIA genes, using the expression profiles provided by the MPGR database. TDC – tryptophan decarboxylase, G10H - Geraniol 10-hydroxylase, 10HGO - 10-hydroxygeraniol oxidoreductase, LAMT – loganic acid methyltransferase, SLS - secologanin synthase, STR - strictosidine synthase, SGD - strictosidine β-D-glucosidase, T16H - tabersonine 16-hydroxylase, OMT – 16-hydoxytabersonine 16-*O*-methyltransferase, NMT - *N*-methyltransferase, D4H - desacetoxyvindoline 4-hydroxylase, DAT - deacetylvindoline 4-*O*-acetyltransferase, MAT – minovincinine 19-hydroxy *O*-acetyltransferase. Up-regulated genes in idioblasts are identified by a red cell before the gene name (Table II) and down-regulated genes in idioblasts are identified by a green cell before the gene name (Table II). The red box highlights a cluster of genes induced by methyl jasmonate, which is particularly associated with the TIA pathway.

Transporters

Overall, the TIA pathway involves reactions taking place in three different subcellular compartments and three different cell types, predicting many transmembrane transport events of TIA intermediates, namely in opposite directions across the same membrane (Fig. 1; Guirimand et al., 2011a; Guirimand et al., 2011b) Logically, it is expected that the expression levels and activity of the respective transporters will be quite important for the regulation of the TIA metabolic fluxes. In this study, 4 ABC transporter genes were up-regulated in idioblasts, two from the subfamily C, one from the subfamily A and one from the subfamily G, while three other were down-regulated, two from subfamily G and one from subfamily B (Table II; Fig. 6 and 7). The other transporters detected were a sulfate transporter, two poorly characterized genes and a subunit from the chloroplastic ATP synthase.

Previously, several ABCB transporters have been implicated in the cellular influx of the alkaloid berberine in the rhizome and other tissues of *Coptis japonica* (Shitan et al., 2003; Shitan N, 2012). ABCG transporters are involved in the secretion of defence terpenoids, secrete lipidic molecules that form cutin and wax layers in the epidermis, and putative ABCG transporters were related with artemisinin yield in *Artemisia annua* (Jasinski et al., 2001; Zhang et al., 2012). ABCC transporters have been implicated in the vacuolar accumulation of several compounds and ions, including glucosylated anthocyanidins, glucuronide flavones, xenobiotic-glutathione conjugates, Cd^{2+} and Hg^{2+}, folate, phytate, etc. (Li et al., 1997; Klein et al., 2000; Liu et al., 2001; Goodman et al., 2004; Nagy et al., 2009; Raichaudhuri et al., 2009; Park et al., 2012; Francisco et al., 2013). In fact, the high diversity of the ABC gene family in plants has been related precisely with the diversity of plant secondary metabolism (Yazaki, 2006). This assumption correlates well with the identification of 42 ABC transporter proteins in the vacuole of *C. roseus* (Chapter III), a plant with a prolific secondary metabolism, unlike previously characterized vacuolar proteomes for Arabidopsis and cauliflower, with less profuse secondary metabolism (Carter et al., 2004; Jaquinod et al., 2007; Schmidt et al., 2007).

Among the idioblast up-regulated ABC transporter genes, the proteins codified by the *ABCC2* and *ABCA1* genes were identified in the vacuolar proteome of *C. roseus* (underlined in Table II). ABCA transporters have been associated mainly with the transport of lipid molecules (Verrier et al., 2008; Kim et al., 2013) while ABCC have been related with the transport of several types of secondary metabolites (above), often to the vacuole. Therefore, *ABCC2* is a likely candidate to transtonoplast transport of TIAs taking place in the idioblasts. Likewise, the up-regulated *ABCC1* and *ABCG1* are candidate to the plasma membrane influx of TIA intermediates that is supposed to

happen in idioblasts. None of the two *ABCG* and one *ABCB* down-regulated genes in idioblasts codifies proteins identified in the vacuolar proteome of *C. roseus* (Table II), so they are not likely candidates to the several transtonoplast transport events of TIA intermediates occurring in epidermal cells (Guirimand et al., 2011a), but they may be candidates to the predicted TIA efflux from epidermal cells (Guirimand et al., 2011b).

Cluster co-expression analysis of the up- and down-regulated transporter genes shows that the up-regulated *ABCC1*, *ABCC2* and *ABCG1*, and the down-regulated *ABCG2* and *ABCG3* genes fall in the highly promising cluster of TIA biosynthesis gene induced by methyl jasmonate in hairy roots. This may indicate that they are all involved in the TIA pathway, and as such are responsive to methyl jasmonate, the up-regulated transporters being expressed in the idioblasts, together with the late part of the pathway, and the down-regulated transporters being expressed in the epidermis, together with the early part of the pathway.

Transcription factors

The ultimate goal of plant metabolic engineering is to identify regulatory master switches of pathways, like has been done for instance for the anthocyanin pathway (Butelli et al., 2008). Therefore, the identification of transcription factors potentially involved in the regulation of the TIA pathway was one of the main goals of this study. Previous TFs implicated in the regulation of TIA biosynthesis enzymes include: two AP2/ERF (ORCA2, ORCA3), one MYB-like (CrBPF1), one WRKY (CrWRKY1), two bHLH (CrMYC1, CrMYC2), and three Cys2/His2-type zinc finger (ZCT1, ZCT2, ZCT3; Memelink and Gantet, 2007; Suttipanta et al., 2011; Zhang et al. 2011). These last three act as repressors, while all the others act as activators, most of them in response to jasmonates or yeast elicitation. However, none of these TFs enabled to increase the levels of the anticancer TIAs, possibly because none of them regulates the idioblast specific, bottleneck steps of VLB biosynthesis. Here, we identified 13 putative transcription factors (TFs) significantly up-regulated in idioblasts (Table II and Fig. 6), including 4 putative *MYB*, 2 *NAC*, 1 *bHLH*, 1 *GTE6*, 1 *homeobox ML1* and 1 *HSF* putative TFs. None of these TFs corresponds to the previously studied TFs in *C. roseus,* and their high expression in idioblasts makes them highly promising concerning the possibility of increasing VLB and VCR levels.

MYB, bHLH and homeobox ML1 TFs have all been involved in cell fate and patterning, namely in: i) trichome initiation, root hair patterning, stomatal differentiation and patterning (MYB; Dubos et al., 2010), ii) epidermal cell differentiation associated with repression of mesophyll cell fate (homeobox-leucine zipper protein MERISTEM L1; Takada et al., 2013), iii) trichrome differentiation and microspore development (bHLH;

Toledo-Ortiz et al., 2003). Therefore, it is possible that the up-regulated *MYB*, *bHLH* and *homeobox ML1* TF may be involved in the differentiation and patterning of idioblasts in *C. roseus* leaves. Interestingly, a bHLH / MYB partnership has been shown to be involved in the differentiation of Arabidopsis trichomes (Payne et al., 2000) and, in Fig. 6, it can be seen that TFup1–bHLH and TFup9-MYB cluster together, suggesting a possible cooperation. In fact, a bHLH / MYB partnership is also active in the regulation of the secondary metabolism pathway of anthocyanins (Heim et al., 2003; Butelli et al., 2008). Moroever, one Arabidopsis bHLH TF has been shown to regulate the biosynthesis of tryptophan, the precursor of the indole moiety from TIAs and a number of MYB TFs are involved in the regulation of different branches of the phenylpropanoid pathway and of glucosinolate biosynthesis in Arabidopsis, all secondary metabolism pathways (Toledo-Ortiz et al., 2003; Dubos et al., 2010). Hence, the putative TFs of these families identified in this study are strong candidates to the regulation of the bottleneck late steps of the TIA pathway specifically expressed in idioblasts.

The idioblast up-regulated putative TFup6-HSFB2a belongs to a TF family that is usually involved in response to stress, especially to heat treatment, and most HSFs act as repressors of target gene expression (Kanchiswamy et al., 2010). Indeed, TFup6-HSFB2a was induced by protoplasting, together with the two NAC and the GTE6 TFs, possibly as a response to the stress induced by this treatment (Fig. 6). In the case of TFup6-HSFB2a, it is tempting to speculate that it may be a repressor of chloroplast biogenesis involved in the low number of these organelles in the idioblasts, which is possibly doing the same in protoplasts, since these cells can obtain sucrose from the medium, and it may be advantageous to channel carbon metabolism to cell wall biosynthesis rather than to chloroplast biogenesis. The other three TFs induced by protoplasting may control defence functions that are activated by protoplast stress and are already particularly strongly expressed in idioblasts, with the TIA pathway actually fitting well in such a profile.

On the other hand, two NAC and one MYB TFs are down-regulated in idioblasts but very strongly up-regulated in the whole leaf protoplast population, showing the distinct behavior of idioblast protoplasts (Fig. 7). Those two TF families have been implicated in different aspects of cell wall biosynthesis, what could explain their induction in protoplasts. Considering such a role, the fact that they are not induced in idioblast protoplasts is difficult to understand. One possible explanation could be that idioblast cells are highly (terminally?) differentiated to play a toxic defence role, and are no longer able to endure the genetic reprograming needed to rebuilt a cell wall from scratch, or they will take much longer to activate that pathway. One sign of their extreme

differentiation is the fact that the ribosomal protein S9 (*RPS9*) gene, the most used housekeeping gene in *C. roseus* is not expressed at all in idioblasts (Fig. 4A).

The fourth down-regulated TF in idioblasts, TFdown1-GTE6, is up-regulated in the root (Fig. 7). Since the root expresses the early steps of the TIA pathway (van der Heijden et al., 2004), also specifically expressed in the epidermis of the leaves, it is possible that this TF may be involved in the regulation of the TIA pathway at the leaf epidermis. In fact, this gene falls in the highly promising cluster of TIA biosynthesis gene induced by methyl jasmonate in hairy roots (Fig. 9), where a set of both up- and down-regulated ABC transporters is included, the rationale being that both the early part of the TIA pathway expressed in the epidermis and the late part of the pathway expressed in idioblasts are responsive to methyl jasmonate. Therefore, the conclusion is that the idioblast up-regulated TFs included in this cluster (TFup1-bHLH, TF4-GTE6, TFup11-NAC and TFup12-NAC; Fig. 9) are likely involved in the regulation of the late TIA pathway in idioblast cells, downstream the methyl jasmonate signal, and that the idioblast down-regulated TFs included in this cluster (TFdown1-GTE6, TFdown3-NAC and TFdown3-NAC; Fig. 9) are likely involved in the regulation of the early TIA in epidermal cells, also downstream the methyl jasmonate signal.

Conclusions

This study shows that the idioblast cells from *C. roseus* leaves present a very distinctive expression profile and behavior during protoplasting, relative to all other cells in the leaves. The main results in what concerns identification of important candidate genes related with the TIA pathway are represented in Fig. 10. Among up- and down-regulated genes in idioblasts, this study identified a P450 that is a good candidate to the bottleneck hydroxylation of AVLB into VLB, 3 ABC transporters that are candidates to tonoplast and plasma membrane transport steps of TIA intermediates in idioblasts, 3 ABC transporters that are candidates to plasma membrane transport steps of TIA intermediates in epidermal cells, 13 TFs that are candidates to the regulation of the late steps of the TIA pathway and / or idioblast differentiation and patterning, and 4 TFs that are candidates to the regulation of the early steps of the TIA pathway. A set of these candidate genes is induced by methyl jasmonate, associating them with several TIA biosynthetic genes already characterized, and another set is induced by protoplasting, associating them with stress. Overall, this work unravels a set of strong candidate genes to key biosynthetic, transport and regulatory steps of the TIA pathway that may develop into important breakthroughs in the field.

Figure 10. Snapshot of the candidate genes to key biosynthetic, transport and regulatory steps of the TIA pathway unraveled by the differential transcript profiling of *C. roseus* leaf idioblast cells isolated by FACS. The putative or documented cell and subcellular localization of the codified proteins is illustrated, and responsiveness to methyl jasmonate (MeJA) and protoplasting is indicated. Full identification of genes is given in Table II. Expression regulation is as observed in Fig. 6, 7 and 9.

ACKNOWLEDGEMENTS

LITERATURE CITED

Birnbaum K, Jung JW, Wang JY, Lambert GM, Hirst JA, Galbraith DW, Benfey PN (2005) Cell type-specific expression profiting in plants via cell sorting of protoplasts from fluorescent reporter lines. Nature Methods **2:** 615-619

Brown S, Renaudin JP, Prevot C, Guern J (1984) Flow-cytometry and sorting of plant-protoplasts-technical problems and physiological results from a study of pH and alkaoids in *Catharanthus roseus*. Physiologie Vegetale **22:** 541-554

Butelli E, Titta L, Giorgio M, Mock H-P, Matros A, Peterek S, Schijlen EGWM, Hall RD, Bovy AG, Luo J, Martin C (2008) Enrichment of tomato fruit with health-promoting anthocyanins by expression of select transcription factors. Nature Biotechnology **26:** 7

Carqueijeiro I, Noronha H, Duarte P, Gerôs HV, Sottomayor M (2013) Vacuolar transport of the medicinal alkaloids from Catharanthus roseus is mediated by a proton driven antiport. Plant Physiology

Carter C, Pan SQ, Jan ZH, Avila EL, Girke T, Raikhel NV (2004) The vegetative vacuole proteorne of Arabidopsis thaliana reveals predicted and unexpected proteins. Plant Cell **16:** 3285-3303

Dixon KS, Hassoun A (2010) Pseudotumor cerebri due to the potentiation of all-trans retinoic acid by voriconazole. Journal of the American Pharmacists Association **50:** 742-744

Duarte P, Pissarra J, Moore I (2008) Processing and trafficking of a single isoform of the aspartic proteinase cardosin a on the vacuolar pathway. Planta **227:** 1255-1268

Dubos C, Stracke R, Grotewold E, Weisshaar B, Martin C, Lepiniec L (2010) MYB transcription factors in Arabidopsis. Trends in plant science **15:** 573-581

Ferreres F, Figueiredo R, Bettencourt S, Carqueijeiro I, Oliveira J, Gil-Izquierdo A, Pereira DM, Valentao P, Andrade PB, Duarte P, Barcelo AR, Sottomayor M (2011) Identification of phenolic compounds in isolated vacuoles of the medicinal plant *Catharanthus roseus* and their interaction with vacuolar class III peroxidase: an H2O2 affair? Journal of Experimental Botany **62:** 2841-2854

Francisco RM, Regalado A, Ageorges A, Burla BJ, Bassin B, Eisenach C, Zarrouk O, Vialet S, Marlin T, Chaves MM, Martinoia E, Nagy R (2013) ABCC1, an ATP Binding Cassette Protein from Grape Berry, Transports Anthocyanidin 3-O-Glucosides. The Plant cell **25:** 1840-1854

Giddings L-A, Liscombe DK, Hamilton JP, Childs KL, DellaPenna D, Buell CR, O'Connor SE (2011) A Stereoselective Hydroxylation Step of Alkaloid Biosynthesis by a Unique Cytochrome P450 in Catharanthus roseus. Journal of Biological Chemistry **286:** 16751-16757

Gongora-Castillo E, Childs KL, Fedewa G, Hamilton JP, Liscombe DK, Magallanes-Lundback M, Mandadi KK, Nims E, Runguphan W, Vaillancourt B, Varbanova-Herde M, DellaPenna D, McKnight TD, O'Connor S, Buell CR (2012) Development of Transcriptomic Resources for Interrogating the Biosynthesis of Monoterpene Indole Alkaloids in Medicinal Plant Species. Plos One **7**

Goodman CD, Casati P, Walbot V (2004) A multidrug resistance-associated protein involved in anthocyanin transport in *Zea mays*. Plant Cell **16:** 1812-1826

Guirimand G, Courdavault V, Lanoue A, Mahroug S, Guihur A, Blanc N, Giglioli-Guivarc'h N, St-Pierre B, Burlat V (2010) Strictosidine activation in Apocynaceae: towards a "nuclear time bomb"? Bmc Plant Biology **10**

Guirimand G, Guihur A, Ginis O, Poutrain P, Héricourt F, Oudin A, Lanoue A, St-Pierre B, Burlat V, Courdavault V (2011a) The subcellular organization of strictosidine biosynthesis in Catharanthus roseus epidermis highlights several trans-tonoplast translocations of intermediate metabolites. FEBS Journal **278:** 749-763

Guirimand G, Guihur A, Poutrain P, Héricourt F, Mahroug S, St-Pierre B, Burlat V, Courdavault V (2011b) Spatial organization of the vindoline biosynthetic pathway in *Catharanthus roseus*. Journal of Plant Physiology **Volume 168:** 549-557

Heim MA, Jakoby M, Werber M, Martin C, Weisshaar B, Bailey PC (2003) The basic helix-loop-helix transcription factor family in plants: A genome-wide study of protein structure and functional diversity. Molecular Biology and Evolution **20:** 735-747

Jacobs D, Gaspari M, van der Greef J, van der Heijden R, Verpoorte R (2005) Proteome analysis of the medicinal plant Catharanthus roseus. Planta **221:** 14

Jaquinod M, Villiers F, Kieffer-Jaquinod S, Hugouvieux V, Bruley C, Garin J, Bourguignon J (2007) A Proteomics Approach Highlights a Myriad of

Transporters in the Arabidopsis thaliana Vacuolar Membrane. Plant signaling & behavior **2:** 413-415

Jasinski M, Stukkens Y, Degand H, Purnelle B, Marchand-Brynaert J, Boutry M (2001) A plant plasma membrane ATP binding cassette-type transporter is involved in antifungal terpenoid secretion. Plant Cell **13:** 1095-1107

Kanchiswamy CN, Muroi A, Maffei ME, Yoshioka H, Sawasaki T, Arimura G-i (2010) Ca2+-dependent protein kinases and their substrate HsfB2a are differently involved in the heat response signaling pathway in Arabidopsis. Plant Biotechnology **27:** 469-473

Kim S, Yamaoka Y, Ono H, Kim H, Shim D, Maeshima M, Martinoia E, Cahoon EB, Nishida I, Lee Y (2013) AtABCA9 transporter supplies fatty acids for lipid synthesis to the endoplasmic reticulum. Proceedings Of The National Academy Of Sciences Of The United States Of America **110:** 773-778

Klein M, Martinoia E, Hoffmann-Thoma G, Weissenbock G (2000) A membrane-potential dependent ABC-like transporter mediates the vacuolar uptake of rye flavone glucuronides: regulation of glucuronide uptake by glutathione and its conjugates. Plant Journal **21:** 289-304

Lancaster JE, Shaw ML, Joyce MDP, McCallum JA, McManus MT (2000) A Novel Alliinase from Onion Roots. Biochemical Characterization and cDNA Cloning. Plant Physiology **122:** 1269-1280

Li Z-S, Lu Y-P, Zhen R-G, Szczypka M, Thiele DJ, Rea PA (1997) A new pathway for vacuolar cadmium sequestration in Saccharomyces cerevisiae: YCF1-catalyzed transport of bis(glutathionato)cadmium. Proceedings of the National Academy of Sciences **94:** 42-47

Liu GS, Sanchez-Fernandez R, Li ZS, Rea PA (2001) Enhanced multispecificity of Arabidopsis vacuolar multidrug resistance-associated protein-type ATP-binding cassette transporter, AtMRP2. Journal of Biological Chemistry **276:** 8648-8656

Loyola-Vargas VM, Galaz-Ávalos RM, Kú-Cauich R (2007) *Catharanthus* biosynthetic enzymes: the road ahead. Phytochemistry Reviews **6:** 307-339

Mahroug S, Burlat V, St-Pierre B (2007) Cellular and sub-cellular organisation of the monoterpenoid indole alkaloid pathway in *Catharanthus roseus*. Phytochemistry Reviews **6:** 363-381

Memelink J, Gantet P (2007) Transcription factors involved in terpenoid indole alkaloid biosynthesis in Catharanthus roseus. Phytochemistry Reviews **6:** 353-362

Menke FLH, Champion A, Kijne JW, Memelink J (1999) A novel jasmonate- and elicitor-responsive element in the periwinkle secondary metabolite biosynthetic

gene Str interacts with a jasmonate- and elicitor-inducible AP2-domain transcription factor, ORCA2. Embo Journal **18:** 4455-4463

Mersey BG, Cutler AJ (1986) Differential distribution of specific indole alkaloids in leaves of Catharanthus roseus Canadian Journal of Botany-Revue Canadienne De Botanique **64:** 1039-1045

Murata J, Roepke J, Gordon H, De Luca V (2008) The leaf epidermome of *Catharanthus roseus* reveals its biochemical specialization. Plant Cell **20:** 524-542

Nagy R, Grob H, Weder B, Green P, Klein M, Frelet-Barrand A, Schjoerring JK, Brearley C, Martinoia E (2009) The Arabidopsis ATP-binding Cassette Protein AtMRP5/AtABCC5 Is a High Affinity Inositol Hexakisphosphate Transporter Involved in Guard Cell Signaling and Phytate Storage. Journal of Biological Chemistry **284:** 33614-33622

Park J, Song W-Y, Ko D, Eom Y, Hansen TH, Schiller M, Lee TG, Martinoia E, Lee Y (2012) The phytochelatin transporters AtABCC1 and AtABCC2 mediate tolerance to cadmium and mercury. The Plant Journal **69:** 278-288

Payne CT, Zhang F, Lloyd AM (2000) GL3 encodes a bHLH protein that regulates trichome development in arabidopsis through interaction with GL1 and TTG1. Genetics **156:** 1349-1362

Pomahacova B, Dusek J, Duskova J, Yazaki K, Roytrakul S, Verpoorte R (2009) Improved accumulation of ajmalicine and tetrahydroalstonine in Catharanthus cells expressing an ABC transporter. Journal of Plant Physiology **166:** 1405-1412

Raichaudhuri A, Peng M, Naponelli V, Chen S, Sánchez-Fernández R, Gu H, Gregory JF, Hanson AD, Rea PA (2009) Plant Vacuolar ATP-binding Cassette Transporters That Translocate Folates and Antifolates in Vitro and Contribute to Antifolate Tolerance in Vivo. Journal of Biological Chemistry **284:** 8449-8460

Rischer H, Oresic M, Seppanen-Laakso T, Katajamaa M, Lammertyn F, Ardiles-Diaz W, Van Montagu MCE, Inze D, Oksman-Caldentey KM, Goossens A (2006) Gene-to-metabolite networks for terpenoid indole alkaloid biosynthesis in Catharanthus roseus cells. Proceedings Of The National Academy Of Sciences Of The United States Of America **103:** 5614-5619

Saeed AI, Sharov V, White J, Li J, Liang W, Bhagabati N, Braisted J, Klapa M, Currier T, Thiagarajan M, Sturn A, Snuffin M, Rezantsev A, Popov D, Ryltsov A, Kostukovich E, Borisovsky I, Liu Z, Vinsavich A, Trush V, Quackenbush J (2003) TM4: A free, open-source system for microarray data management and analysis. Biotechniques **34:** 374-+

Saldanha AJ (2004) Java Treeview-extensible visualization of microarray data. Bioinformatics **20:** 3246-3248

Schmidt UG, Endler A, Schelbert S, Brunner A, Schnell M, Neuhaus HE, Marty-Mazars D, Marty F, Baginsky S, Martinoia E (2007) Novel tonoplast transporters identified using a proteomic approach with vacuoles isolated from cauliflower buds. Plant Physiology **145:** 216-229

Shitan N, Bazin I, Dan K, Obata K, Kigawa K, Ueda K, Sato F, Forestier C, Yazaki K (2003) Involvement of CjMDR1, a plant multidrug-resistance-type ATP-binding cassette protein, in alkaloid transport in Coptis japonica. Proceedings Of The National Academy Of Sciences Of The United States Of America **100:** 751-756

Shitan N DF, Dan K, Kato N, Ueda K, Sato F, Forestier C, Yazaki K (2012) Characterization of *Coptis japonica* CjABCB2, an ATP-binding cassette protein involved in alkaloid transport. Phytochemistry

Shukla AK, Shasany AK, Gupta MM, Khanuja SPS (2006) Transcriptome analysis in Catharanthus roseus leaves and roots for comparative terpenoid indole alkaloid profiles. Journal of Experimental Botany **57:** 3921-3932

St-Pierre B, Vazquez-Flota FA, De Luca V (1999) Multicellular compartmentation of Catharanthus roseus alkaloid biosynthesis predicts intercellular translocation of a pathway intermediate. Plant Cell **11:** 887-900

Suttipanta N, Pattanaik S, Kulshrestha M, Patra B, Singh SK, Yuan L (2011) The Transcription Factor CrWRKY1 Positively Regulates the Terpenoid Indole Alkaloid Biosynthesis in Catharanthus roseus. Plant Physiology **157**: 2081-2093

Takada S, Takada N, Yoshida A (2013) ATML1 promotes epidermal cell differentiation in Arabidopsis shoots. Development **140:** 1919-1923

Toledo-Ortiz G, Huq E, Quail PH (2003) The Arabidopsis basic/helix-loop-helix transcription factor family. Plant Cell **15:** 1749-1770

van der Heijden R, Jacobs DI, Snoeijer W, Hallared D, Verpoorte R (2004) The Catharanthus alkaloids: Pharmacognosy and biotechnology. Current Medicinal Chemistry **11:** 607-628

Verpoorte R, Lata B, Sadowska A, eds (2007) Biology and Biochemistry of *Catharanthus roseus* (L.) G. Don Vol 2-3. Springer Verlag

Verrier PJ, Bird D, Buria B, Dassa E, Forestier C, Geisler M, Klein M, Kolukisaoglu U, Lee Y, Martinoia E, Murphy A, Rea PA, Samuels L, Schulz B, Spalding EP, Yazaki K, Theodoulou FL (2008) Plant ABC proteins - a unified nomenclature and updated inventory. Trends in plant science **13:** 151-159

Vuylsteke M, Peleman JD, van Eijk MJT (2007a) AFLP-based transcript profiling (cDNA-AFLP) for genome-wide expression analysis. Nature Protocols **2:** 1399-1413

Yazaki K (2006) ABC transporters involved in the transport of plant secondary metabolites. Febs Letters **580:** 1183-1191

Zhang H, Hedhili S, Montiel G, Zhang Y, Chatel G, Pre M, Gantet P, Memelink J (2011) The basic helix-loop-helix transcription factor CrMYC2 controls the jasmonate-responsive expression of the ORCA genes that regulate alkaloid biosynthesis in Catharanthus roseus. Plant Journal **67**: 61-71

Zhang L, Lu X, Shen Q, Chen Y, Wang T, Zhang F, Wu S, Jiang W, Liu P, Zhang L, Wang Y, Tang K (2012) Identification of Putative Artemisia annua ABCG Transporter Unigenes Related to Artemisinin Yield Following Expression Analysis in Different Plant Tissues and in Response to Methyl Jasmonate and Abscisic Acid Treatments. Plant Molecular Biology Reporter **30:** 838-847

Chapter
VI

Conclusions and future

perspectives

CONCLUSIONS AND FUTURE PERSPECTIVES

In this thesis, the metabolism and transmembrane transport of the highly valuable medicinal alkaloids from *C. roseus* was investigated, using biochemical and omic approaches. *C. roseus* accumulates in the leaves low levels of the important anticancer terpenoid indole alkaloids (TIAs) vinblastine (VLB) and vincristine (VCR), making of this plant one of the best characterized medicinal plants. However, although much is known about the biosynthesis and regulation of TIAs in *C. roseus*, gene / enzyme characterization is still lacking for many biosynthetic steps, the membrane transport mechanisms of TIAs are basically uncharacterized despite their importance for TIA accumulation, and no effective regulatory master switch of the TIA pathway has been identified to date.

Therefore, one of the primary objectives of this thesis was to characterize the transmembrane transport mechanism responsible for the accumulation of TIAs in their final sequestration target, the vacuole. This specific transport step was selected among the multiple transport events of the TIA pathway, due to the fact that vacuoles are the final accumulation target of TIAs, and therefore the most likely to have an important influence in the output of TIA fluxes. On the other hand, although technically challenging, this transport step was also probably the most amenable to experimental characterization. In chapter II, a thorough characterization of the membrane transport mechanism for vacuolar accumulation of the main TIAs present in *C. roseus* leaves was performed. Results revealed that TIAs are accumulated in the vacuoles of mesophyll cells by a specific proton antiport system, dependent on the transtonoplast pH gradient generated by the V-H$^+$-ATPase and the V-H$^+$-PPase, in agreement with previous observations for the alkaloids berberine in *C. japonica* and nicotine in tobacco. Therefore, the results from Chapter II further support the H$^+$ antiport mechanism as a general system for vacuolar accumulation of alkaloids in plants, with MATE transporters being prime candidates for this transport. Chapter II also establishes a number of tools for the characterization of membrane transport of alkaloids in *C. roseus* that may now be very useful for the characterization of the many other transmembrane transport steps occurring in the TIA pathway.

In chapter III, highly pure intact vacuoles and tonoplast membranes were used to perform the characterization of the proteome of the toxic vacuoles of *C. roseus* leaf cells, aiming to identify putative transtonoplast TIA transporters and missing TIA biosynthetic enzymes, at the same time the complexity of biological functions of the vacuoles were further investigated. In fact, the vacuole proteome of *C. roseus* not only provided several

candidate MATE transporter candidate genes to the vacuolar proton / TIA antiport characterized in chapter II, but also highlighted known and novel aspects of vacuoles biological functions. As a whole, the proteome of the toxic vacuoles from *C. roseus* leaves indicates, apart from the well-known involvement in lytic reactions and in ion and sugar homeostasis, a high commitment of this organelle with secondary metabolism and defence indicated by the high levels of strictosidine synthase, a newly discovered and very significant role in redox homeostasis, the presence of a significant metabolic activity, and the possible association of innumerable transporters and signalling proteins in membrane microdomains. In total, 1886 putative proteins were identified, standing now as an invaluable tool for future studies of vacuole and protein function. An exciting clue raised by this vacuole proteome study, was whether catalase and the Rubisco small subunit may be "moonlighting" proteins, exhibiting further activities distinct from their classically identified functions.

In chapters IV and V, in order to identify putative candidate genes for the missing, bottleneck biosynthetic steps of VLB and VCR and for their transcriptional regulators, an ambitious strategy was set, based on the fact that the late, bottleneck steps of VLB biosynthesis occur in specialized mesophyll cells called idioblasts. This strategy involved the isolation of the specialized idioblast cells from the mesophyll tissue where they are embedded, followed by their differential transcription profiling. Accordingly, in chapter IV, a methodology for the isolation of idioblast protoplasts by means of fluorescence activated cell sorting (FACS) of leaf protoplasts was established, taking advantage of the distinctive autofluorescences of idioblasts. The optimized buffer and FCAS method enabled the isolation of a highly pure and viable population of idioblast protoplasts, compatible with the implementation of subsequent transcriptomic, metabolomic and proteomic studies. This FACS method, allowing the isolation of intact leaf protoplast populations according to their autofluorescence, is likely applicable to many other situations involving specific plant cell types.

The isolated idioblast cells were then submitted to differential transcription profiling by cDNA-AFLP in Chapter V, in order to unravel important candidate genes for the crucial part of the TIA pathway, including related biosynthetic enzymes, transporters and transcriptional regulators. This transcriptional screening showed that the idioblast cells from *C. roseus* leaves present a very distinctive expression profile relative to all other cells in the leaves, and it was possible to identify a P450 that is a good candidate to the bottleneck hydroxylation of AVLB into VLB, 3 ABC transporters that are candidates to tonoplast and plasma membrane transport steps of TIA intermediates in idioblasts, 3 ABC transporters that are candidates to plasma membrane transport steps of TIA intermediates in epidermal cells, 13 TFs that are candidates to the regulation of the late

steps of the TIA pathway and / or idioblast differentiation and patterning, and 4 TFs that are candidates to the regulation of the early steps of the TIA pathway. Overall, the work of chapter V unravels a set of strong candidate genes to key biosynthetic, transport and regulatory steps of the TIA pathway, that may develop into important breakthroughs in the field.

At present, several of the MATE and ABC transporter candidate genes, as well as the P450 gene and several of the transcription factors identified in this thesis (chapters III and V) are being isolated and cloned in our laboratory, to proceed with their functional characterization. One of the major limitations that has been hindering research and applications in *C. roseus* and its TIA pathway, is the lack of an efficient method for the production of transgenic *C. roseus* plants. However, very recently two protocols for the production of transgenic *C. roseus* plants were published (Verma and Mathur 2011; Wang et al. 2012). So, one of the priorities of future work should be to confirm the reproducibility of these protocols, in order to be able to test and use the genes identified here in planta.

The characterization of the differential metabolome of idioblasts is also imperative, to definitely ascertain the metabolic differentiation status of these cells and confirm the assumptions that have been made concerning the specific accumulation of VLB and VCR in idioblasts. On the other hand, the full characterization of the transcriptional idioblastome by deep sequencing is now a tangible possibility, and should produce exciting results concerning the TIA pathway, its regulation, and the differentiation of idioblasts.

In summary, the results obtained in the course of this thesis have provided novel and important information regarding the transmembrane transport of TIAs, as well as a set of highly relevant candidate genes that will feed research in the field for many years, and may guarantee, in the future, the successful manipulation of the TIA pathway in *C. roseus* to achieve higher levels of the anticancer VLB and VCR.

LITERATURE CITED

Verma P, Mathur AK (2011) *Agrobacterium tumefaciens*-mediated transgenic plant production via direct shoot bud organogenesis from pre-plasmolyzed leaf explants of *Catharanthus roseus* Biotechnol Lett **33**: 1053–1060

Wang Q, Xing S, Pan Q, Yuan F, Zhao J, Tian Y, Chen Y, Wang G, Tang K (2012) Development of efficient *Catharanthus roseus* regeneration and transformation system using agrobacterium tumefaciens and hypocotyls as explants. BMC Biotechnology **12**: 34